Electronic Supplementary Information (ESI)

PIDA-Mediated Synthesis of Kynurenine Derivatives by Oxidative Fragmentation of Tryptophan Scaffold

Chinmay K. Jena,[a,c] Aurobindo Patnaik, [a,c] Sushree S. Nayak,[a,c] Supriya Kumari, [a,b] Ankita Panda,[a,c] Manjusha Dixit [b,c] and Nagendra K. Sharma*[a,c]

[a]School of Chemical Sciences, National Institute of Science Education and Research (NISER),

Jatani-752050, Odisha, India.

[b]School of Biological Sciences, National Institute of Science Education and Research (NISER),

Jatani-752050, Odisha, India.

[c] Homi Bhabha National Institute (HBNI)-Mumbai, Anushaktinagar, Mumbai, 400 094, India

*Corresponding author. Tel.: 0674-249-4141; fax: +91 (674) 2494004; E-mail: nagendra@niser.ac.in

Contents

1. NMR and Mass Spectra of Tryptophan Derivatives (**2a-2l**/**4a-4m**/**6a-6i**)

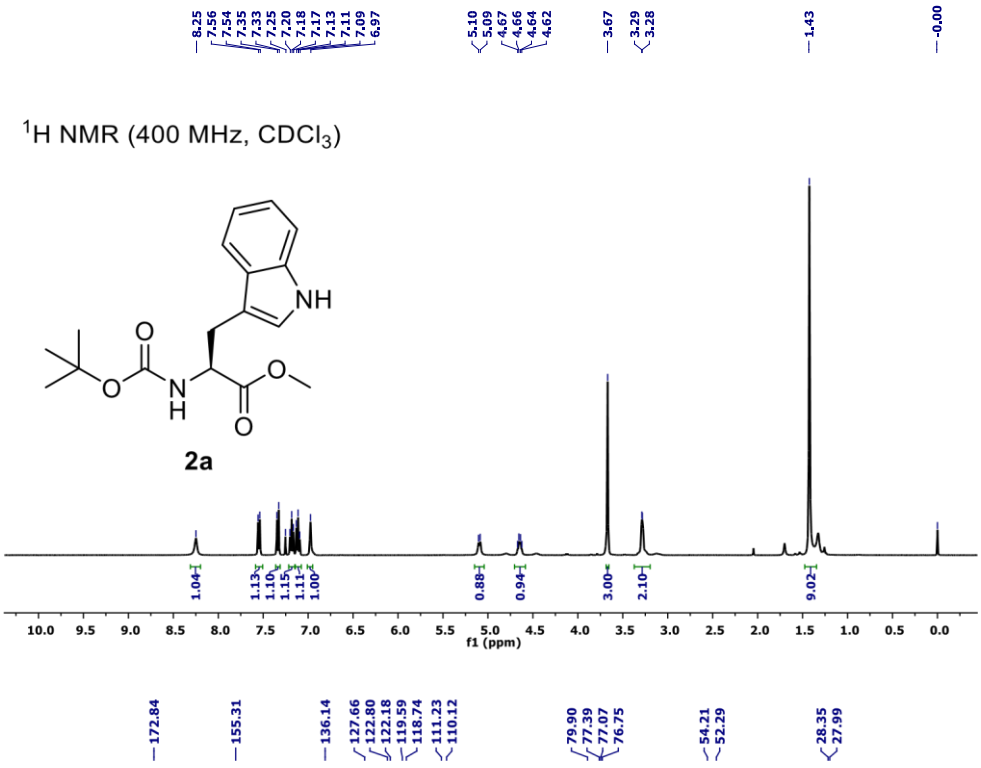

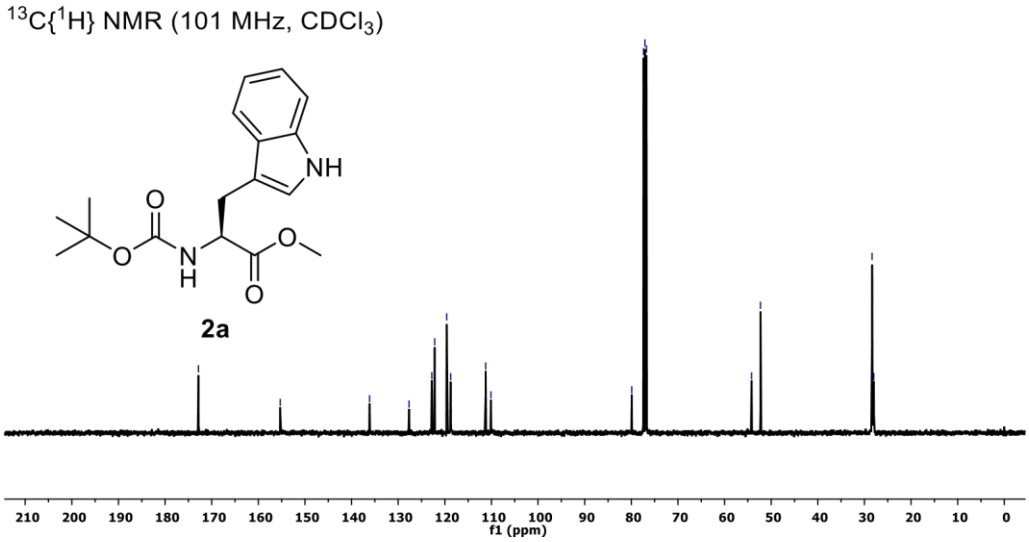

Fig S1. ^{1}H, ^{13}C $\{^{1}H\}$ NMR spectra of tryptophan derivative **2a**.

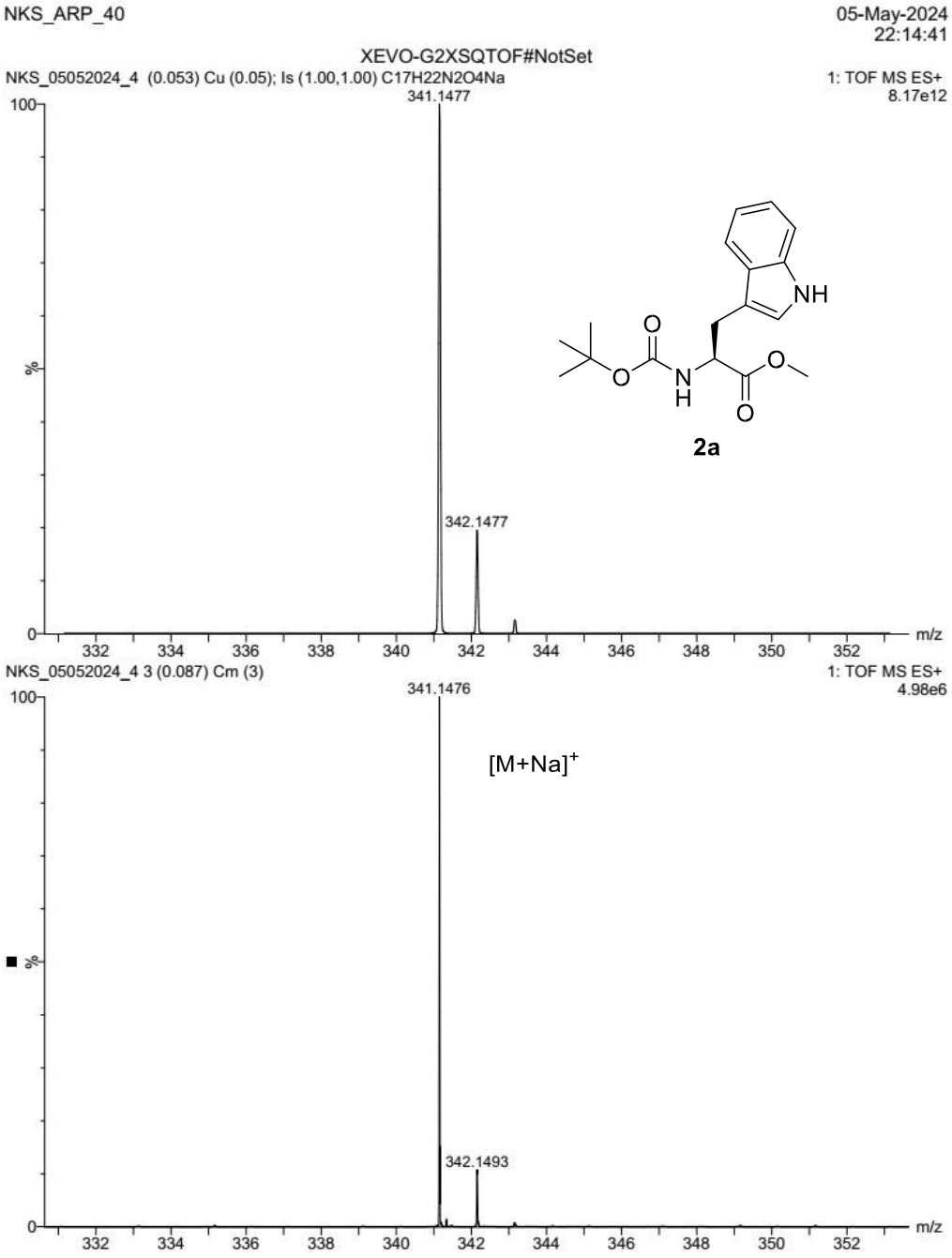

Fig S2. ESI-HRMS spectra of tryptophan derivative **2a**.

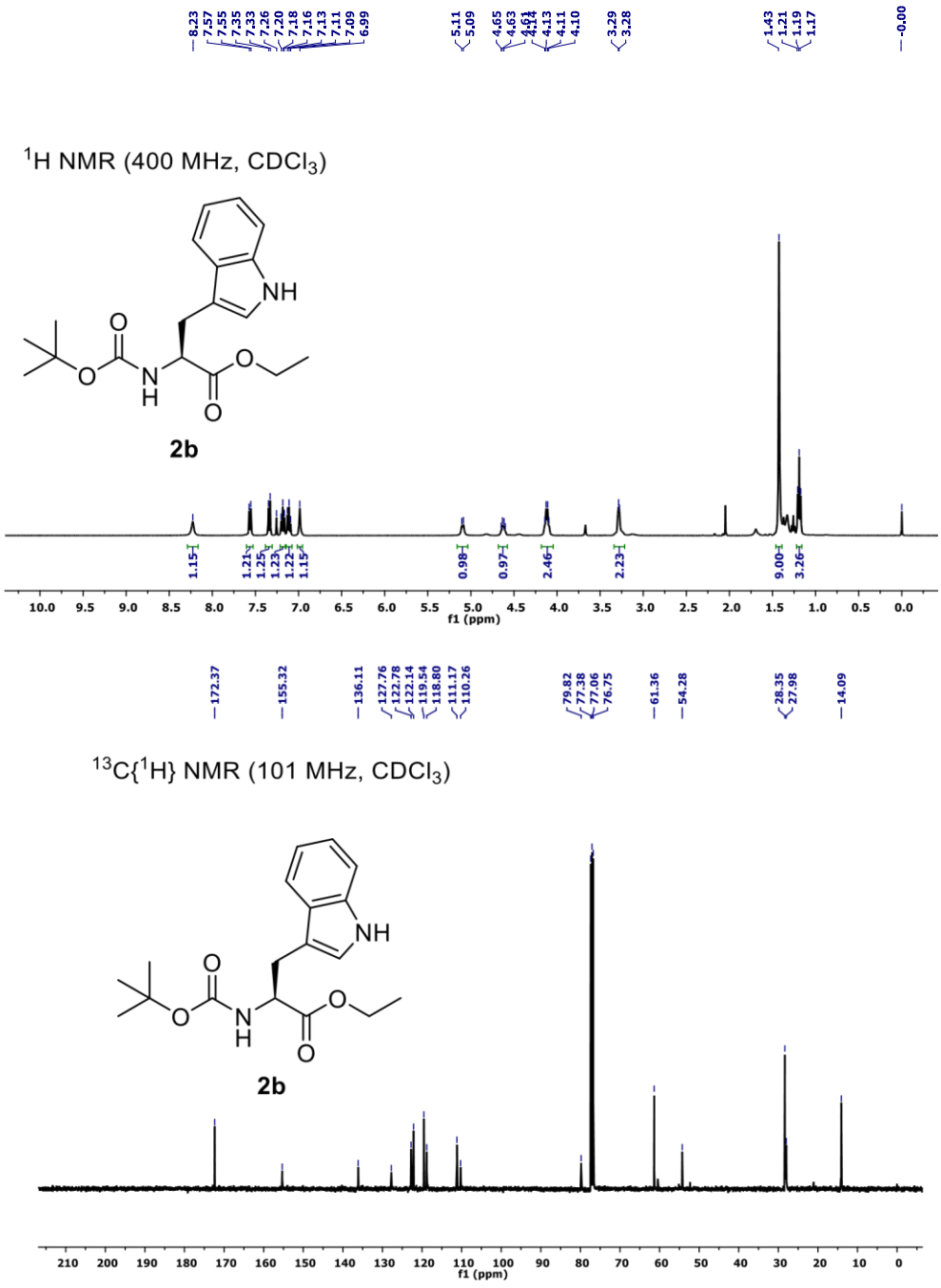

Fig S3. ^{1}H, ^{13}C $\{^{1}H\}$ NMR spectra of tryptophan derivative **2b**.

5
7.33
7 11
6.99
7

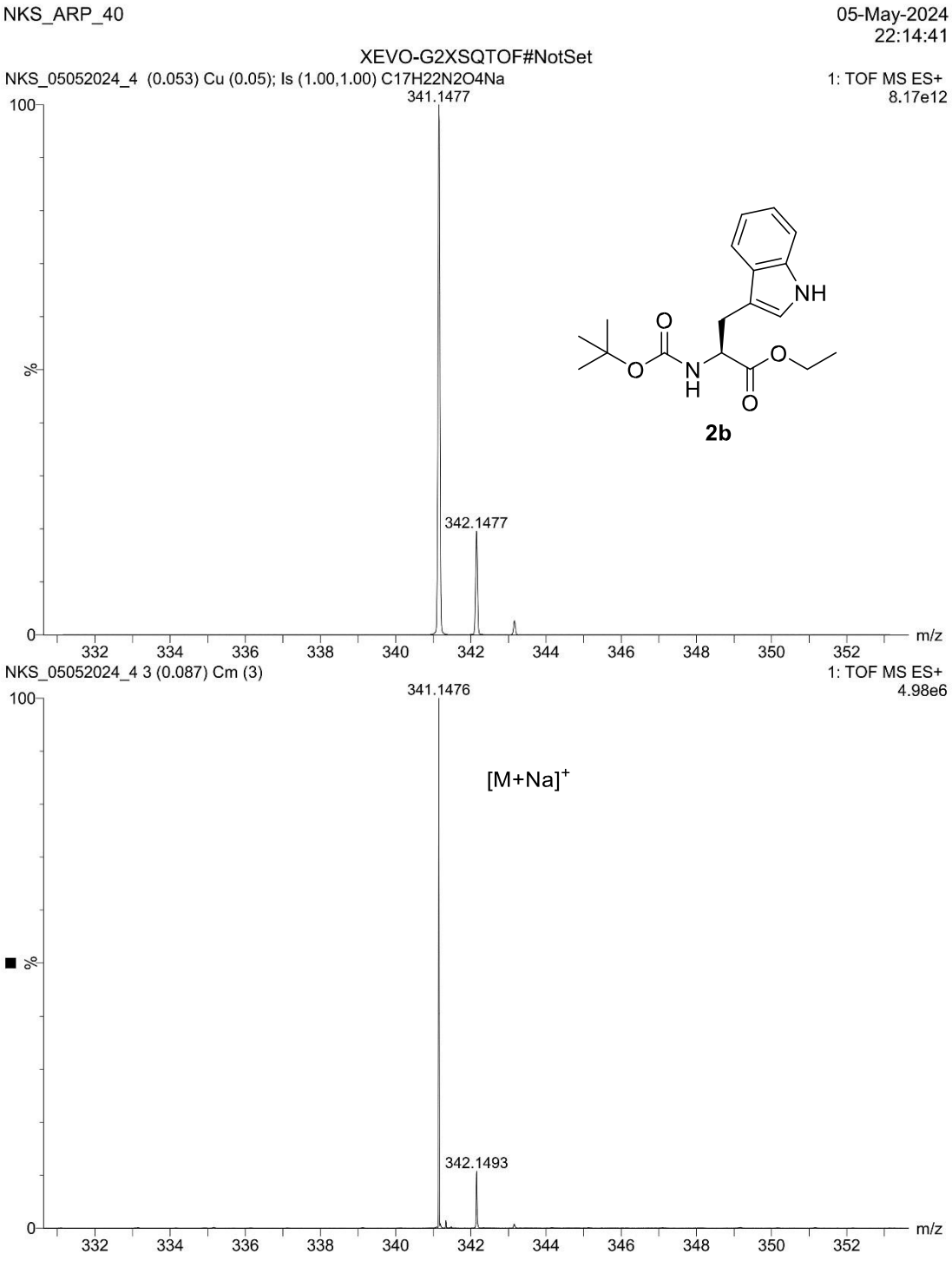

Fig S4. ESI-HRMS spectra of tryptophan derivative **2b**.

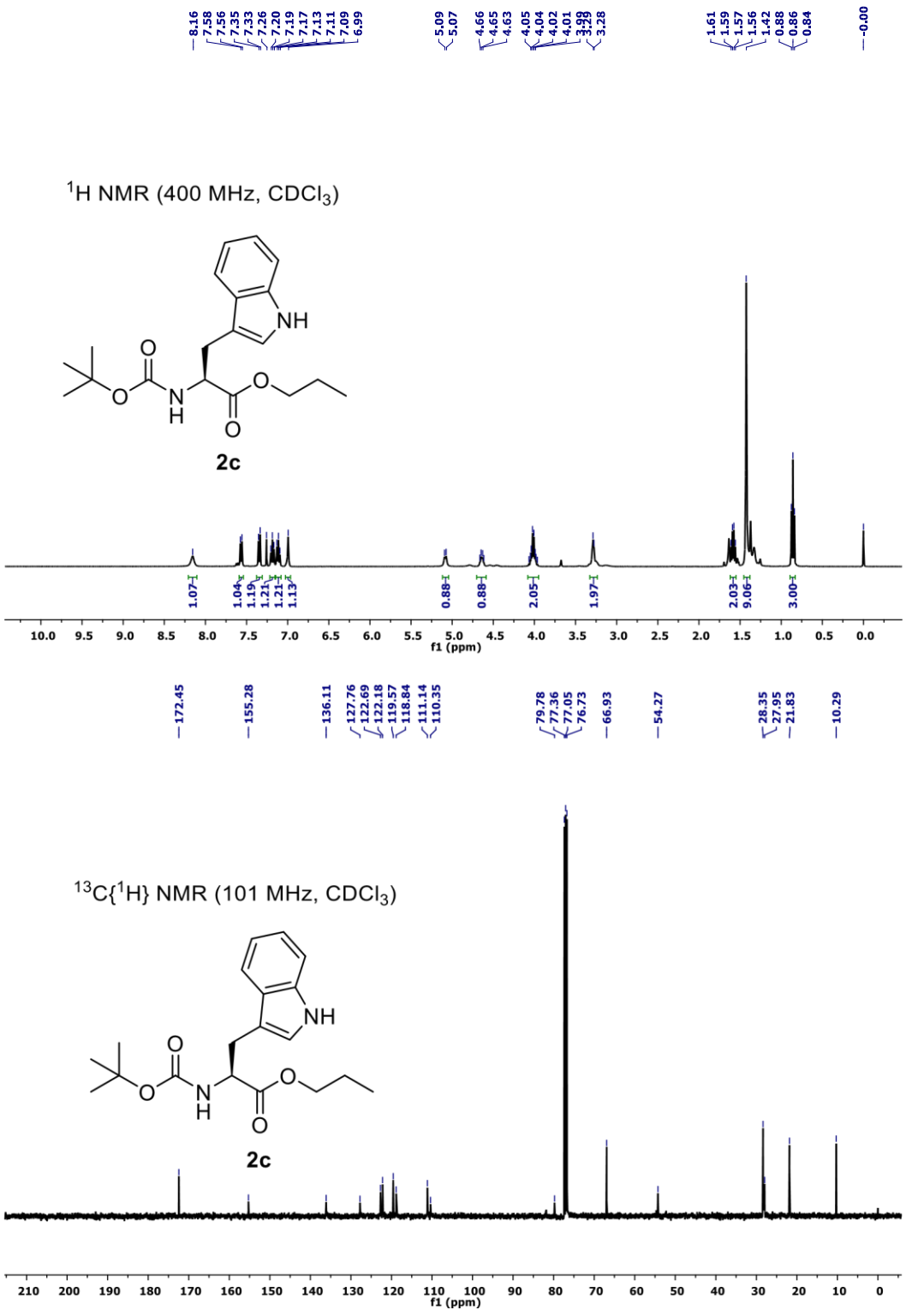
8.16
7.58
7.56
7.35
7.33
7.26
7.20
7.19
7.17
7.13
7.11
7.09
6.99
5.09
5.07
4.66
4.65
4.63
4.05
4.04
4.02
4.01
3.99
3.29
3.28
1.61
1.59
1.57
1.56
1.42
0.88
0.86
0.84
-0.00
1H NMR (400 MHz, CDCl3)
NH
O
O
N
H
O
O
2c
1.07
1.04
1.19
1.21
1.21
1.13
0.88
0.88
2.05
1.97
2.03
9.06
3.00
10.0 9.5 9.0 8.5 8.0 7.5 7.0 6.5 6.0 5.5 5.0 4.5 4.0 3.5 3.0 2.5 2.0 1.5 1.0 0.5 0.0
f1 (ppm)
172.45
155.28
136.11
127.76
122.69
122.18
119.57
118.84
111.14
110.35
79.78
77.36
77.05
76.73
66.93
54.27
28.35
27.95
21.83
10.29
13C{1H} NMR (101 MHz, CDCl3)
NH
O
O
N
H
O
O
2c
210 200 190 180 170 160 150 140 130 120 110 100 90 80 70 60 50 40 30 20 10 0
f1 (ppm)

Fig S5. ^{1}H, ^{13}C $\{^{1}H\}$ NMR spectra of tryptophan derivative **2c**.

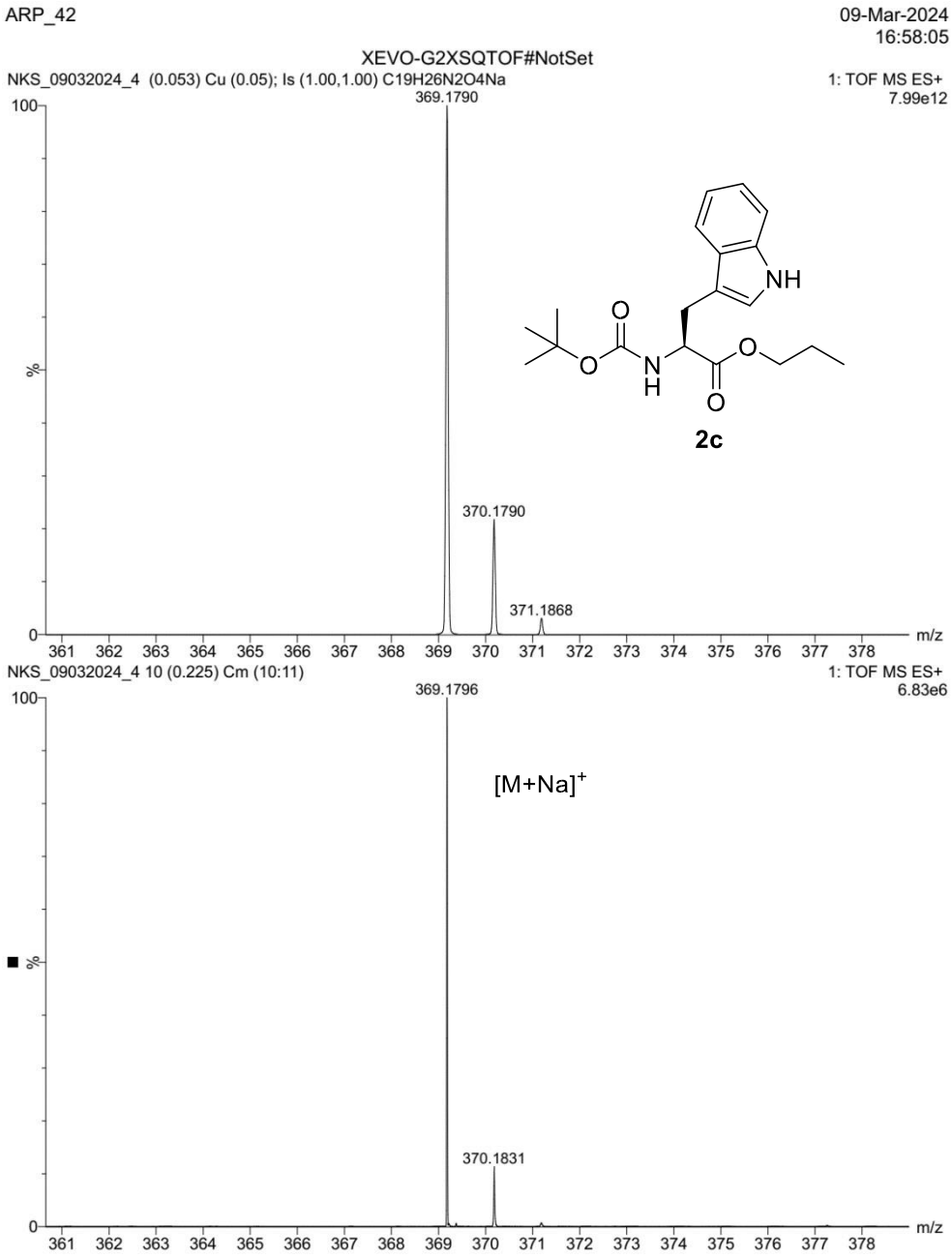

Fig S6. ESI-HRMS spectra of tryptophan derivative **2c**.

5
7.33
7 11
6.99
7

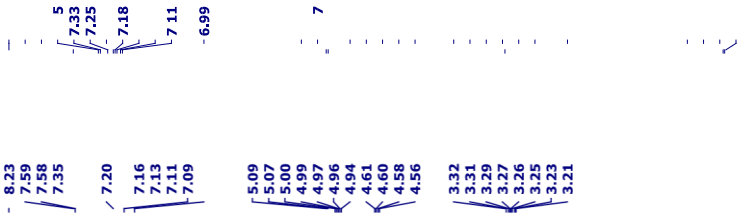

^{1}H NMR (400 MHz, $CDCl_3$)

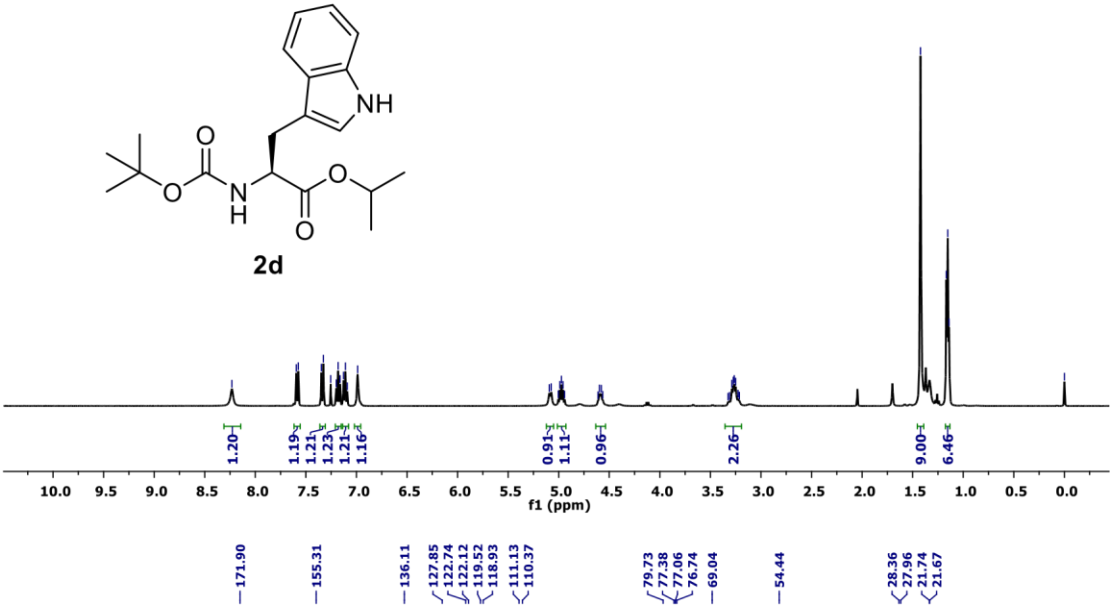

2d

^{13}C{^{1}H} NMR (101 MHz, $CDCl_3$)

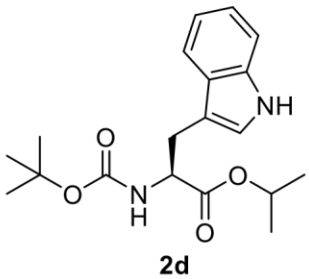

2d

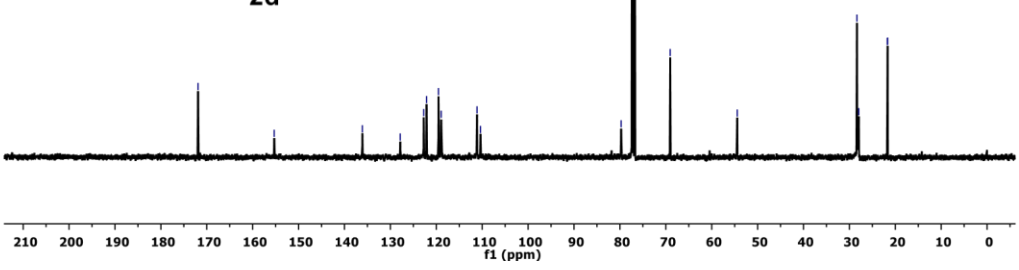

Fig S7. ^{1}H, ^{13}C $\{^{1}H\}$ NMR spectra of tryptophan derivative **2d**.

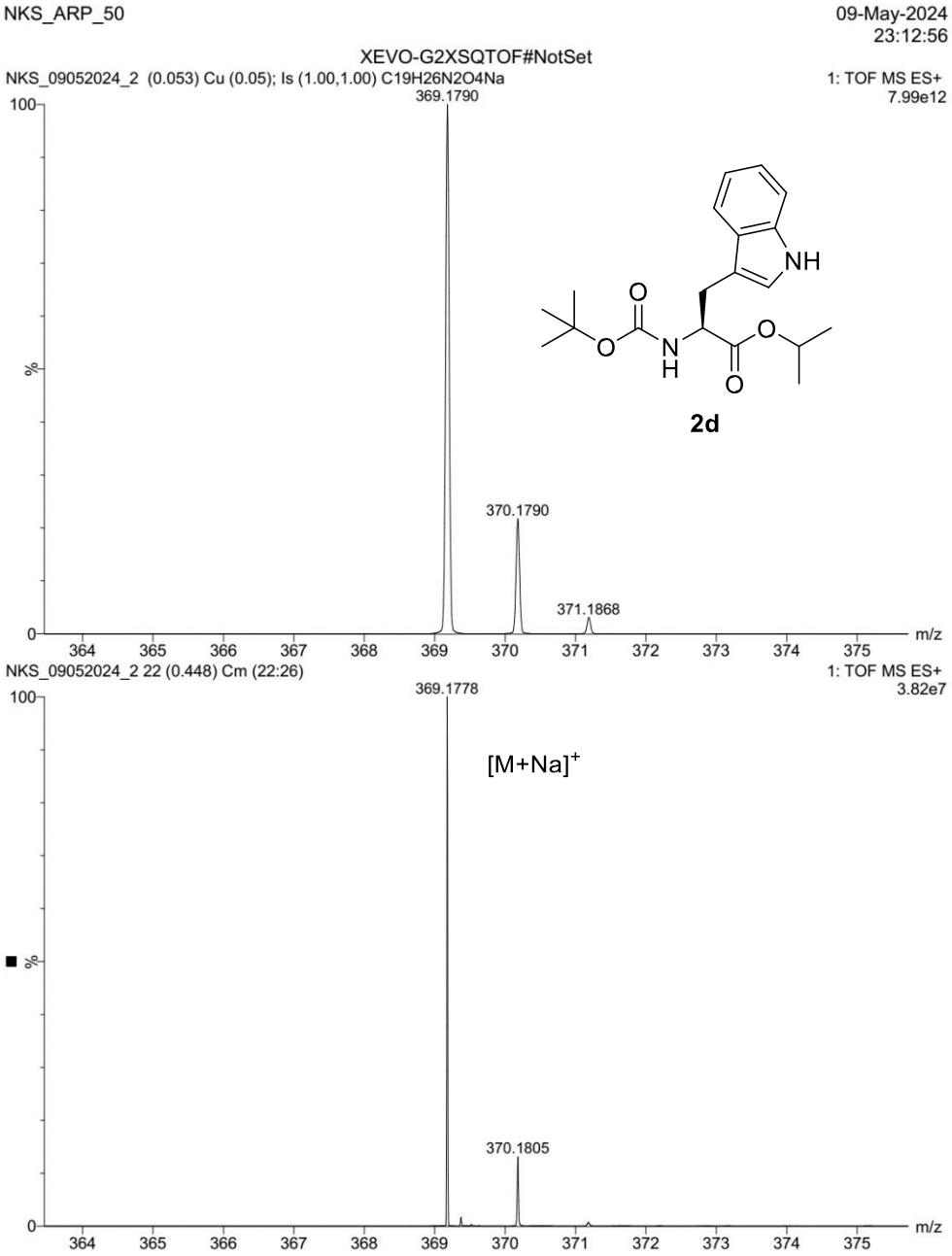

Fig S8. ESI-HRMS spectra of tryptophan derivative **2d**.

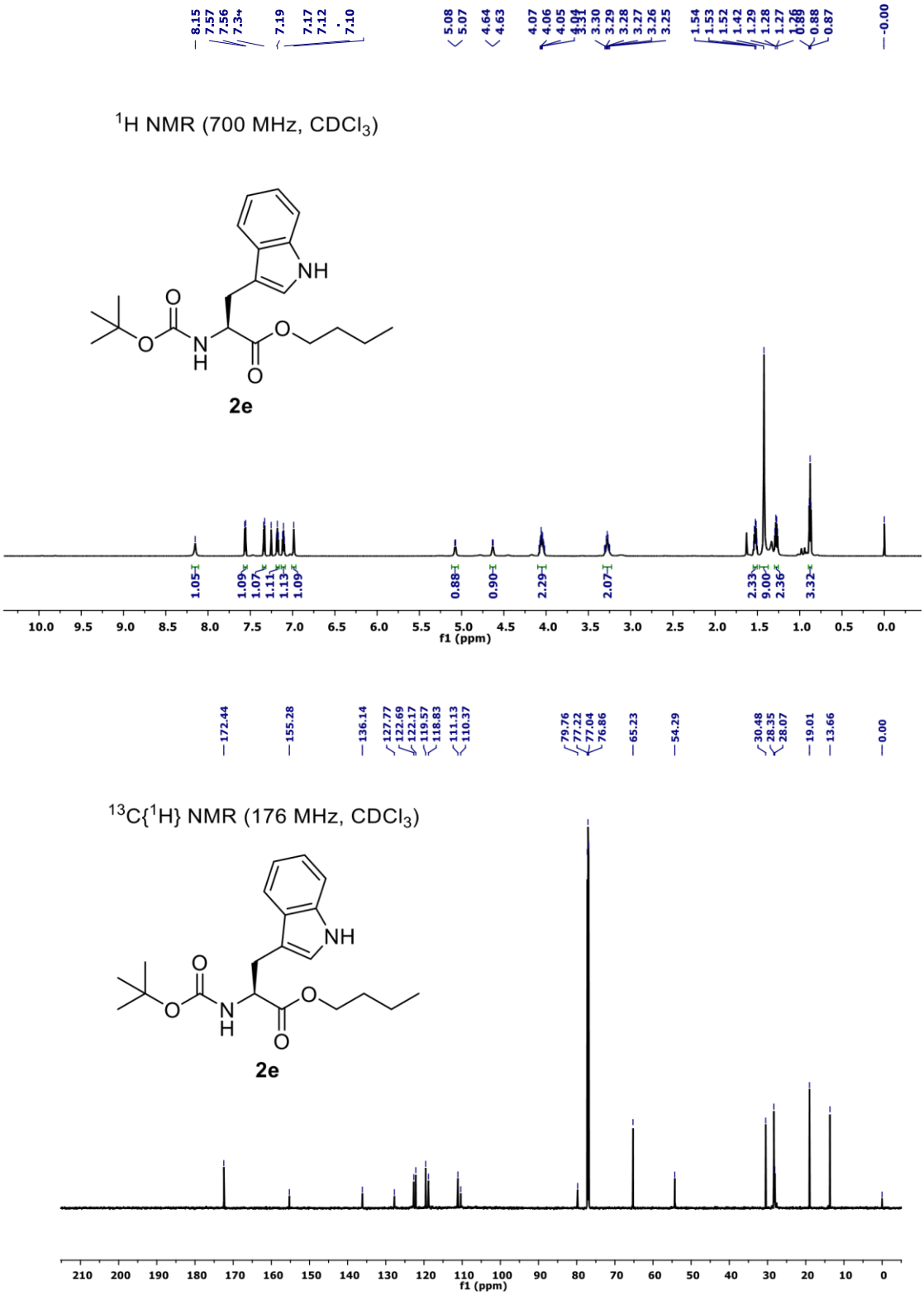

Fig S9. ^{1}H, ^{13}C $\{^{1}H\}$ NMR spectra of tryptophan derivative **2e**.

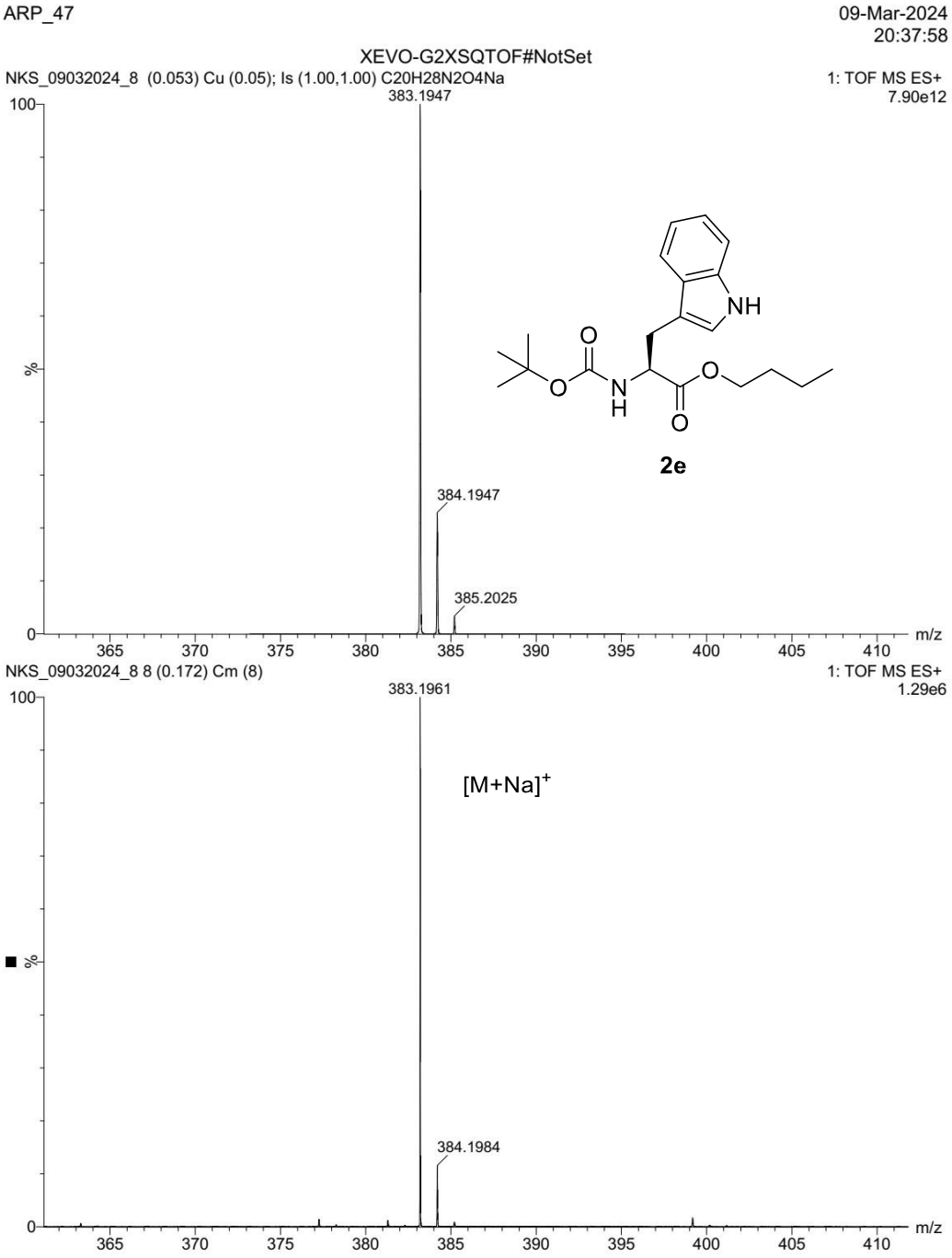

Fig S10. ESI-HRMS spectra of tryptophan derivative **2e**.

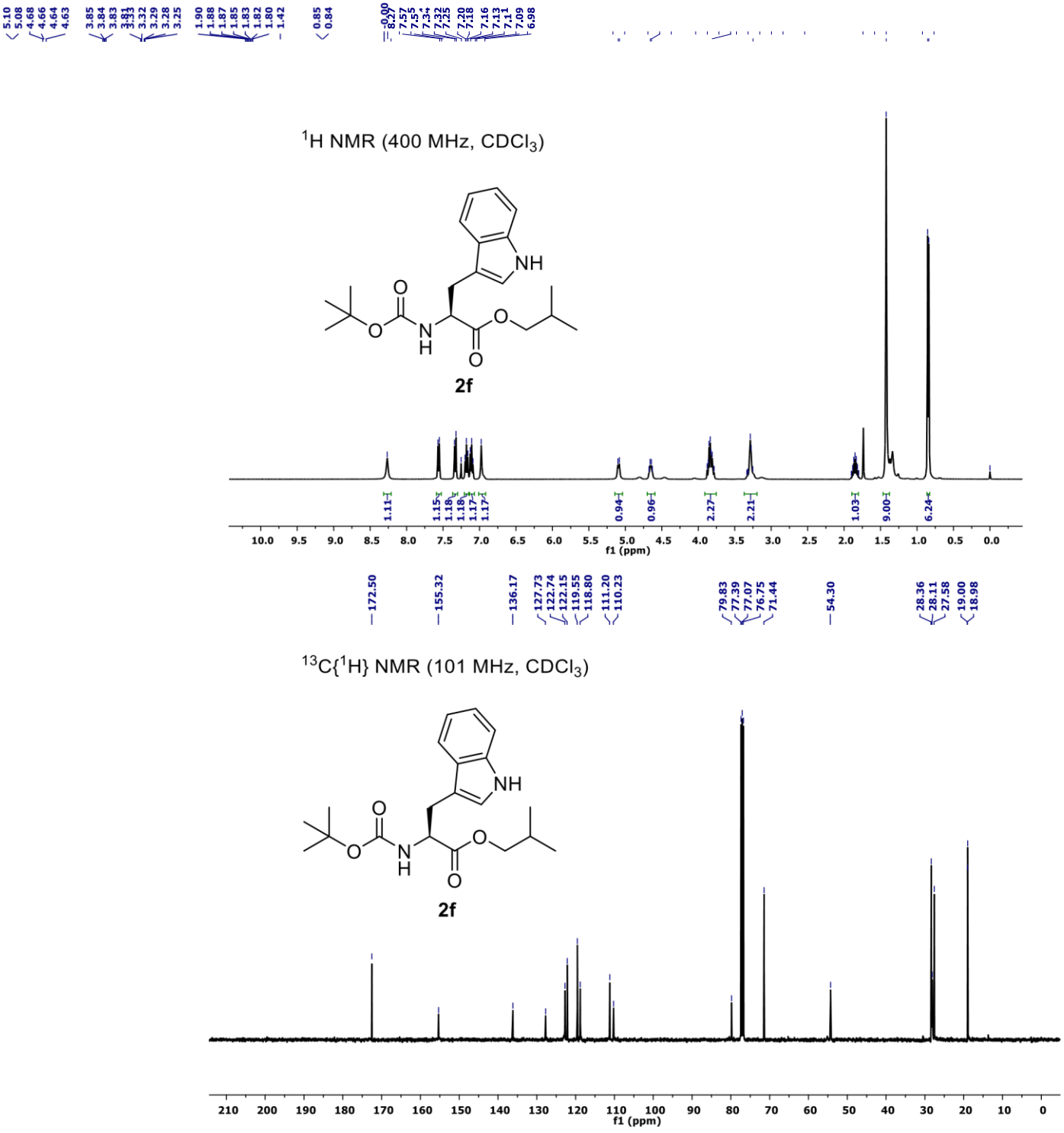

Fig S11. ^{1}H, ^{13}C {^{1}H} NMR spectra of tryptophan derivative **2f**.

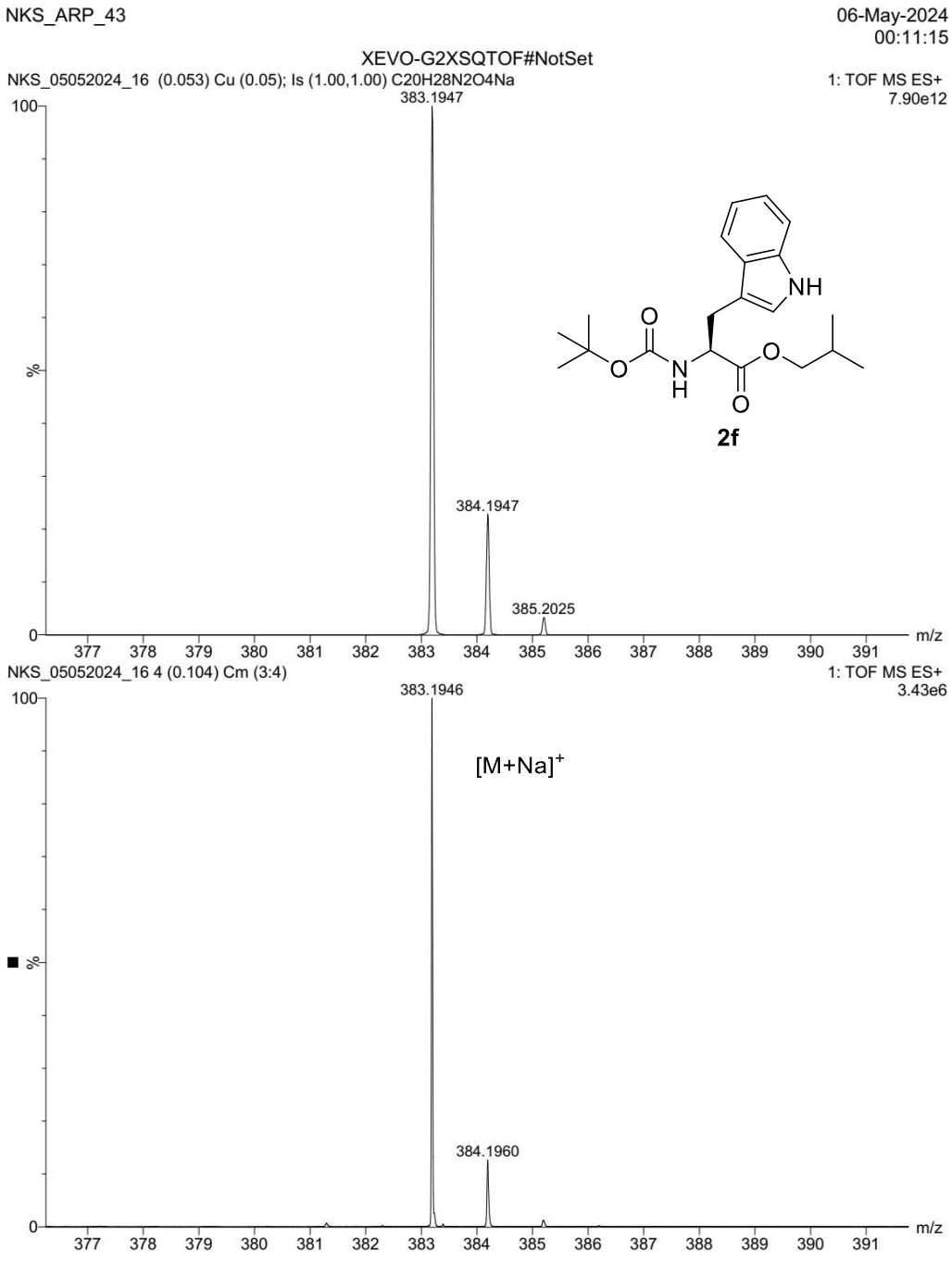

Fig S12. ESI-HRMS spectra of tryptophan derivative **2f**.

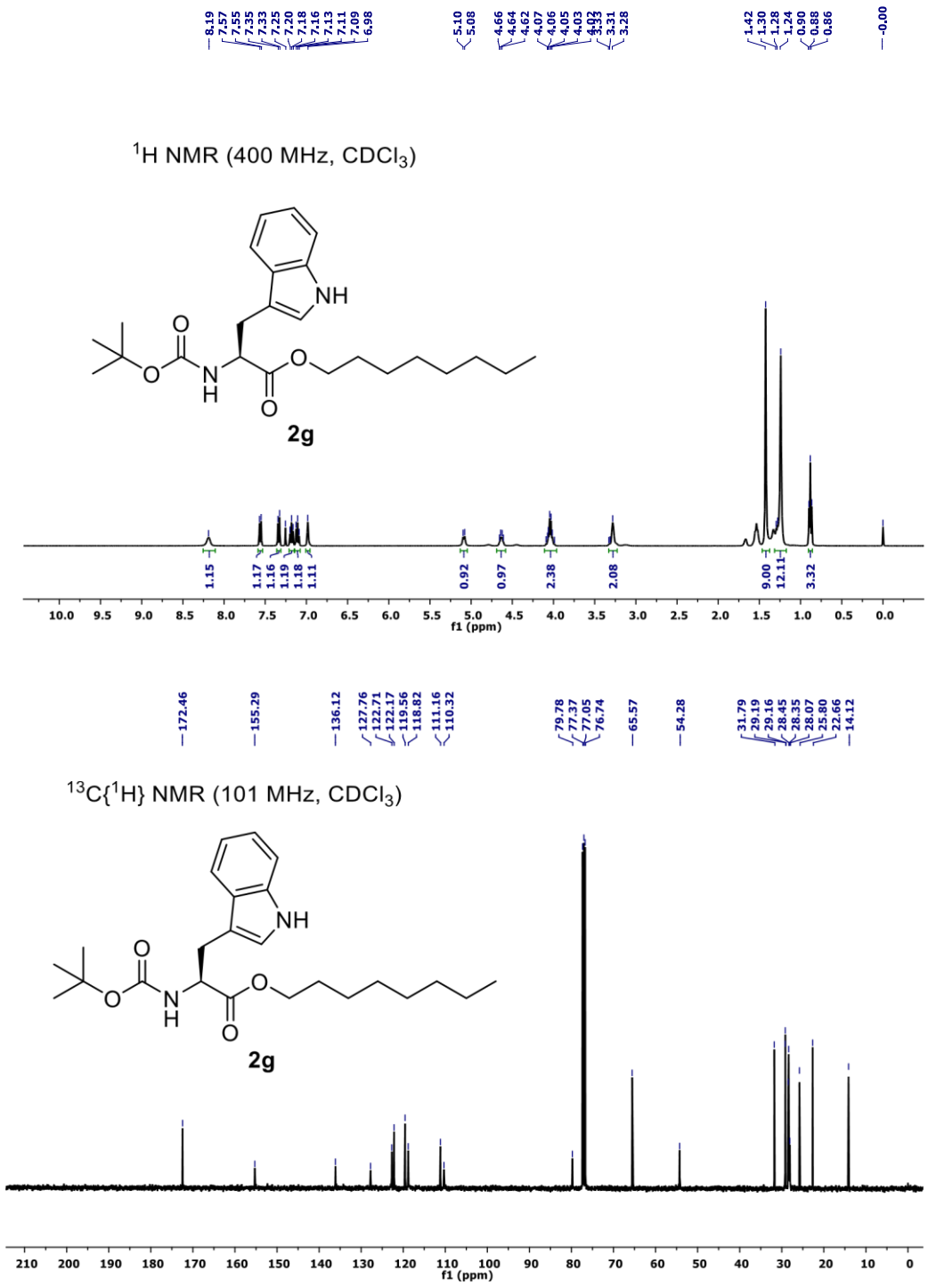

Fig S13. ^{1}H, ^{13}C $\{^{1}H\}$ NMR spectra of tryptophan derivative **2g**.

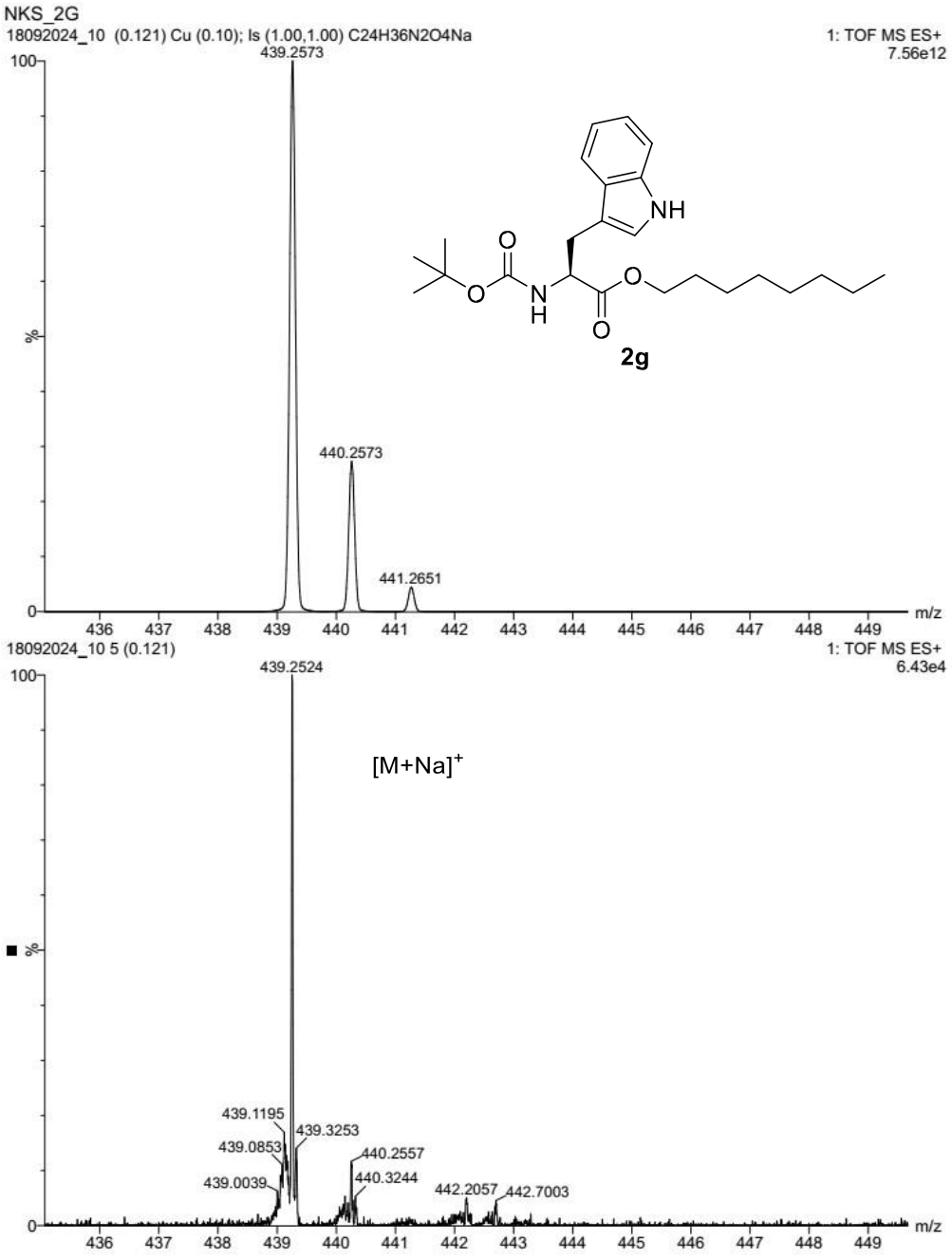

Fig S14. ESI-HRMS spectra of tryptophan derivative **2g**.


57
5

^{1}H NMR (400 MHz, $CDCl_3$)

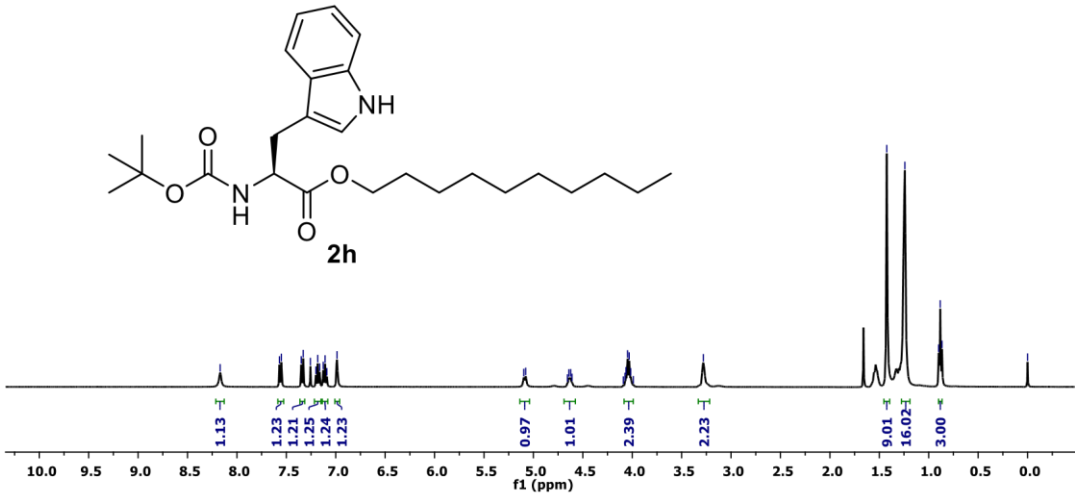

^{13}C{^{1}H} NMR (101 MHz, $CDCl_3$)

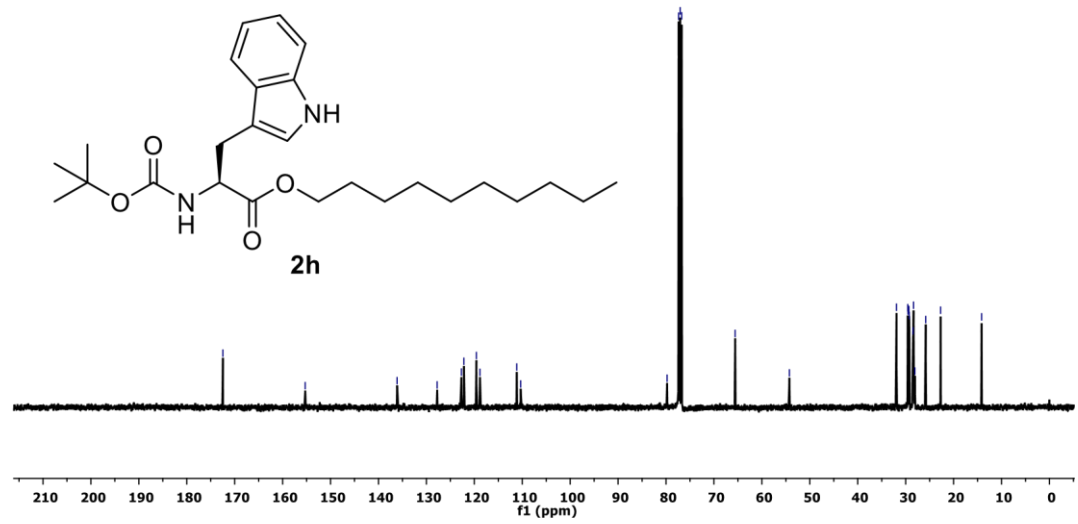

Fig S15. ^{1}H, ^{13}C $\{^{1}H\}$ NMR spectra of tryptophan derivative **2h**.

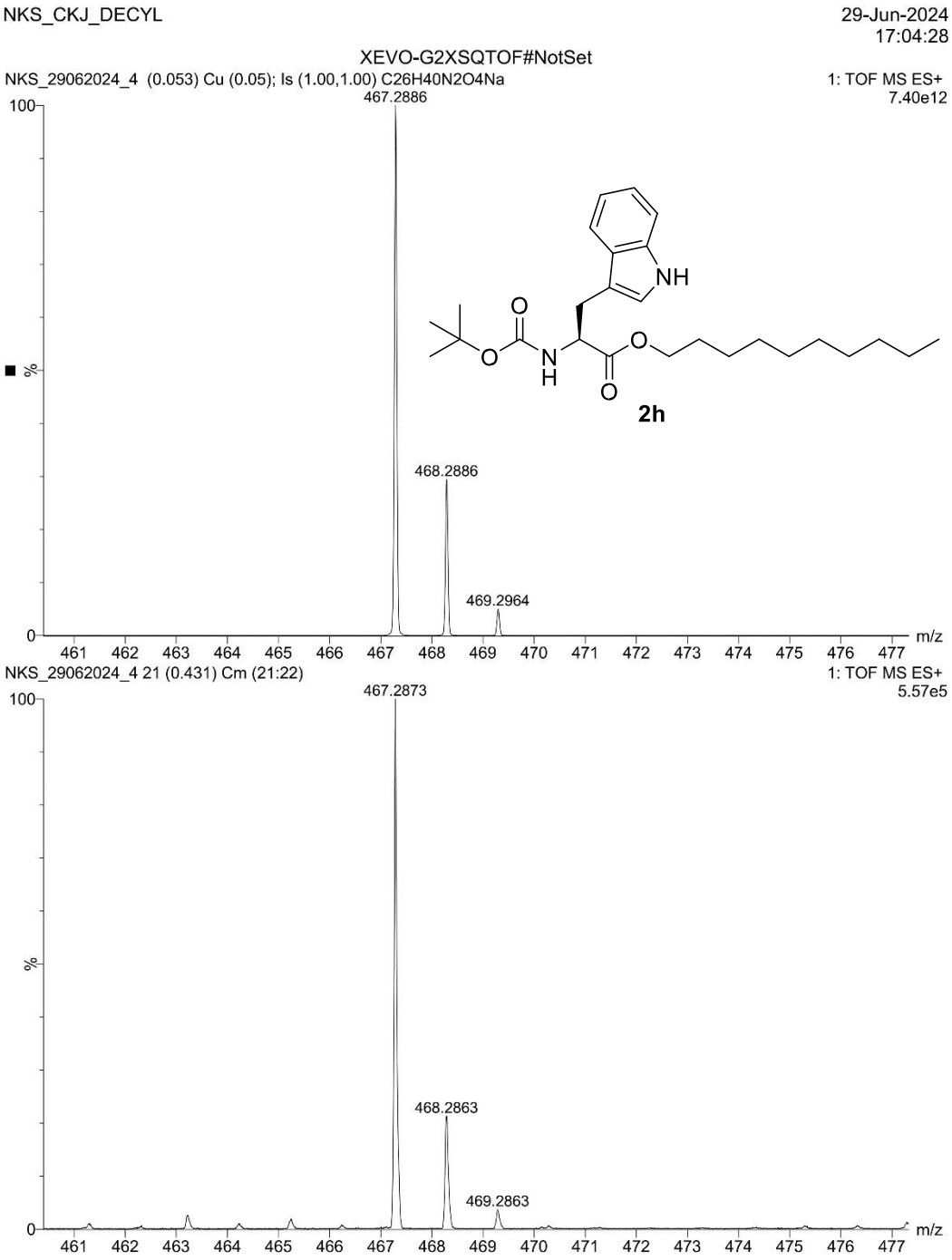

Fig S16. ESI-HRMS spectra of tryptophan derivative **2h**.

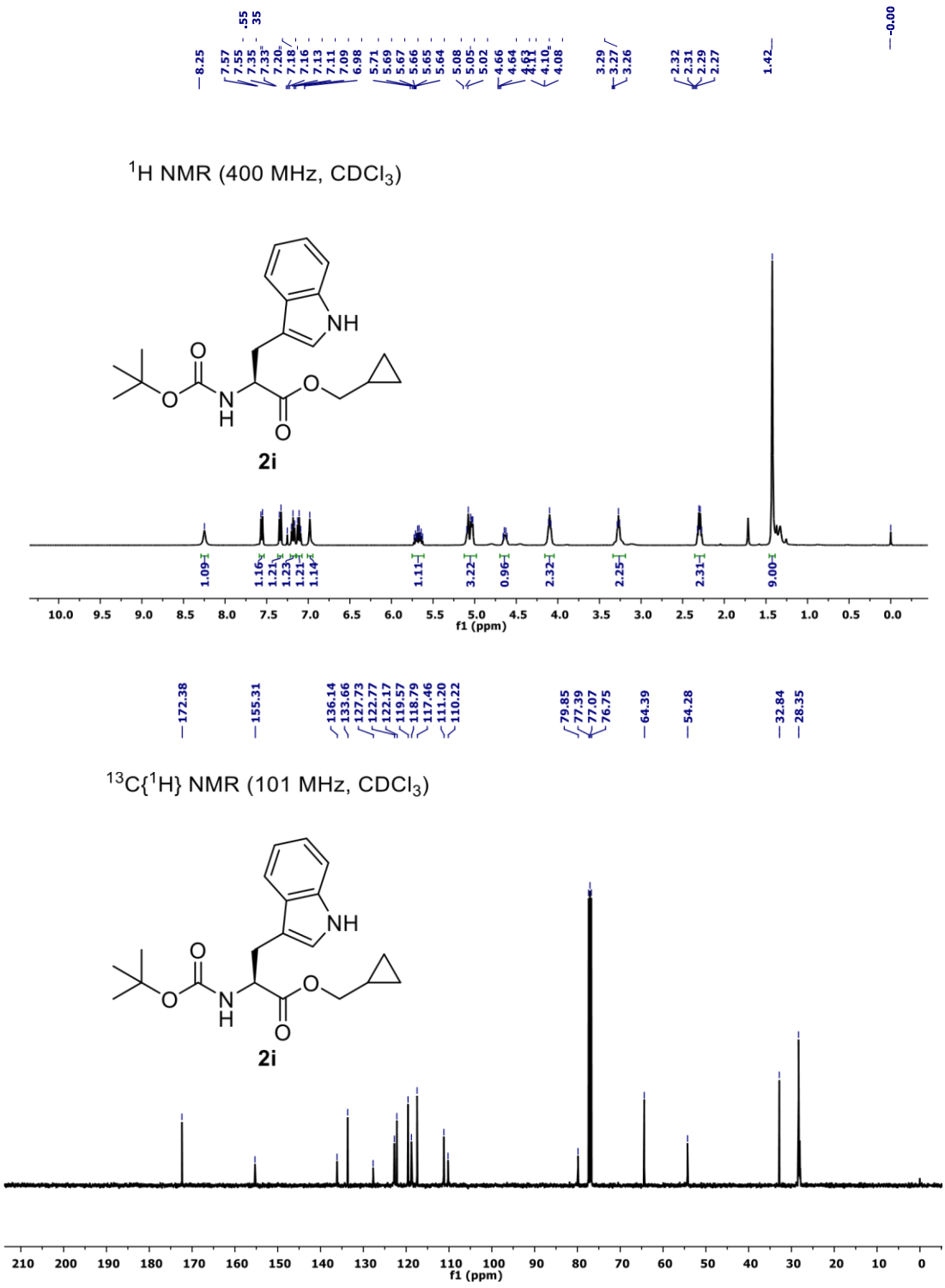

Fig S17. ^{1}H, ^{13}C $\{^{1}H\}$ NMR spectra of tryptophan derivative **2i**.

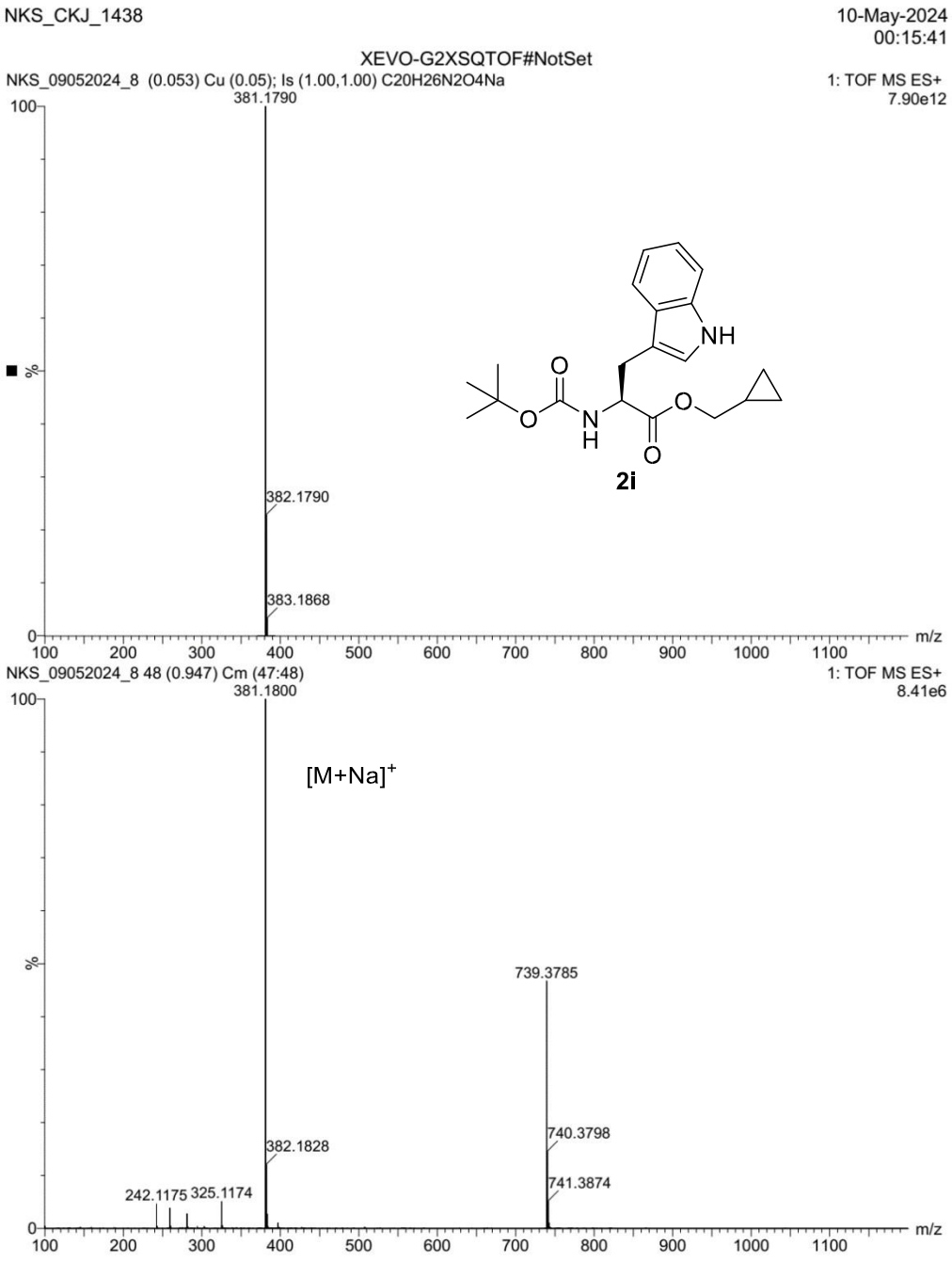

Fig S18. ESI-HRMS spectra of tryptophan derivative **2i**.

^{1}H NMR (400 MHz, $CDCl_3$)

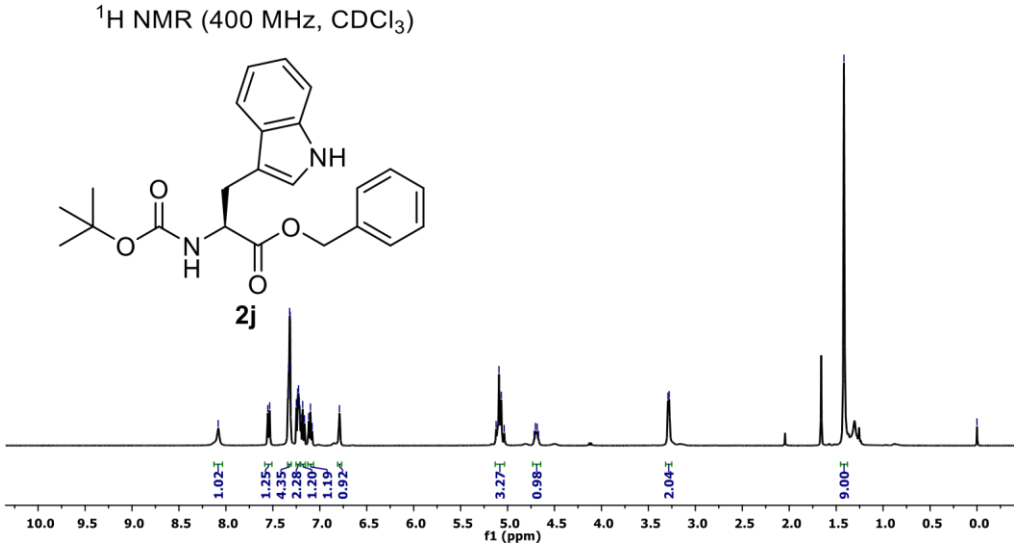

$^{13}C\{^{1}H\}$ NMR (101 MHz, $CDCl_3$)

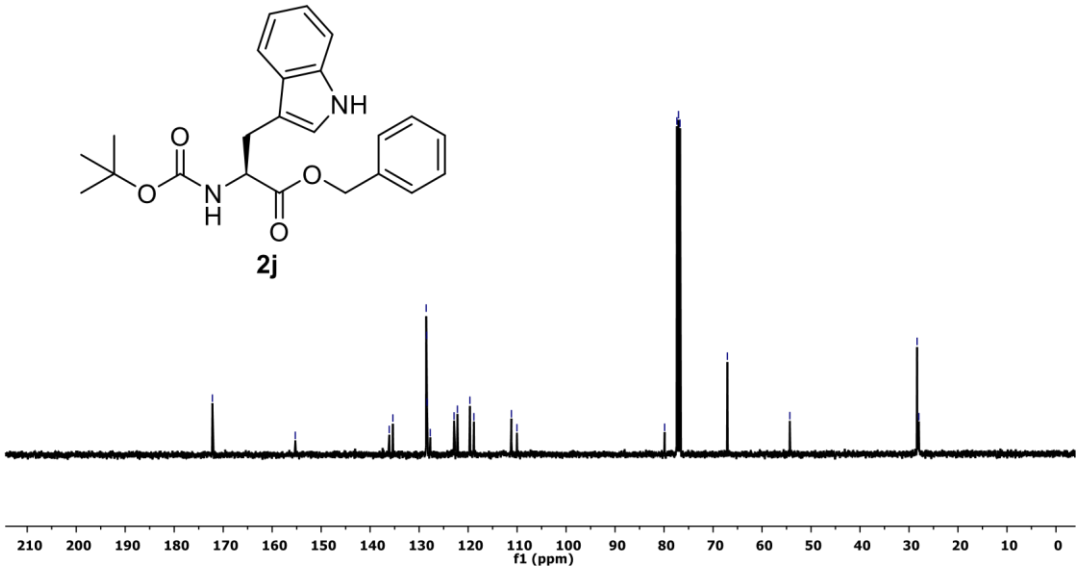

Fig S19. ^{1}H, ^{13}C $\{^{1}H\}$ NMR spectra of tryptophan derivative **2j**.

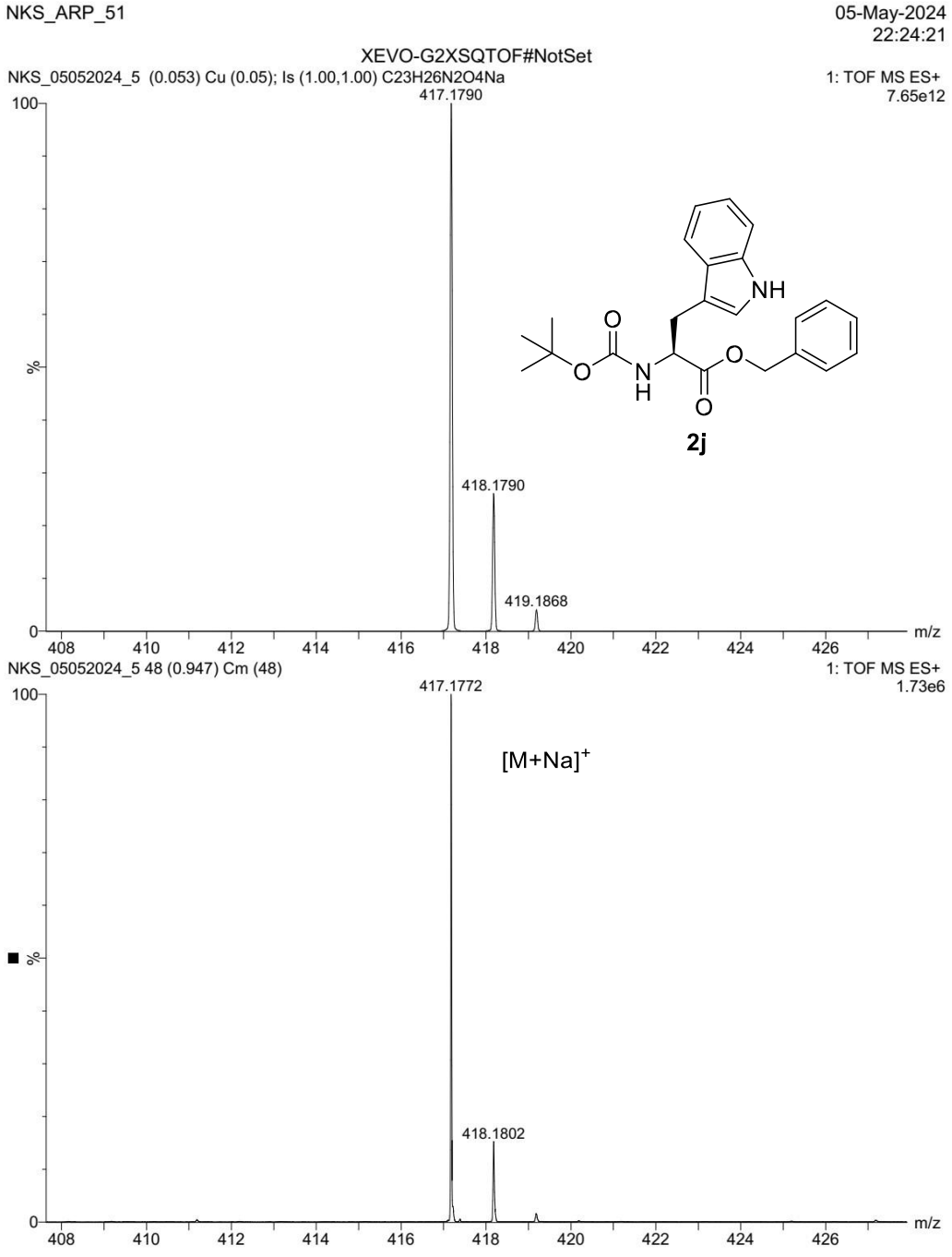

Fig S20. ESI-HRMS spectra of tryptophan derivative **2j**.

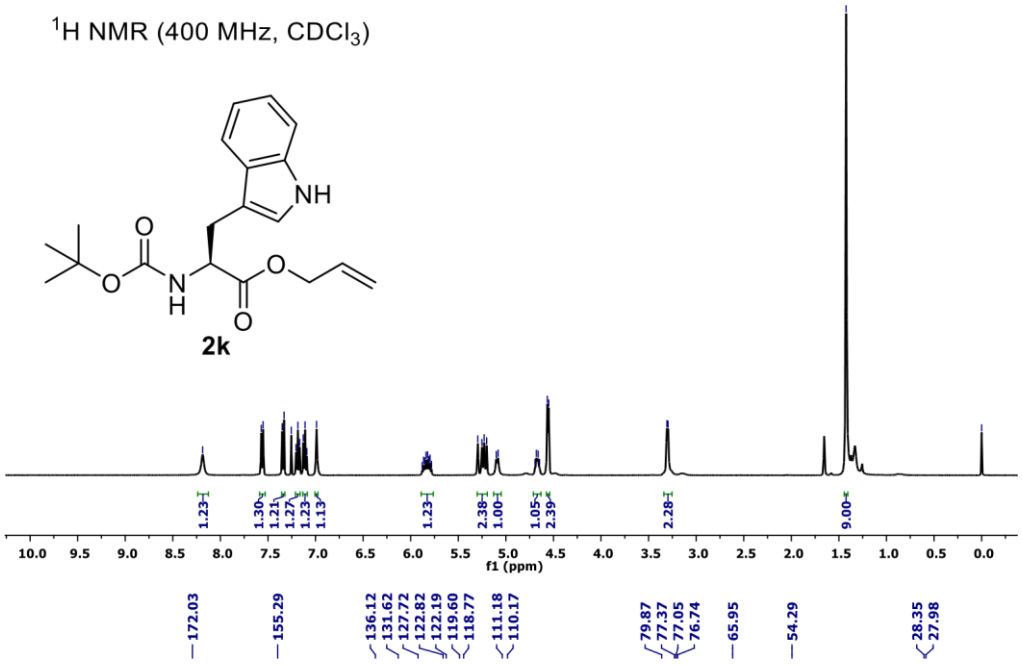

Fig ^{1}H, ^{13}C $\{^{1}H\}$ NMR spectra of tryptophan derivative

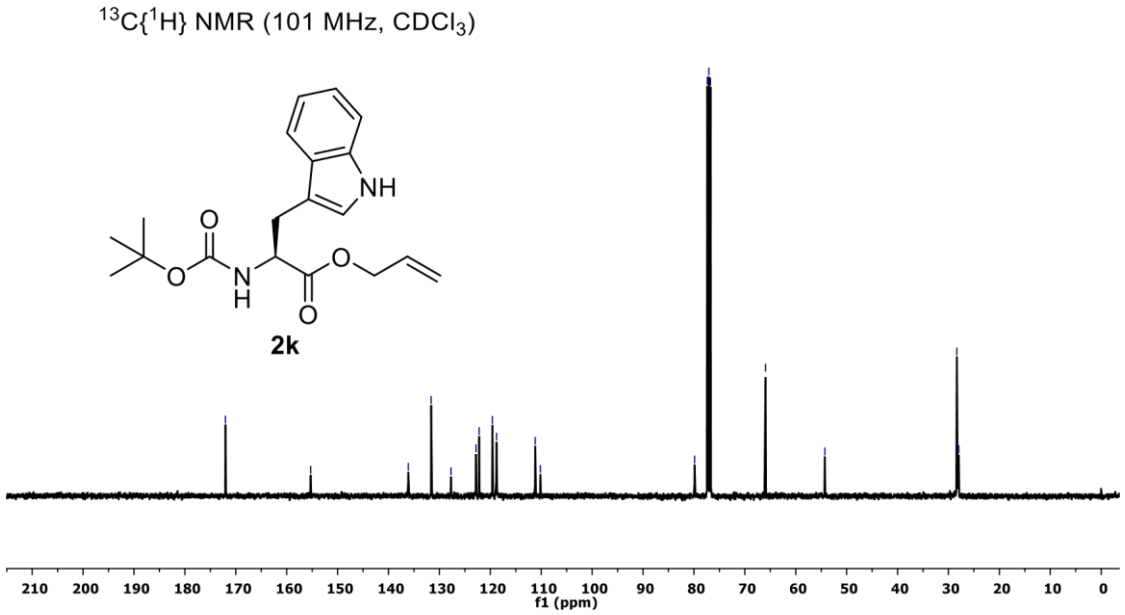
$^{13}C\{^{1}H\}$ NMR (101 MHz, $CDCl_3$)
NH
O
O
N
H
O
O
2k
210 200 190 180 170 160 150 140 130 120 110 100 90 80 70 60 50 40 30 20 10 0
f1 (ppm)

S21. **2k**.

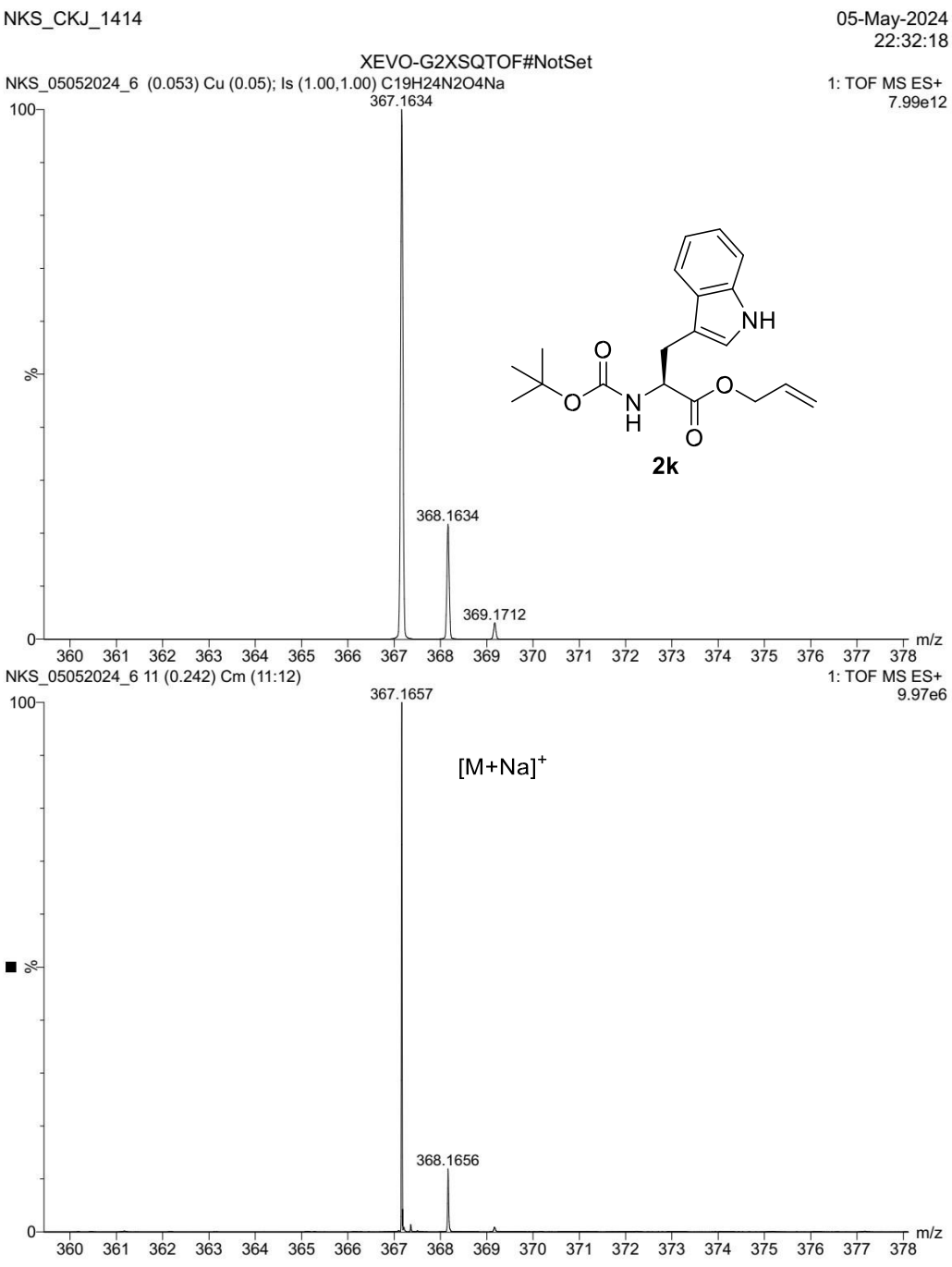
NKS_CKJ_1414
05-May-2024
22:32:18
XEVO-G2XSQTOF#NotSet
NKS_05052024_6 (0.053) Cu (0.05); Is (1.00,1.00) C19H24N2O4Na
1: TOF MS ES+
7.99e12
367.1634
368.1634
369.1712
2k
NKS_05052024_6 11 (0.242) Cm (11:12)
1: TOF MS ES+
9.97e6
367.1657
[M+Na]+
368.1656
m/z

Fig

Fig S22. ESI-HRMS spectra of tryptophan derivative **2k**.

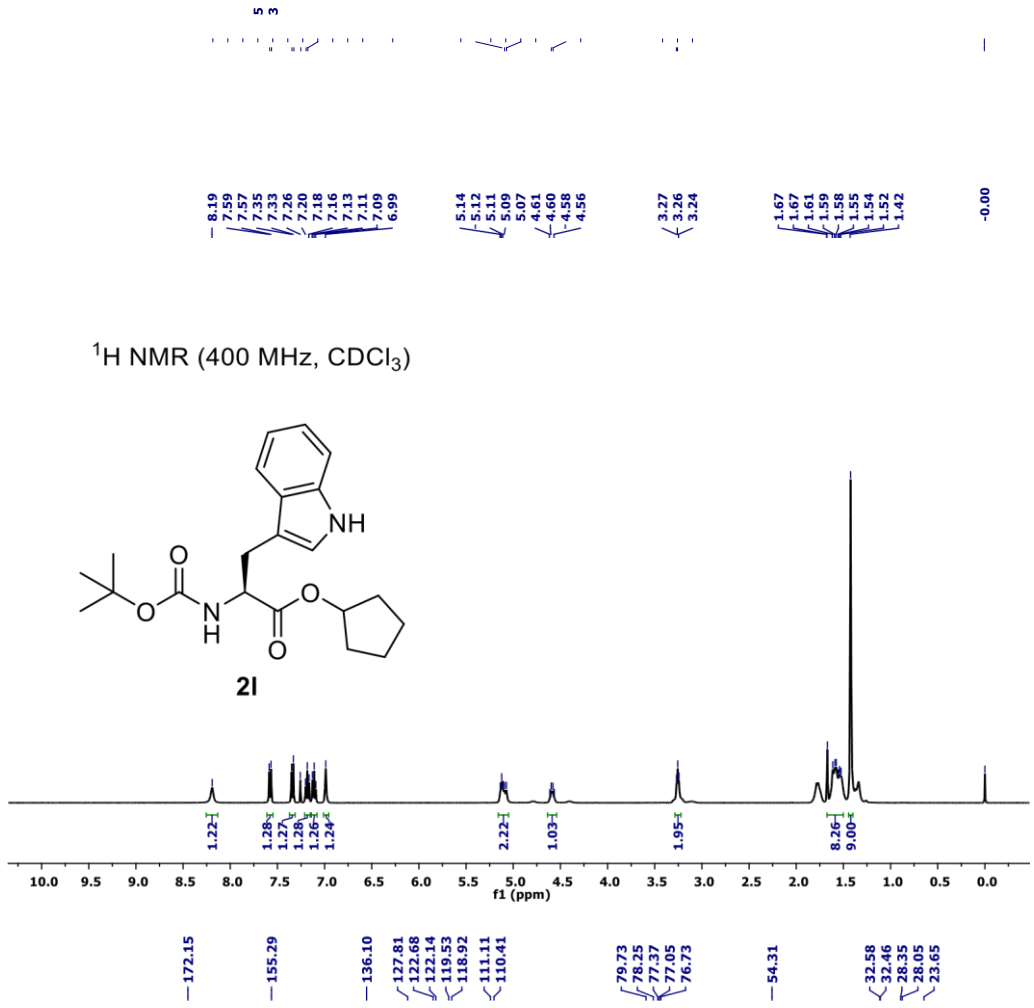

Fig ^{1}H, ^{13}C {^{1}H} NMR spectra of tryptophan derivative

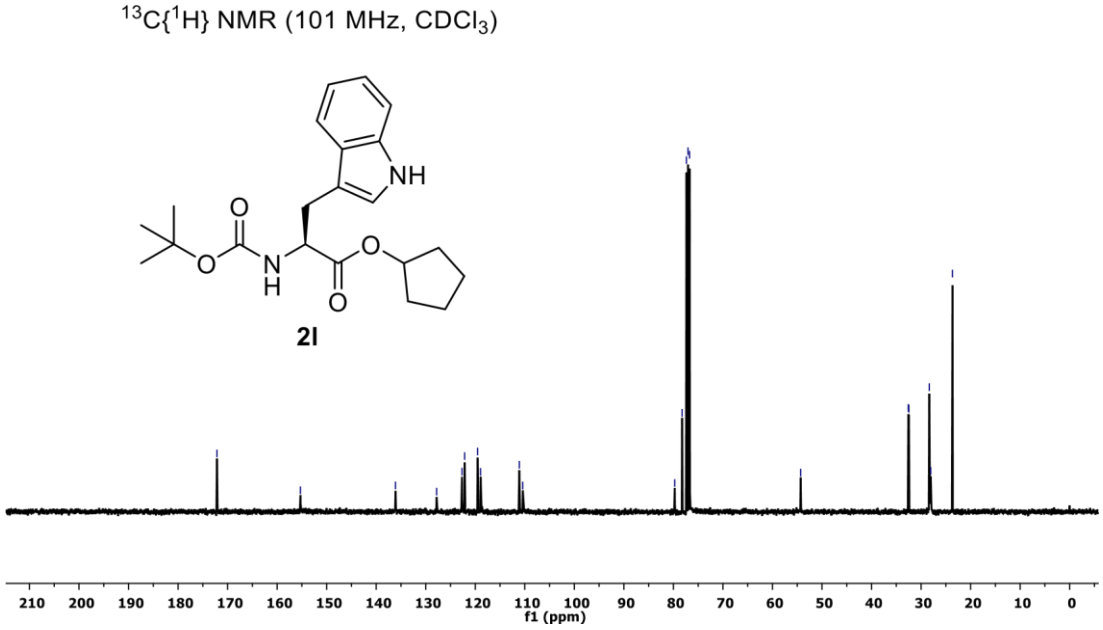
$^{13}C\{^{1}H\}$ NMR (101 MHz, $CDCl_3$)
NH
O
O
N
H
O
O
2l
210 200 190 180 170 160 150 140 130 120 110 100 90 80 70 60 50 40 30 20 10 0
f1 (ppm)

S23. **2l**.

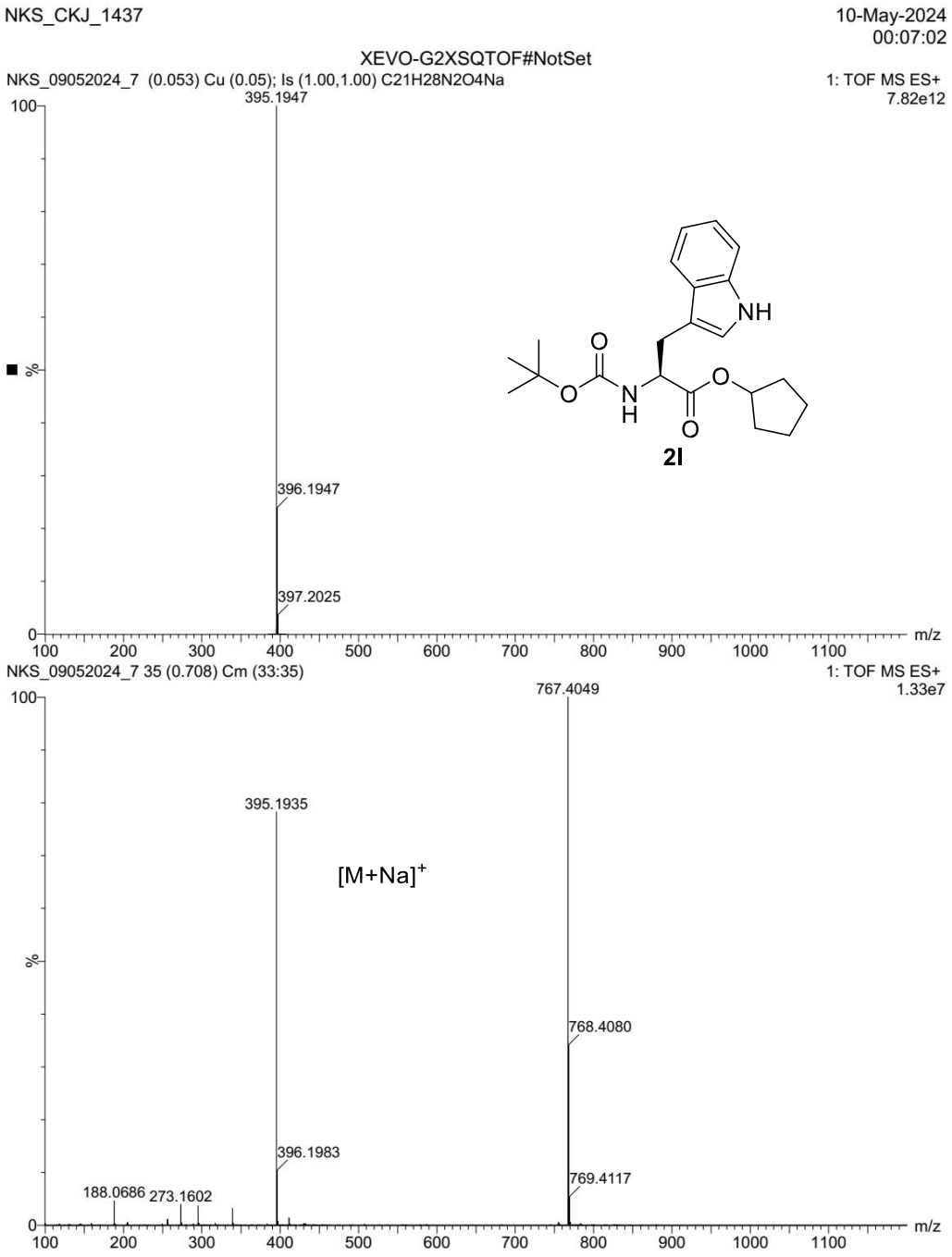

Fig H, ^{13}C{^{1}H} NMR spectra of tryptophan derivative

Fig S24. ESI-HRMS spectra of tryptophan derivative **2l**.

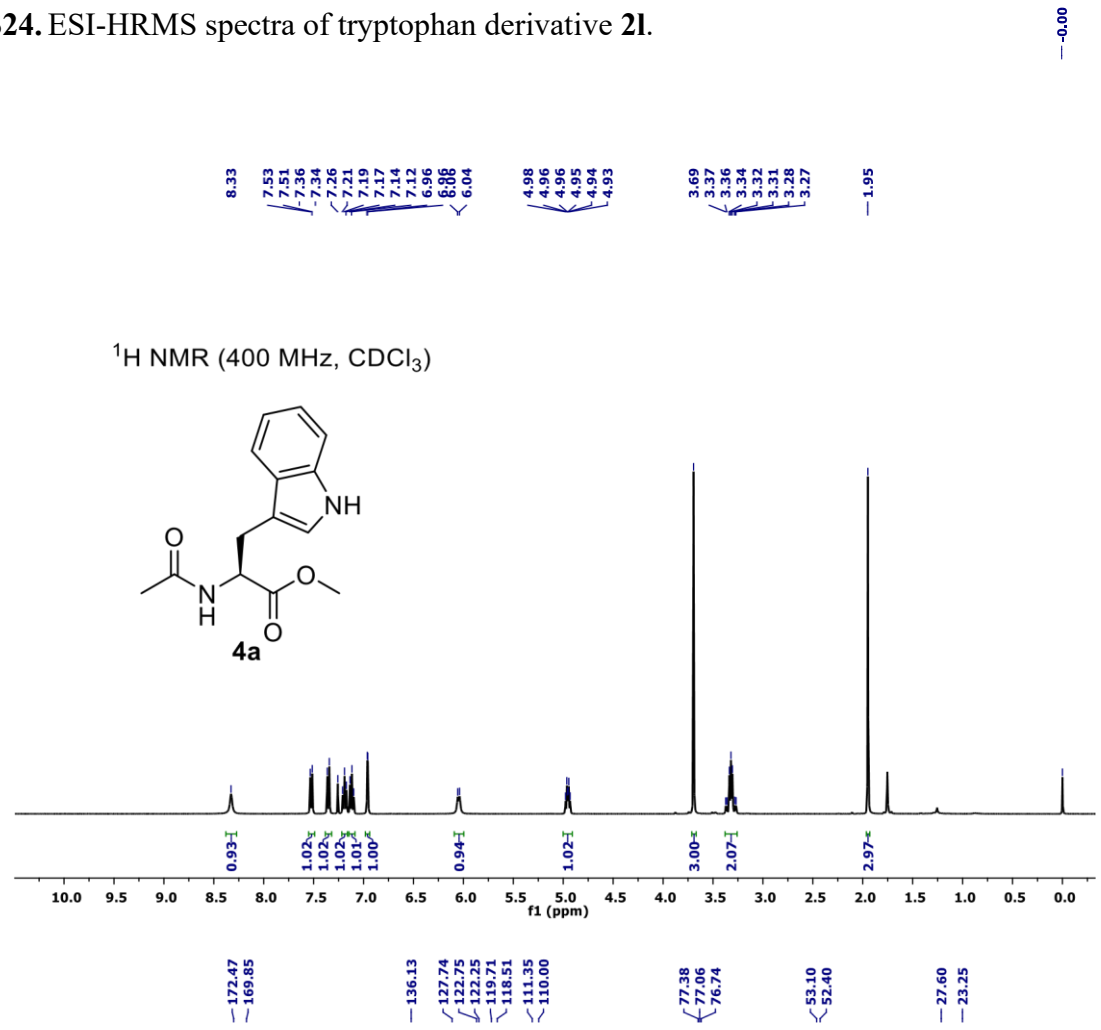

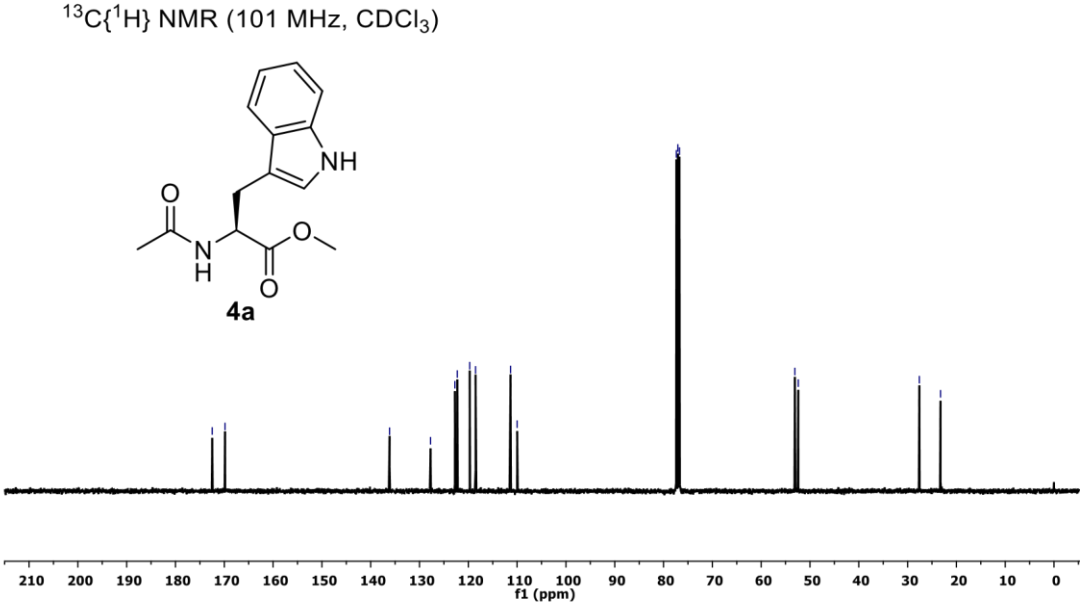

S25. **4a**.

Fig ^{1}H, ^{13}C $\{^{1}H\}$ NMR spectra of tryptophan derivative

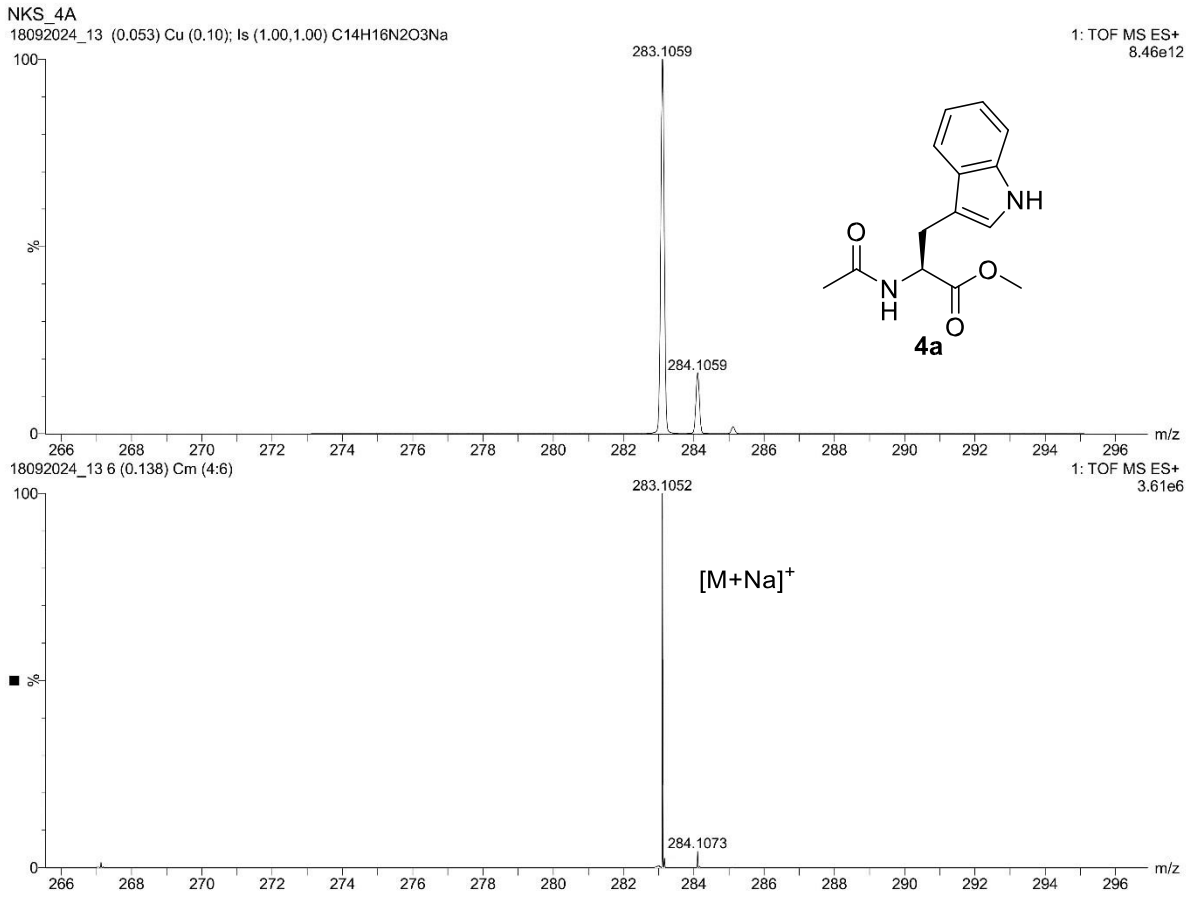

Fig S26. ESI-HRMS spectra of tryptophan derivative **4a**.

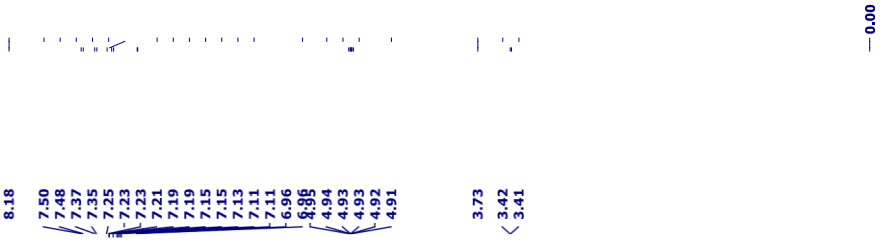

^{1}H NMR (400 MHz, $CDCl_3$)

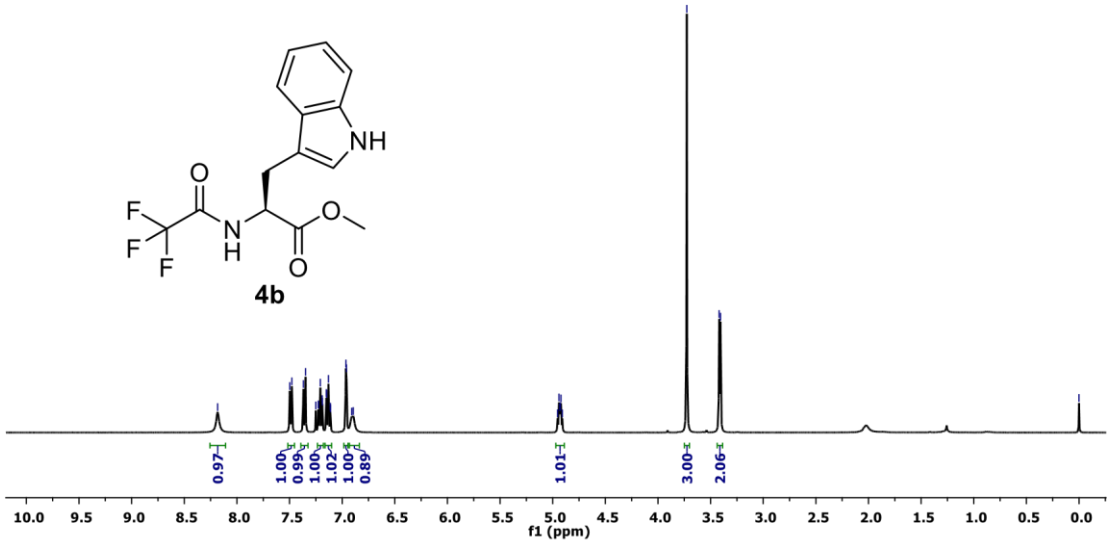

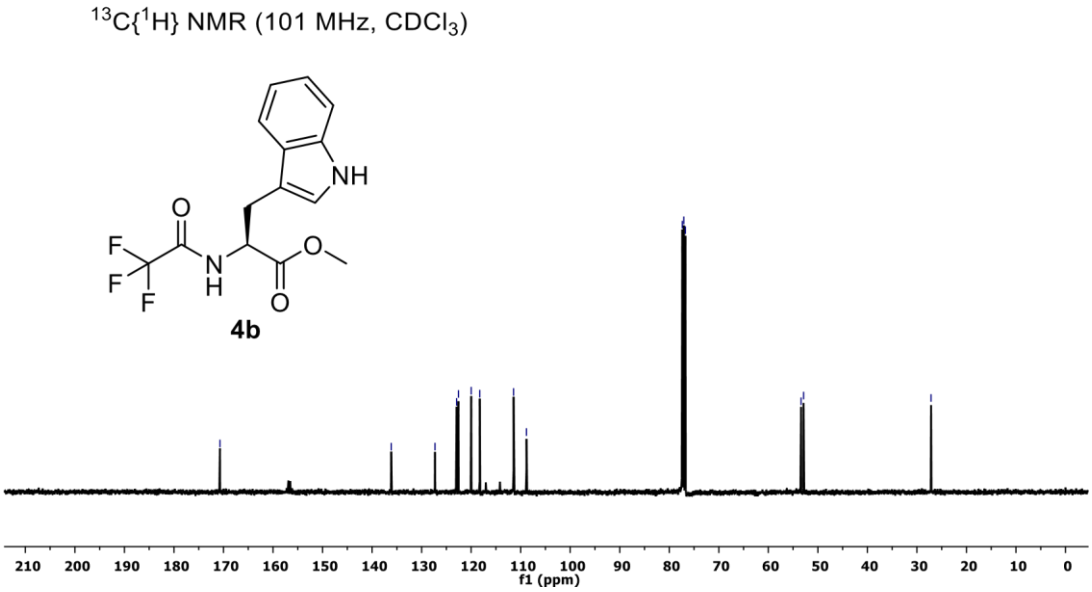

Fig S27. ^{1}H, ^{13}C $\{^{1}H\}$ NMR spectra of tryptophan derivative **4b**.

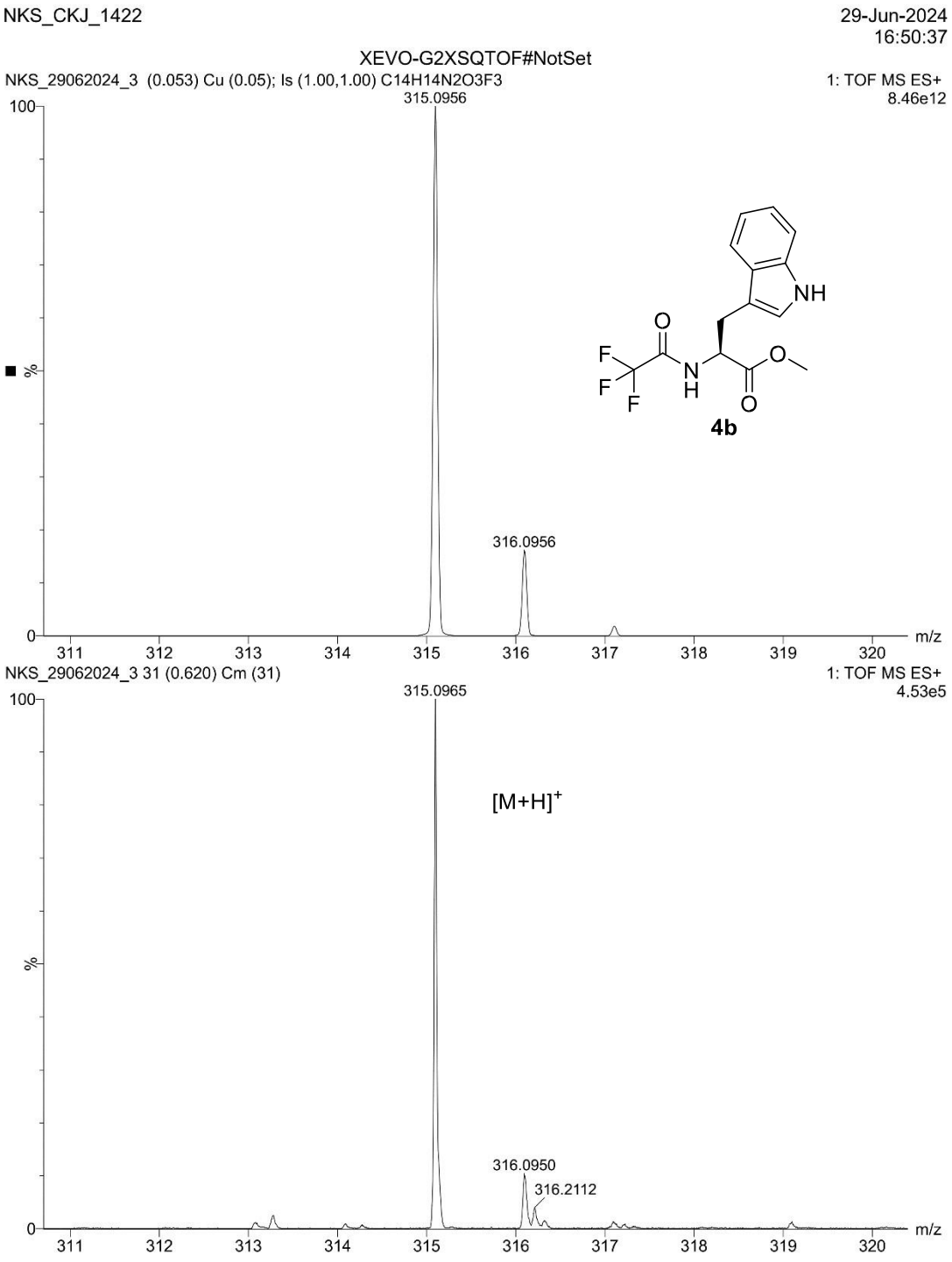

Fig S28. ESI-HRMS spectra of tryptophan derivative **4b**.

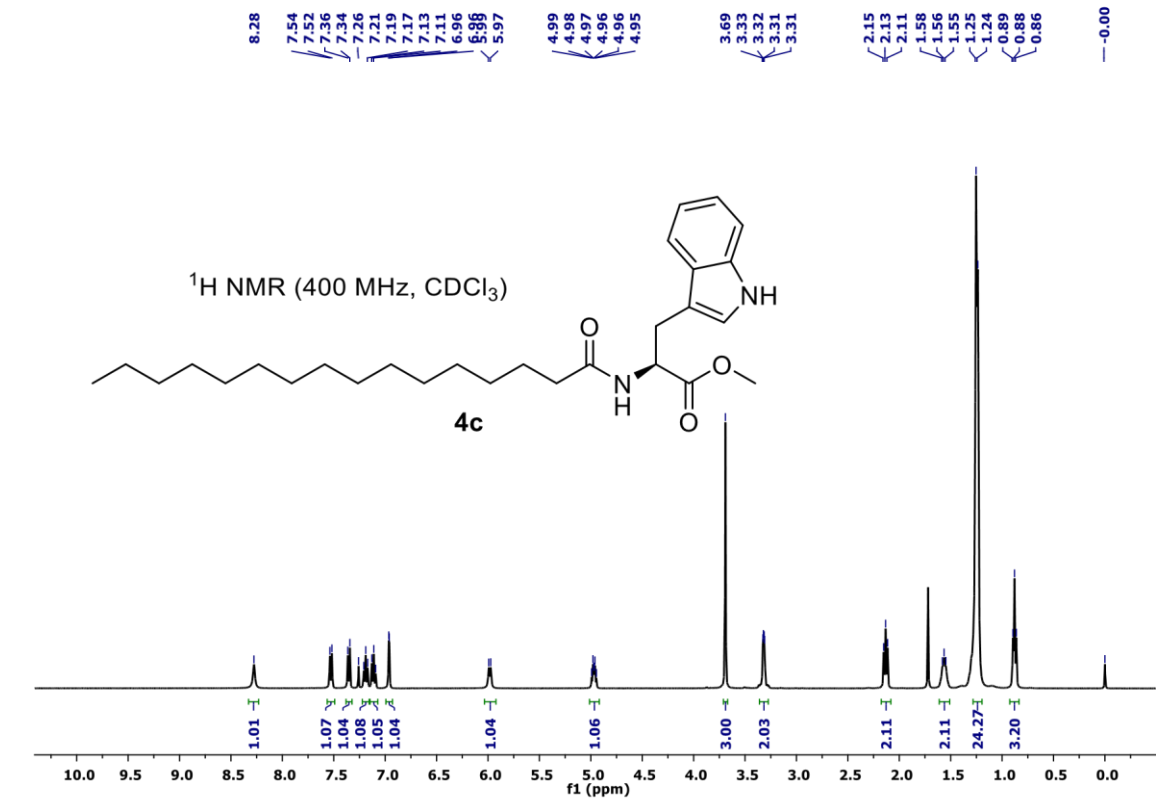
^{1}H NMR (400 MHz, CDCl$_3$)
4c
f1 (ppm)

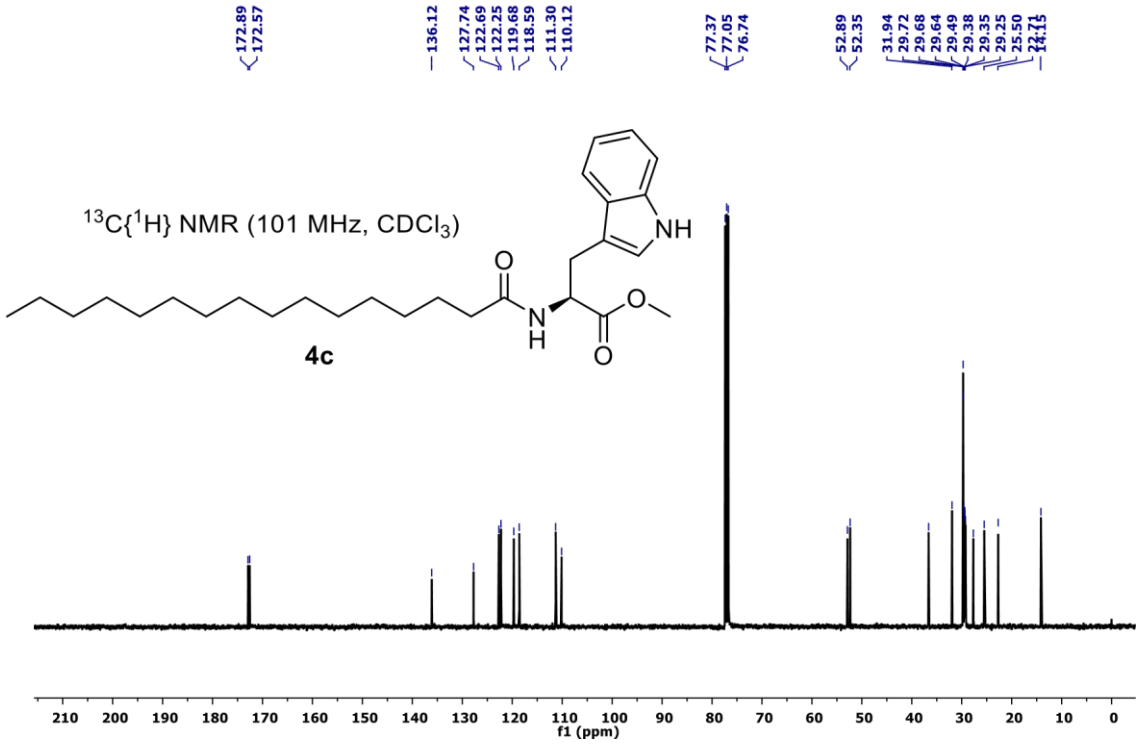
^{13}C{^{1}H} NMR (101 MHz, CDCl$_3$)
4c
f1 (ppm)

Fig S29. ^{1}H, ^{13}C $\{^{1}H\}$ NMR spectra of tryptophan derivative **4c**.

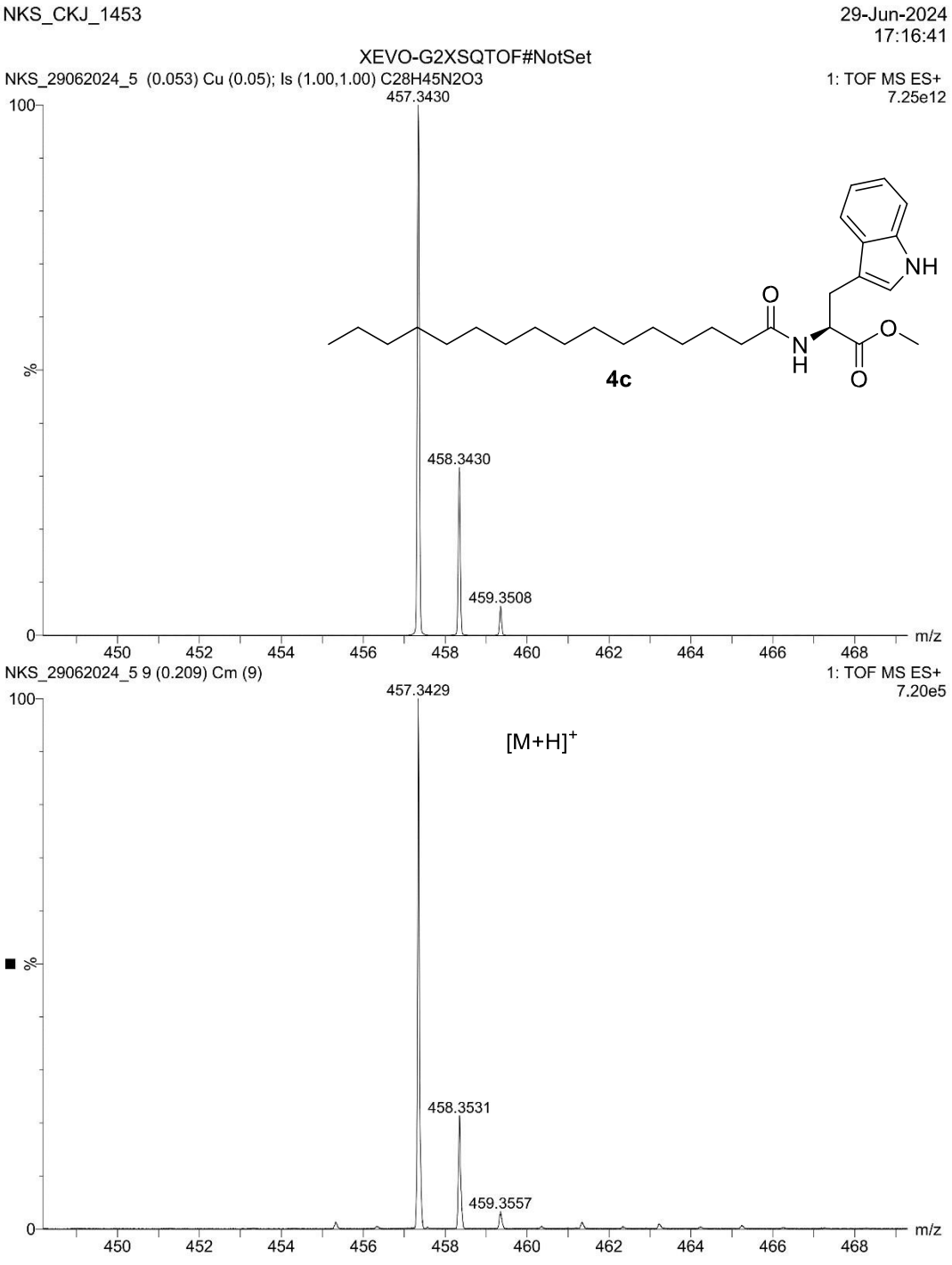

Fig S30. ESI-HRMS spectra of tryptophan derivative **4c**.

8.15
7.59
7.58
7.58
7.57
7.21
7.19
7.10
7.08
7.06
7.04
7.02
7.00
6.94
6.94
5.28
5.26
5.25
5.24
4.27
4.26
4.26
4.24
4.24
4.23
3.74
3.73
3.72

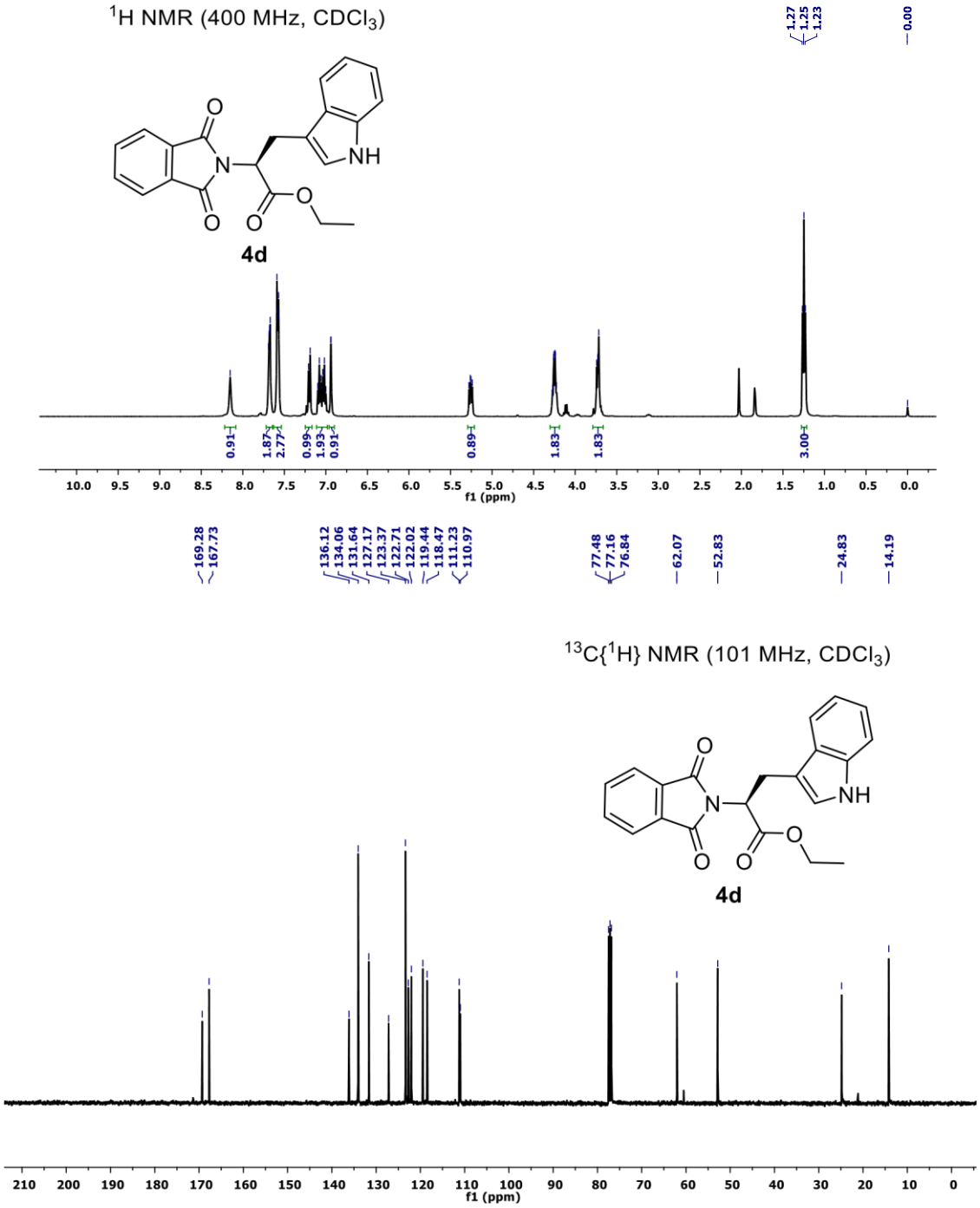

Fig S31. ^{1}H, ^{13}C $\{^{1}H\}$ NMR spectra of tryptophan derivative **4d**.

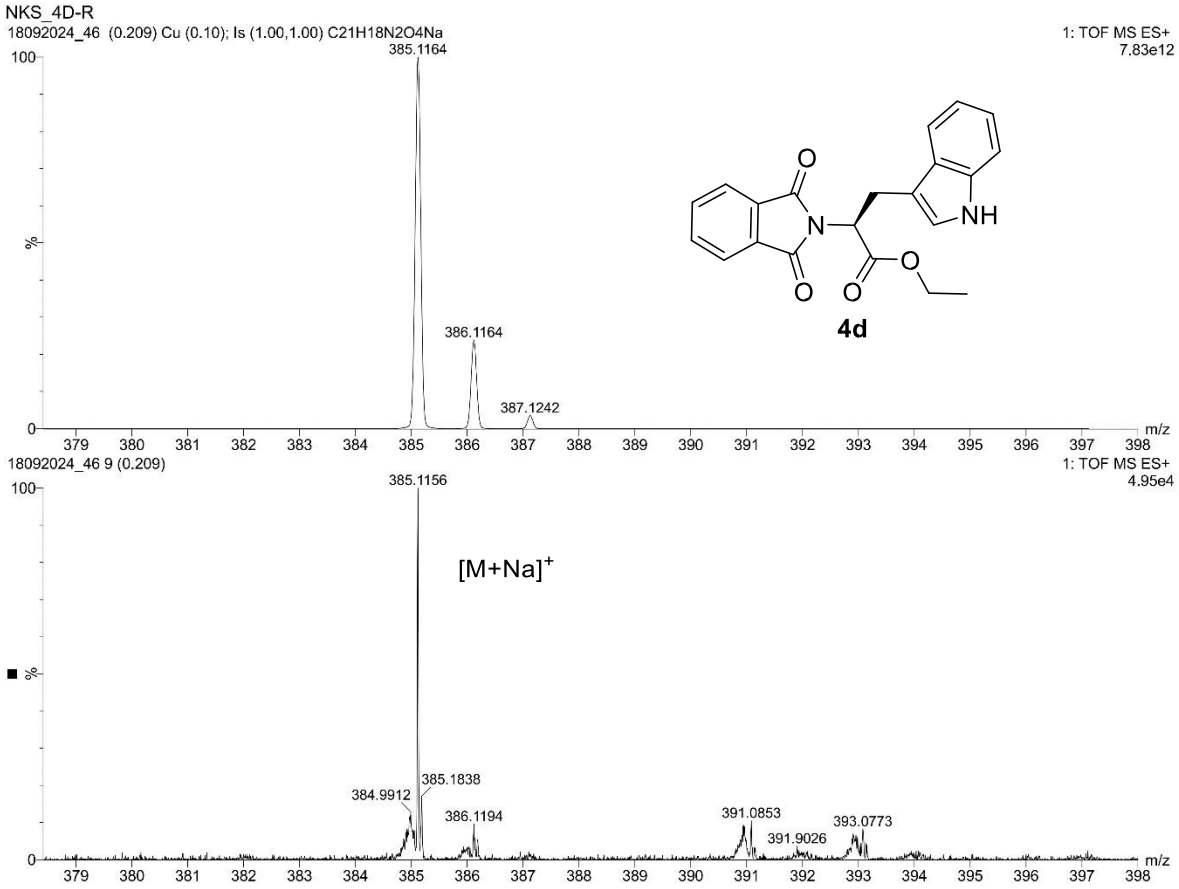

Fig S32. ESI-HRMS spectra of tryptophan derivative **4d**.

Fig ^{1}H, ^{13} H} NMR spectra of tryptophan derivative

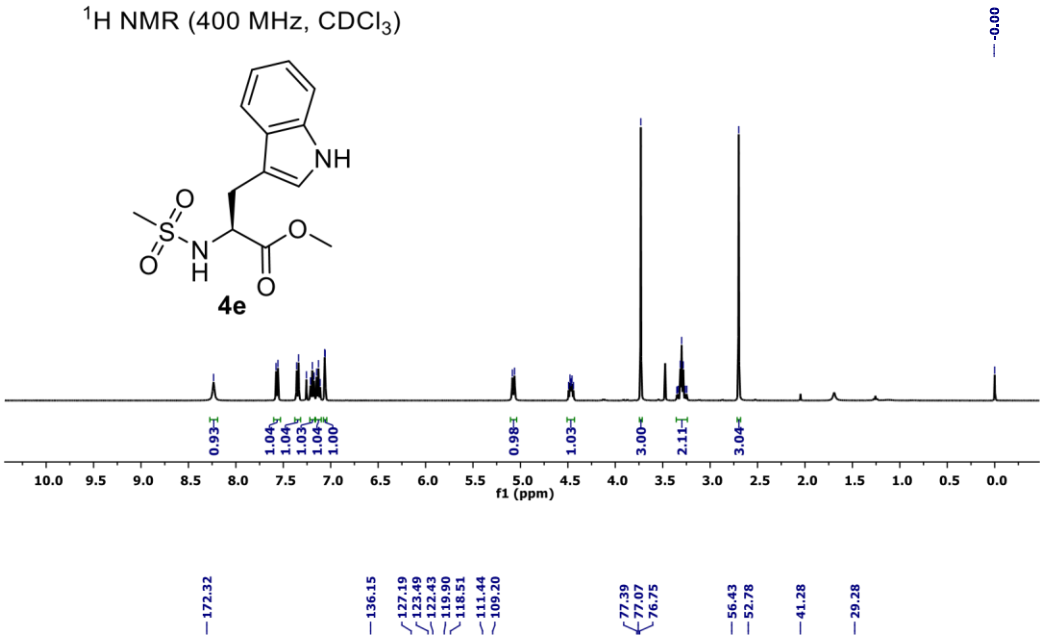
^{1}H NMR (400 MHz, CDCl$_3$)
4e
0.93
1.04
1.04
1.03
1.04
1.00
0.98
1.03
3.00
2.11
3.04
f1 (ppm)

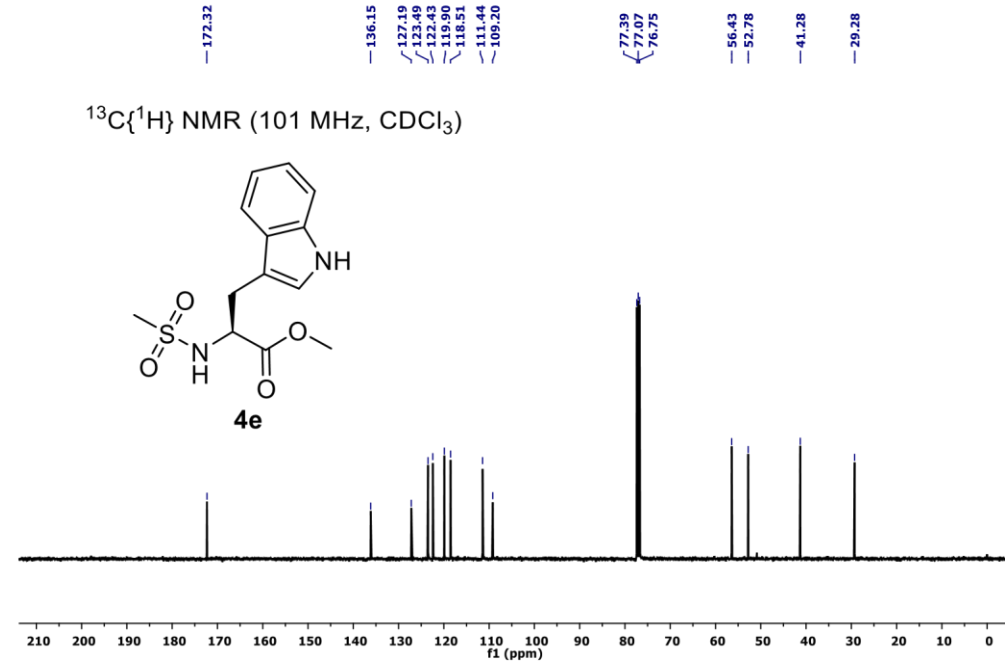
^{13}C{^{1}H} NMR (101 MHz, CDCl$_3$)
4e
172.32
136.15
127.19
123.49
122.43
119.90
118.51
111.44
109.20
77.39
77.07
76.75
56.43
52.78
41.28
29.28
f1 (ppm)

S33. C {^{1} **4e**.

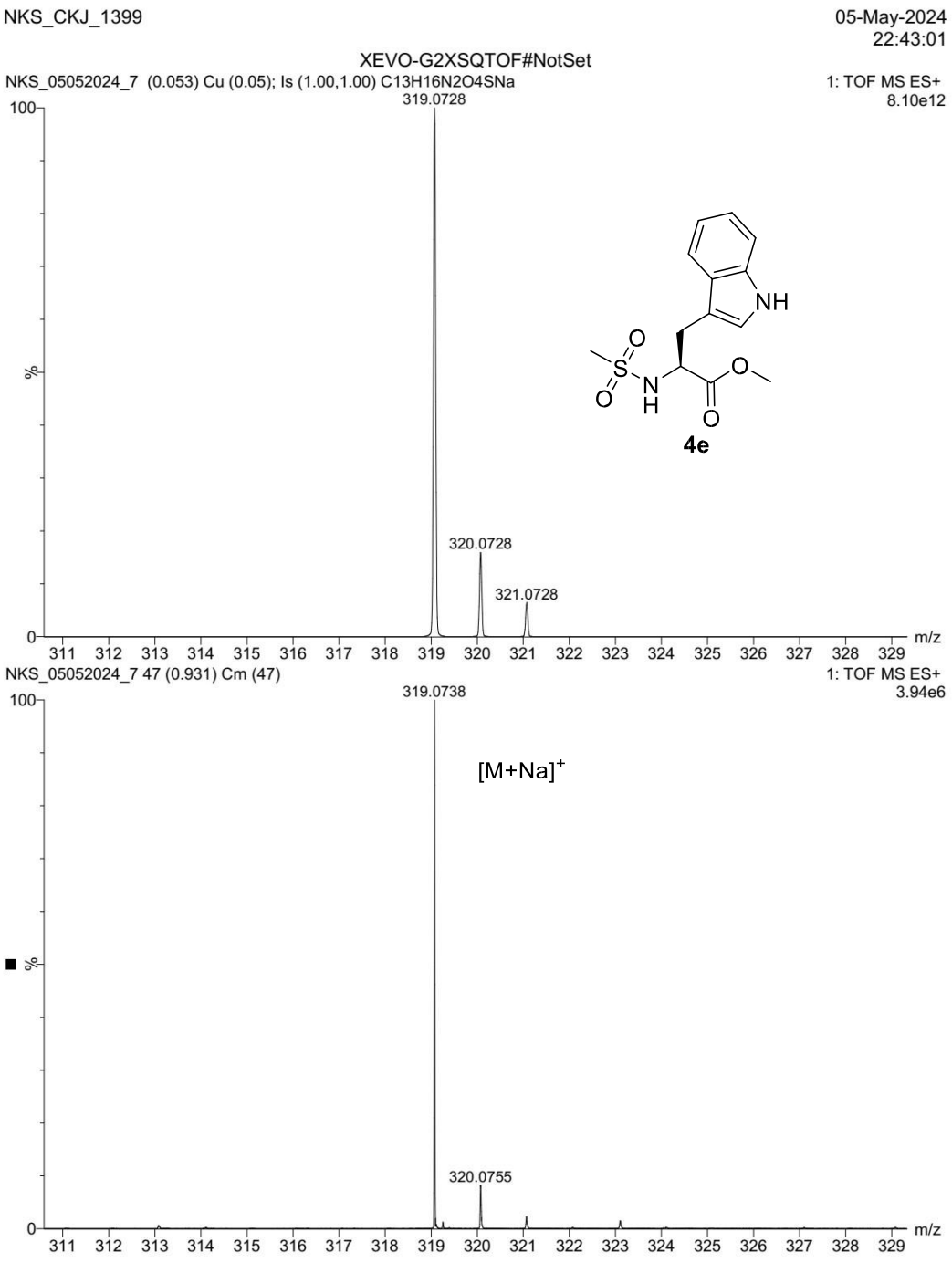
NKS_CKJ_1399
05-May-2024
22:43:01
XEVO-G2XSQTOF#NotSet
NKS_05052024_7 (0.053) Cu (0.05); Is (1.00,1.00) C13H16N2O4SNa
1: TOF MS ES+
8.10e12
319.0728
320.0728
321.0728
4e
NKS_05052024_7 47 (0.931) Cm (47)
1: TOF MS ES+
3.94e6
319.0738
[M+Na]+
320.0755
%
m/z

Fig

Fig S34. ESI-HRMS spectra of tryptophan derivative **4e**.

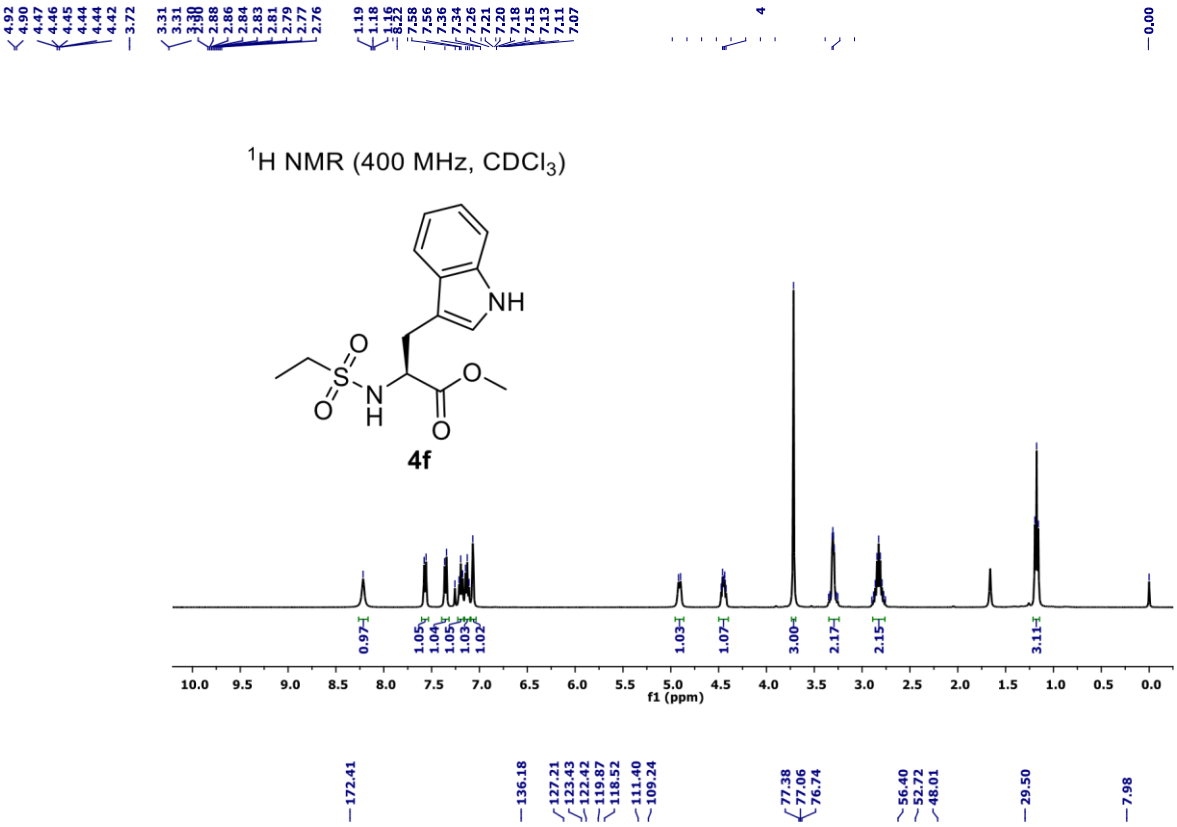

Fig ^{1}H, ^{13} H} NMR spectra of tryptophan derivative

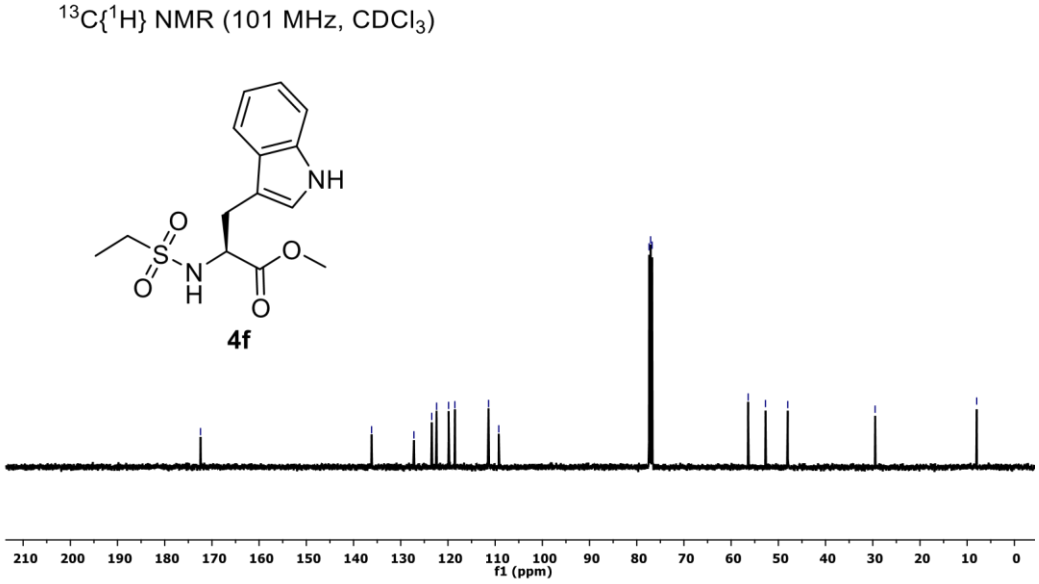
$^{13}C\{^{1}H\}$ NMR (101 MHz, $CDCl_3$)
NH
O
S
O
N
H
O
O
4f
210 200 190 180 170 160 150 140 130 120 110 100 90 80 70 60 50 40 30 20 10 0
f1 (ppm)

S35. C {^{1} **4f**.

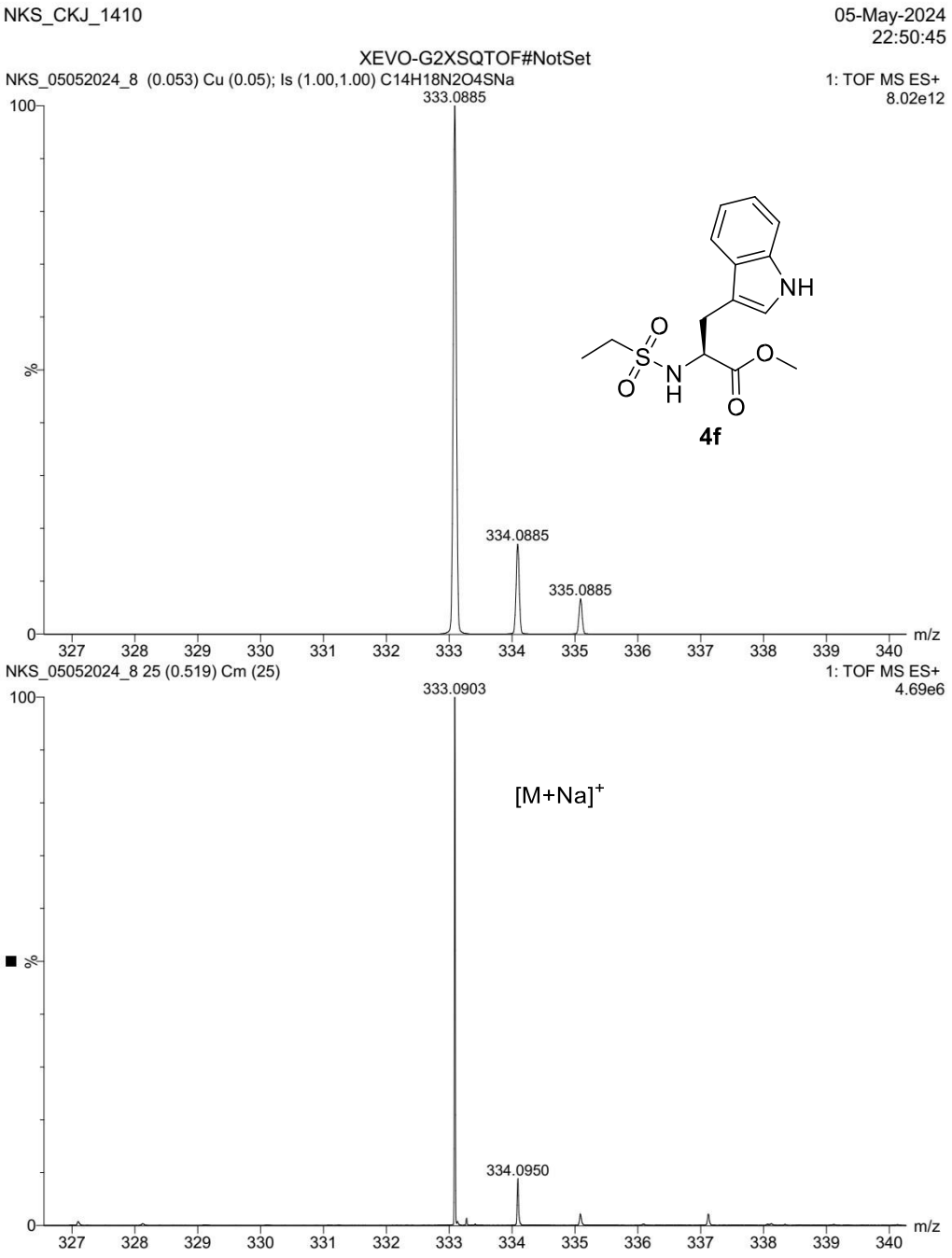
NKS_CKJ_1410
05-May-2024
22:50:45
XEVO-G2XSQTOF#NotSet
NKS_05052024_8 (0.053) Cu (0.05); Is (1.00,1.00) C14H18N2O4SNa
1: TOF MS ES+
8.02e12
333.0885
334.0885
335.0885
4f
m/z
NKS_05052024_8 25 (0.519) Cm (25)
1: TOF MS ES+
4.69e6
333.0903
[M+Na]+
334.0950

Fig

Fig S36. ESI-HRMS spectra of tryptophan derivative **4f**.

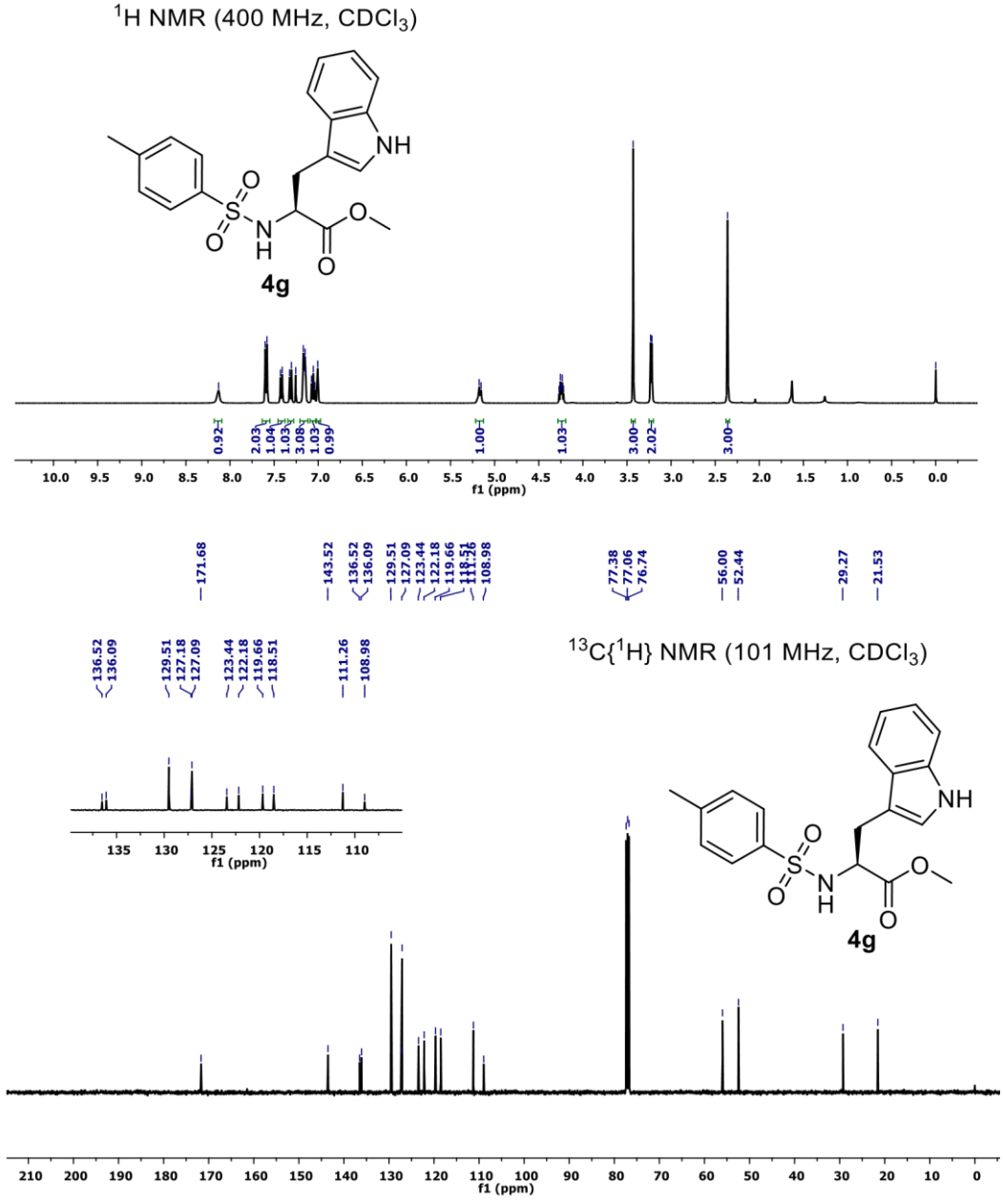

S37. C {[1] **4g**.

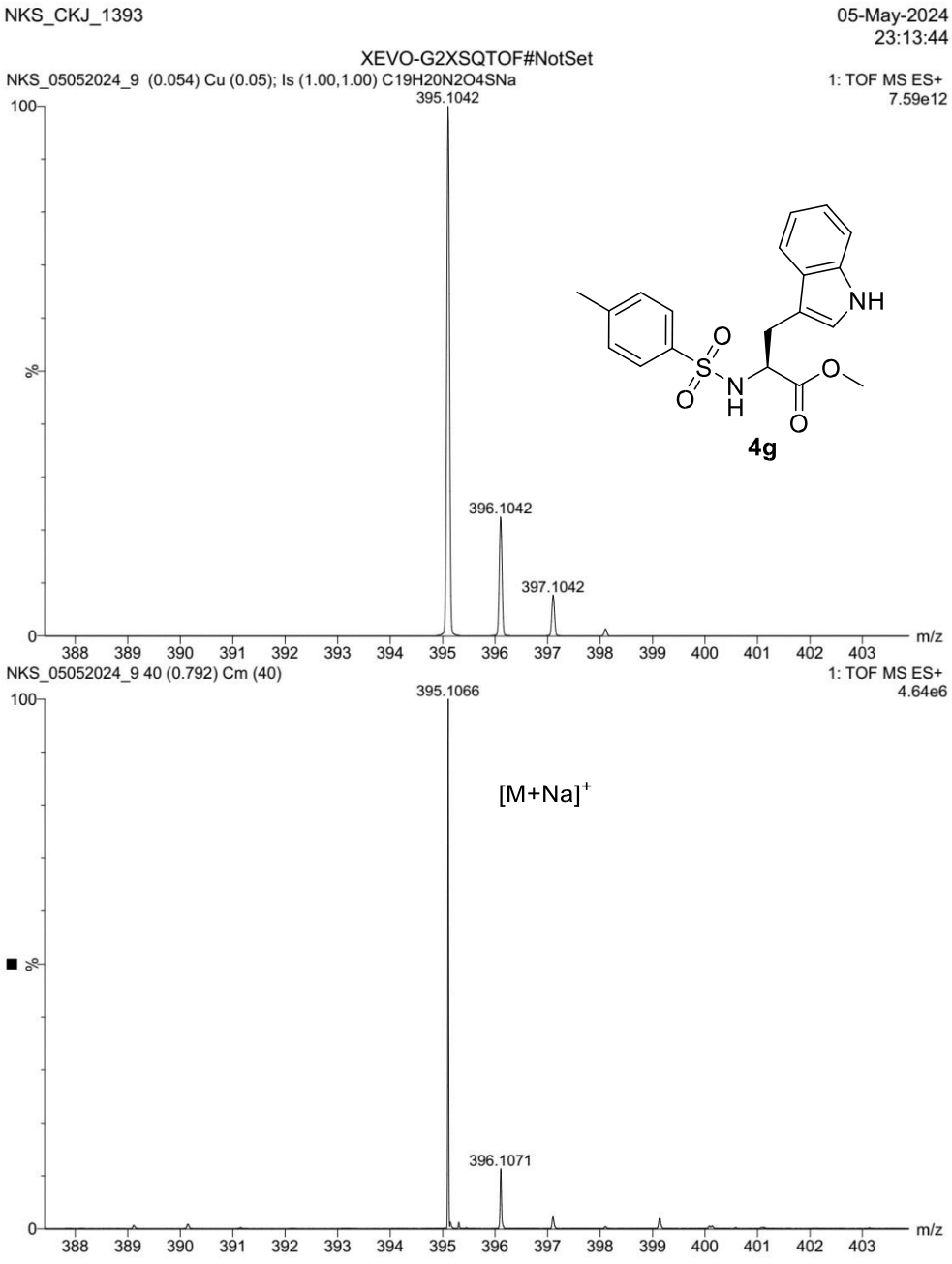
NKS_CKJ_1393
05-May-2024
23:13:44
XEVO-G2XSQTOF#NotSet
NKS_05052024_9 (0.054) Cu (0.05); Is (1.00,1.00) C19H20N2O4SNa
1: TOF MS ES+
7.59e12
395.1042
396.1042
397.1042
4g
NKS_05052024_9 40 (0.792) Cm (40)
1: TOF MS ES+
4.64e6
395.1066
[M+Na]+
396.1071
%
m/z
100
0
388 389 390 391 392 393 394 395 396 397 398 399 400 401 402 403

Fig

Fig S38. ESI-HRMS spectra of tryptophan derivative **4g**.

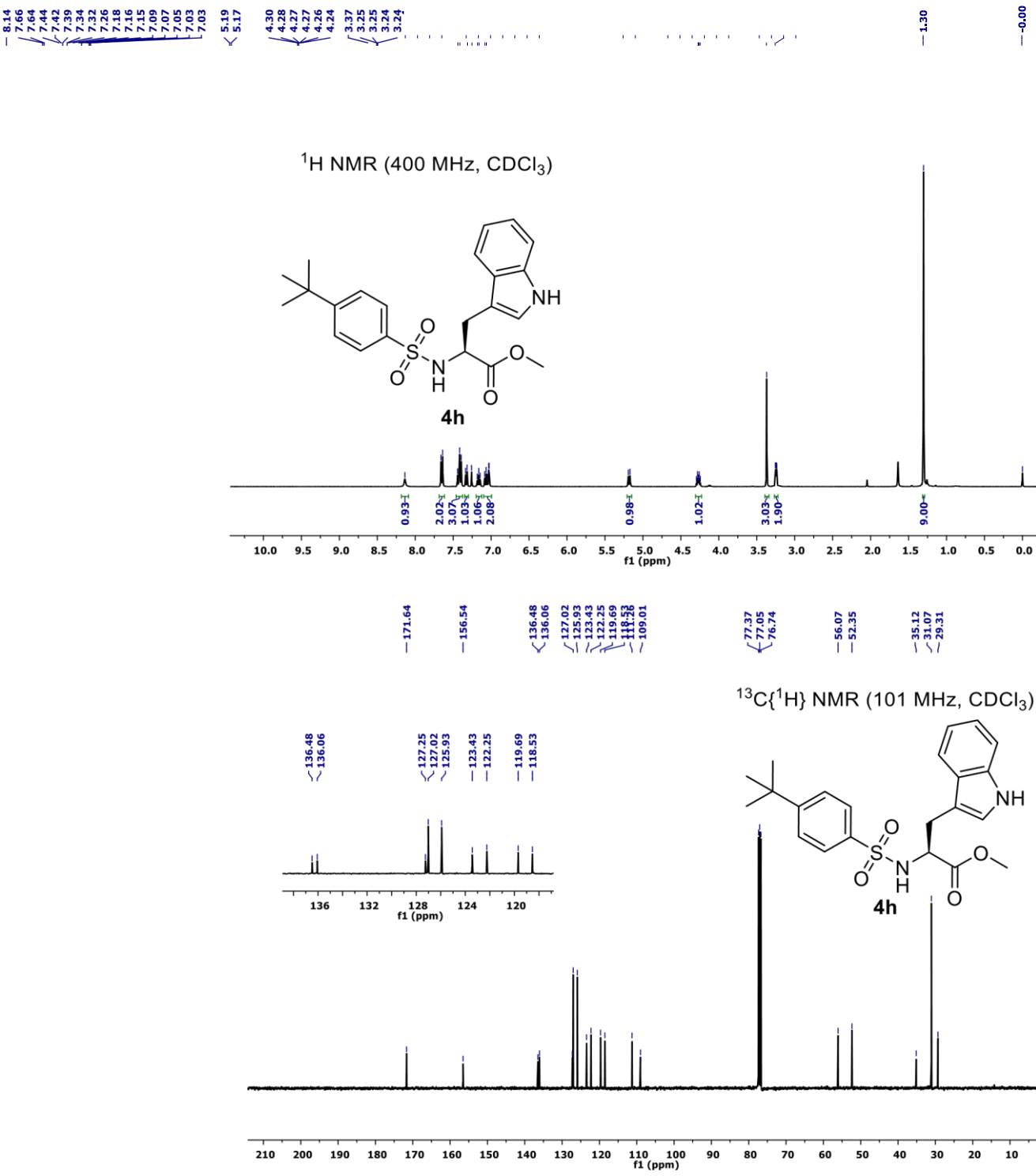

Fig S39. ^{1}H, ^{13}C $\{^{1}H\}$ NMR spectra of tryptophan derivative **4h**.

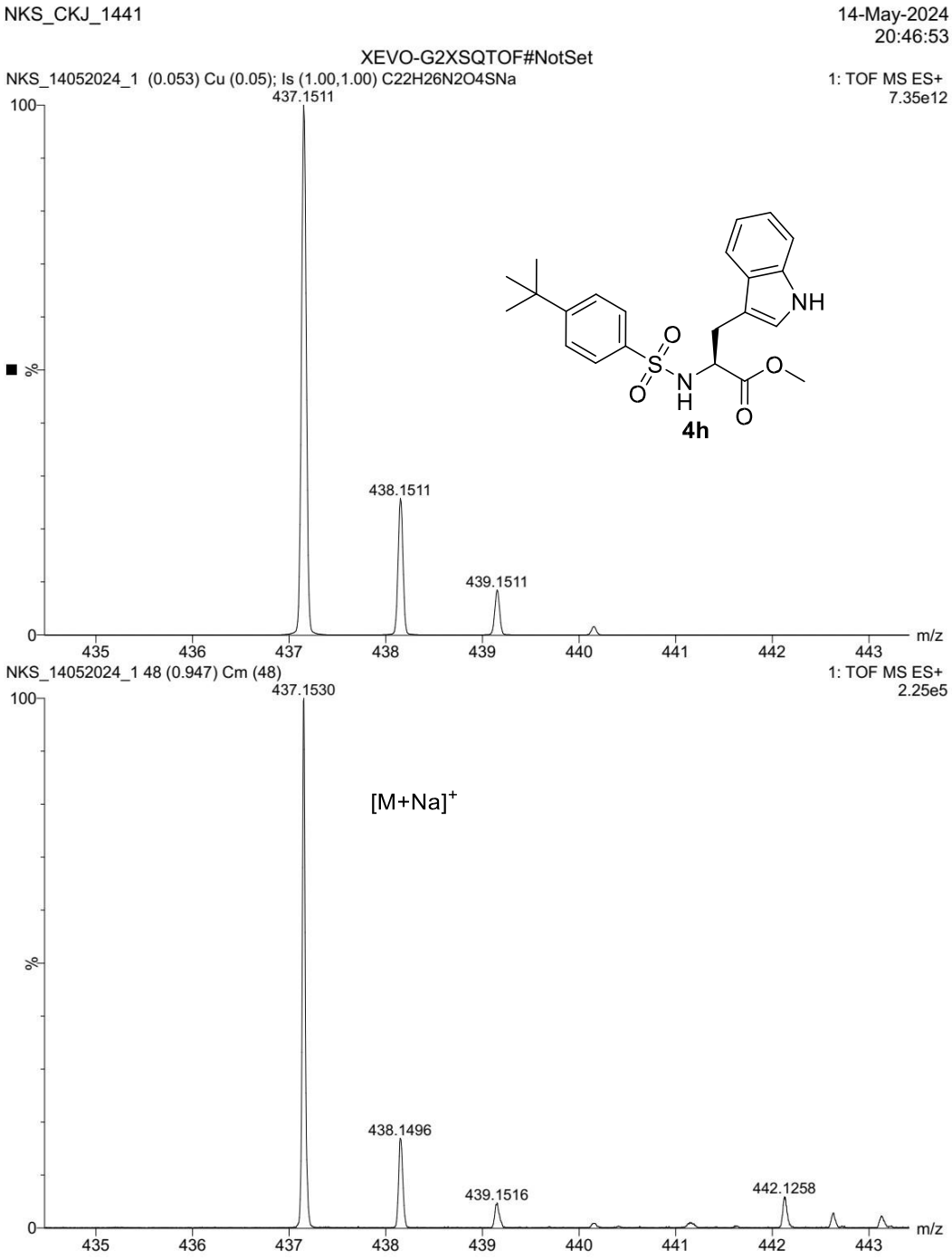

Fig S40. ESI-HRMS spectra of tryptophan derivative **4h**.

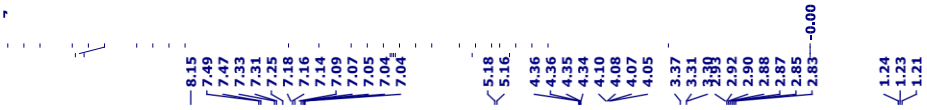

^{1}H NMR (400 MHz, $CDCl_3$)

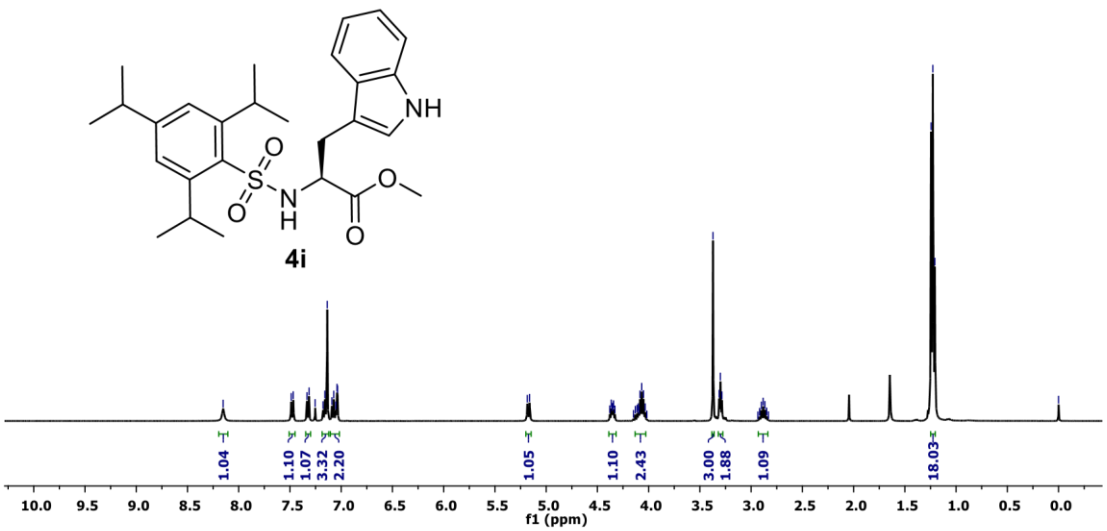

^{13}C{^{1}H} NMR (101 MHz, $CDCl_3$)

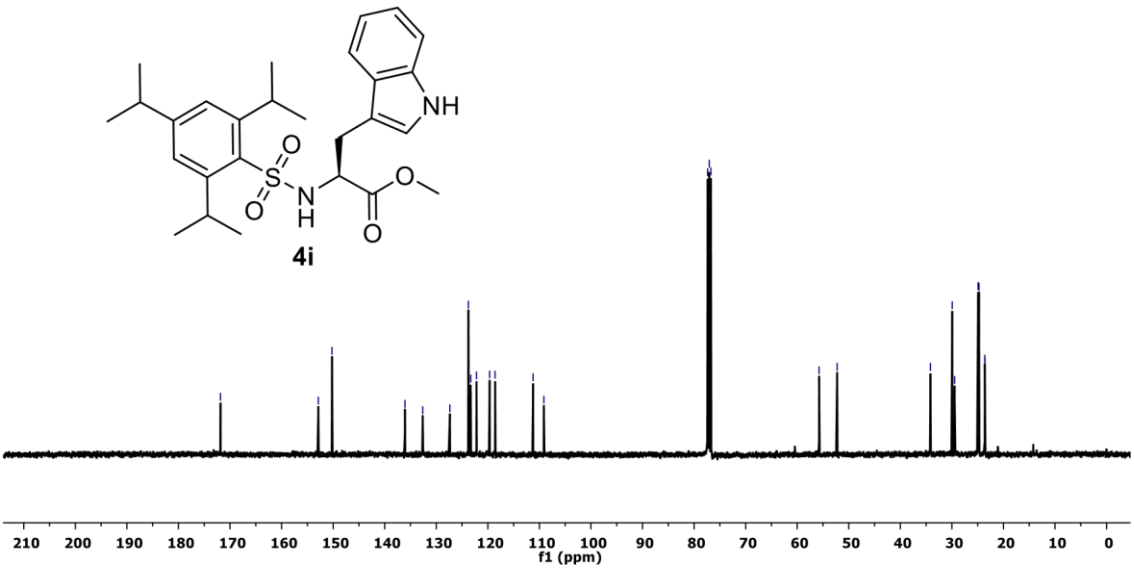

Fig S41. ^{1}H, ^{13}C $\{^{1}H\}$ NMR spectra of tryptophan derivative **4i**.

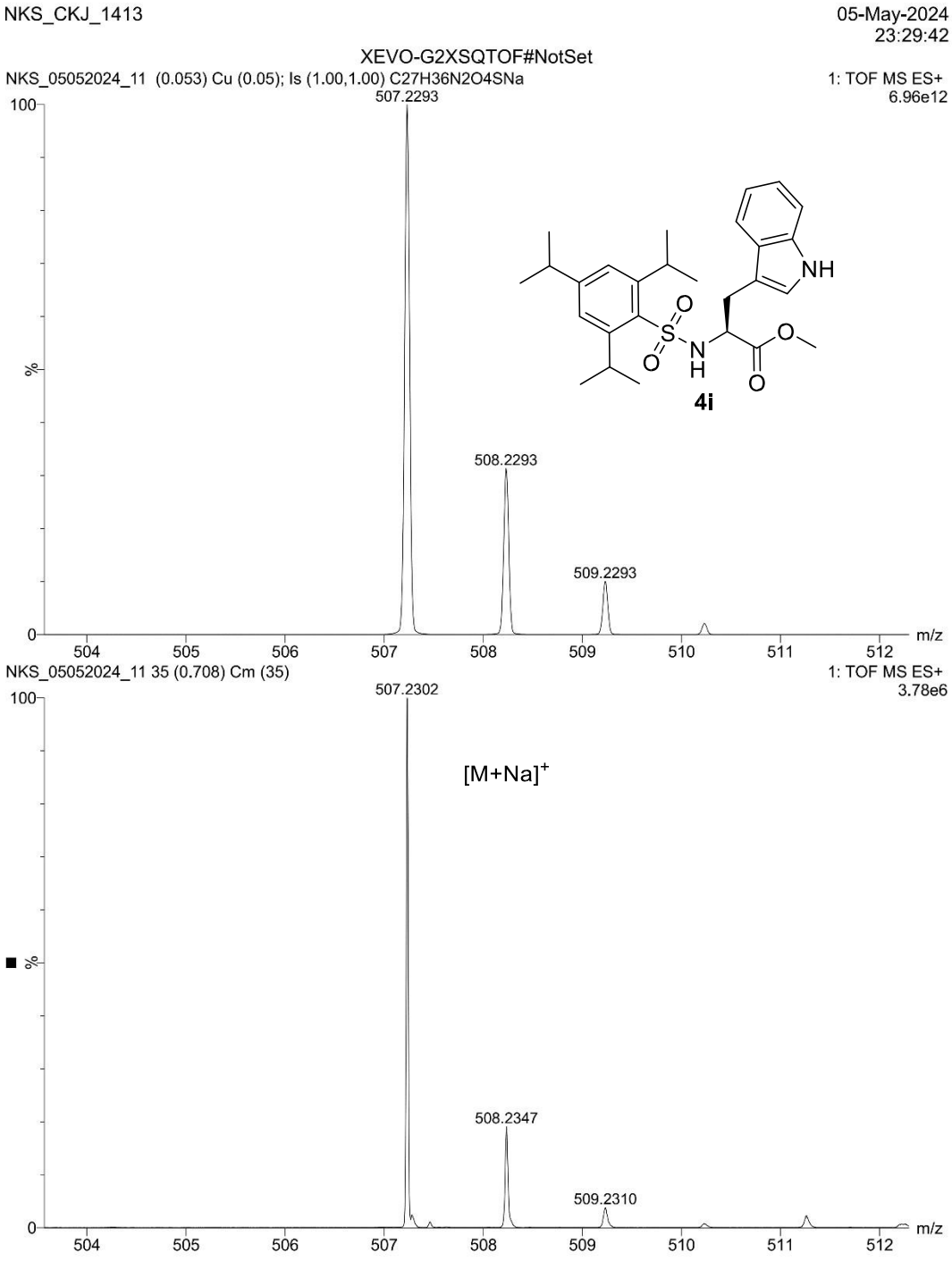

Fig S42. ESI-HRMS spectra of tryptophan derivative **4i**.

10.74
8.85
8.83
7.95
7.93
7.55
7.53
7.27
7.25
7.12
7.10
7.05
7.04
6.94
6.93
6.92
6.90
6.90
4.05
4.04
4.03
4.02
4.02
4.00
3.57
3.38
3.38
3.37
3.37
3.11
3.09
3.07
3.06
2.90
2.87
2.86
2.84
2.51
2.51
2.50
0.00

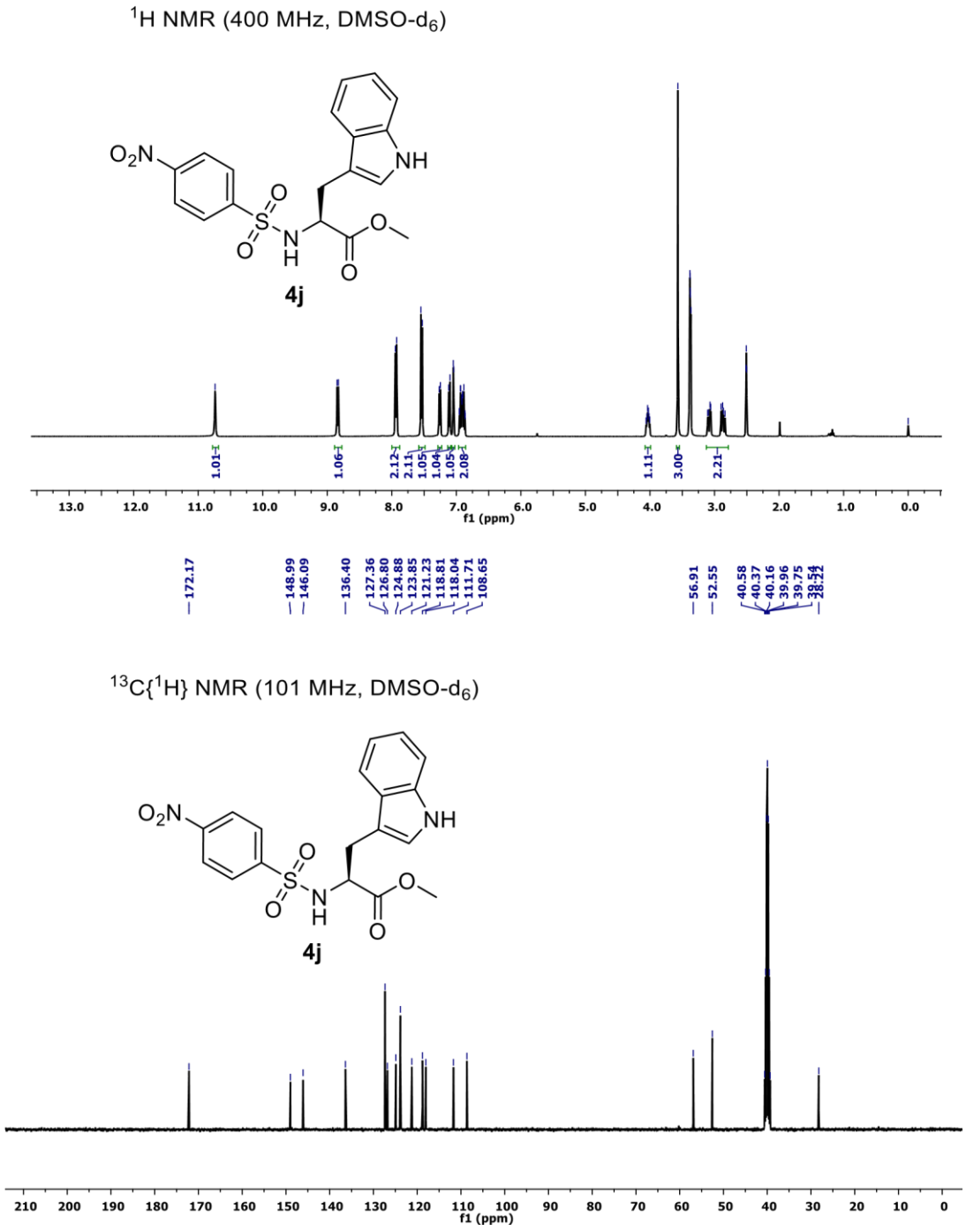

Fig S43. ^{1}H, ^{13}C {^{1}H} NMR spectra of tryptophan derivative **4j**.

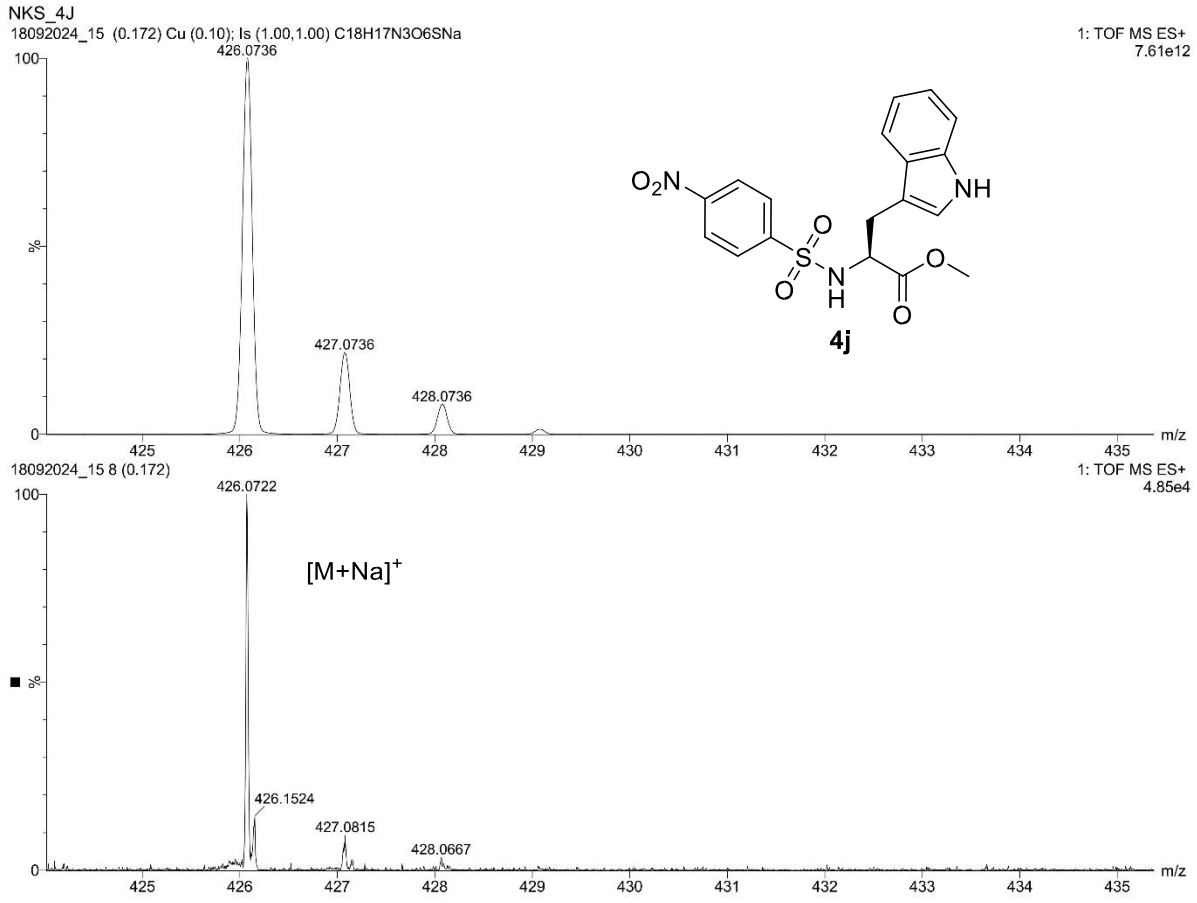

Fig S44. ESI-HRMS spectra of tryptophan derivative **4j**.

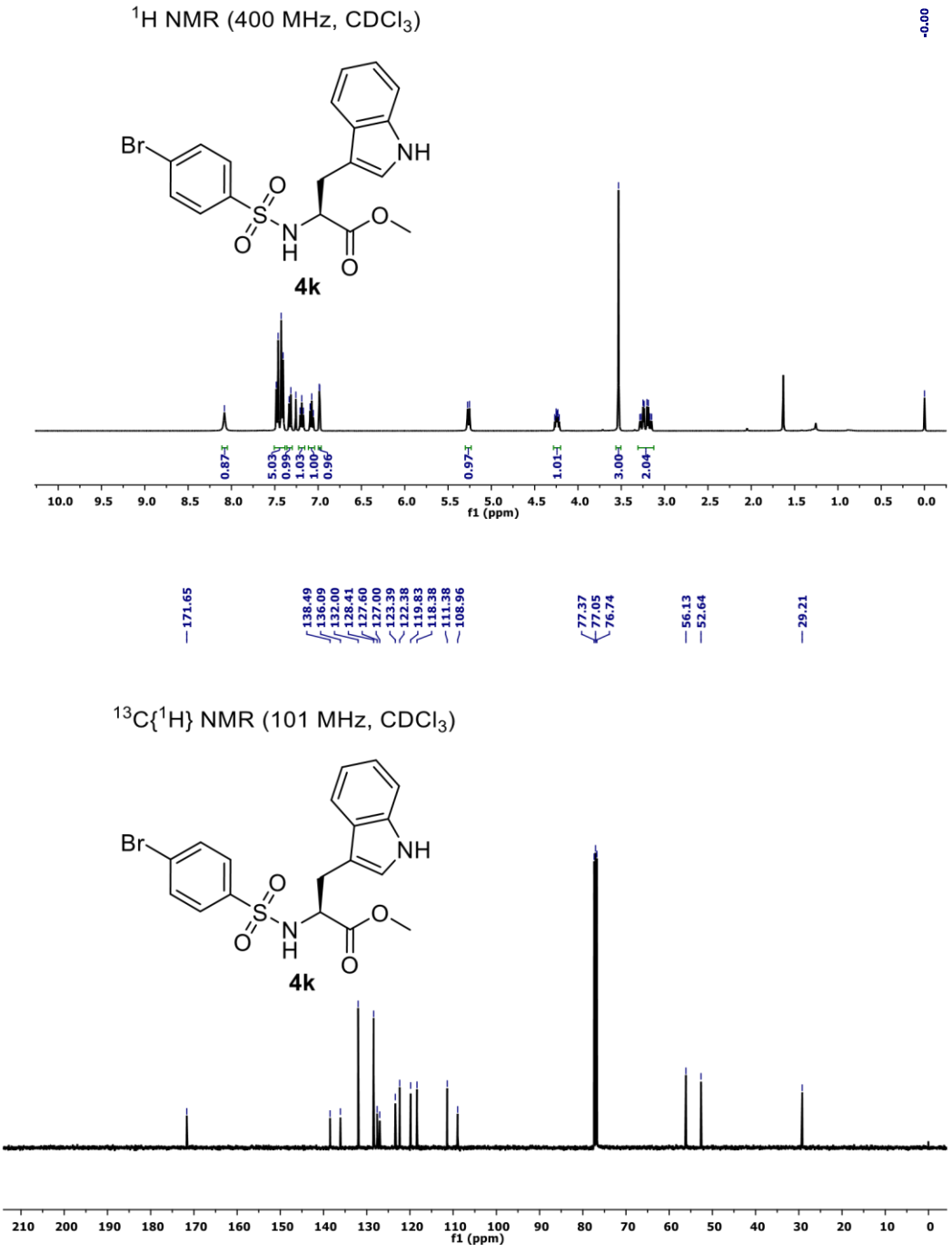

Fig S45. ^{1}H, ^{13}C $\{^{1}H\}$ NMR spectra of tryptophan derivative **4k**.

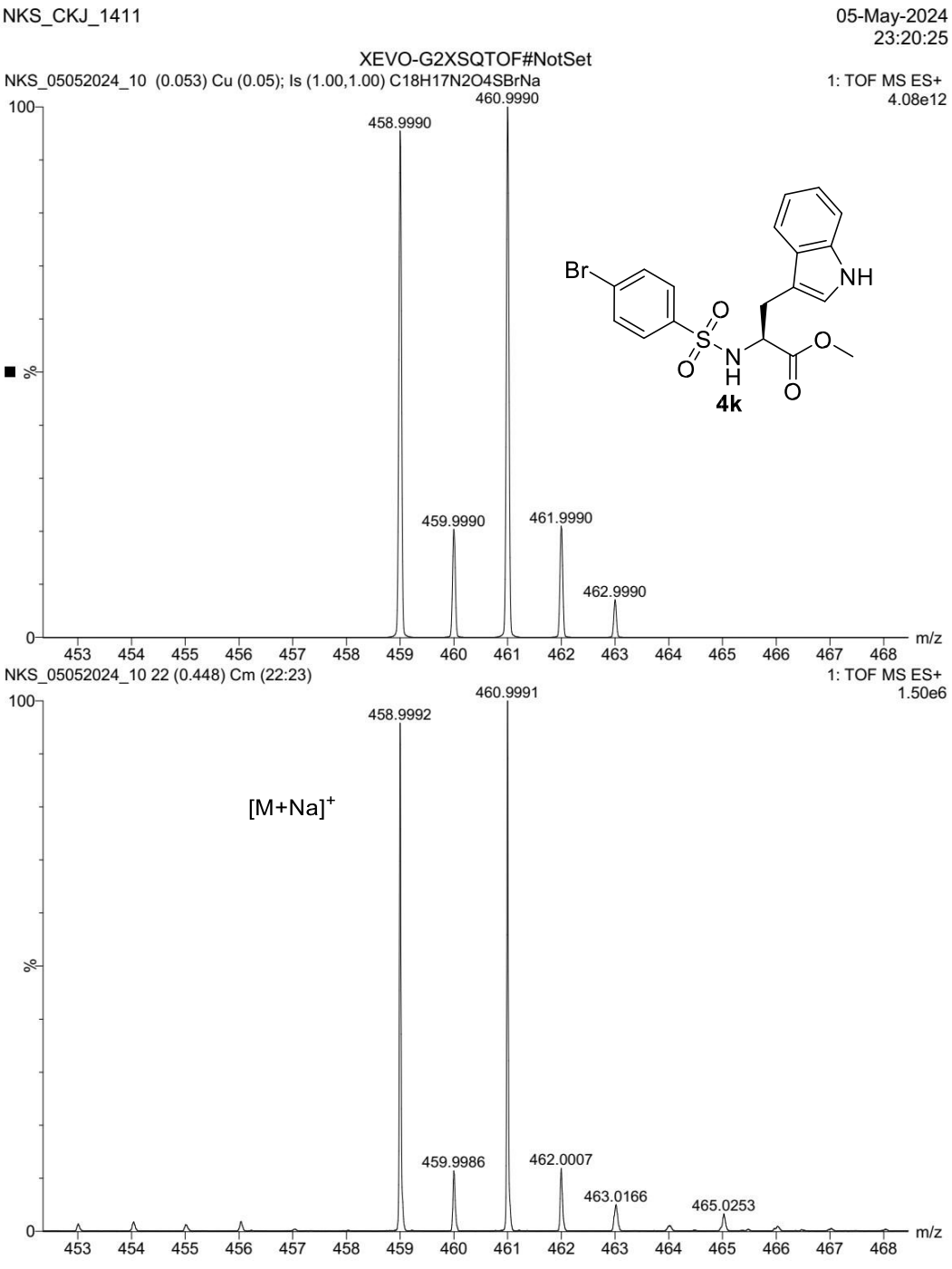
NKS_CKJ_1411
05-May-2024
23:20:25
XEVO-G2XSQTOF#NotSet
NKS_05052024_10 (0.053) Cu (0.05); Is (1.00,1.00) C18H17N2O4SBrNa
1: TOF MS ES+
4.08e12
460.9990
458.9990
459.9990
461.9990
462.9990
Br
NH
O
S
O
N
H
O
O
4k
%
m/z
NKS_05052024_10 22 (0.448) Cm (22:23)
1: TOF MS ES+
1.50e6
460.9991
458.9992
[M+Na]+
459.9986
462.0007
463.0166
465.0253

Fig S46. ESI-HRMS spectra of tryptophan derivative **4k**.

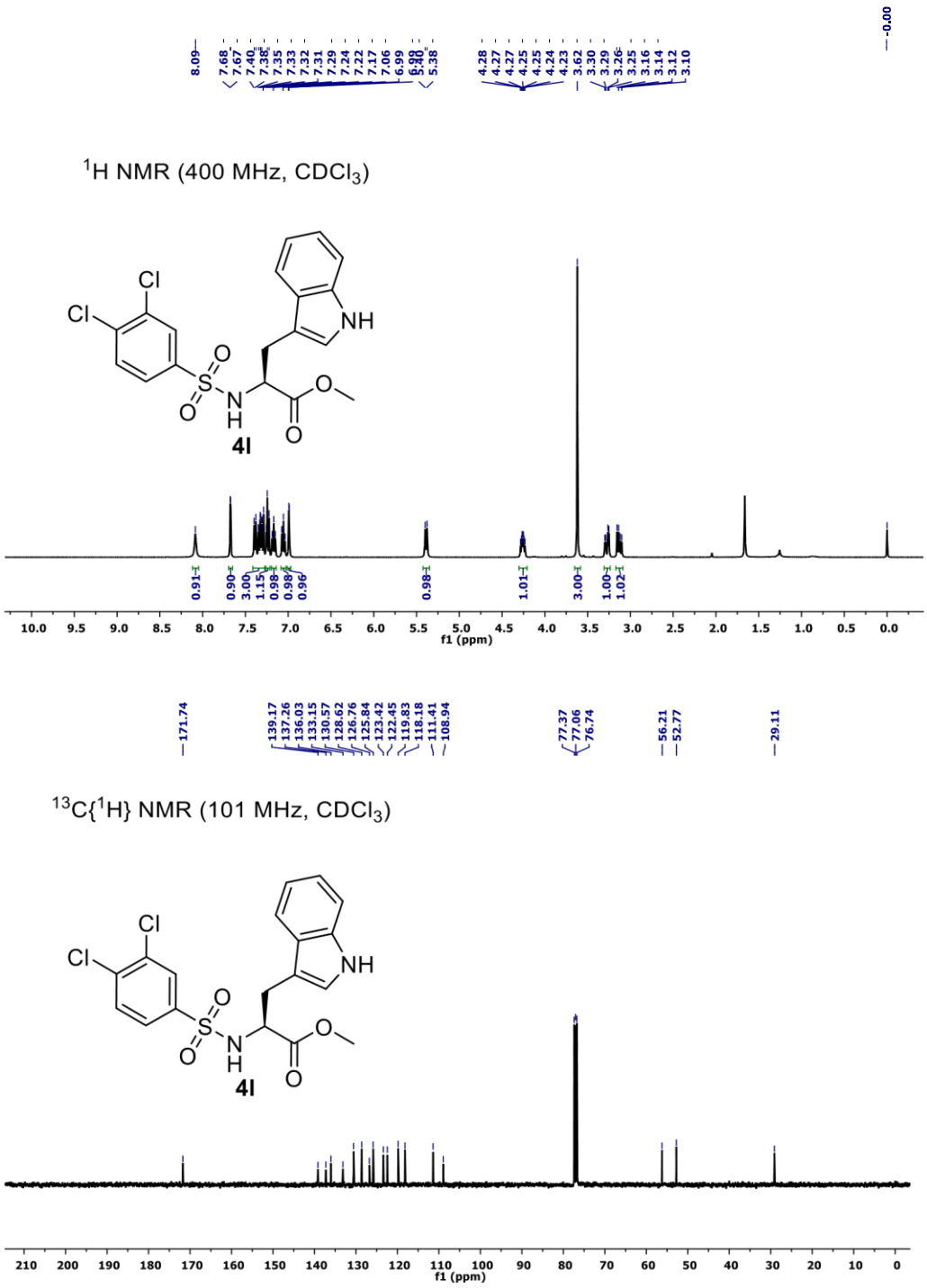

Fig S47. ^{1}H, ^{13}C $\{^{1}H\}$ NMR spectra of tryptophan derivative **4l**.

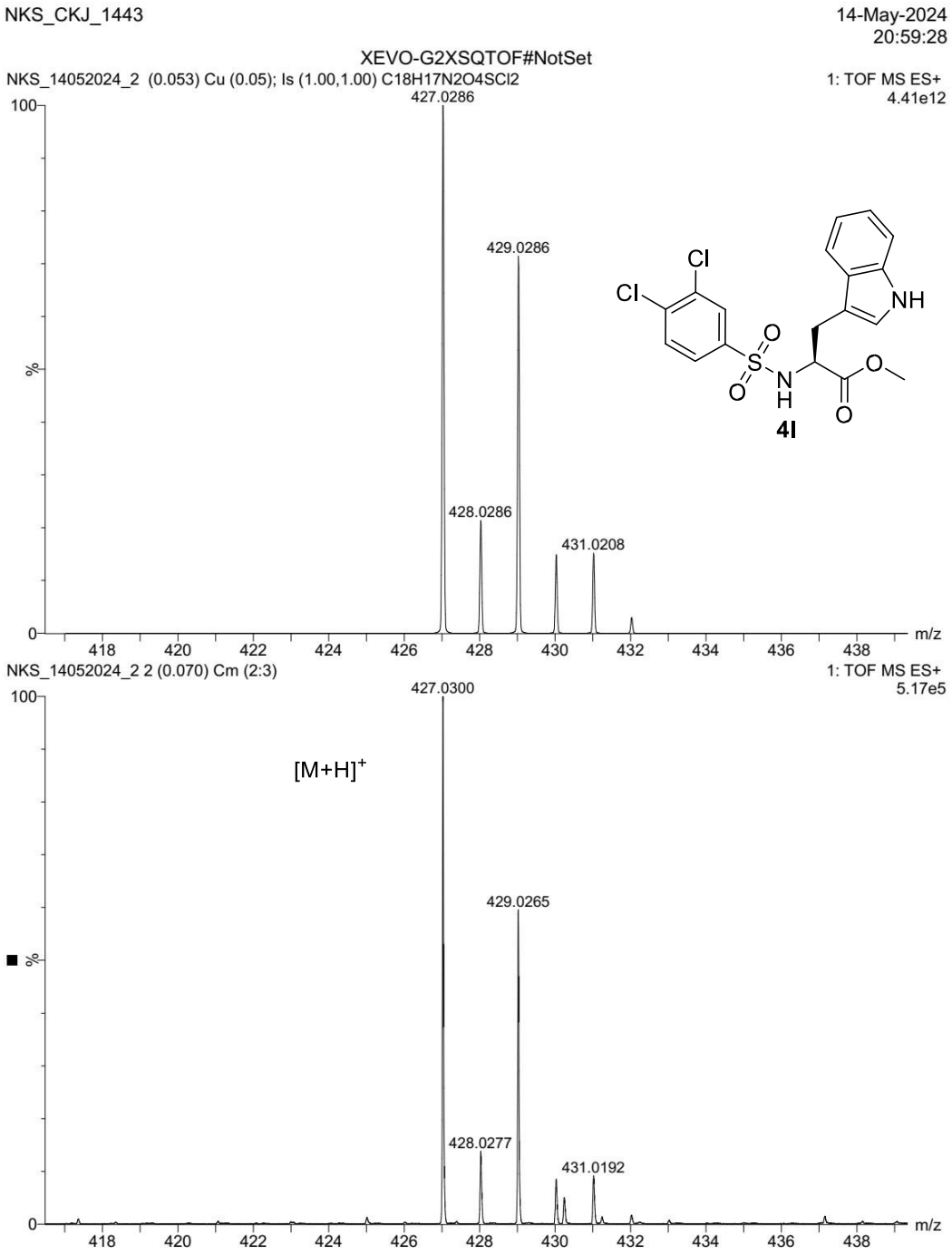

Fig S48. ESI-HRMS spectra of tryptophan derivative **4l**.

^{1}H NMR (400 MHz, $CDCl_3$)

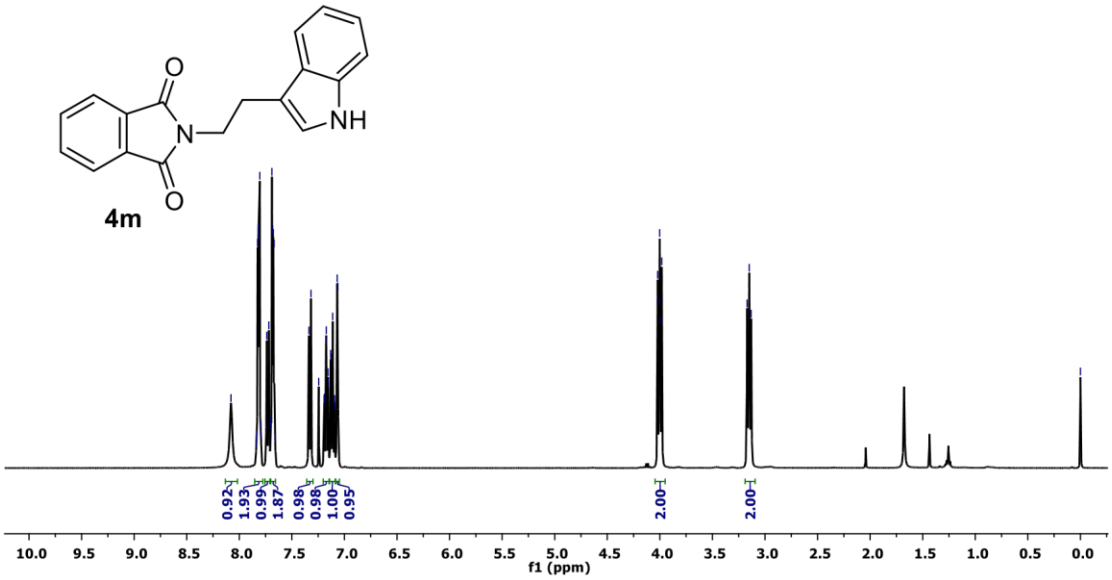

^{13}C{^{1}H} NMR (101 MHz, $CDCl_3$)

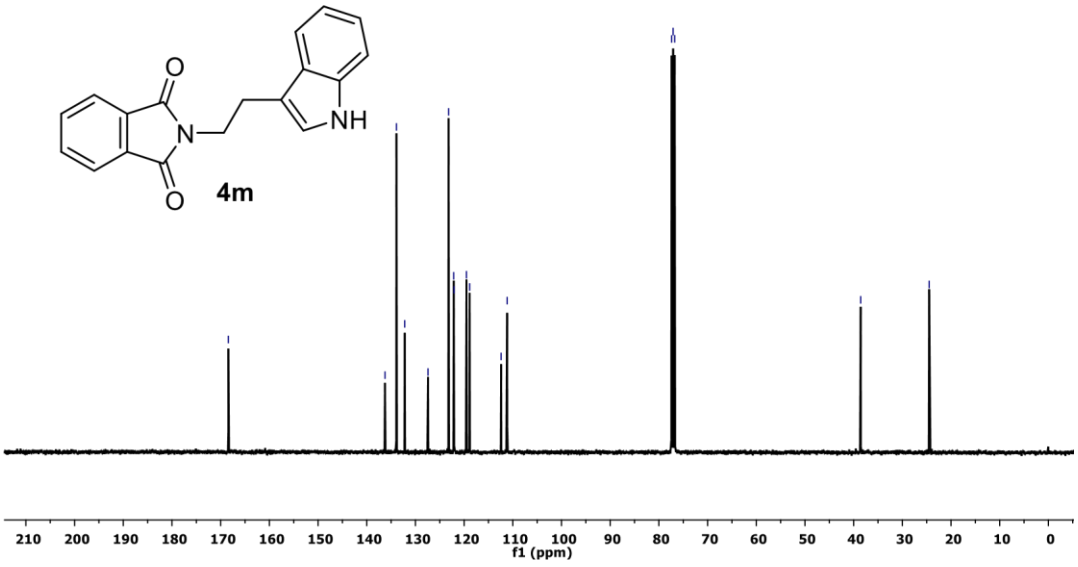

Fig S49. ^{1}H, ^{13}C $\{^{1}H\}$ NMR spectra of tryptophan derivative **4m**.

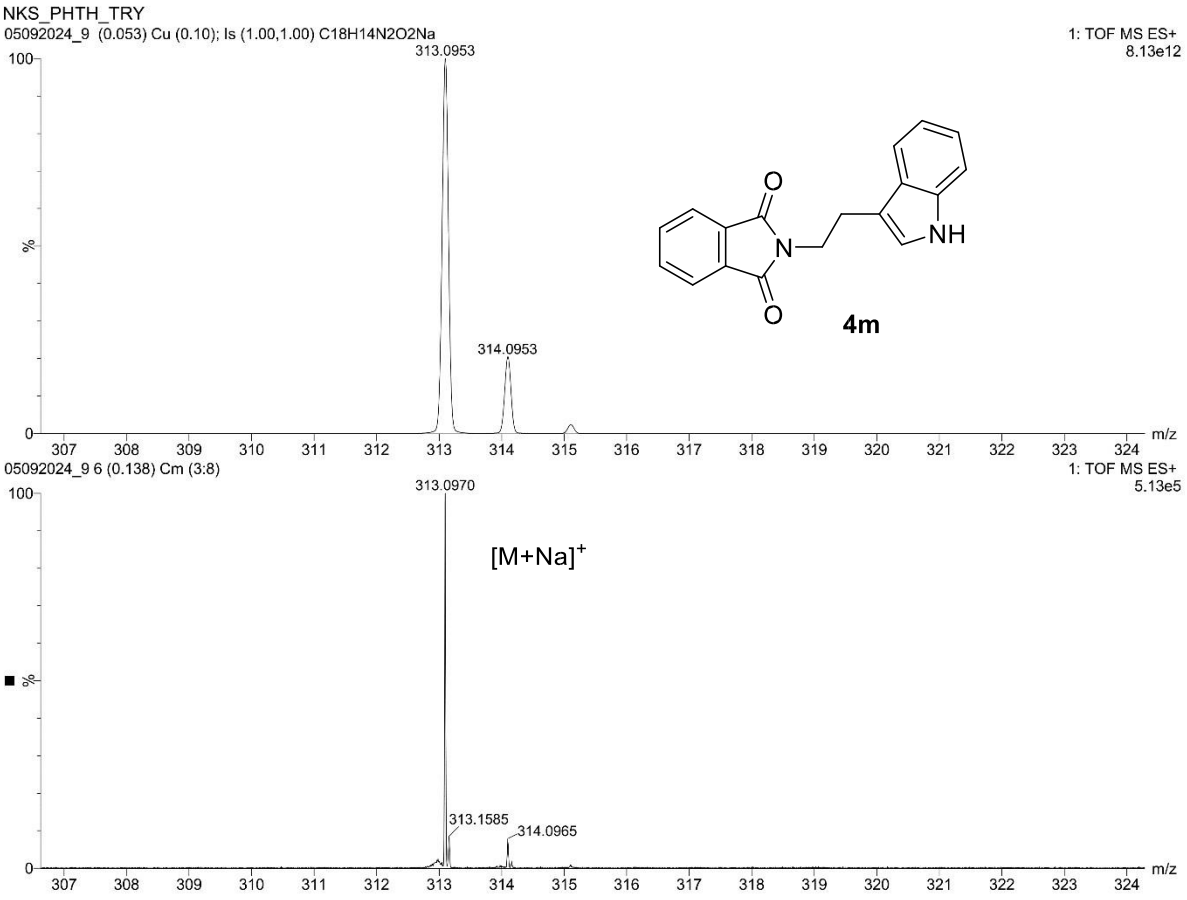

Fig S50. ESI-HRMS spectra of tryptophan derivative **4m**.

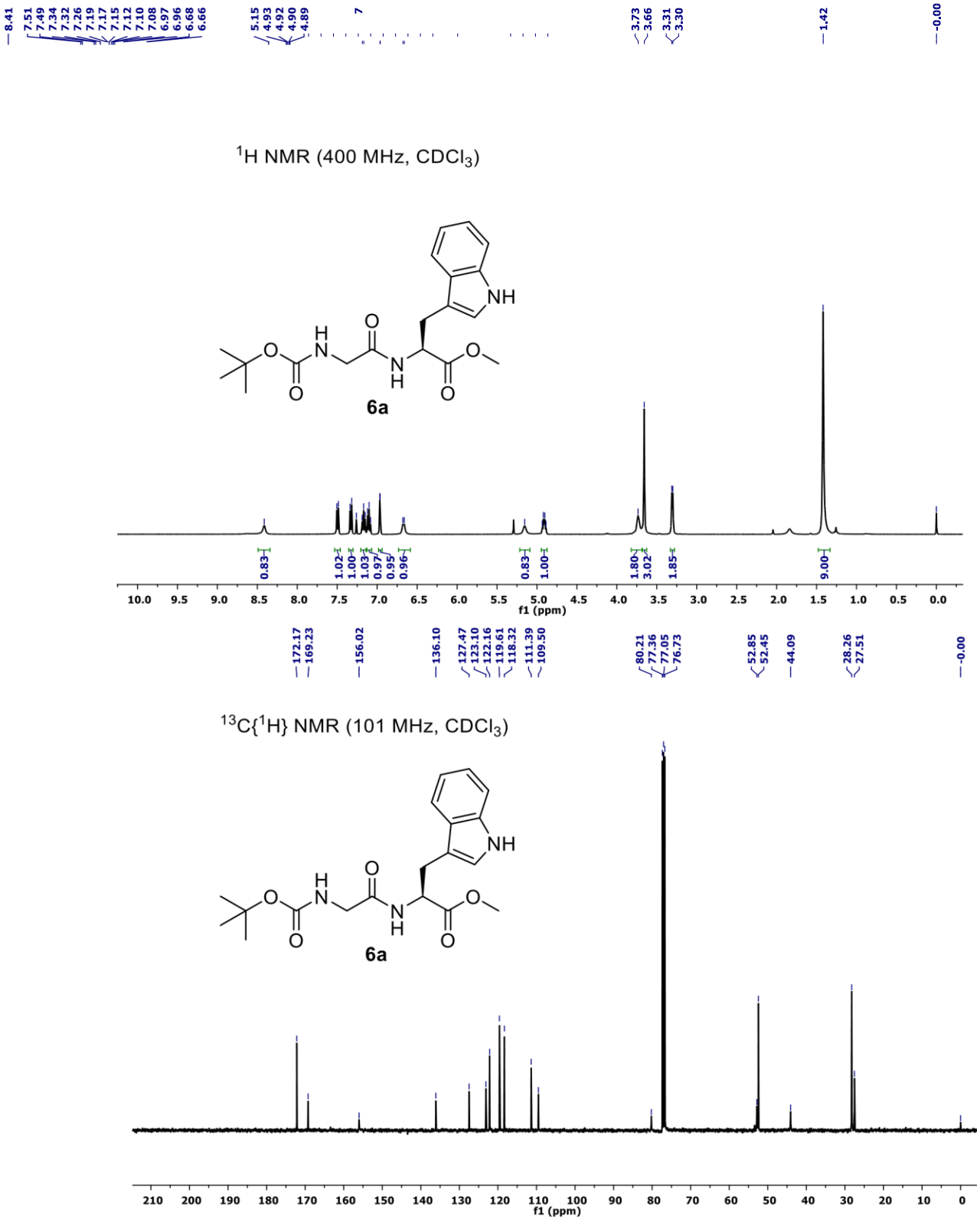

Fig S51. ^{1}H, ^{13}C $\{^{1}H\}$ NMR spectra of tryptophan-containing dipeptide **6a**.

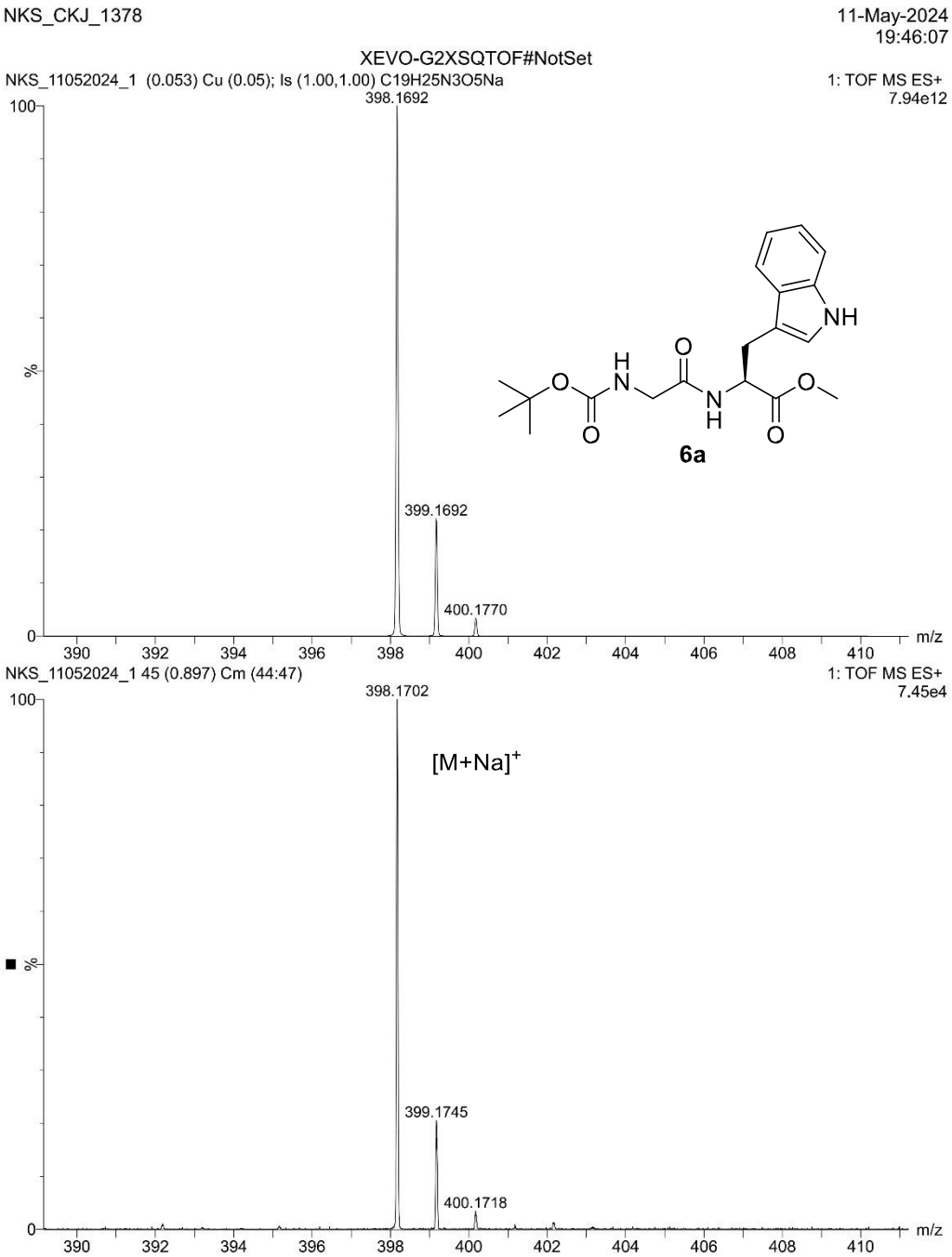
NKS_CKJ_1378
11-May-2024
19:46:07
XEVO-G2XSQTOF#NotSet
NKS_11052024_1 (0.053) Cu (0.05); Is (1.00,1.00) C19H25N3O5Na
1: TOF MS ES+
7.94e12
398.1692
399.1692
400.1770
6a
NKS_11052024_1 45 (0.897) Cm (44:47)
1: TOF MS ES+
7.45e4
398.1702
[M+Na]+
399.1745
400.1718
%
m/z
100
0
390
392
394
396
398
400
402
404
406
408
410

Fig S52. ESI-HRMS spectra of tryptophan-containing dipeptide **6a**.

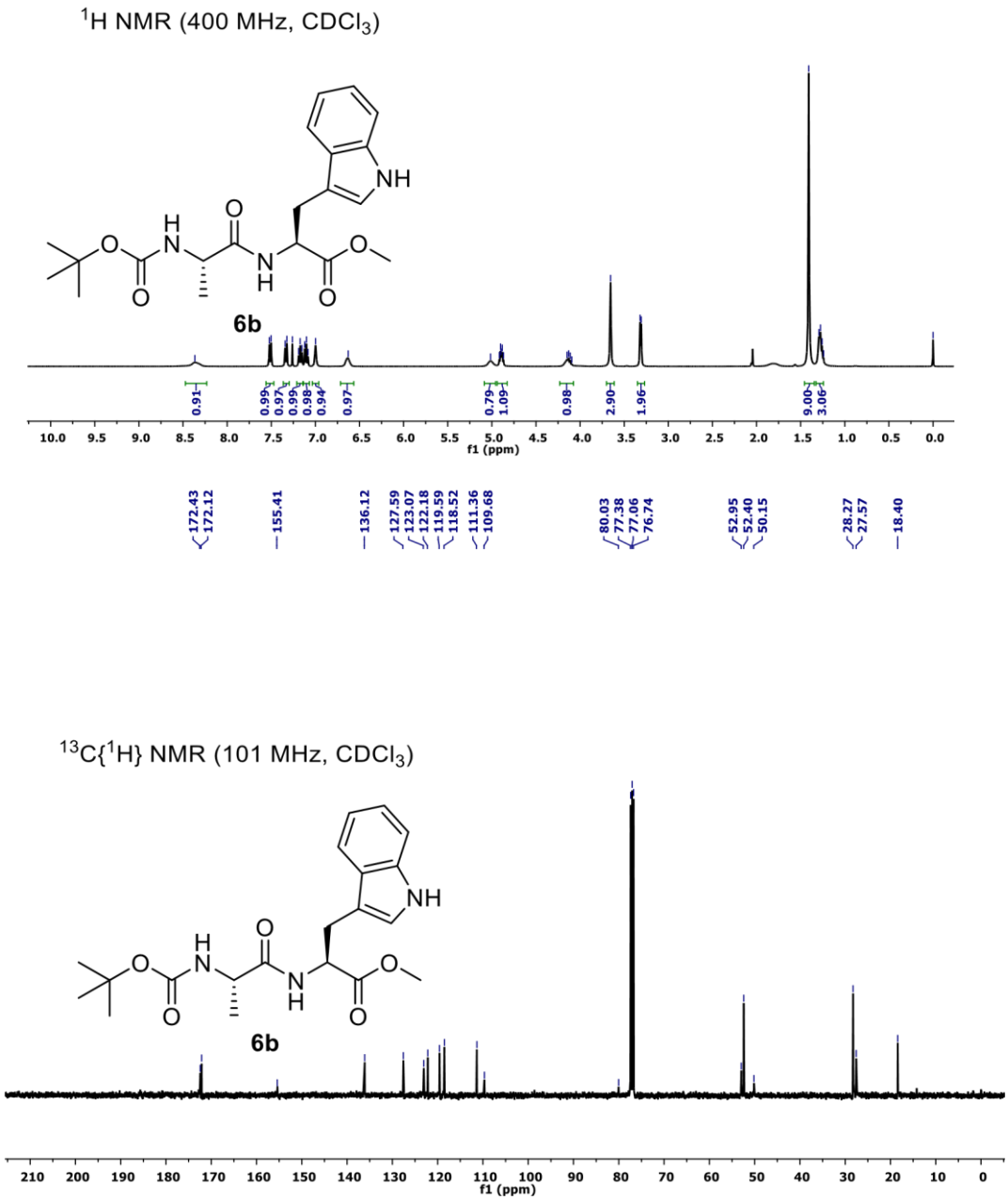

Fig S53. ^{1}H, ^{13}C $\{^{1}H\}$ NMR spectra of tryptophan-containing dipeptide **6b**.

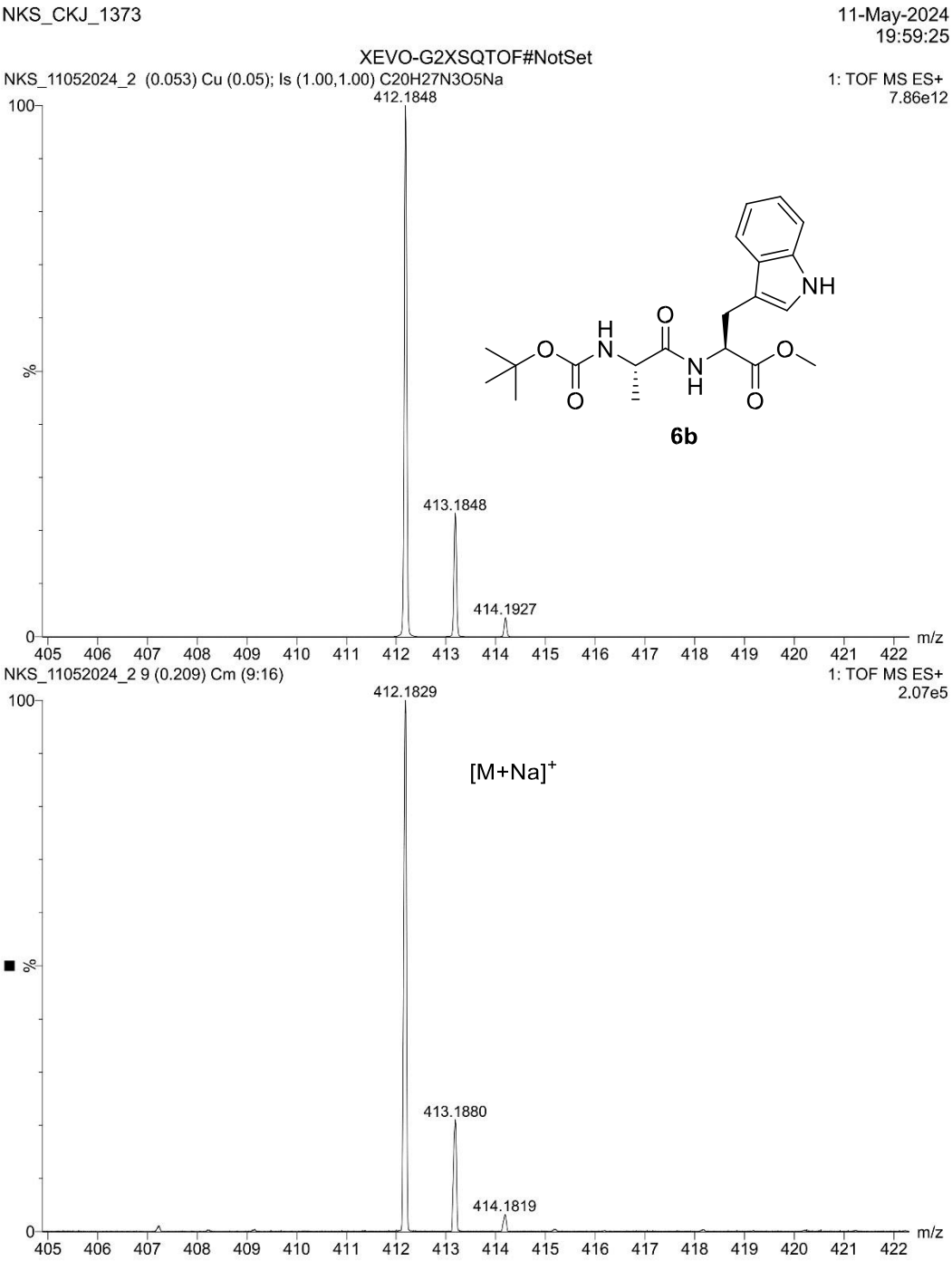

Fig S54. ESI-HRMS spectra of tryptophan-containing dipeptide **6b**.

Fig S55. ^{1}H, ^{13}C $\{^{1}H\}$ NMR spectra of tryptophan-containing dipeptide **6c**.

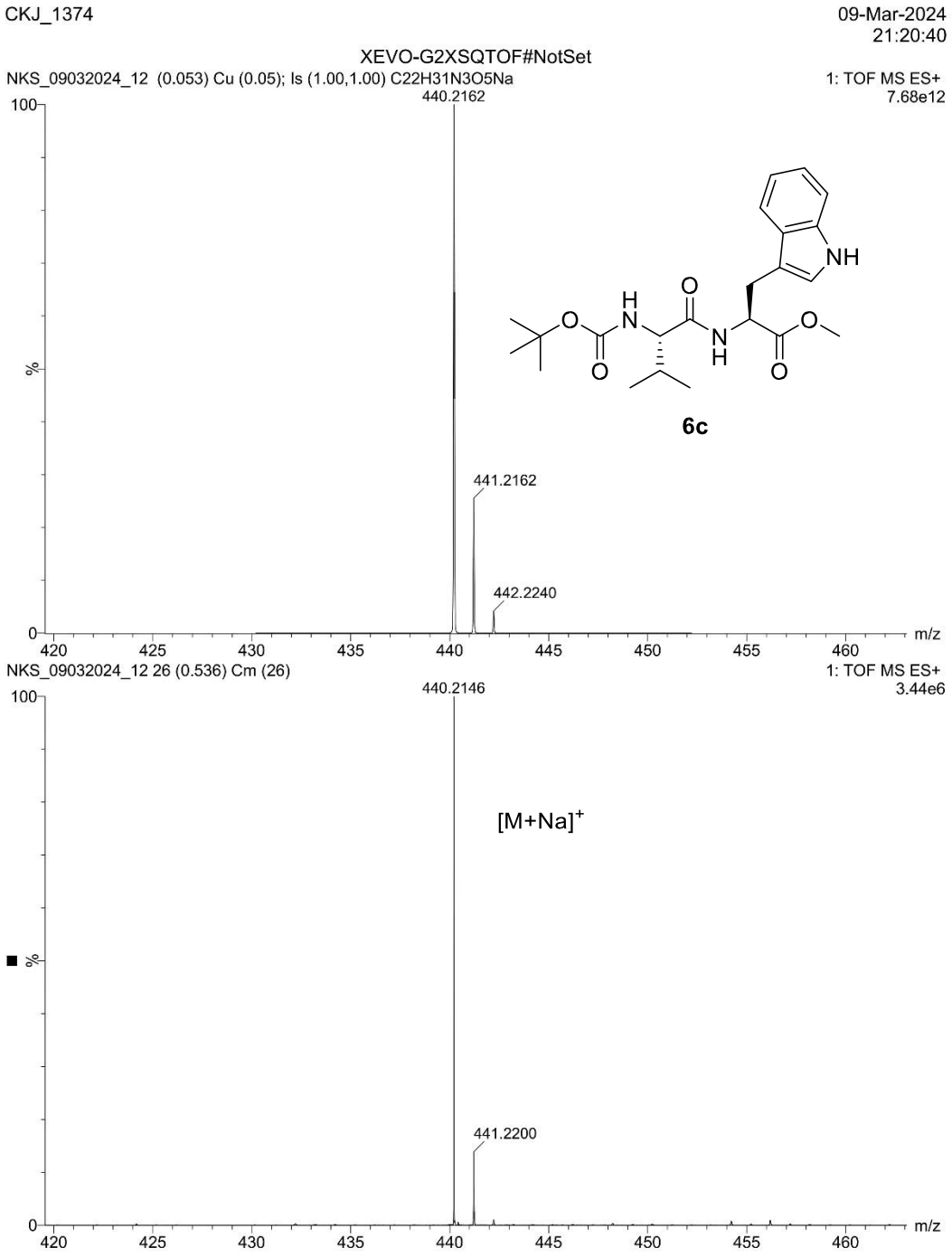

Fig S56. ESI-HRMS spectra of tryptophan-containing dipeptide **6c**.

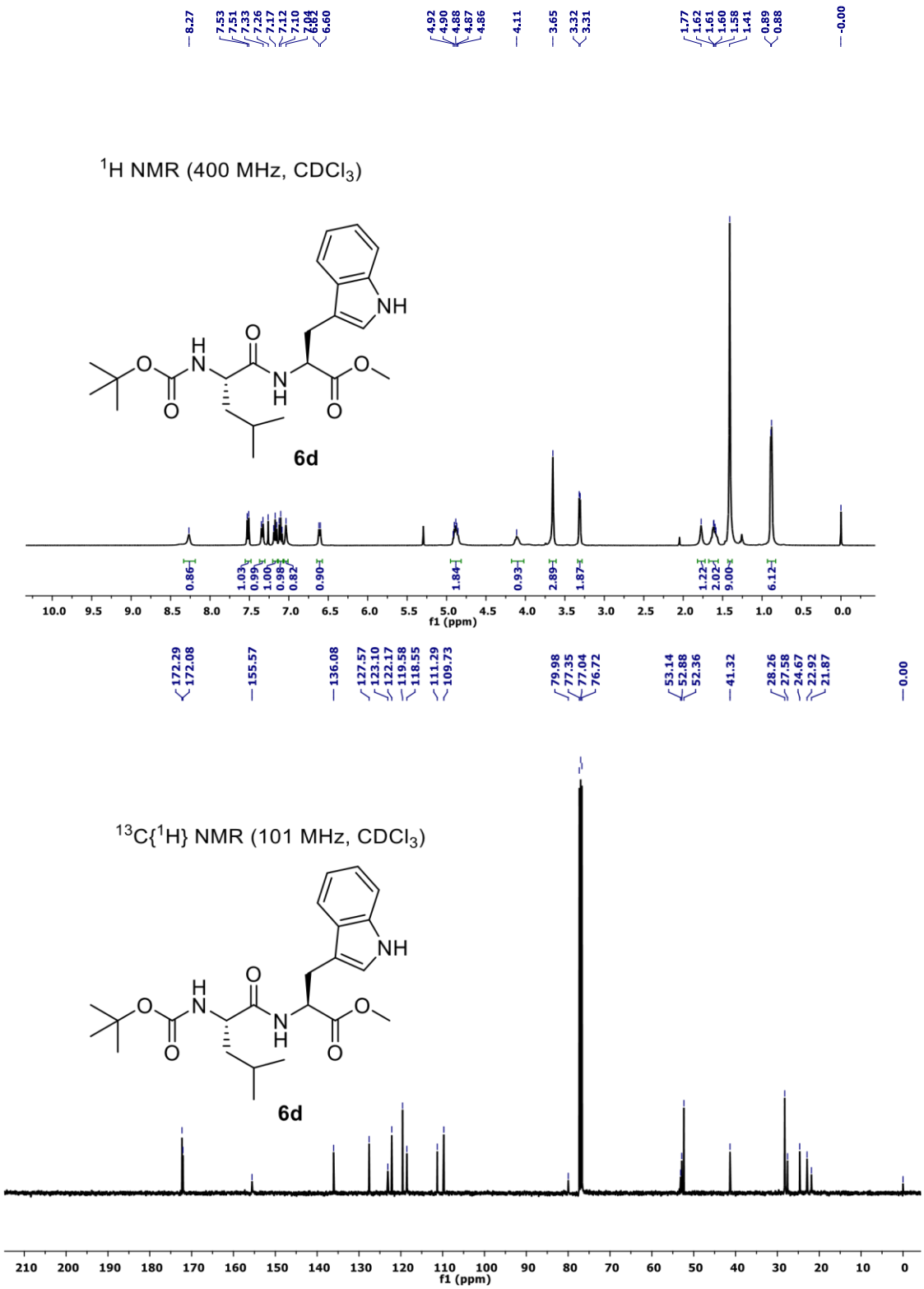

Fig S57. ^{1}H, ^{13}C $\{^{1}H\}$ NMR spectra of tryptophan-containing dipeptide **6d**.

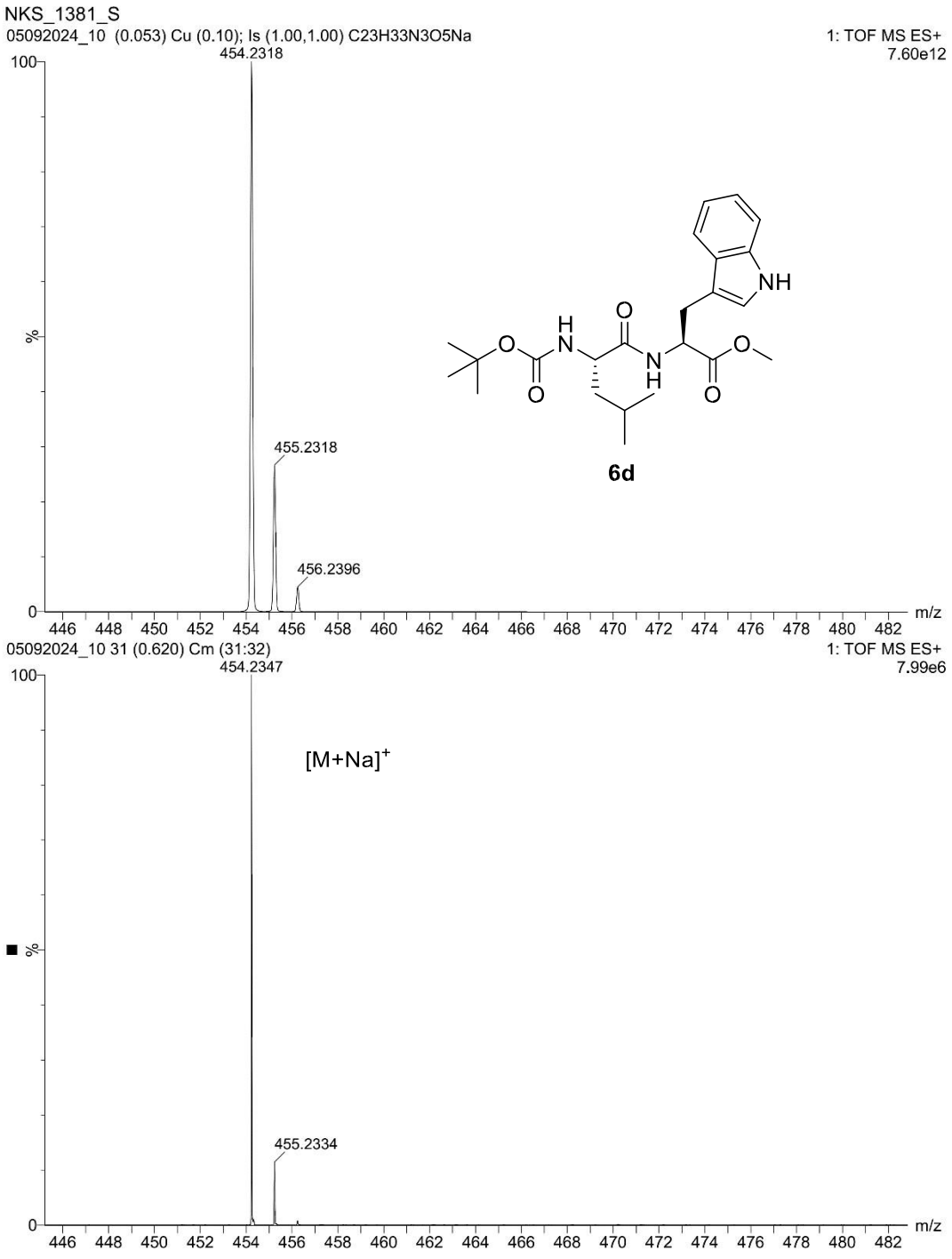
NKS_1381_S
05092024_10 (0.053) Cu (0.10); Is (1.00,1.00) C23H33N3O5Na
1: TOF MS ES+
7.60e12
454.2318
455.2318
456.2396
100
%
0
446 448 450 452 454 456 458 460 462 464 466 468 470 472 474 476 478 480 482
m/z
6d
05092024_10 31 (0.620) Cm (31:32)
1: TOF MS ES+
7.99e6
454.2347
[M+Na]+
455.2334
100
%
0
446 448 450 452 454 456 458 460 462 464 466 468 470 472 474 476 478 480 482
m/z

Fig S58. ESI-HRMS spectra of tryptophan-containing dipeptide **6d**.

Fig ^{1}H, ^{13}C $\{^{1}H\}$ NMR spectra of tryptophan-containing dipeptide

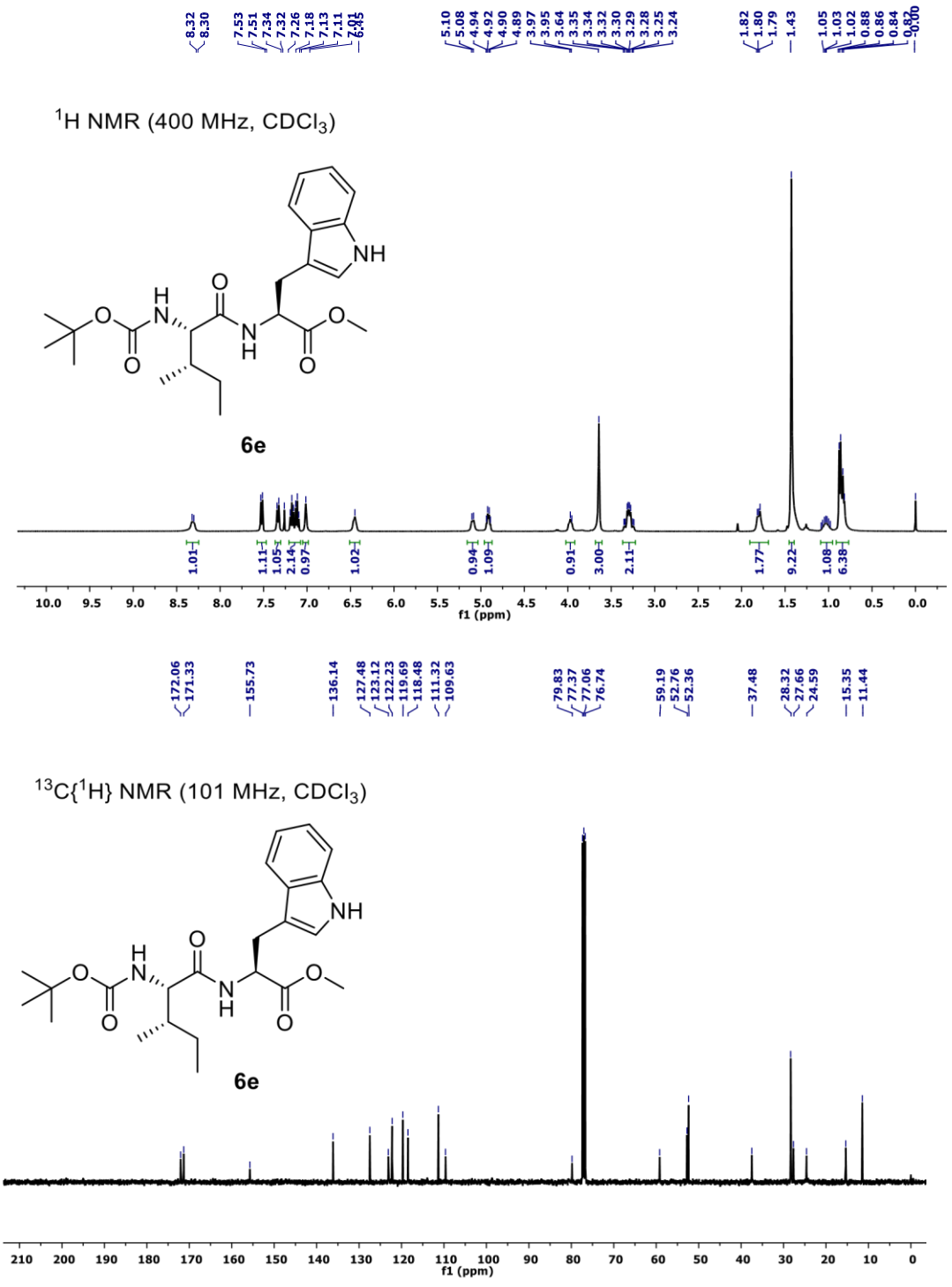

S59. **6e**.

Fig ^{1}H, ^{13}C $\{^{1}H\}$ NMR spectra of tryptophan-containing dipeptide

Fig ^{1}H, ^{13}C $\{^{1}H\}$ NMR spectra of tryptophan-containing dipeptide

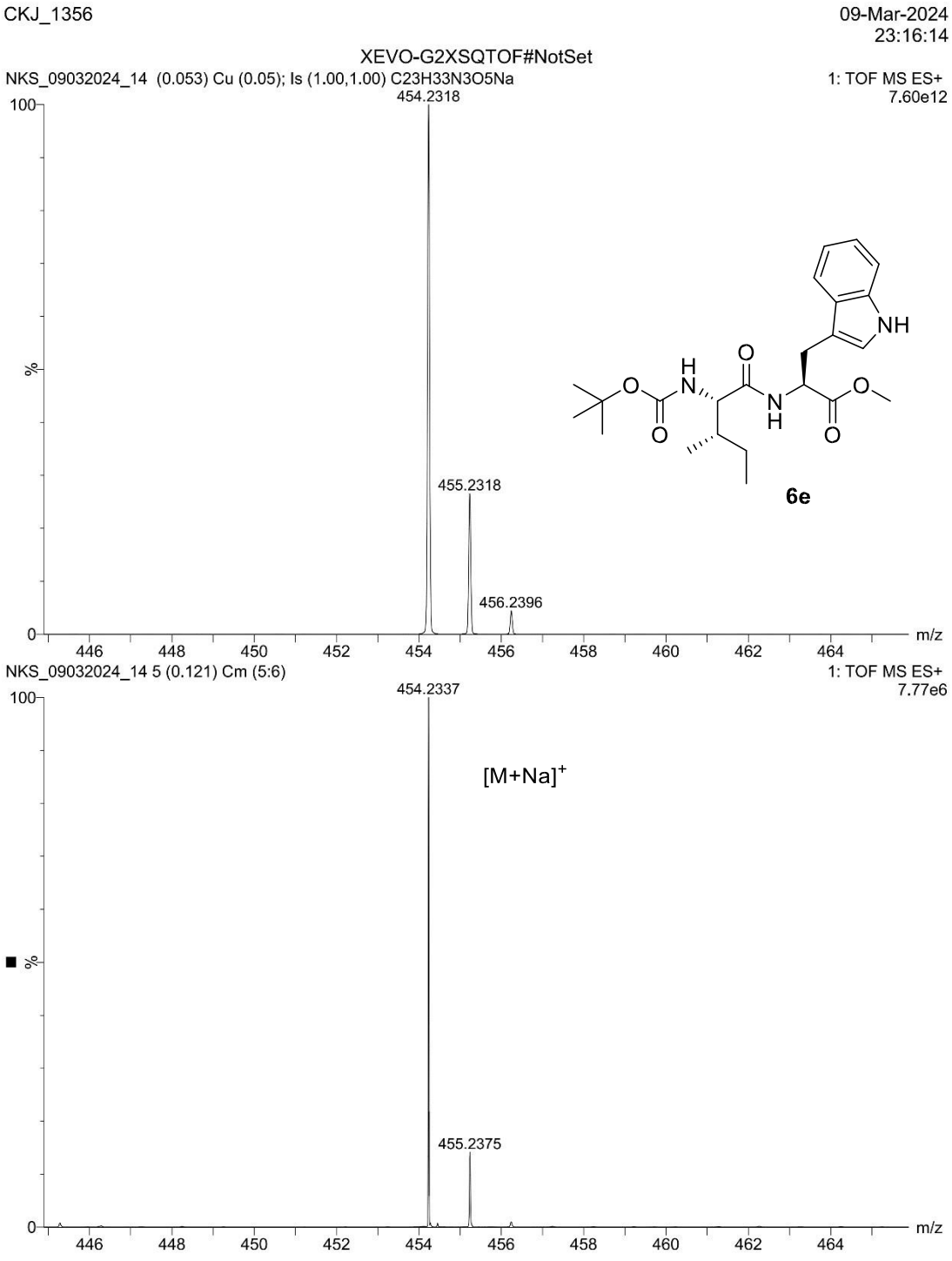

Fig S60. ESI-HRMS spectra of tryptophan-containing dipeptide **6e**.

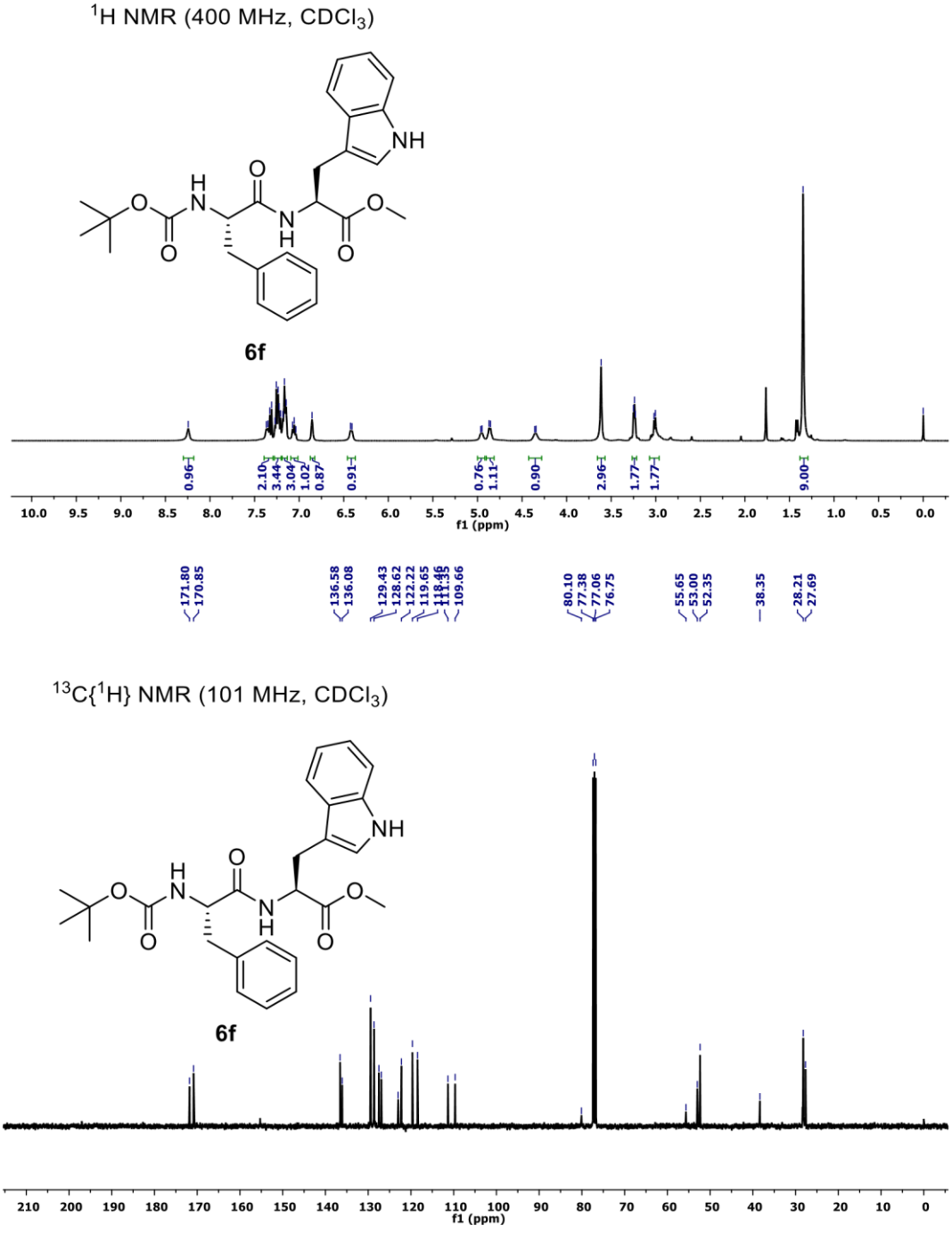

Fig ^{1}H, ^{13}C {^{1}H} NMR spectra of tryptophan-containing dipeptide

S61. **6f**.

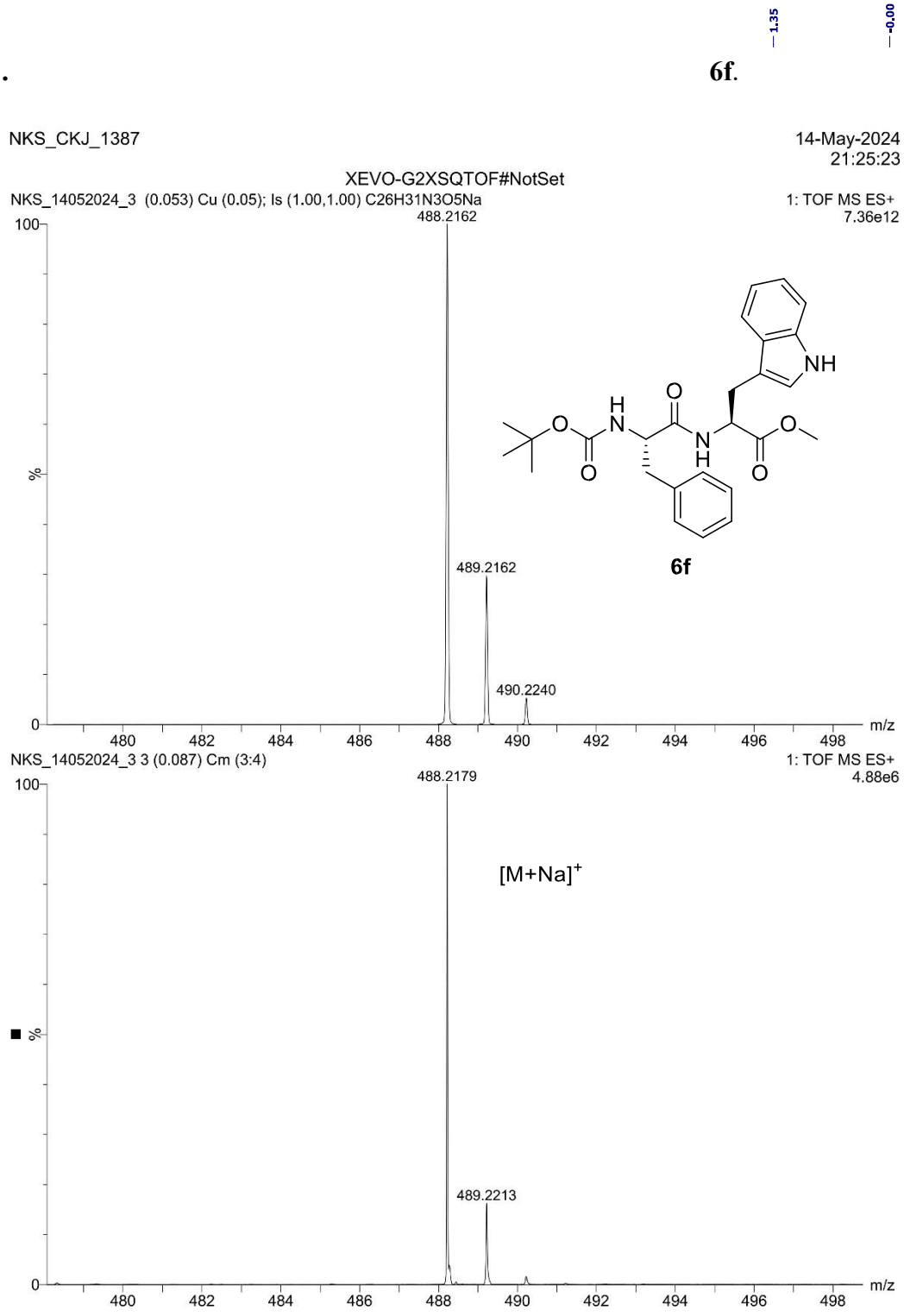

Fig S62. ESI-HRMS spectra of tryptophan-containing dipeptide **6f**.

Fig ^{1}H, ^{13}C $\{^{1}H\}$ NMR spectra of tryptophan-containing dipeptide

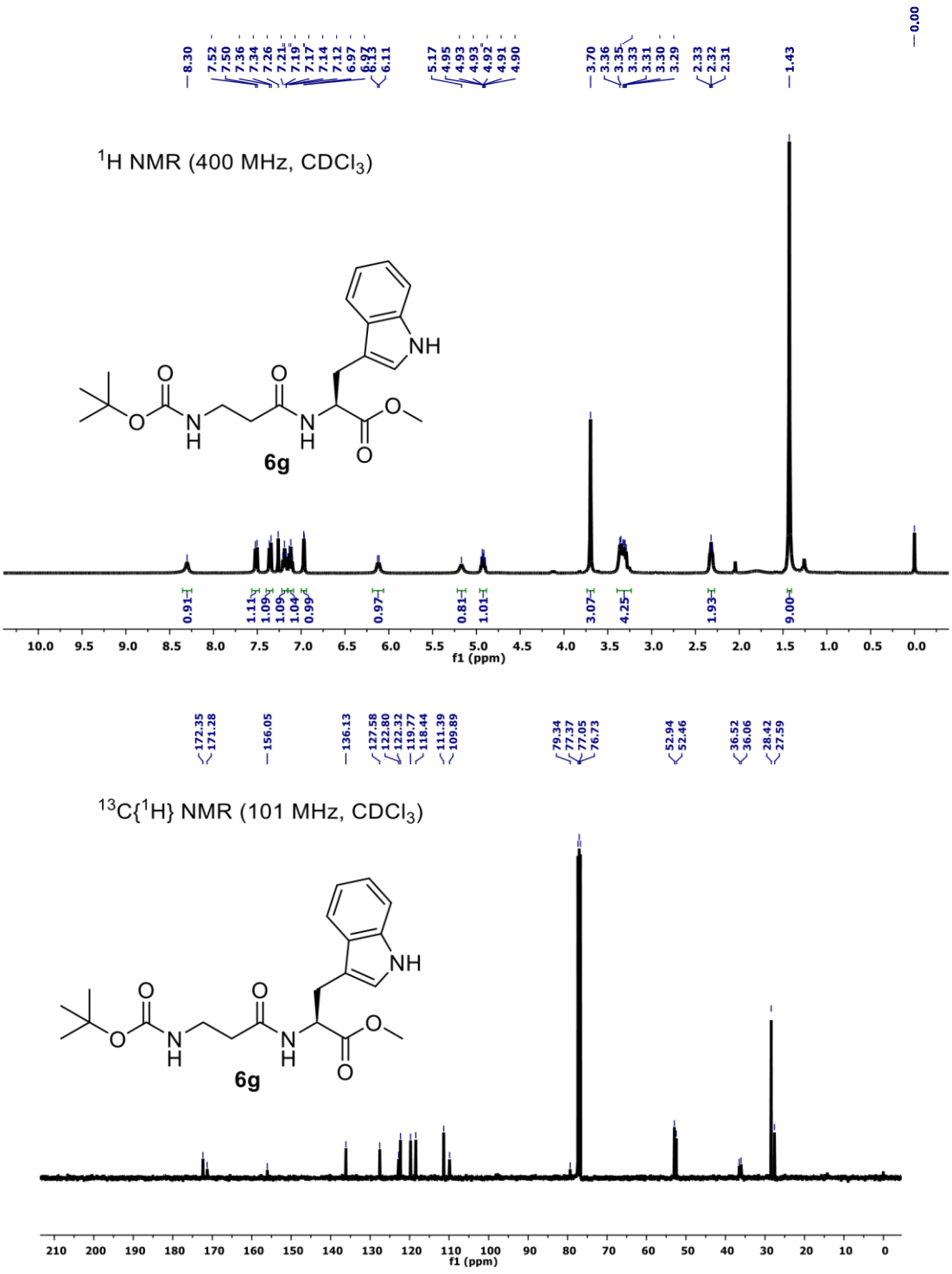

Fig S63. ^{1}H, ^{13}C $\{^{1}H\}$ NMR spectra of tryptophan-containing dipeptide **6g**.

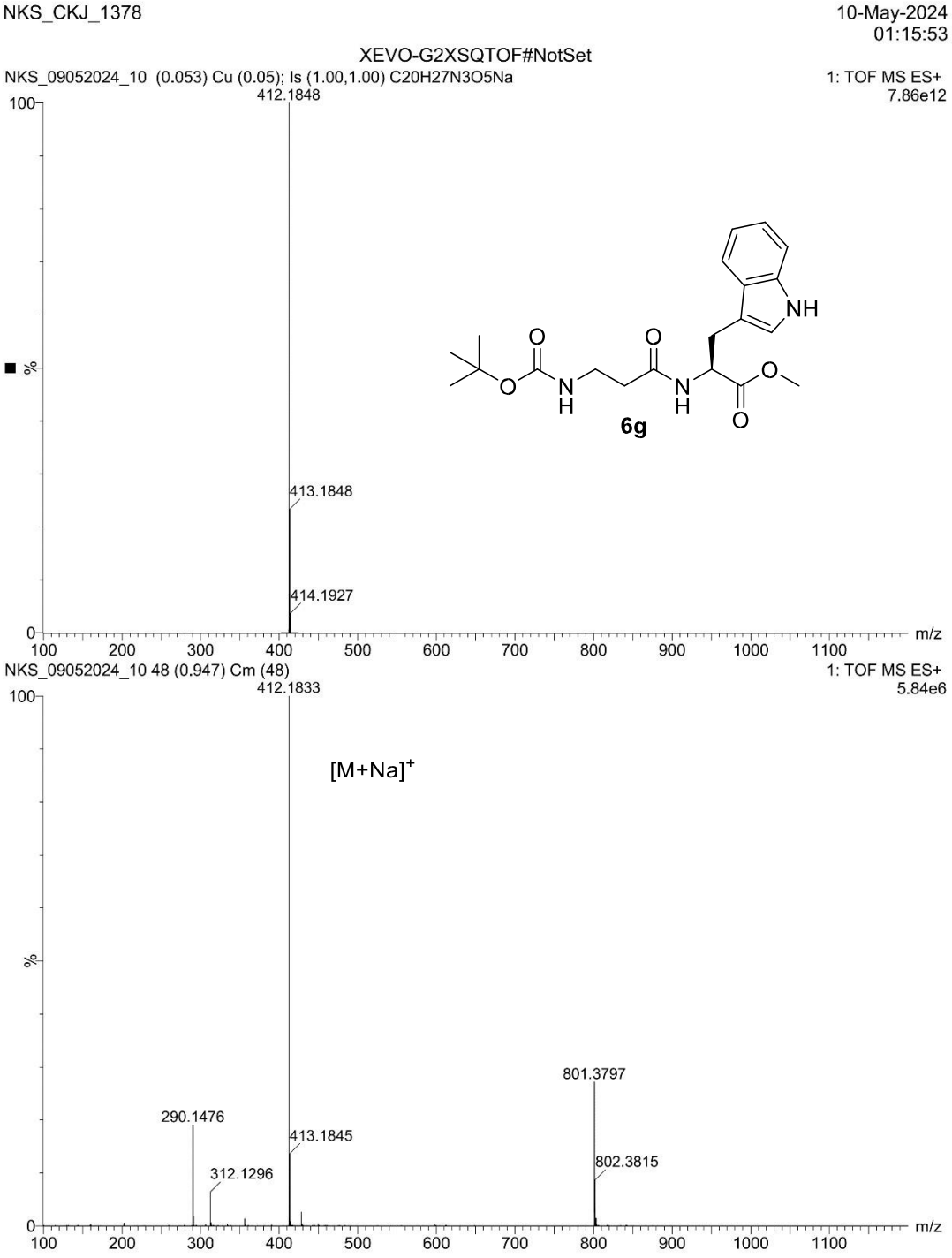

Fig S64. ESI-HRMS spectra of tryptophan-containing dipeptide **6g**.

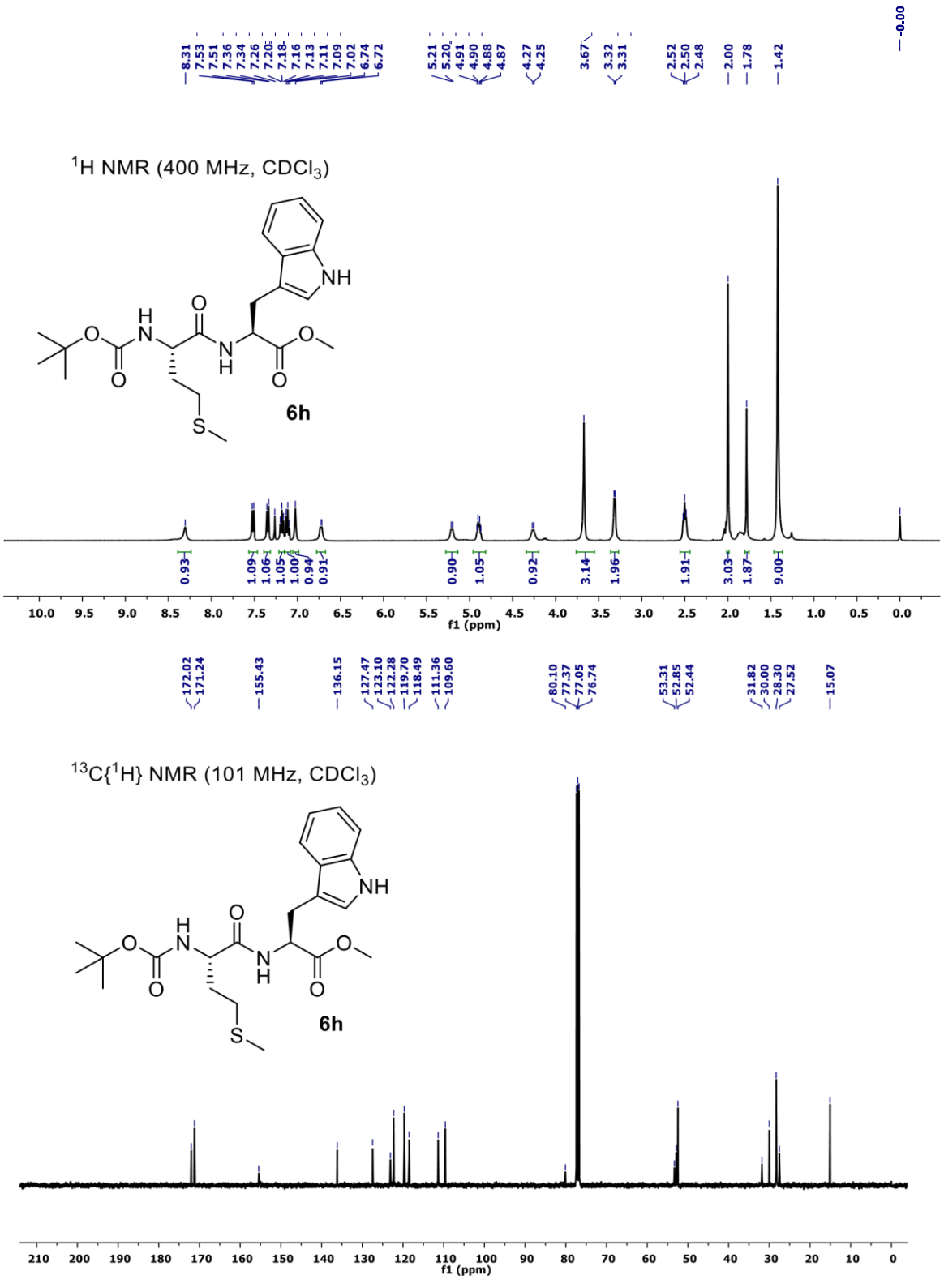

Fig S65. ^{1}H, ^{13}C $\{^{1}H\}$ NMR spectra of tryptophan-containing dipeptide **6h**.

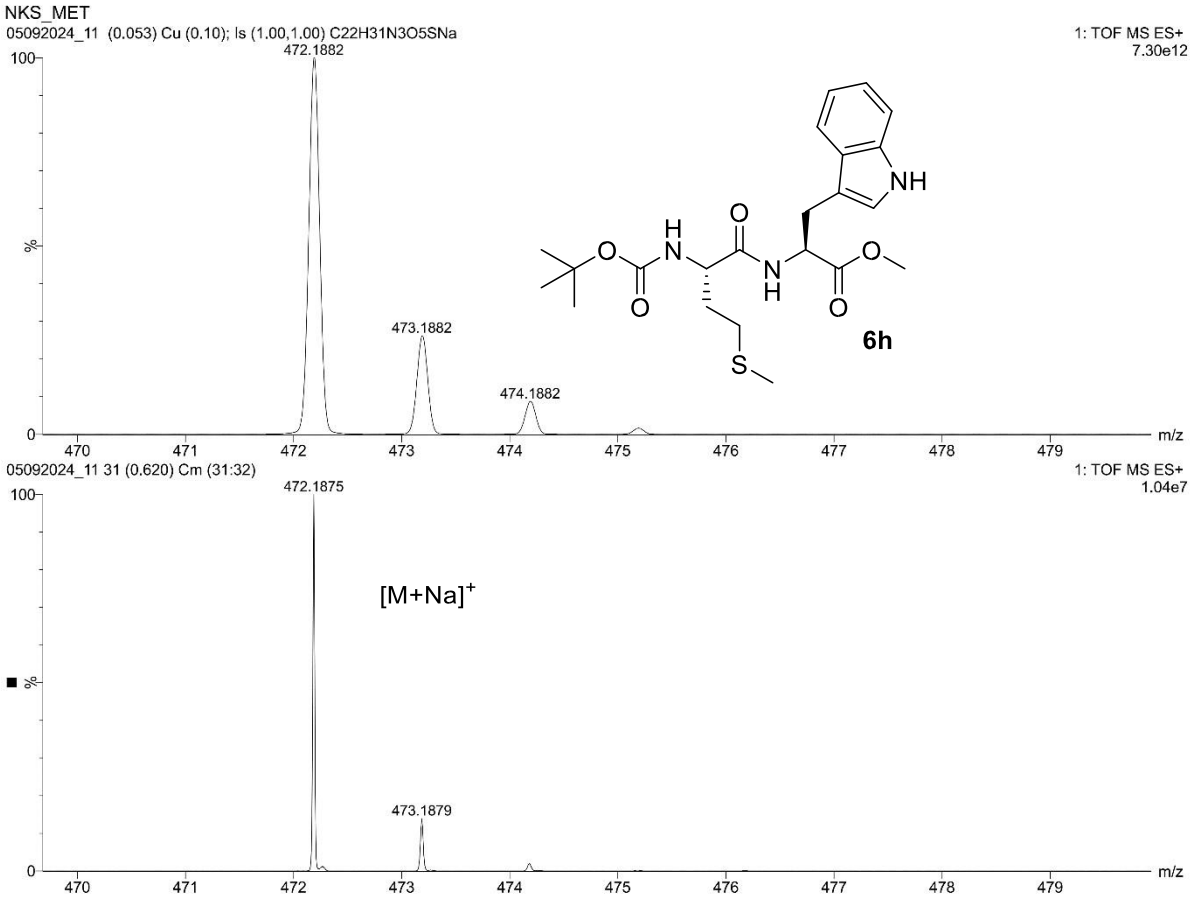

Fig S66. ESI-HRMS spectra of tryptophan-containing dipeptide **6h**.

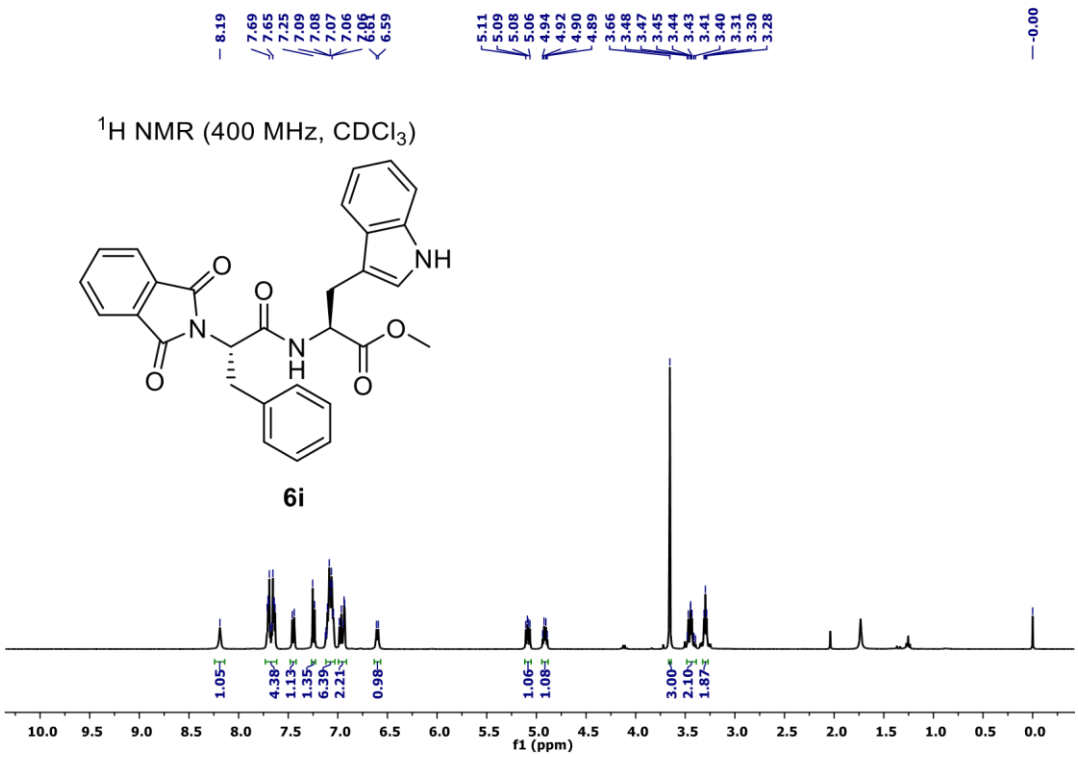
8.19
7.69
7.65
7.25
7.09
7.08
7.07
7.06
6.81
6.59
5.11
5.09
5.08
5.06
4.94
4.92
4.90
4.89
3.66
3.48
3.47
3.45
3.44
3.43
3.41
3.40
3.31
3.30
3.28
-0.00
1H NMR (400 MHz, CDCl3)
NH
O
N
H
6i
1.05
4.38
1.13
1.35
6.39
2.21
0.98
1.06
1.08
3.00
2.10
1.87
10.0 9.5 9.0 8.5 8.0 7.5 7.0 6.5 6.0 5.5 5.0 4.5 4.0 3.5 3.0 2.5 2.0 1.5 1.0 0.5 0.0
f1 (ppm)

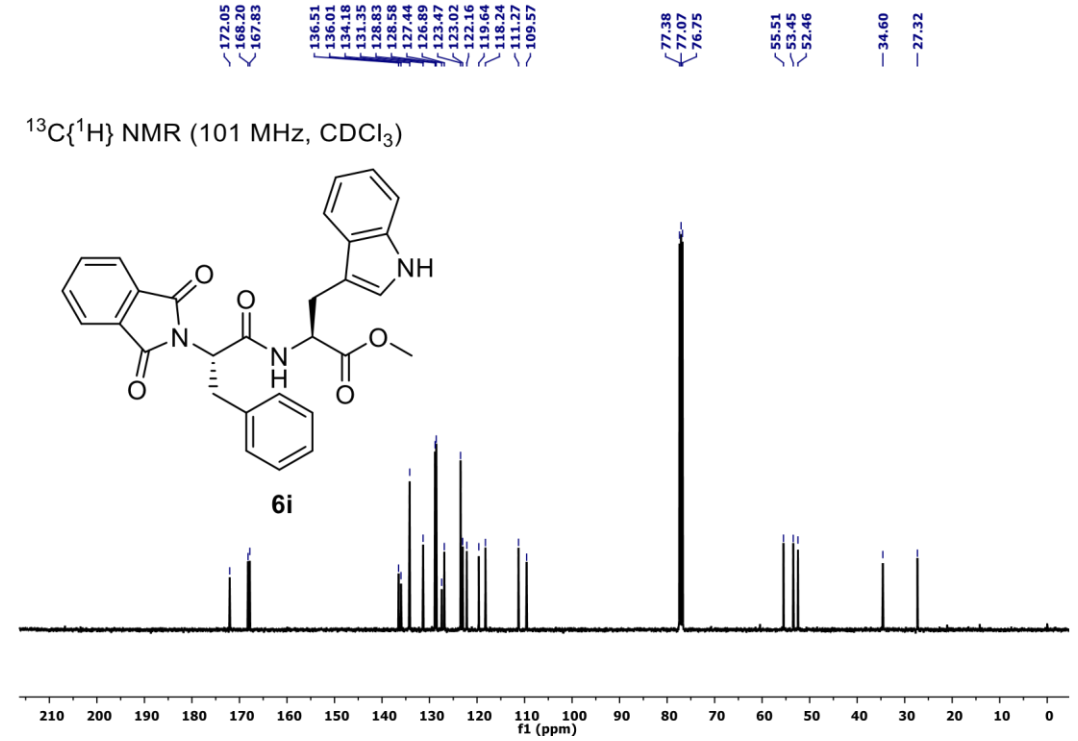
172.05
168.20
167.83
136.51
136.01
134.18
131.35
128.83
128.58
127.44
126.89
123.47
123.02
122.16
119.64
118.24
111.27
109.57
77.38
77.07
76.75
55.51
53.45
52.46
34.60
27.32
13C{1H} NMR (101 MHz, CDCl3)
NH
O
N
H
6i
210 200 190 180 170 160 150 140 130 120 110 100 90 80 70 60 50 40 30 20 10 0
f1 (ppm)

Fig S67. ^{1}H, ^{13}C $\{^{1}H\}$ NMR spectra of tryptophan-containing dipeptide **6i**.

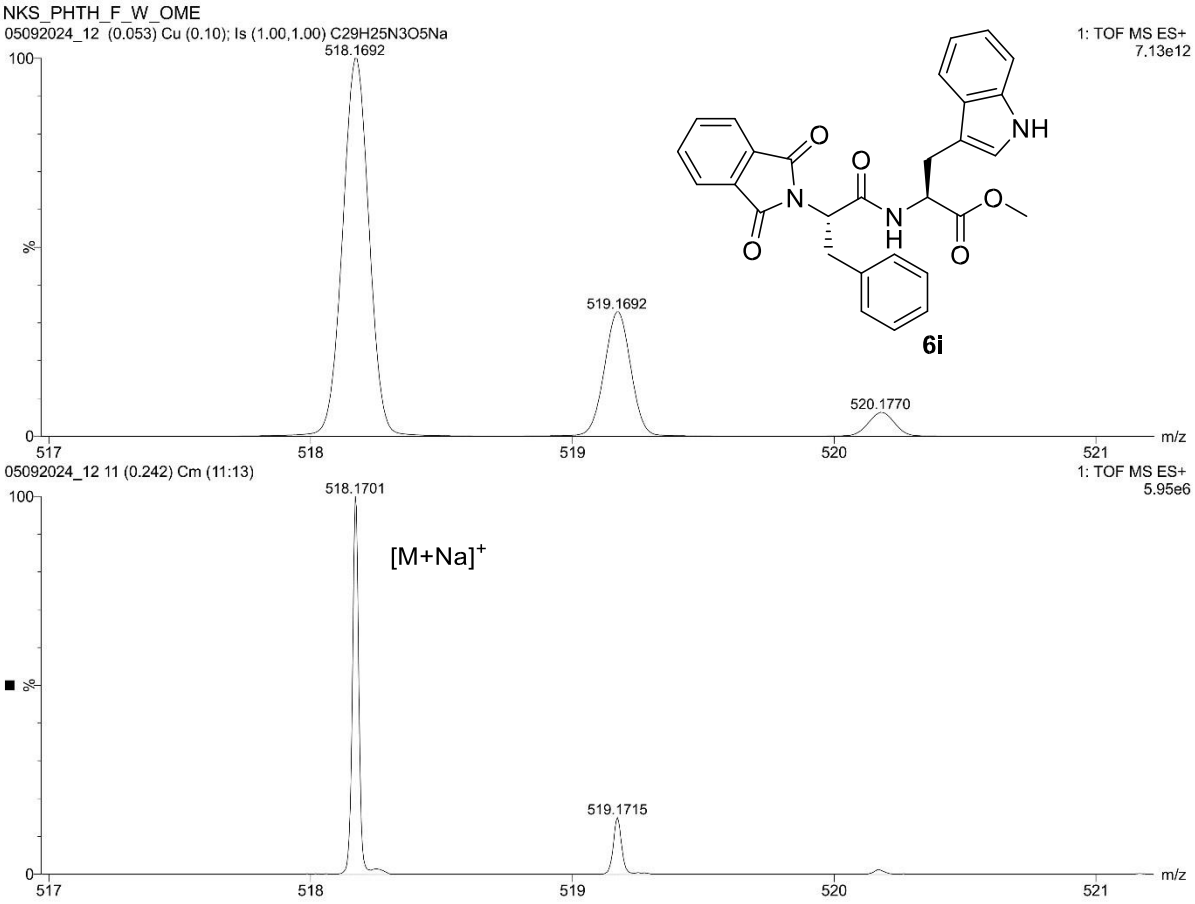

Fig S68. ESI-HRMS spectra of tryptophan-containing dipeptide **6i**.

2. NMR and Mass Spectra of Kynurenine Derivatives (**3a-3l**/**5a-5m**/**7a-7i**)

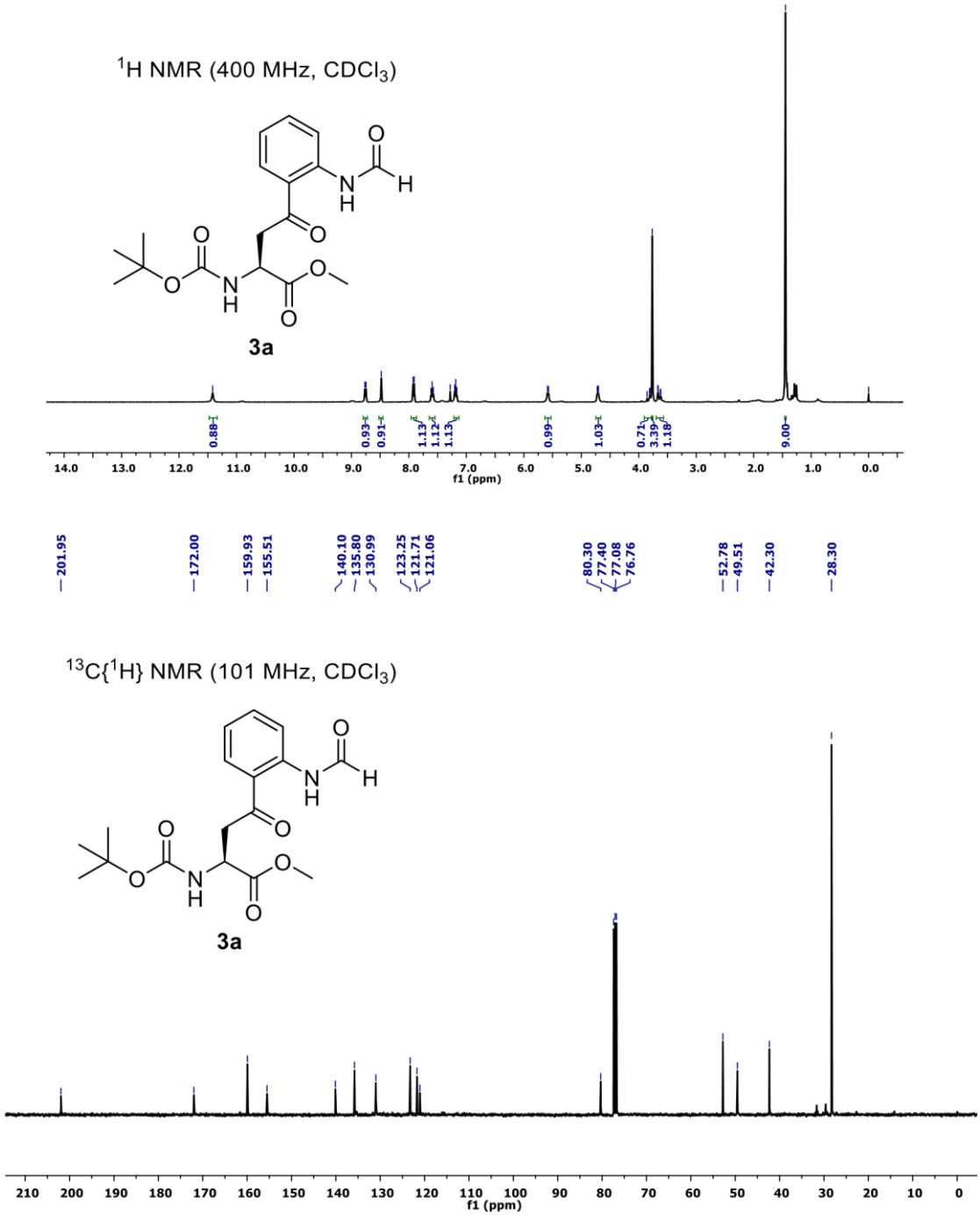

Fig S69. ^{1}H, ^{13}C $\{^{1}H\}$ NMR spectra of kynurenine derivative **3a**.

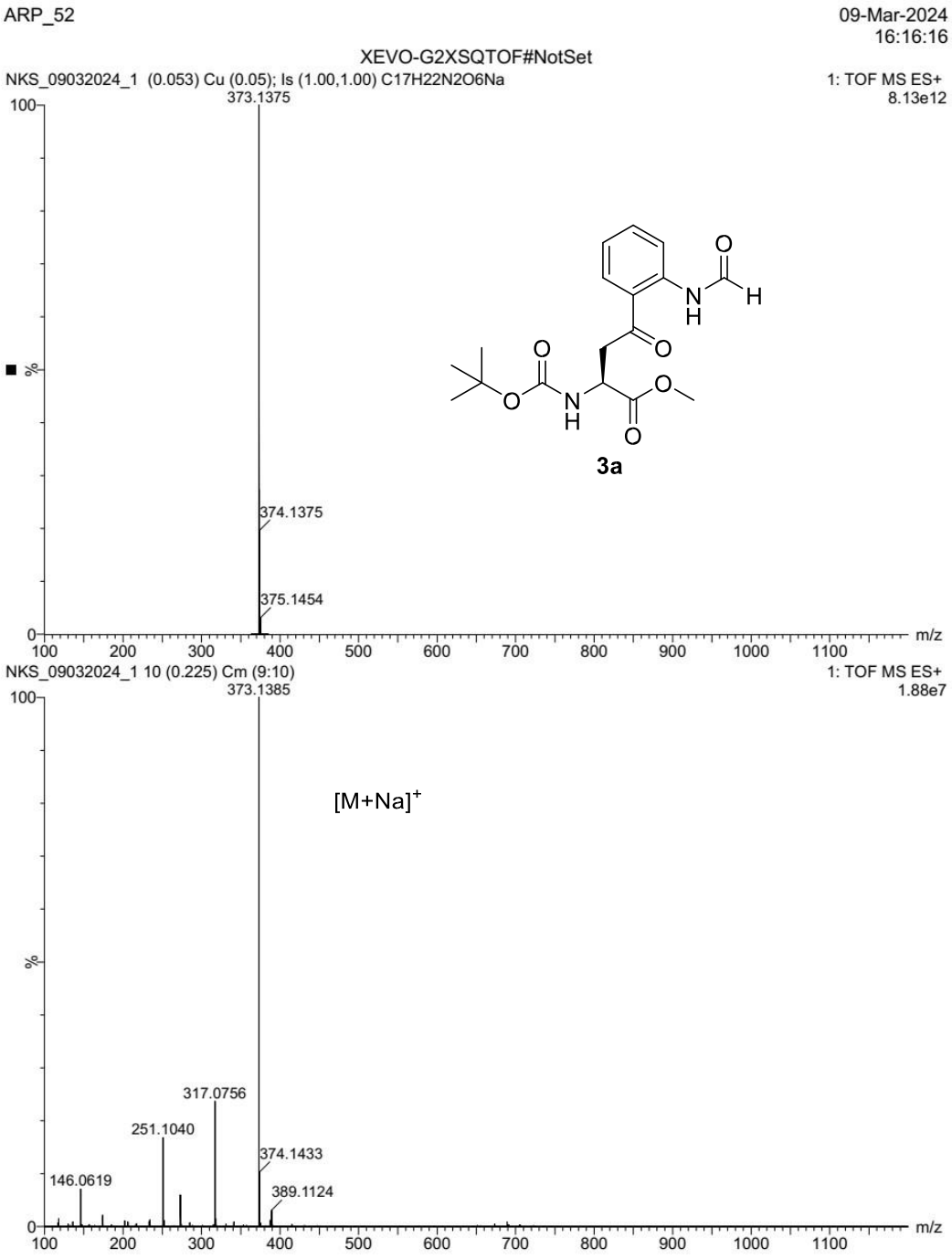

Fig S70. ESI-HRMS spectra of kynurenine derivative **3a**.

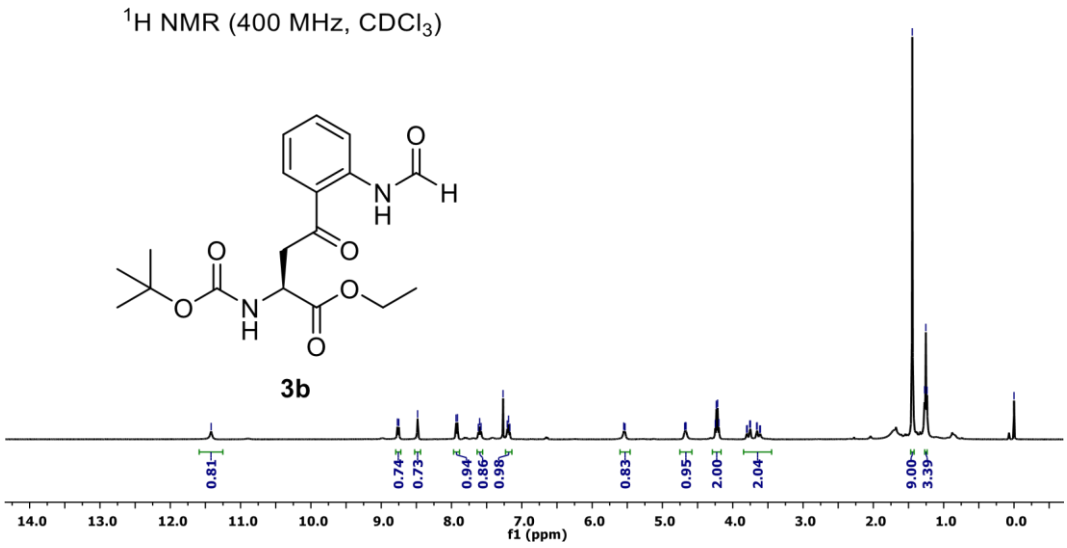

Fig ^{1}H, ^{13}C $\{^{1}$ of

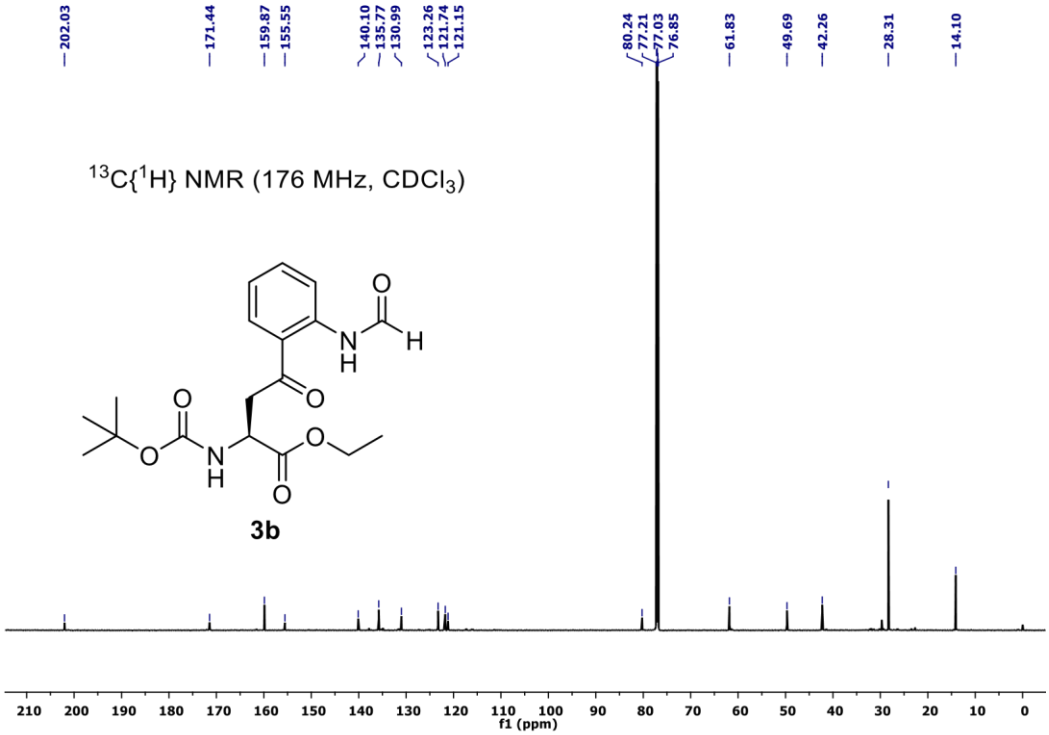

S71. H} NMR spectra kynurenine derivative **3b**.

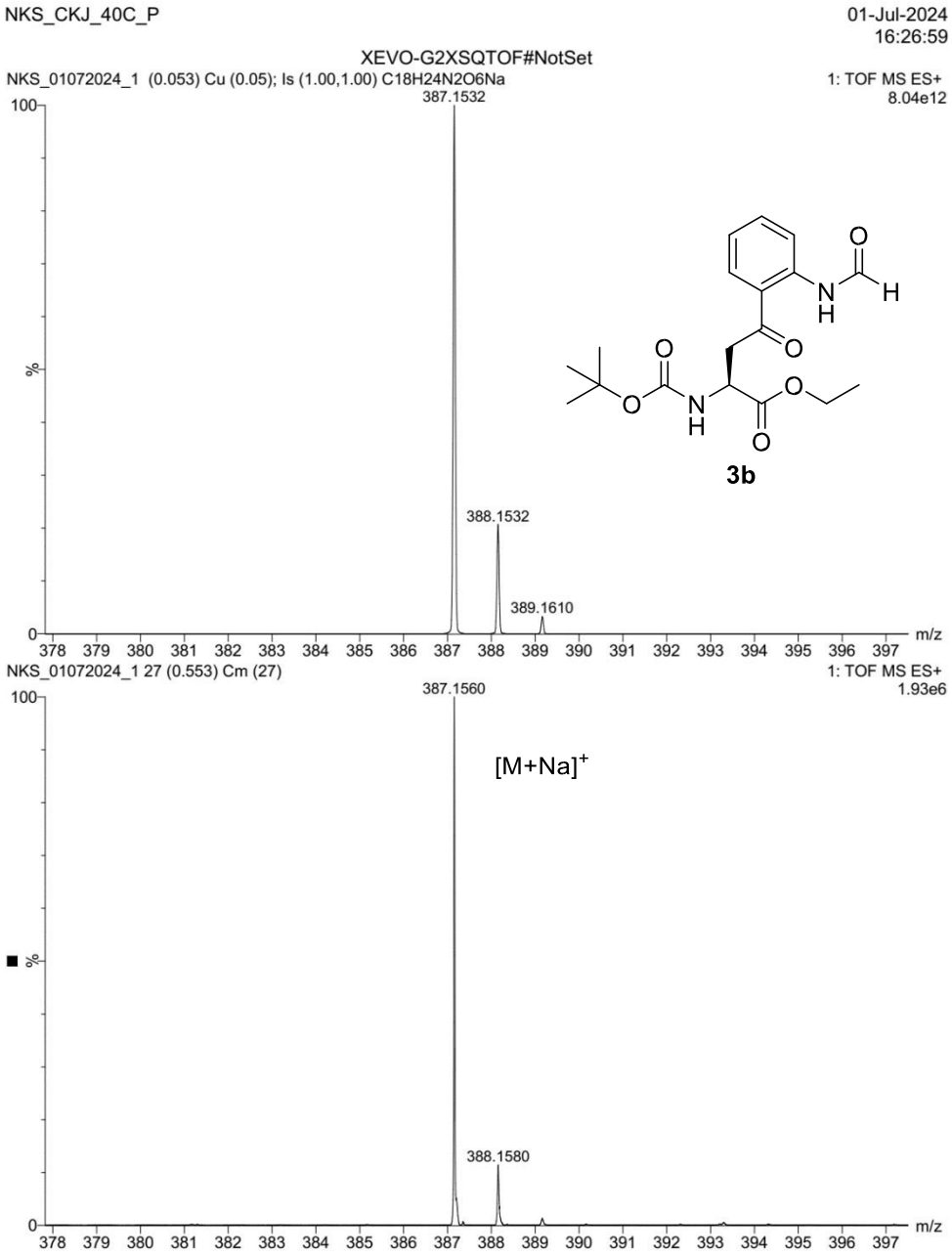

Fig ^{1}H, ^{13}C {^{1} of

Fig S72. ESI-HRMS spectra of kynurenine derivative **3b**.

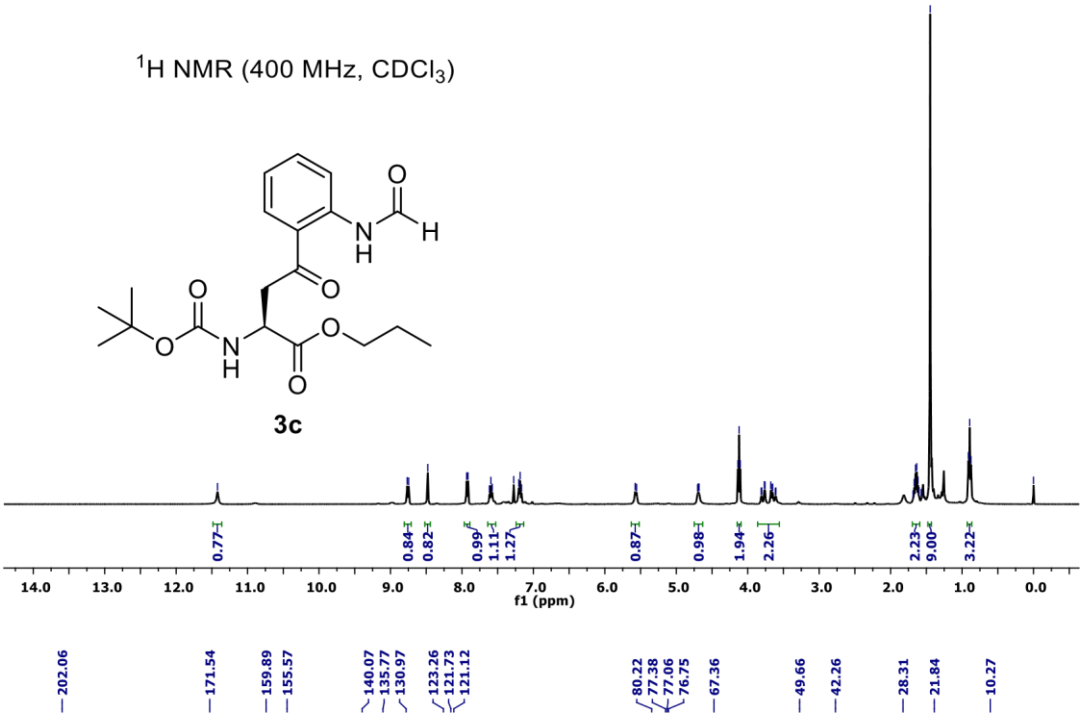

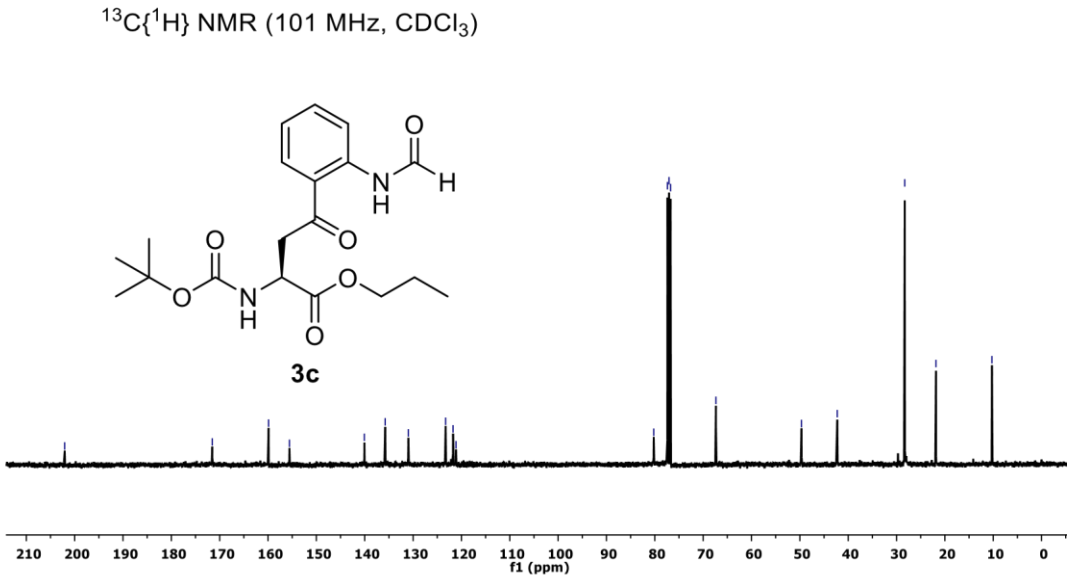

S73. H} NMR spectra kynurenine derivative **3c**.

Fig ^{1}H, ^{13}C {^{1} of

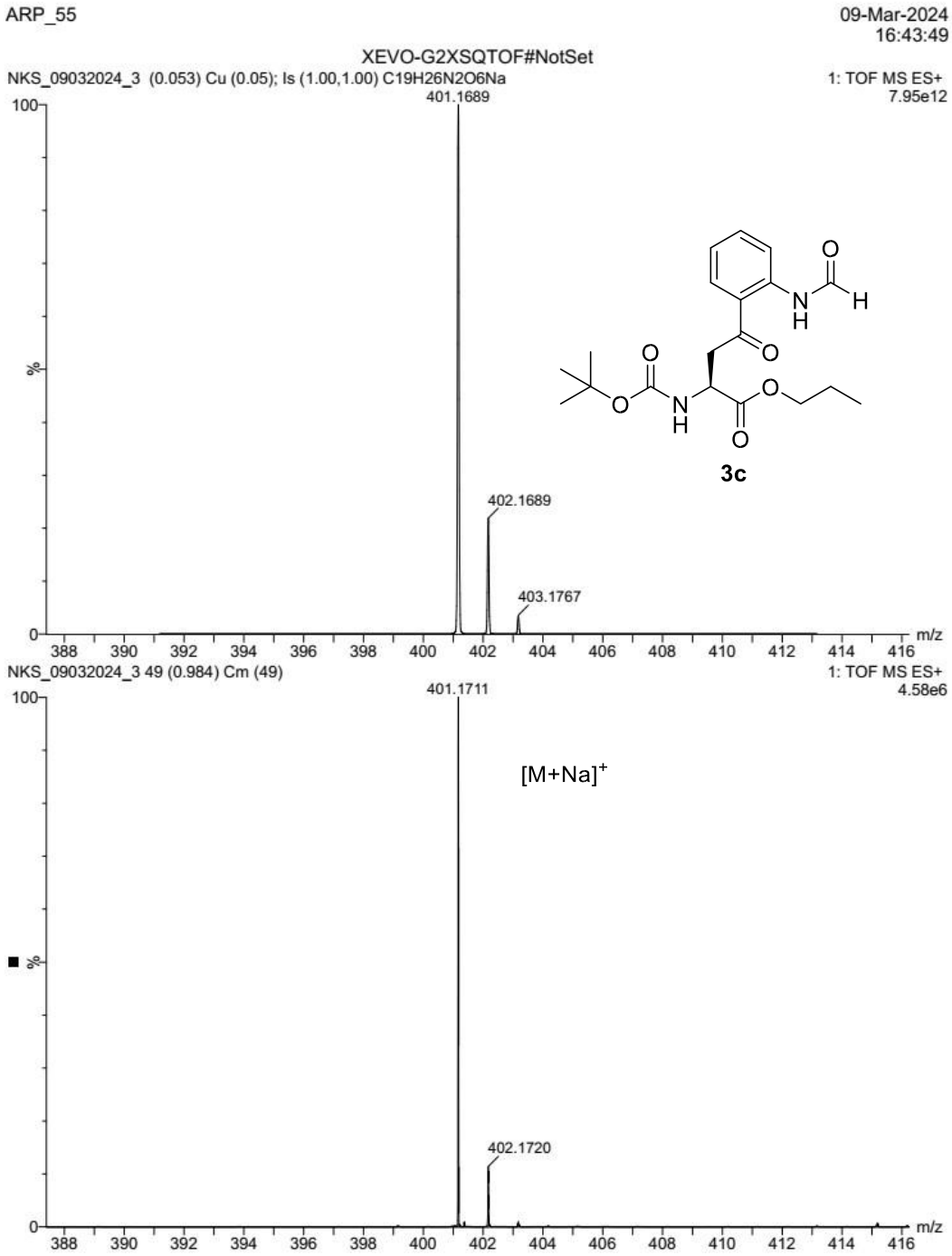

Fig S74. ESI-HRMS spectra of kynurenine derivative **3c**.

Fig ^{1}H, ^{13}C {^{1} of

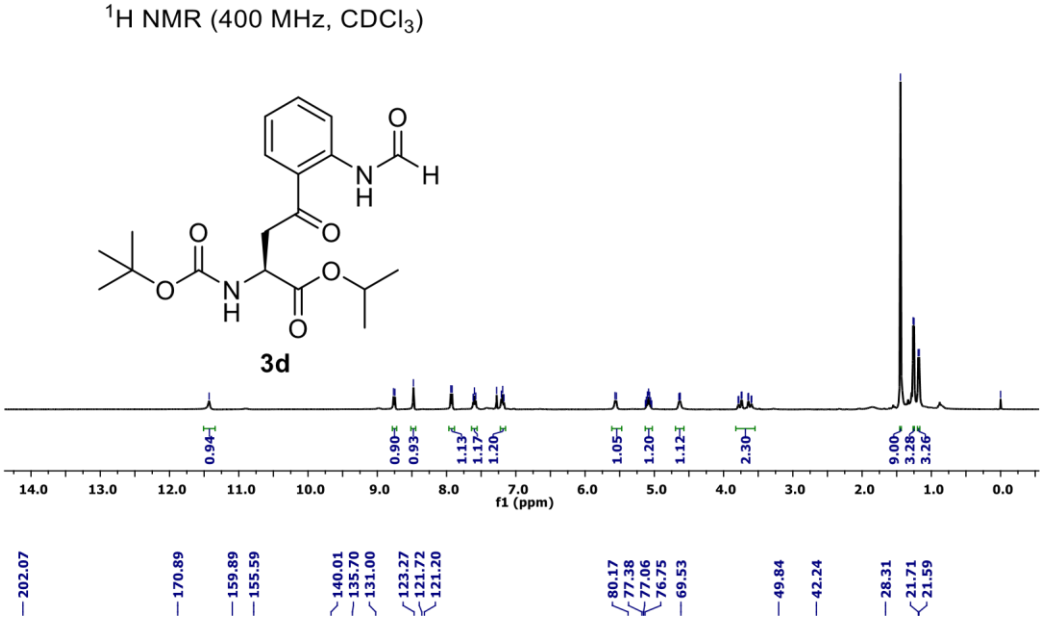

Fig ^{1}H, ^{13}C {^{1} of

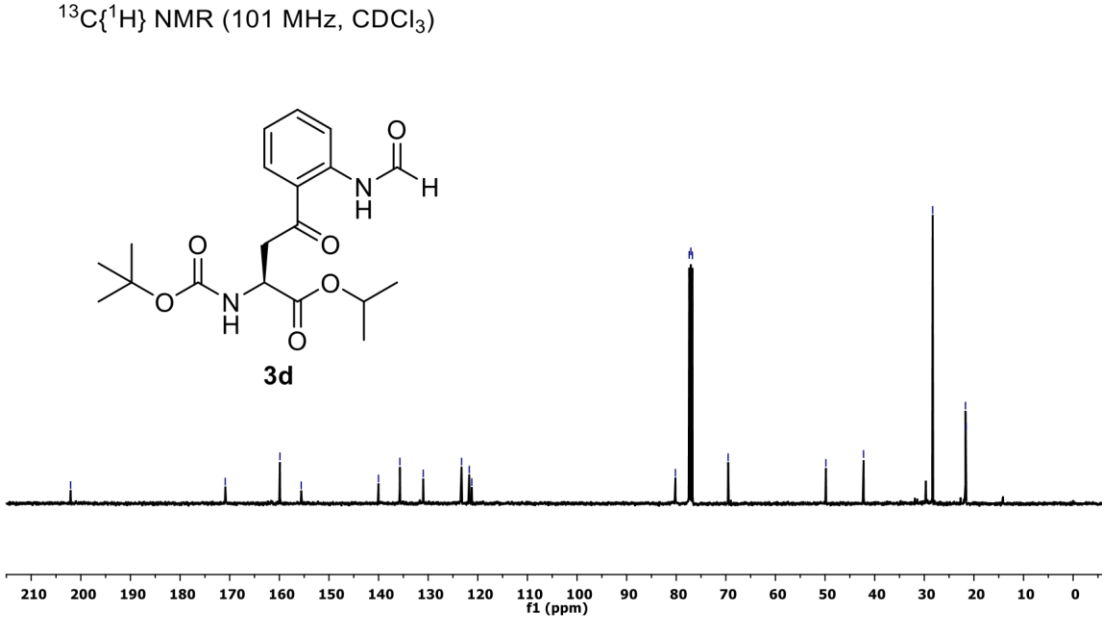

S75. H} NMR spectra kynurenine derivative **3d**.

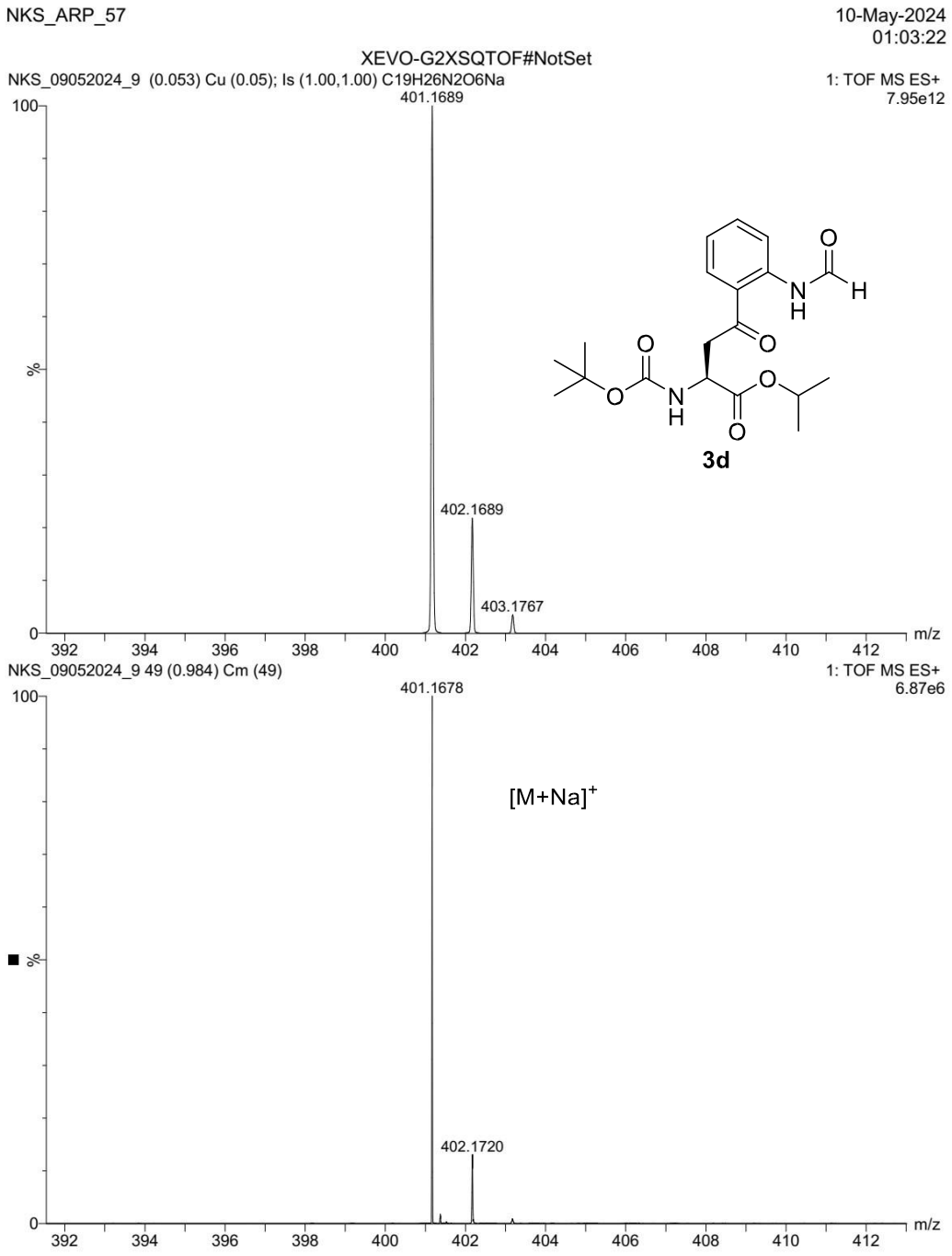

Fig S76. ESI-HRMS spectra of kynurenine derivative **3d**.

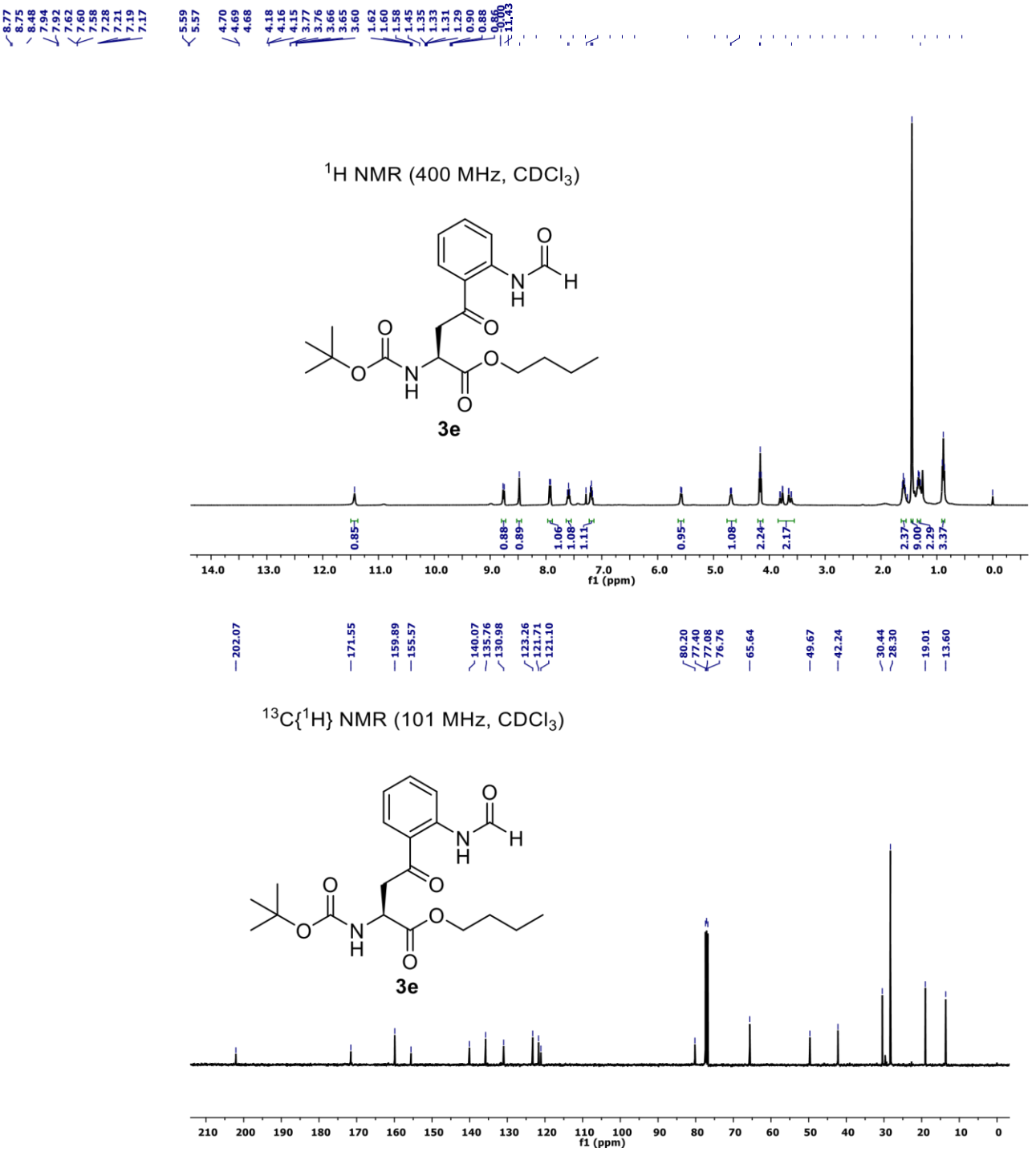

Fig S77. ^{1}H, ^{13}C $\{^{1}H\}$ NMR spectra of kynurenine derivative **3e**.

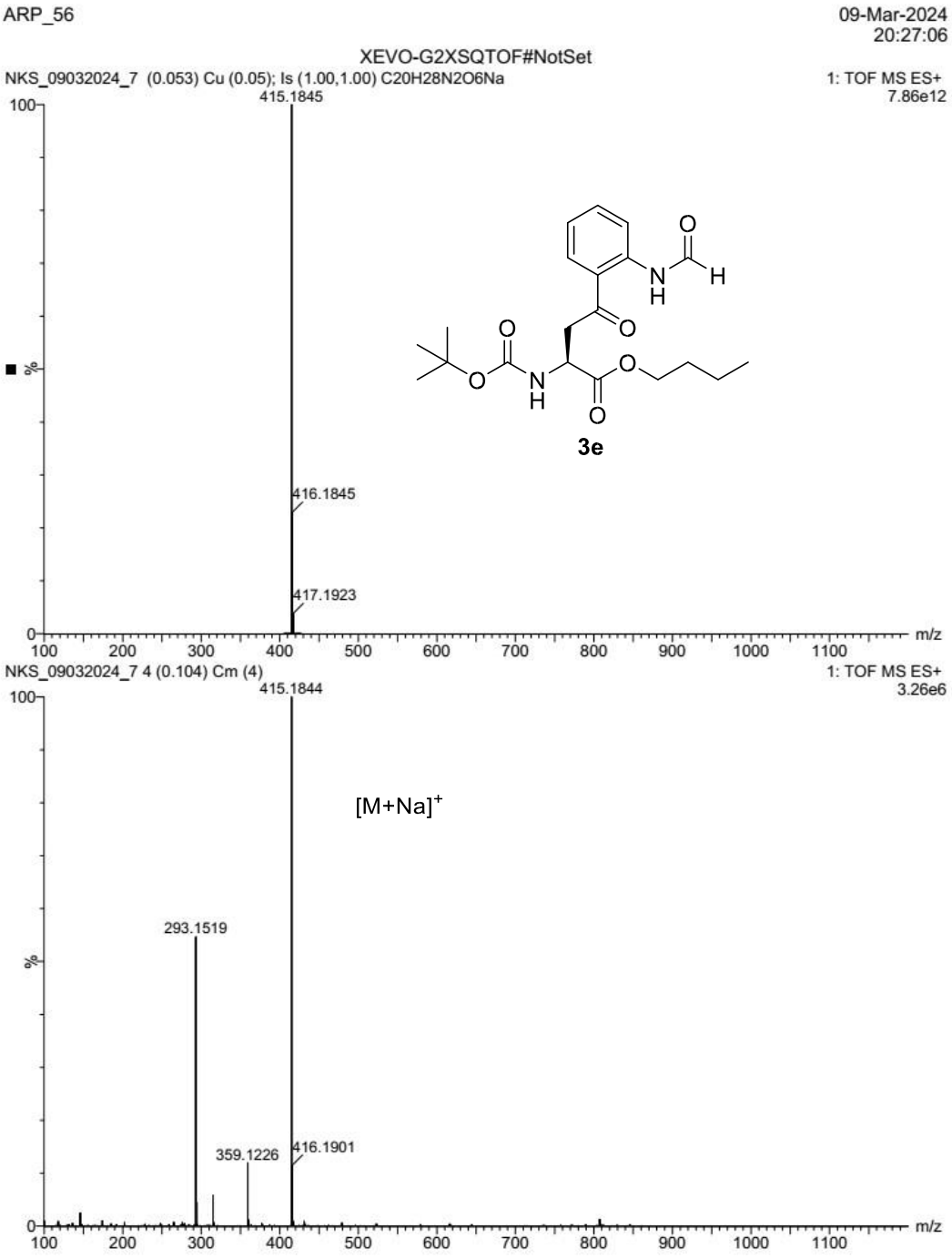

Fig S78. ESI-HRMS spectra of kynurenine derivative **3e**.

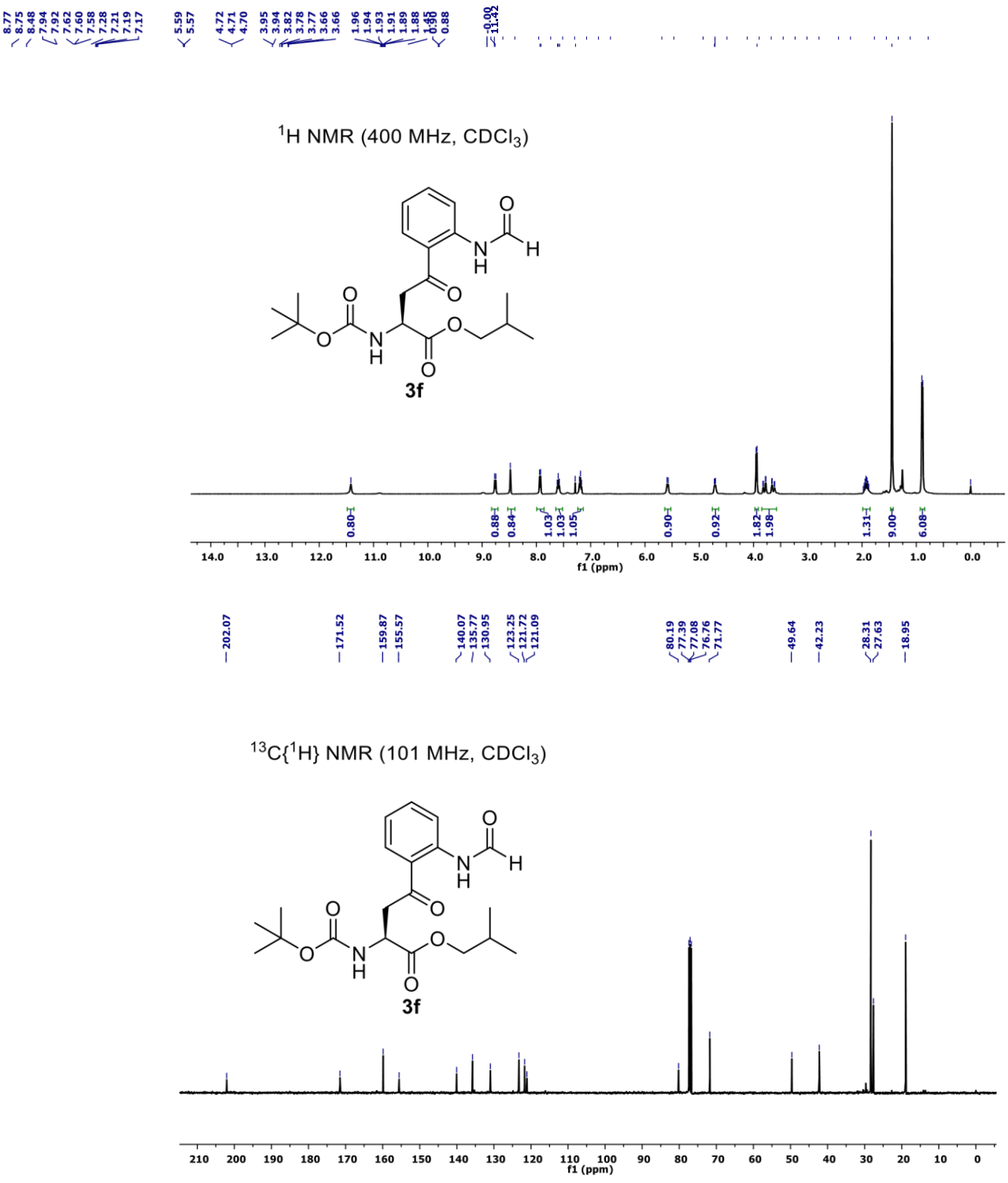

Fig S79. ^{1}H, ^{13}C $\{^{1}H\}$ NMR spectra of kynurenine derivative **3f**.

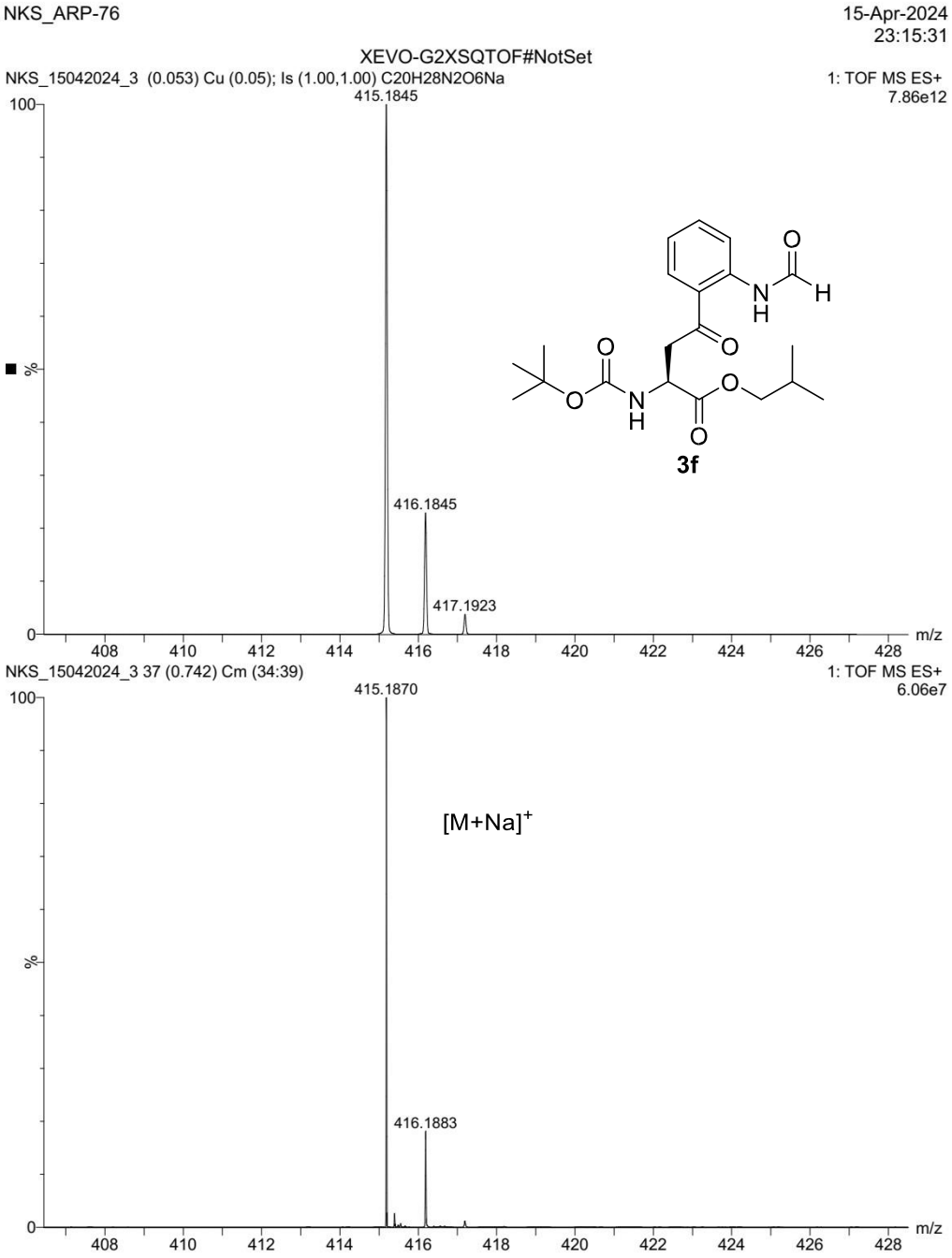

Fig S80. ESI-HRMS spectra of kynurenine derivative **3f**.

^{1}H NMR (400 MHz, $CDCl_3$)

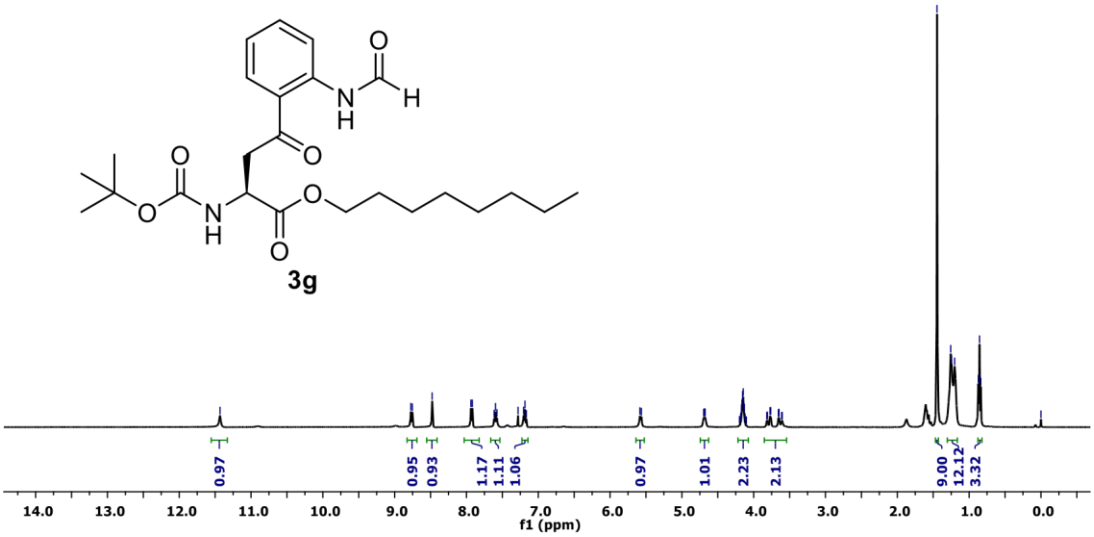

^{13}C{^{1}H} NMR (101 MHz, $CDCl_3$)

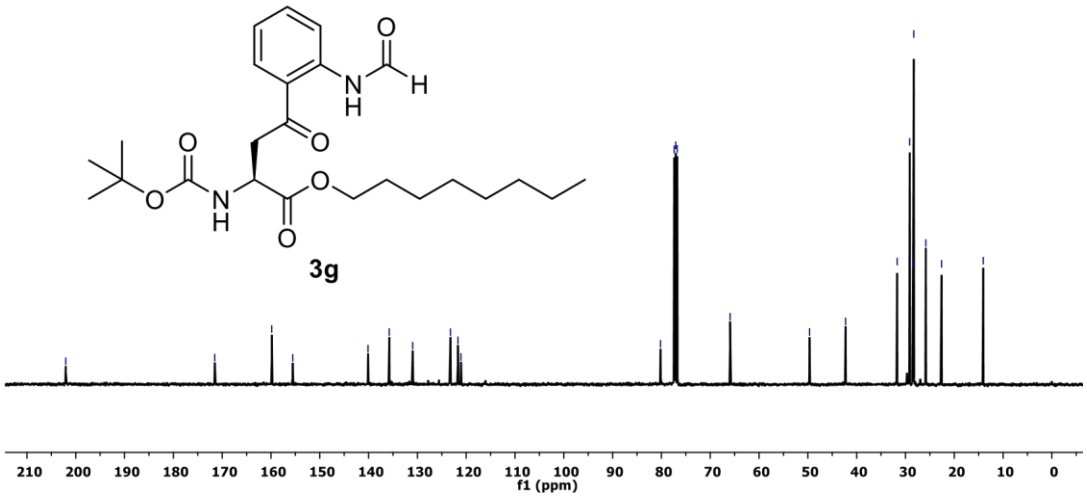

Fig S81. ^{1}H, ^{13}C $\{^{1}H\}$ NMR spectra of kynurenine derivative **3g**.

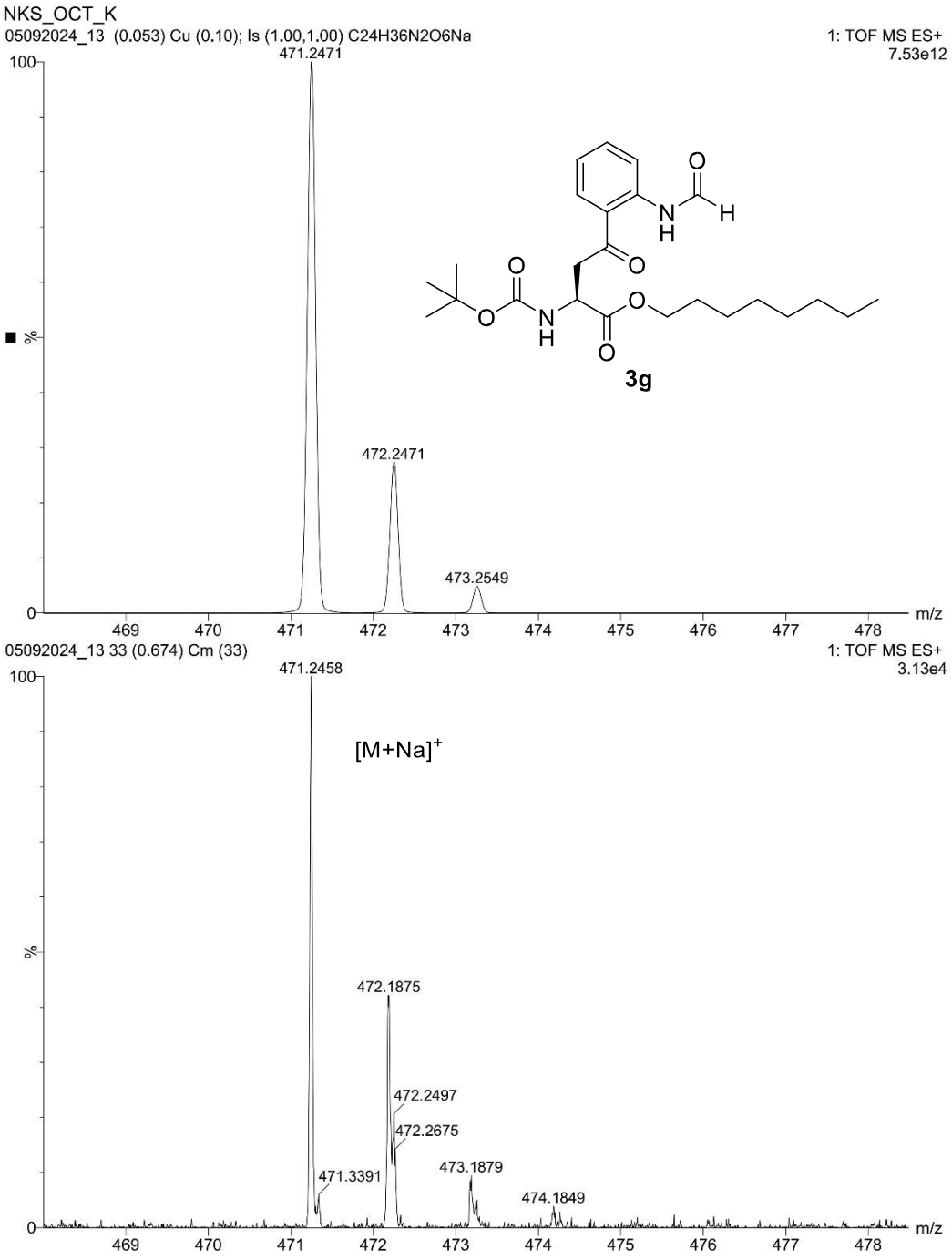

Fig S82. ESI-HRMS spectra of kynurenine derivative **3g**.

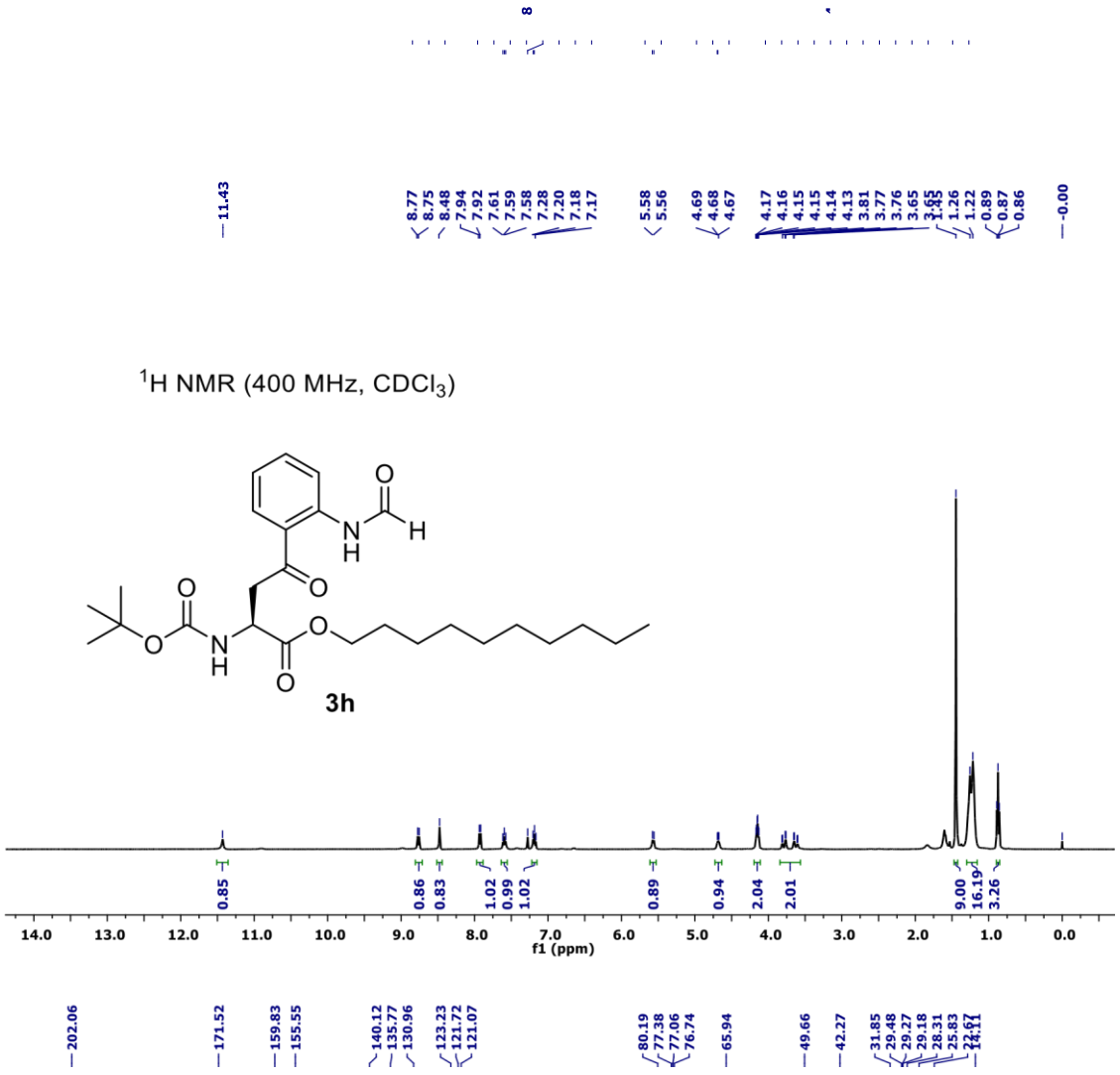
^{1}H NMR (400 MHz, $CDCl_3$)
3h
f1 (ppm)

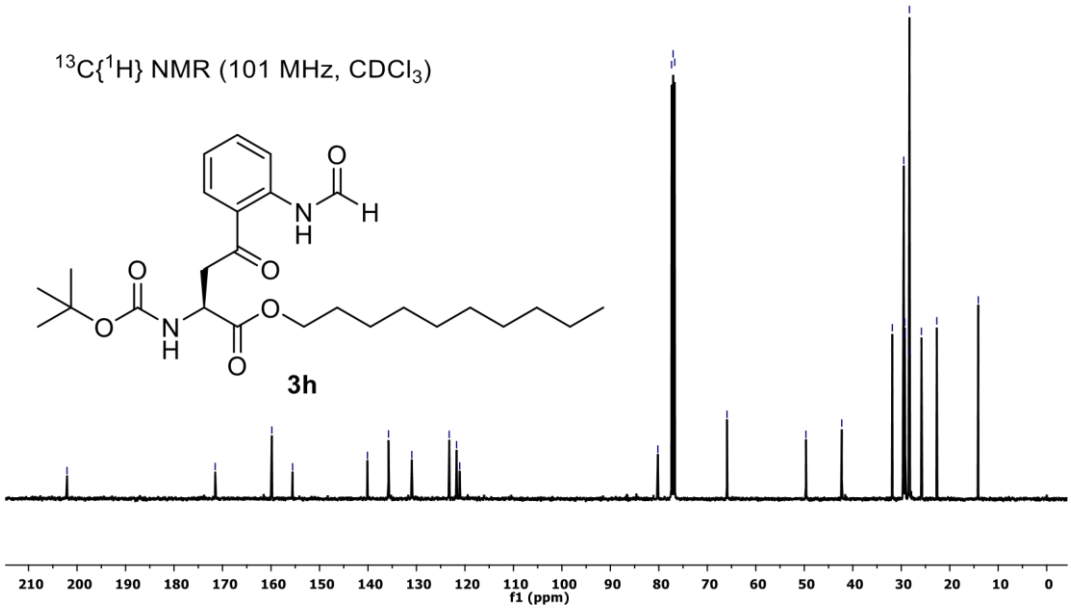

Fig S83. ^{1}H, ^{13}C $\{^{1}H\}$ NMR spectra of kynurenine derivative **3h**.

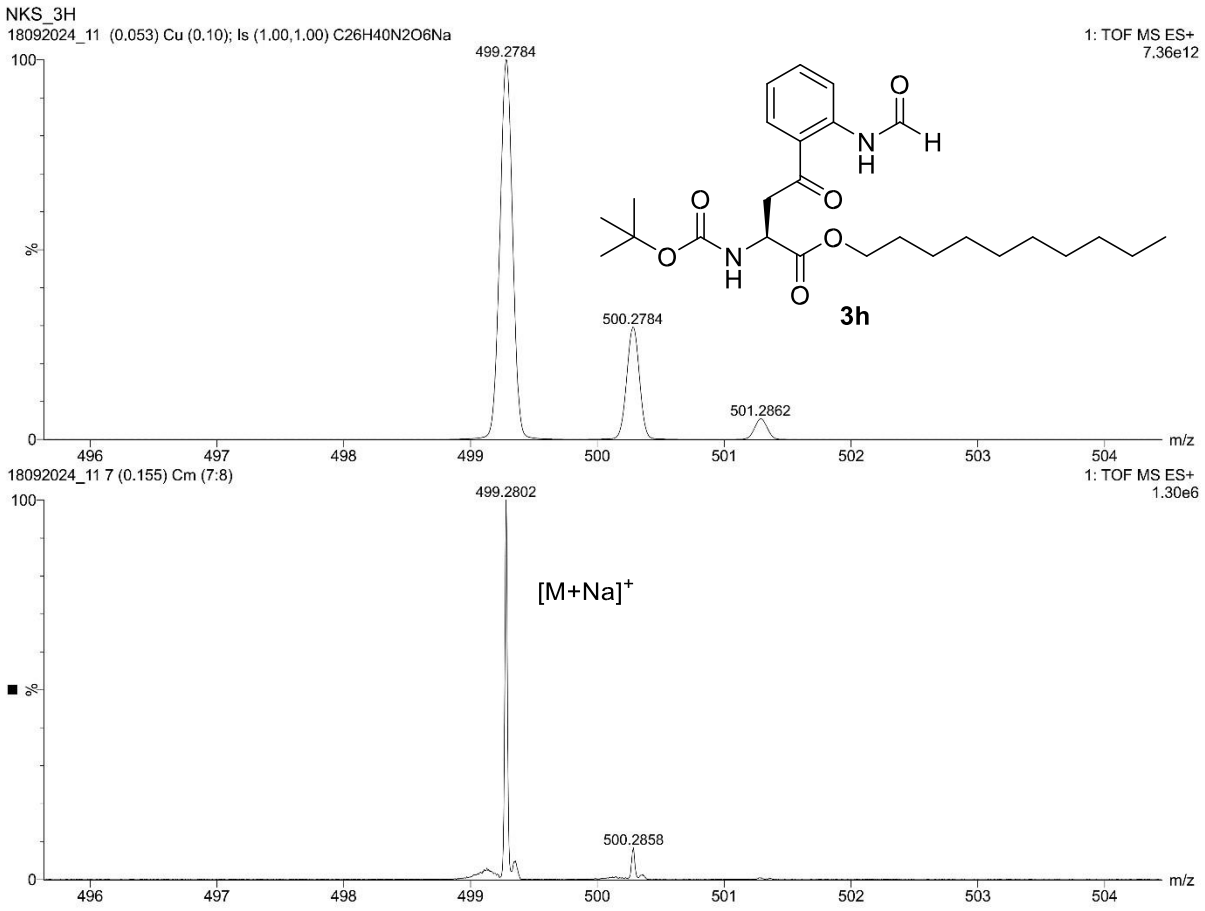

Fig S84. ESI-HRMS spectra of kynurenine derivative **3h**.

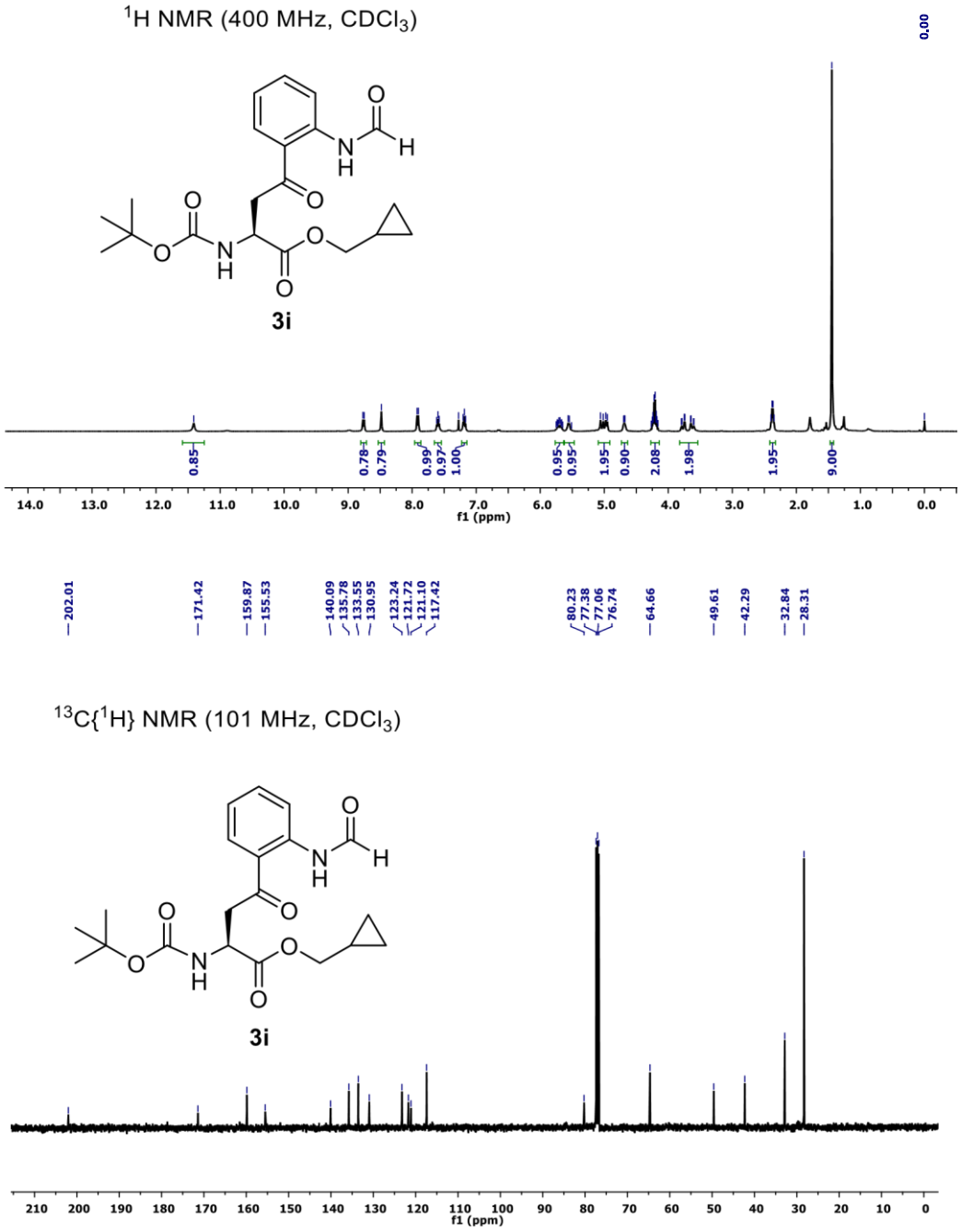

Fig S85. ^{1}H, ^{13}C {^{1}H} NMR spectra of kynurenine derivative **3i**.

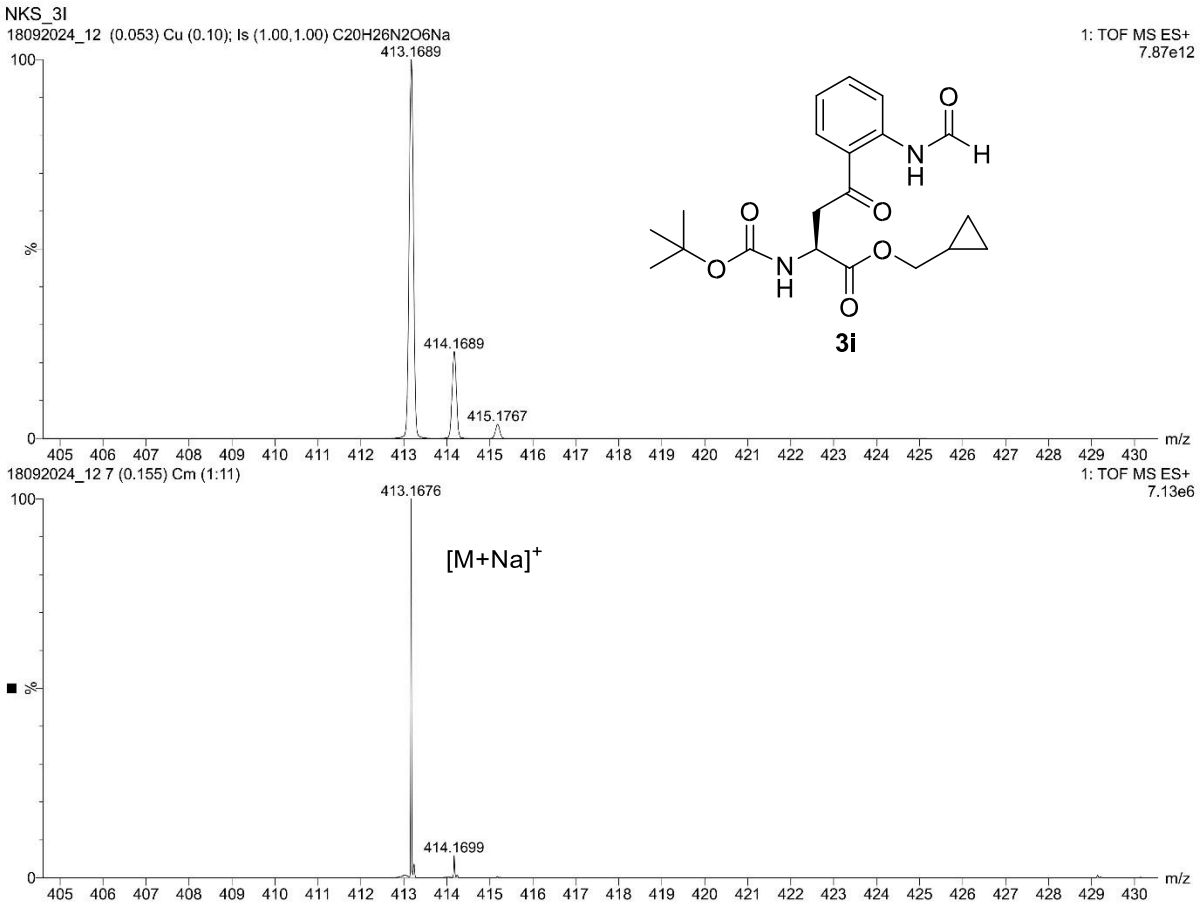

Fig S86. ESI-HRMS spectra of kynurenine derivative **3i**.

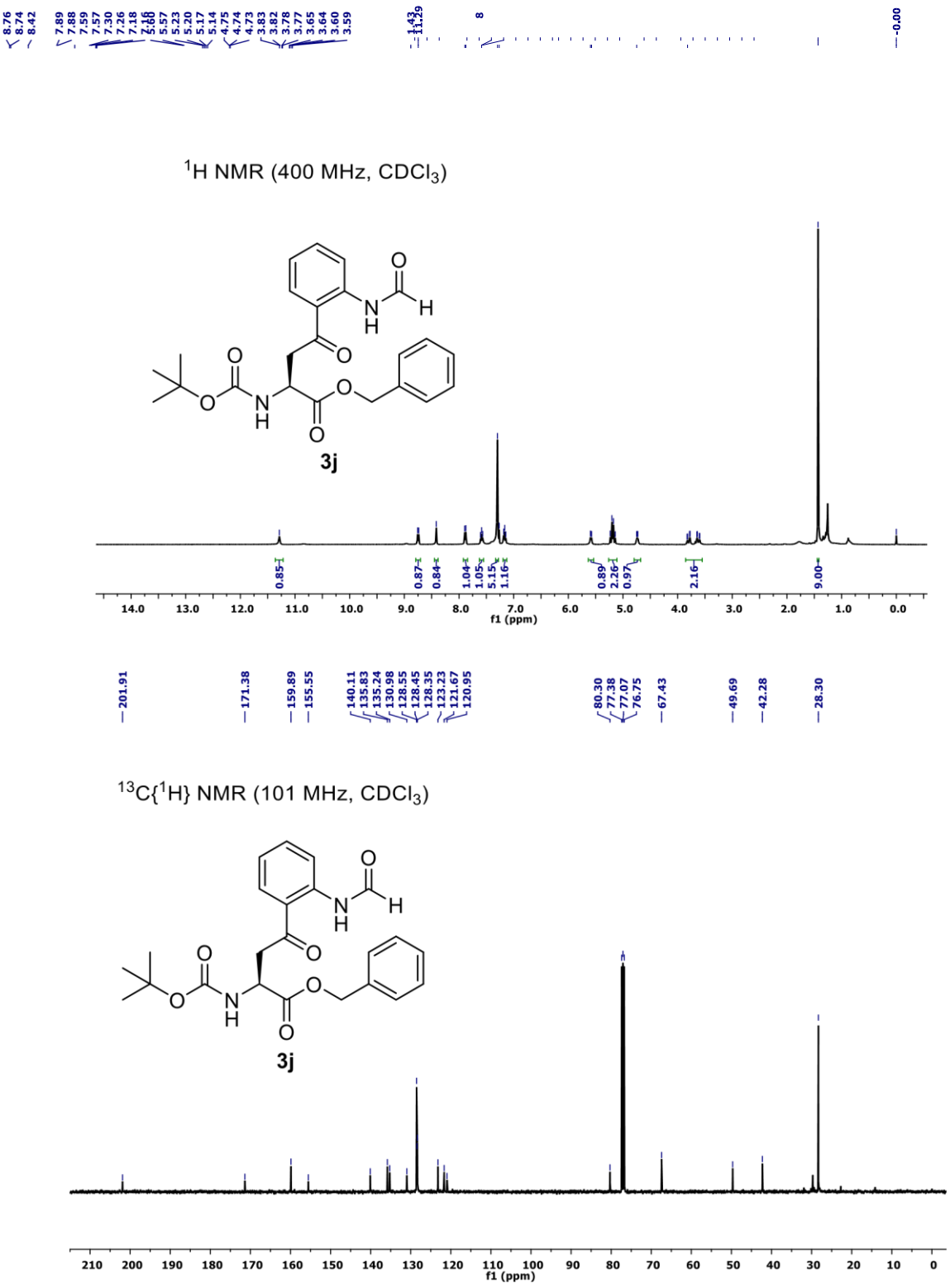

Fig S87. ^{1}H, ^{13}C $\{^{1}H\}$ NMR spectra of kynurenine derivative **3j**.

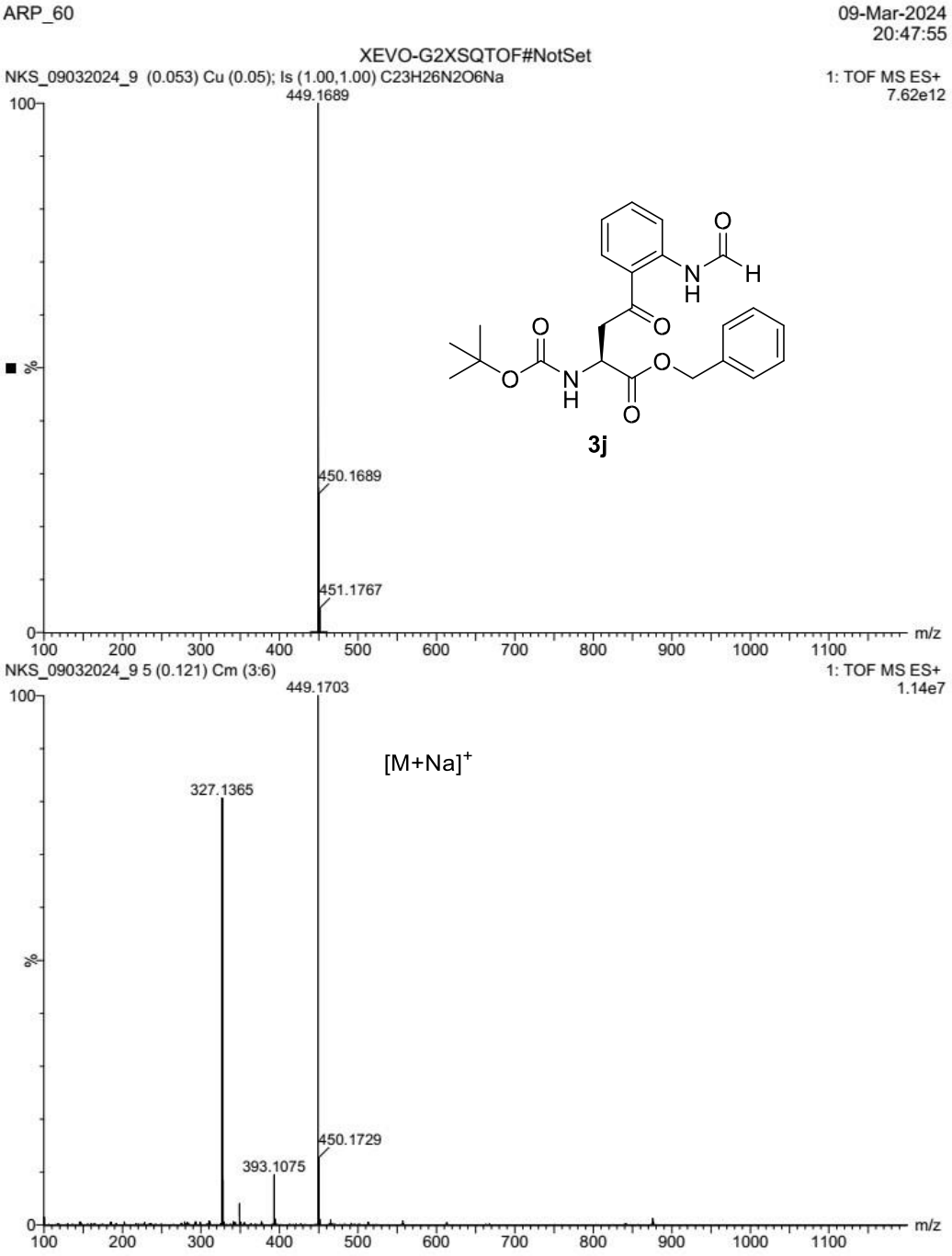
ARP_60
09-Mar-2024
20:47:55
XEVO-G2XSQTOF#NotSet
NKS_09032024_9 (0.053) Cu (0.05); Is (1.00,1.00) C23H26N2O6Na
1: TOF MS ES+
7.62e12
449.1689
450.1689
451.1767
3j
NKS_09032024_9 5 (0.121) Cm (3:6)
1: TOF MS ES+
1.14e7
449.1703
[M+Na]+
327.1365
450.1729
393.1075
m/z

Fig S88. ESI-HRMS spectra of kynurenine derivative **3j**.

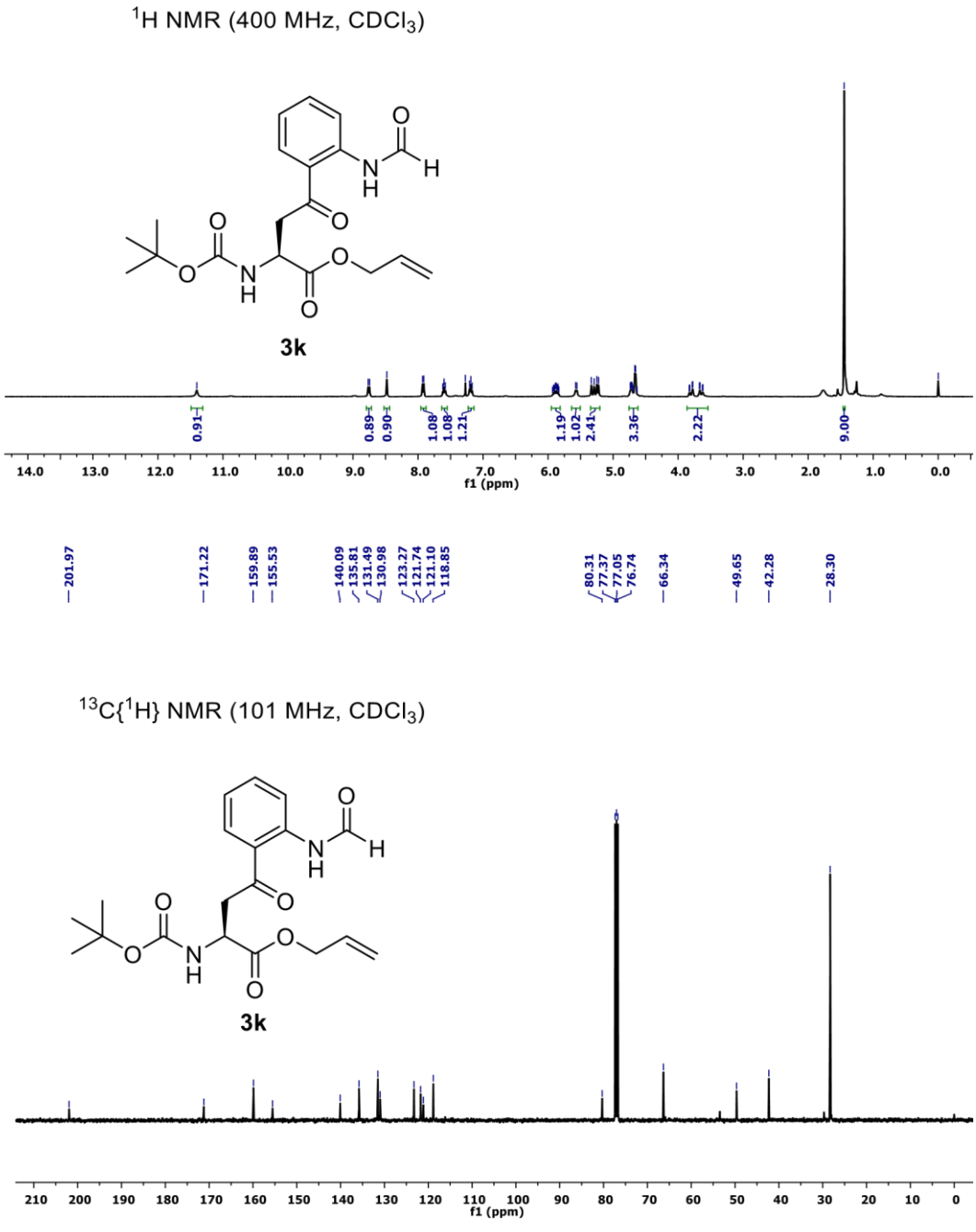

Fig S89. ^{1}H, ^{13}C $\{^{1}H\}$ NMR spectra of kynurenine derivative **3k**.

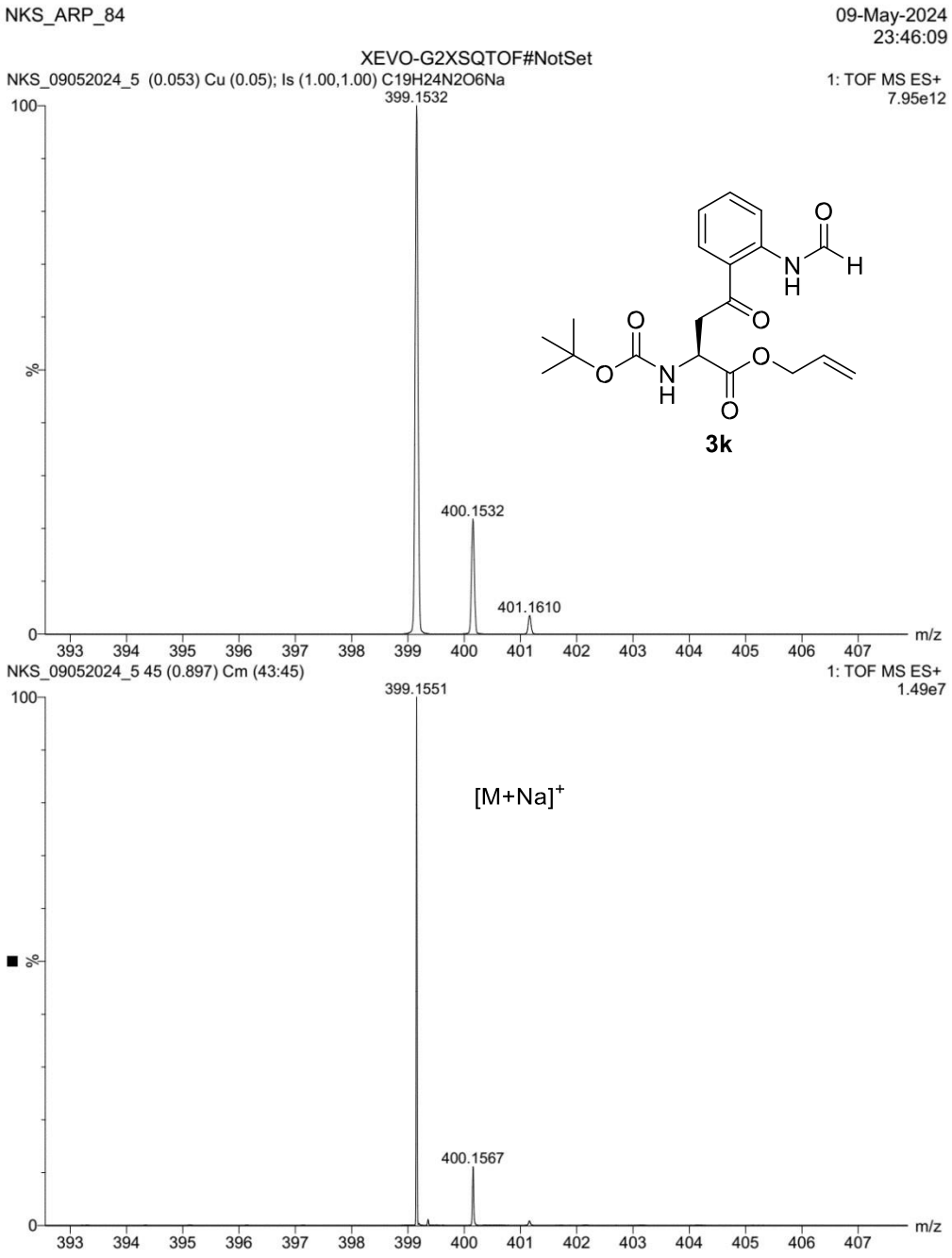

Fig S90. ESI-HRMS spectra of kynurenine derivative **3k**.

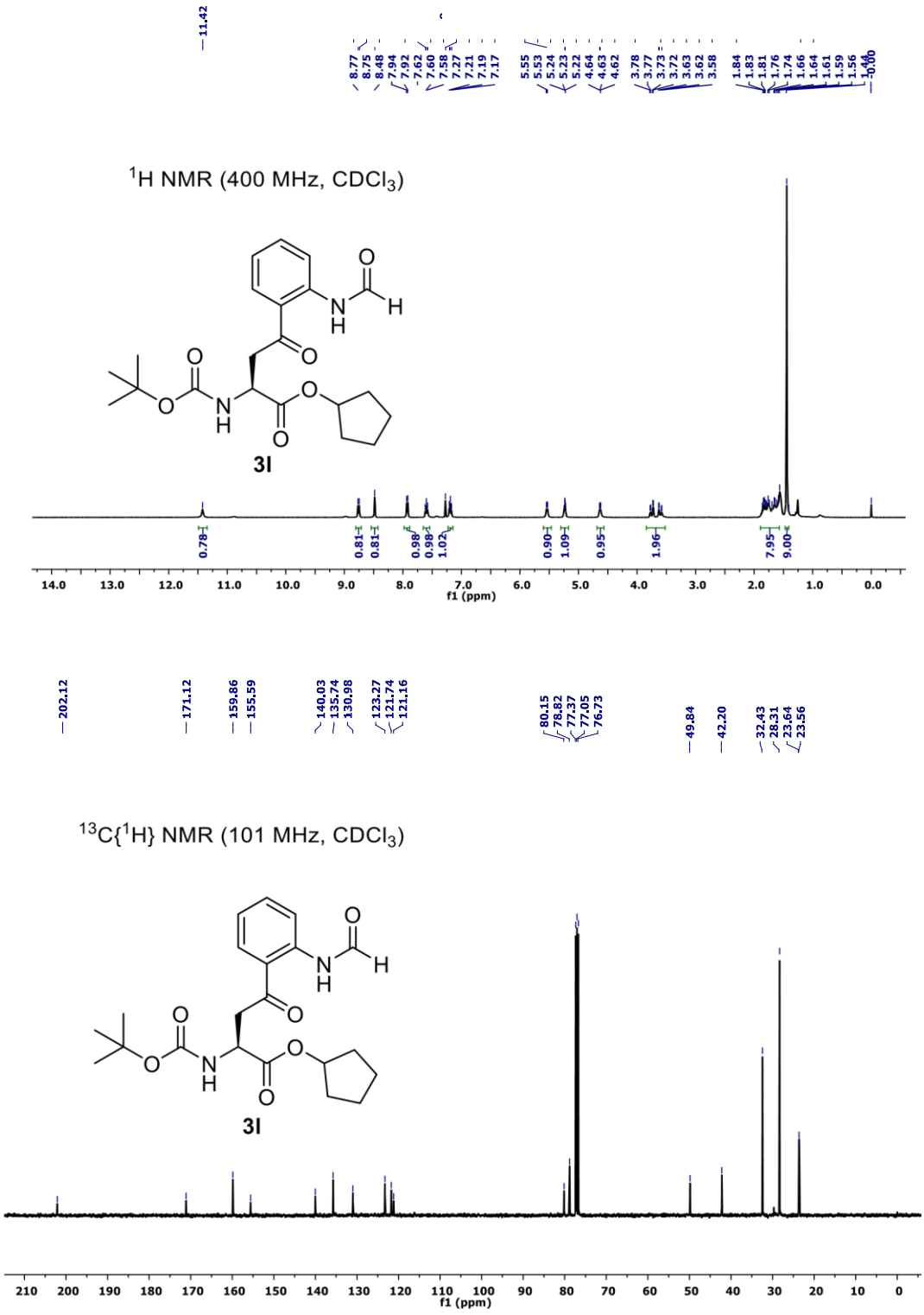

Fig S91. ^{1}H, ^{13}C $\{^{1}H\}$ NMR spectra of kynurenine derivative **3l**.

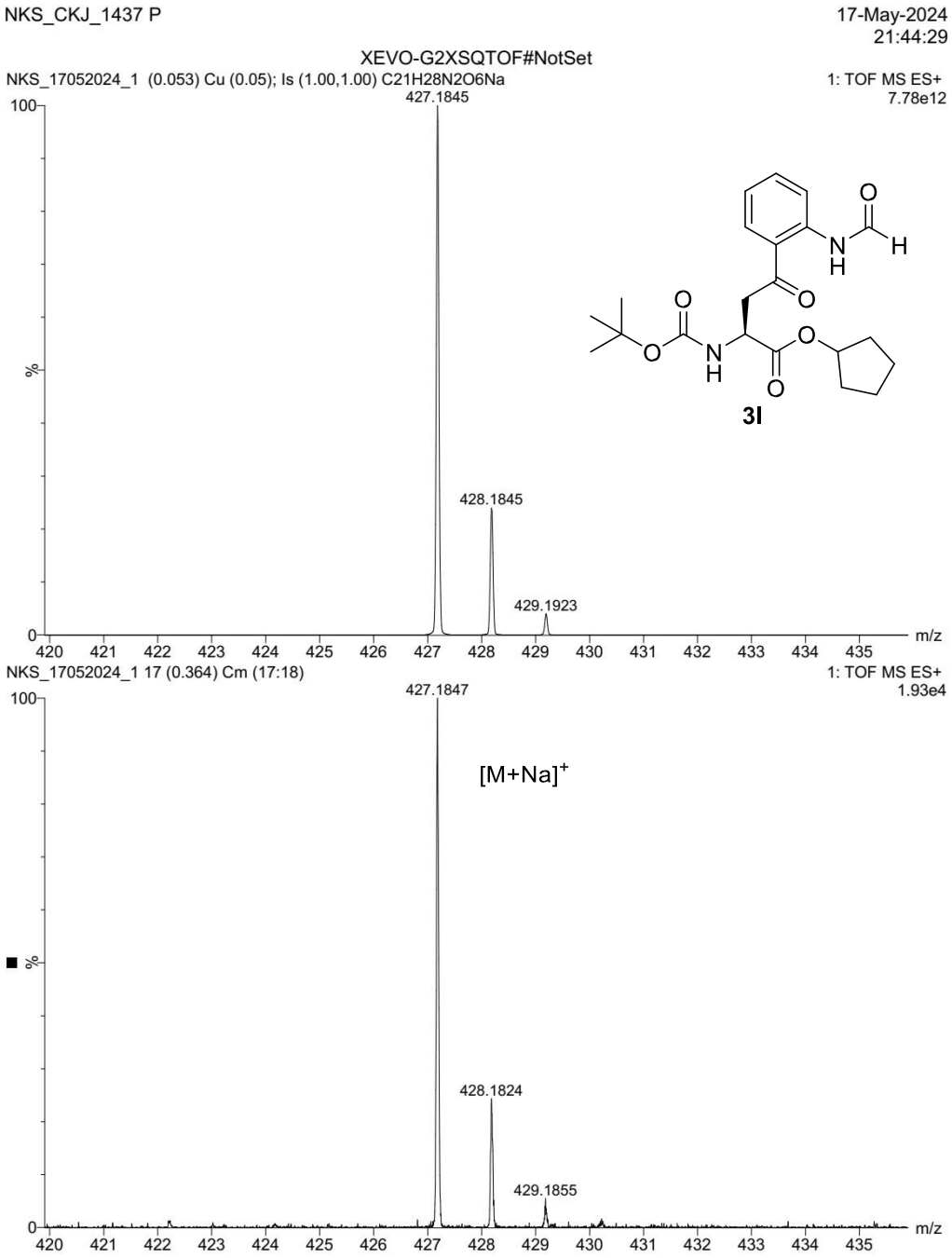

Fig S92. ESI-HRMS spectra of kynurenine derivative **3l**.

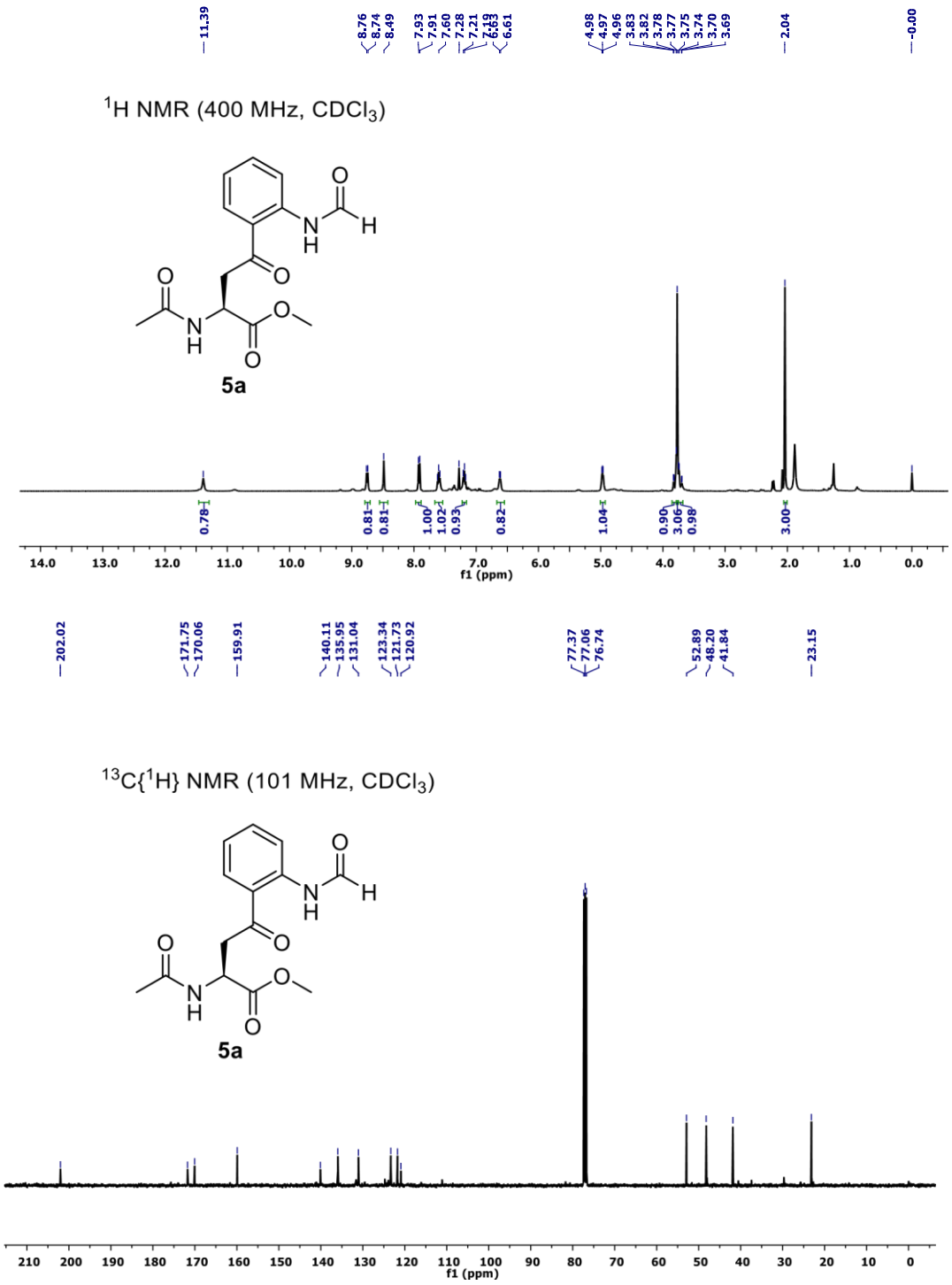

Fig S93. ^{1}H, ^{13}C $\{^{1}H\}$ NMR spectra of kynurenine derivative **5a**.

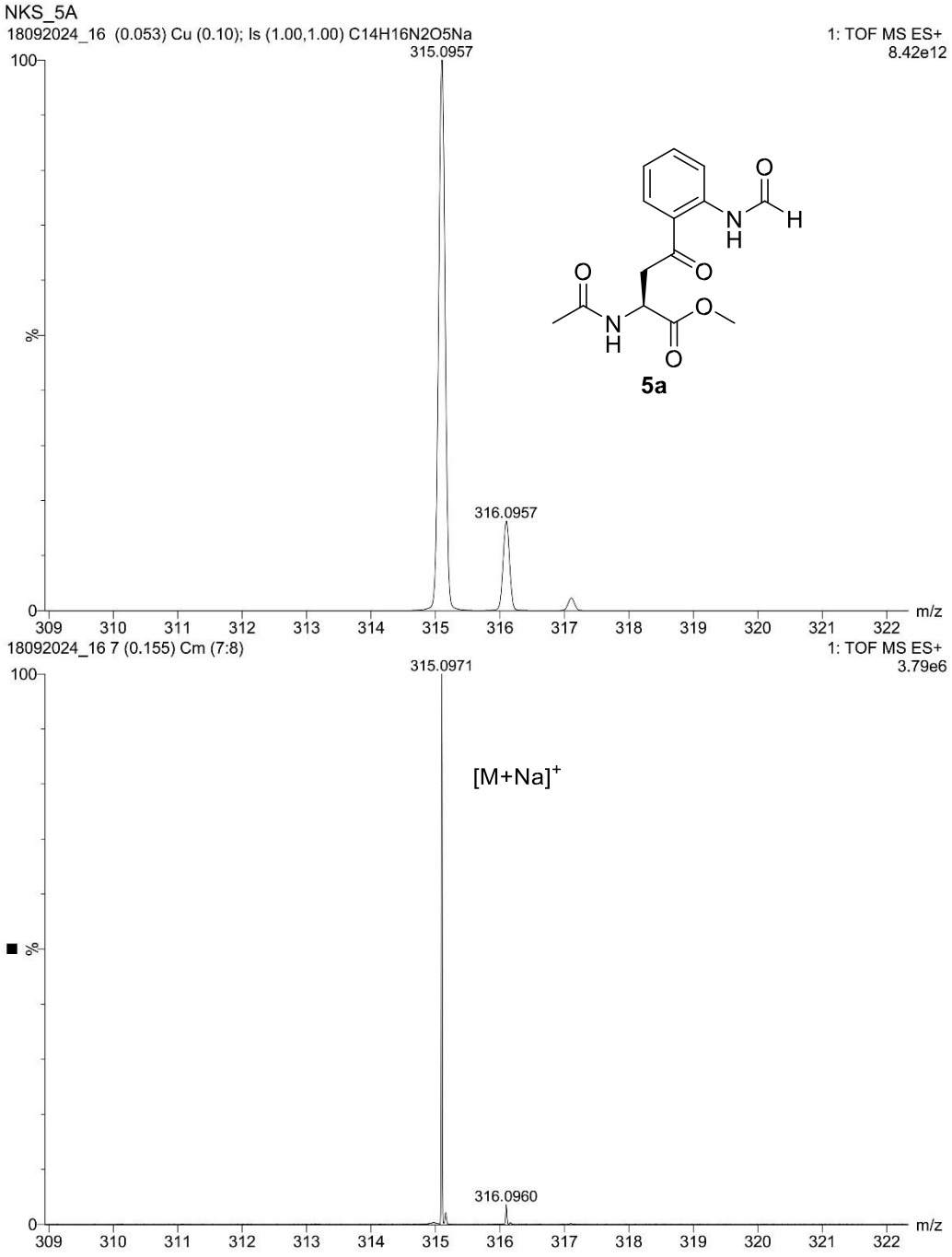

Fig S94. ESI-HRMS spectra of kynurenine derivative **5a**.

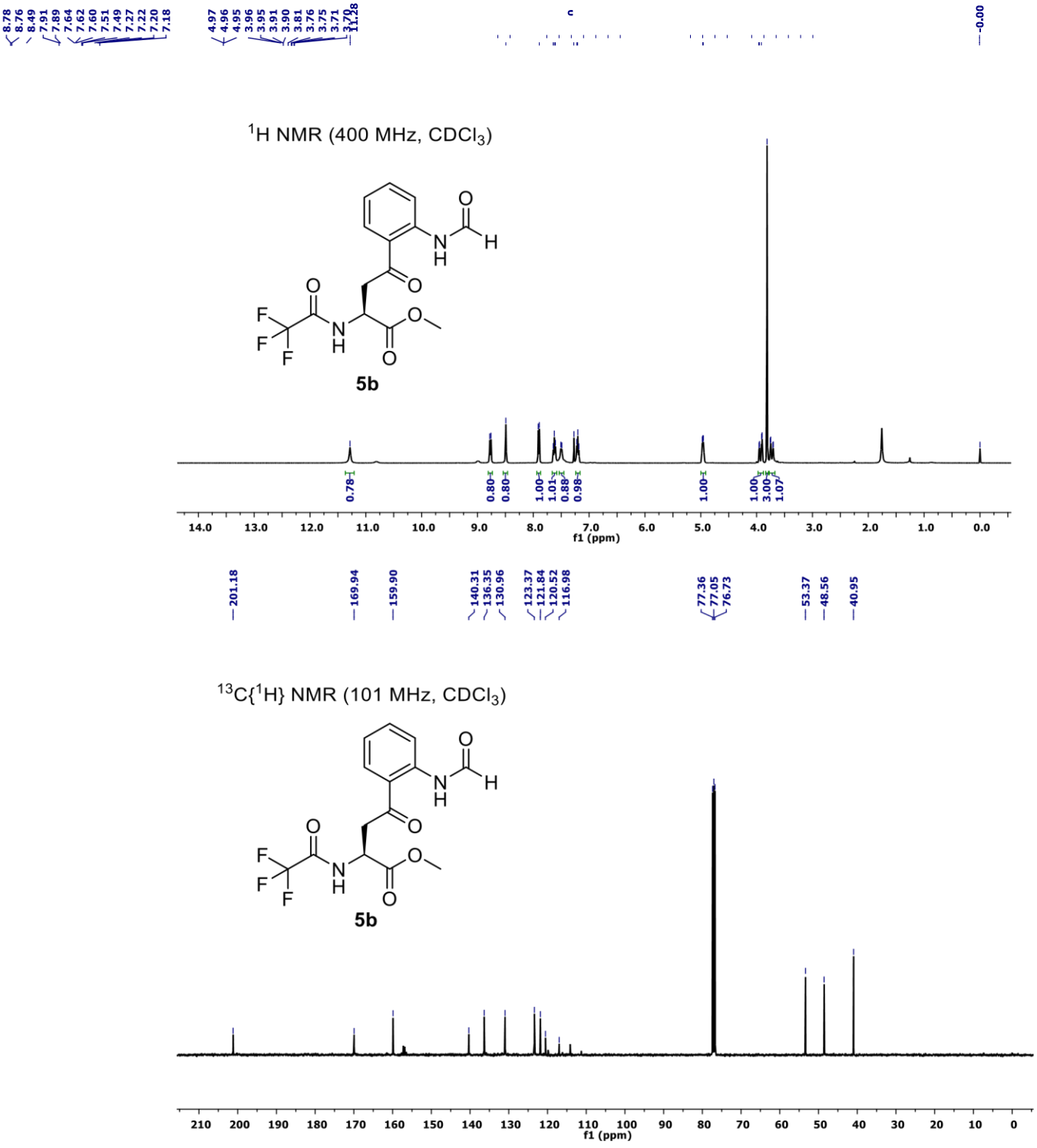

Fig S95. ^{1}H, ^{13}C $\{^{1}H\}$ NMR spectra of kynurenine derivative **5b**.

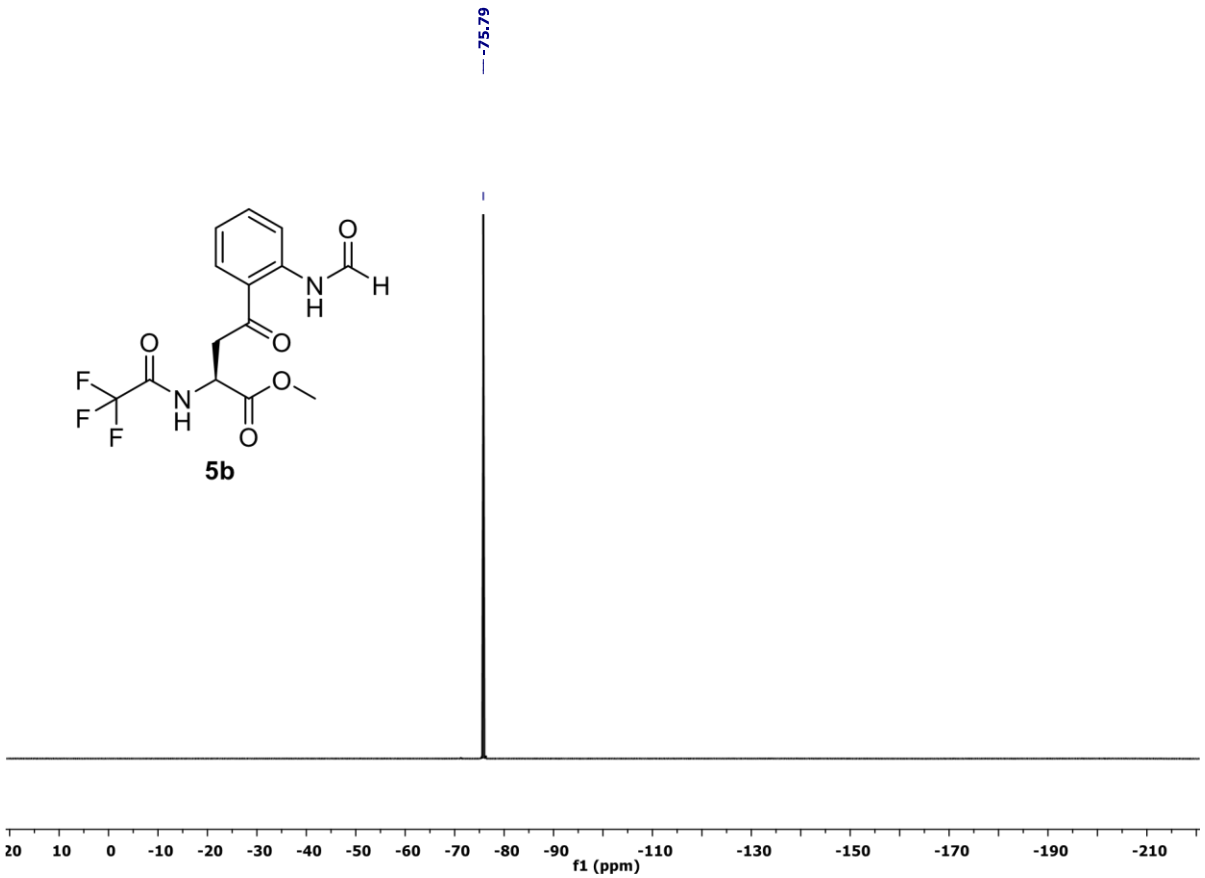

Fig S96. ^{19}F NMR spectra (in $CDCl_3$) of kynurenine derivative **5b**.

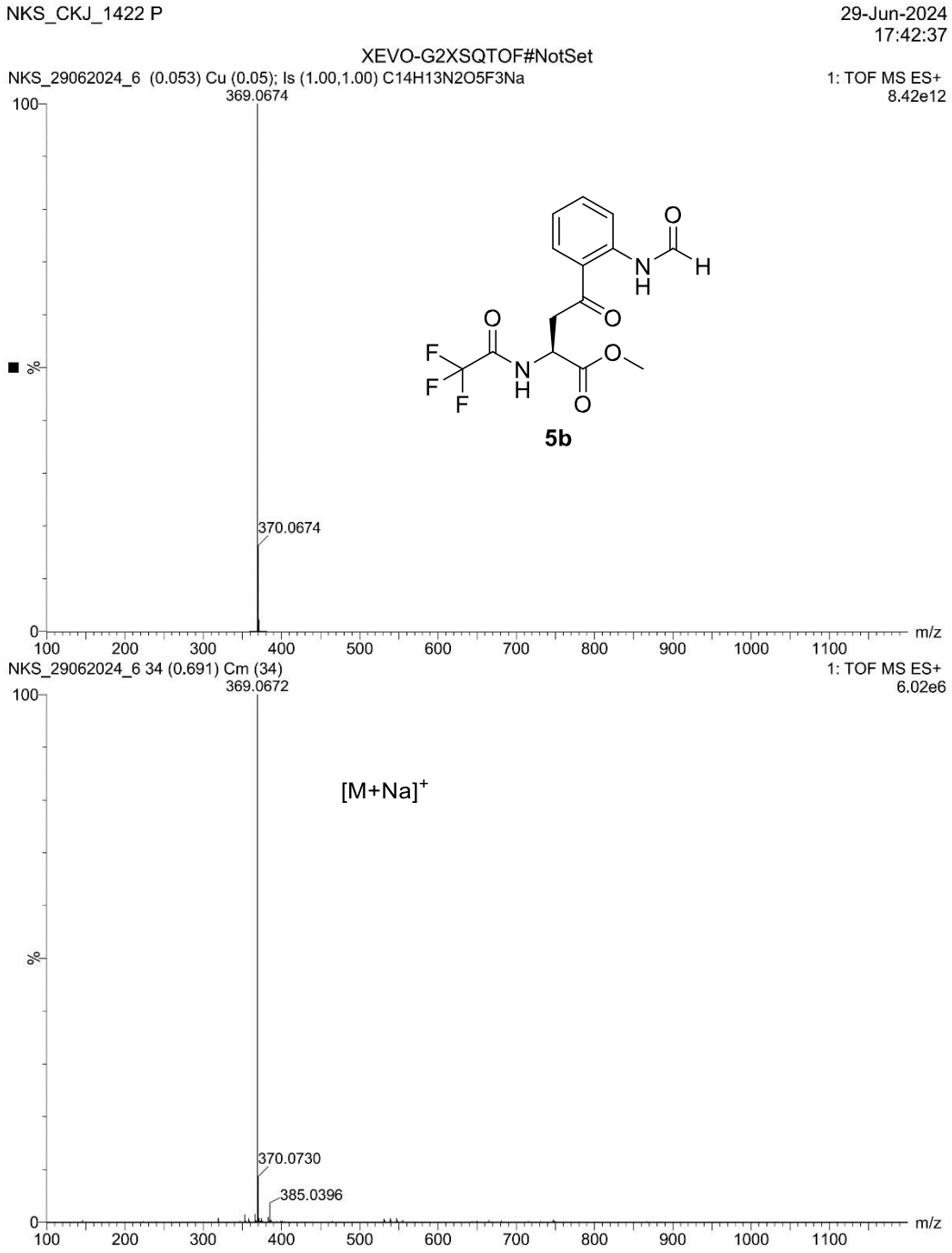

Fig S97. ESI-HRMS spectra of kynurenine derivative **5b**.

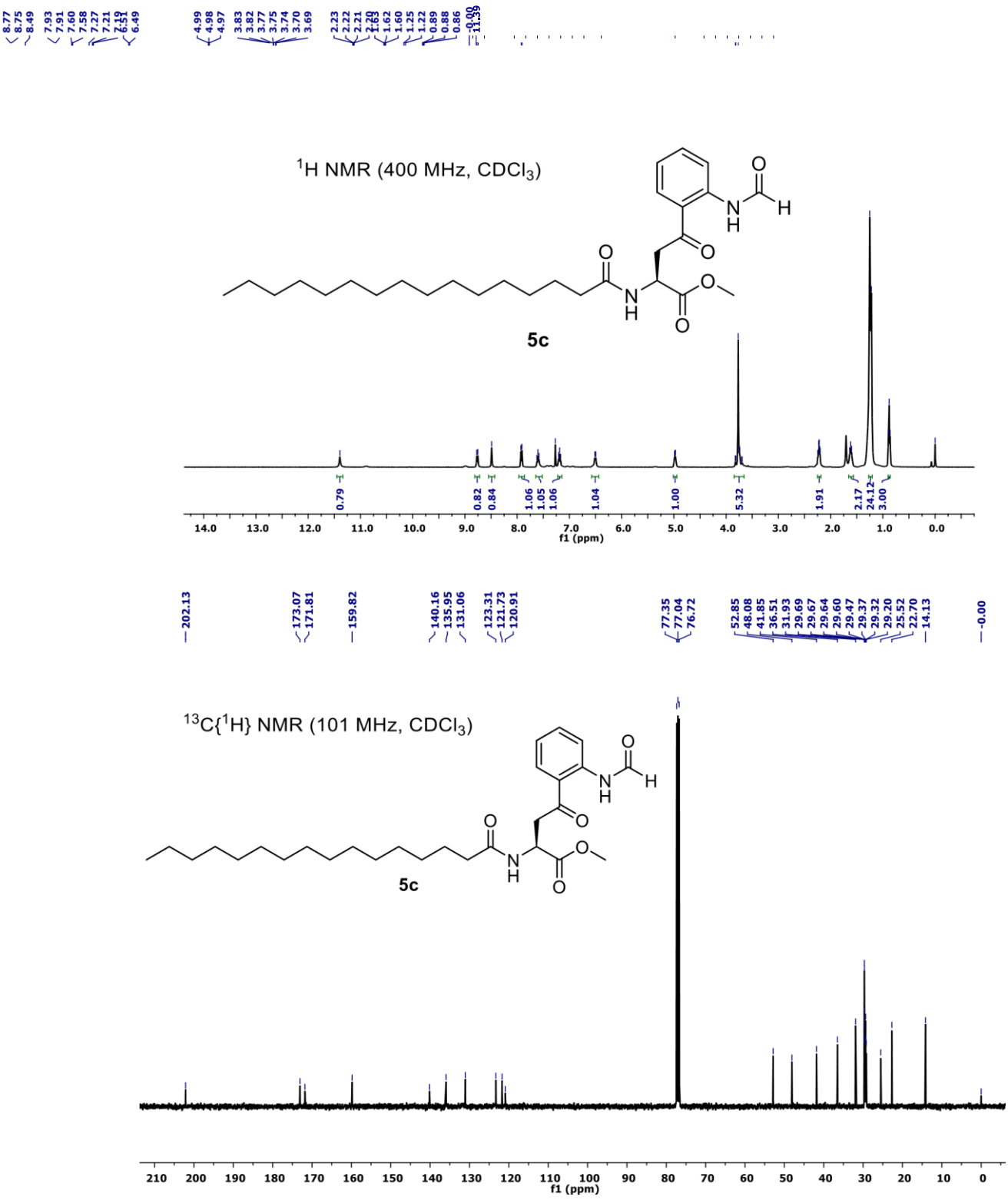

Fig S98. ^{1}H, ^{13}C {^{1}H} NMR spectra of kynurenine derivative **5c**.

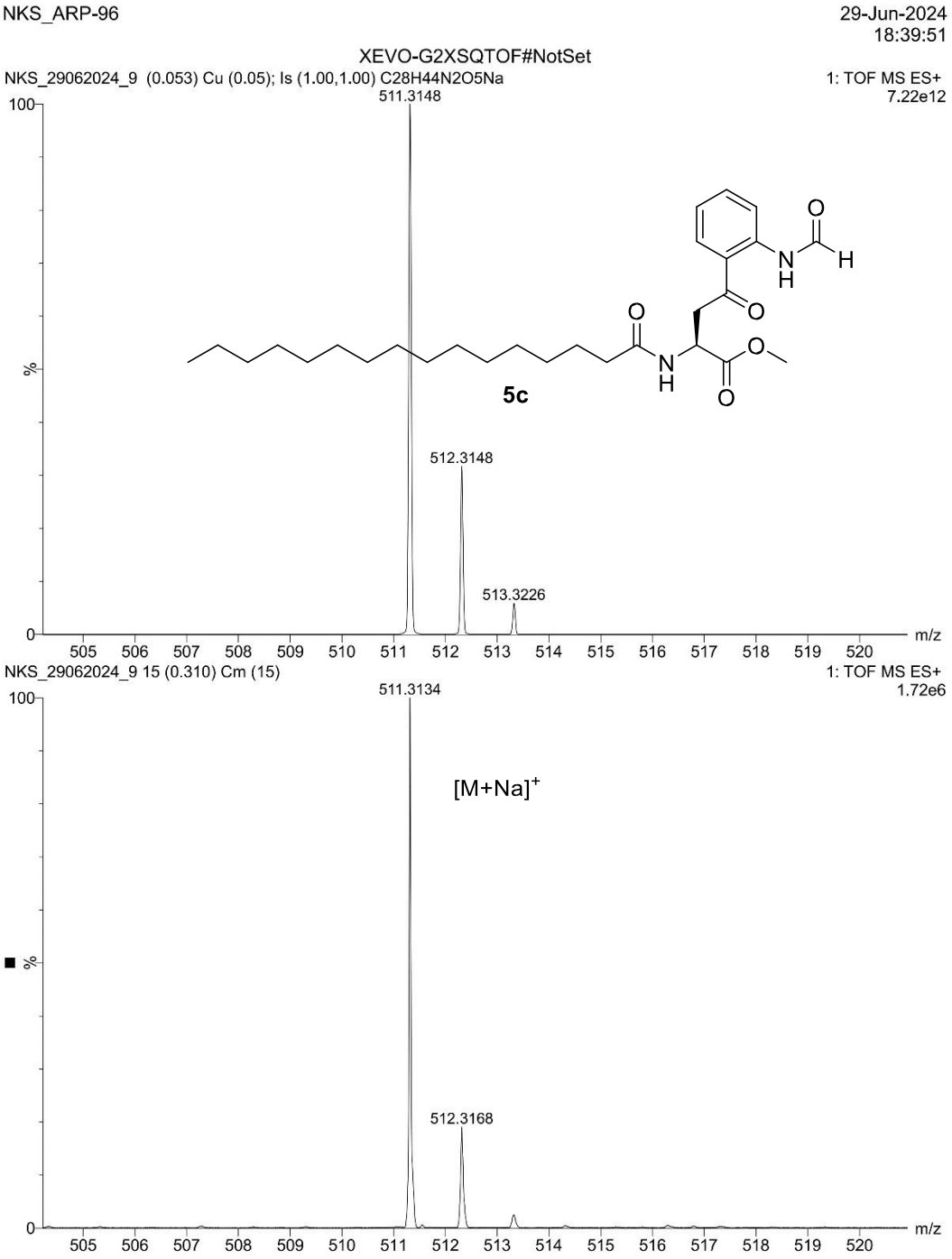

Fig S99. ESI-HRMS spectra of kynurenine derivative **5c**.

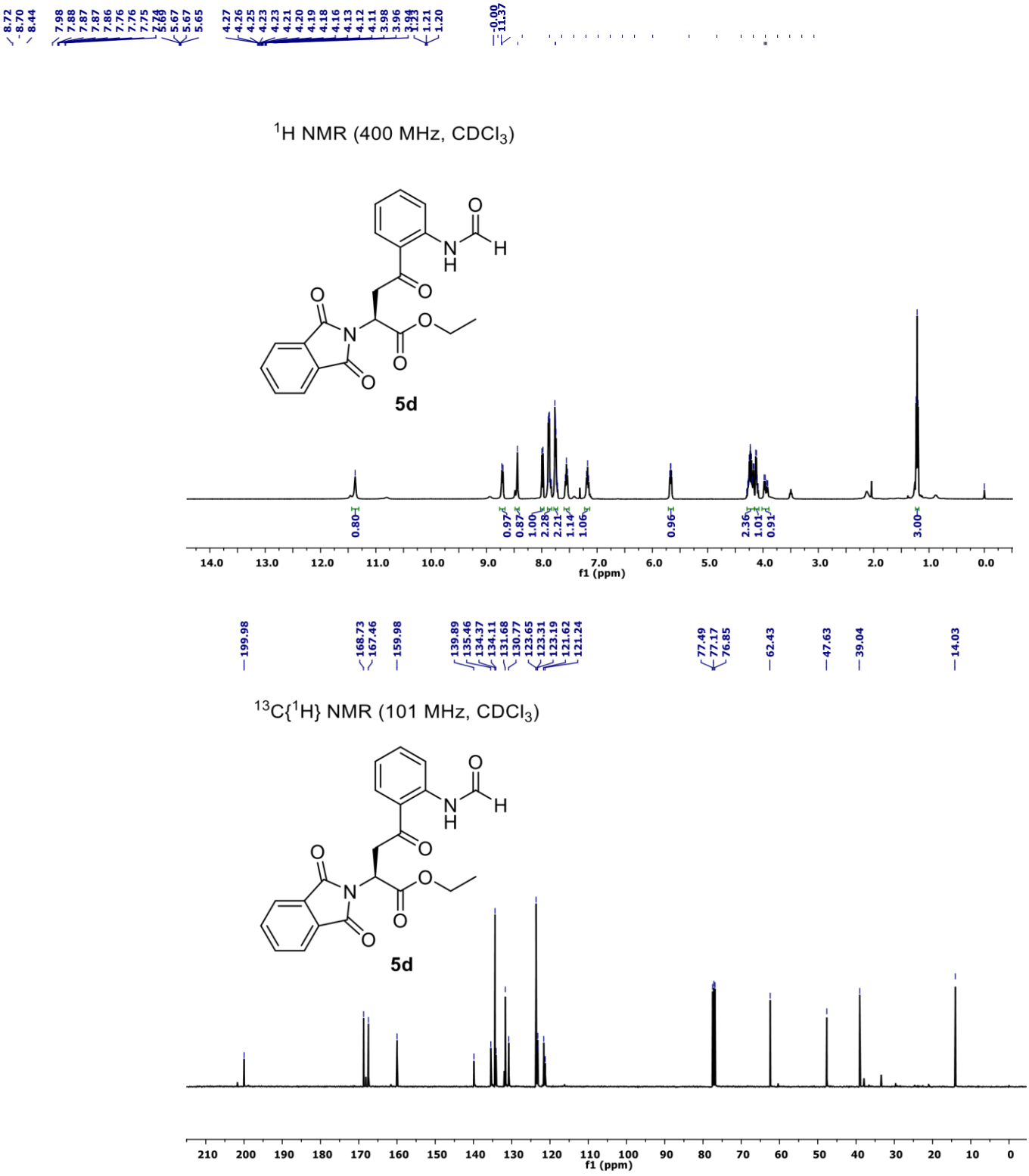

Fig S100. ^{1}H, ^{13}C $\{^{1}H\}$ NMR spectra of kynurenine derivative **5d**.

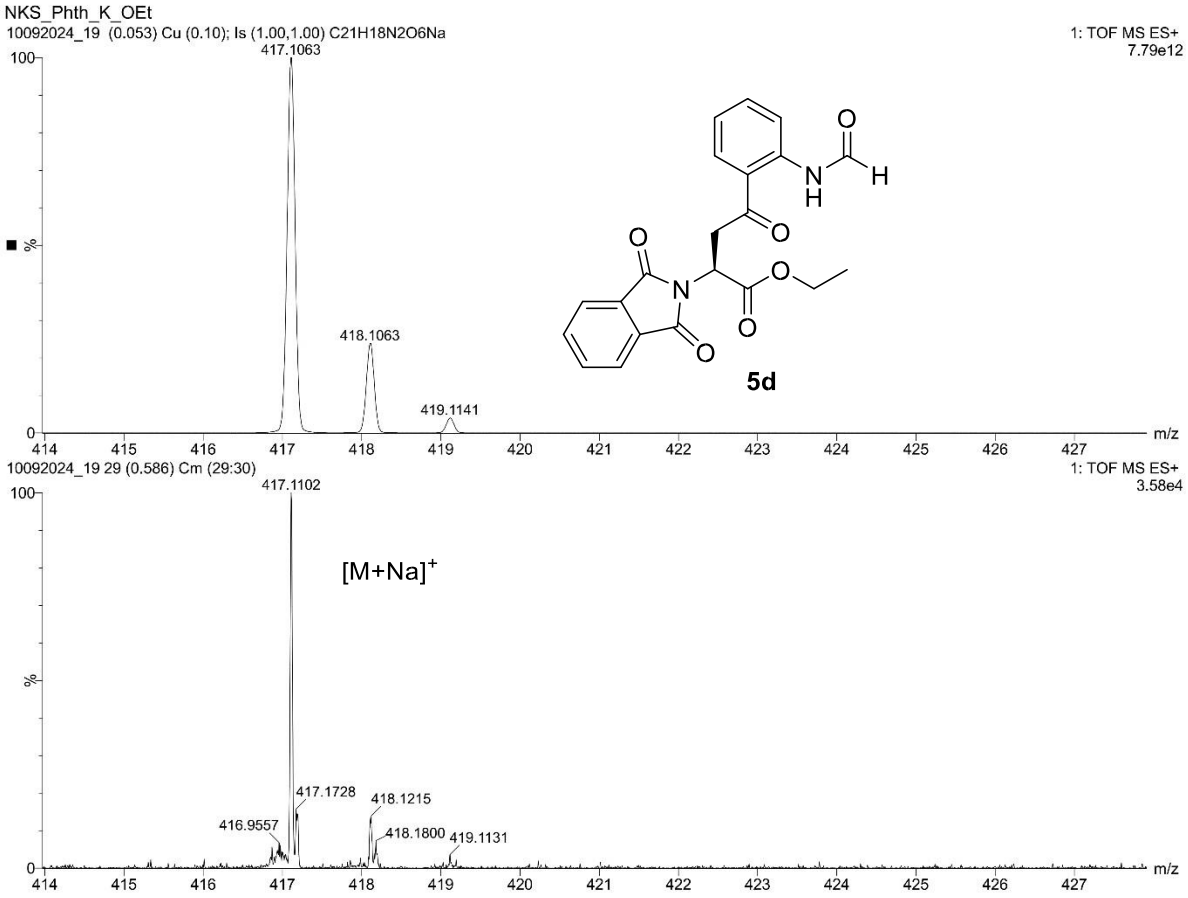

Fig S101. ESI-HRMS spectra of kynurenine derivative **5d**.

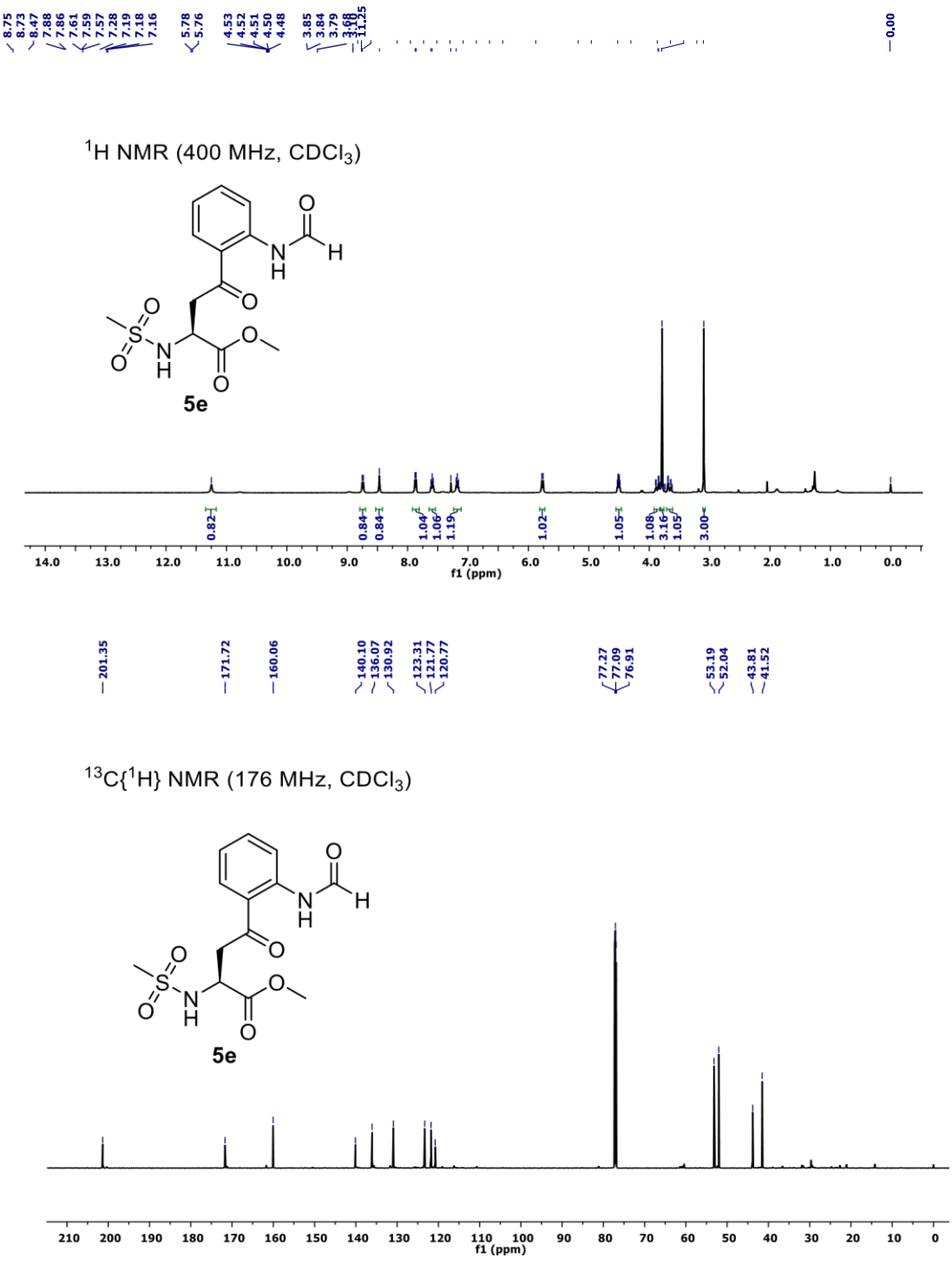

Fig S102. ^{1}H, ^{13}C $\{^{1}H\}$ NMR spectra of kynurenine derivative **5e**.

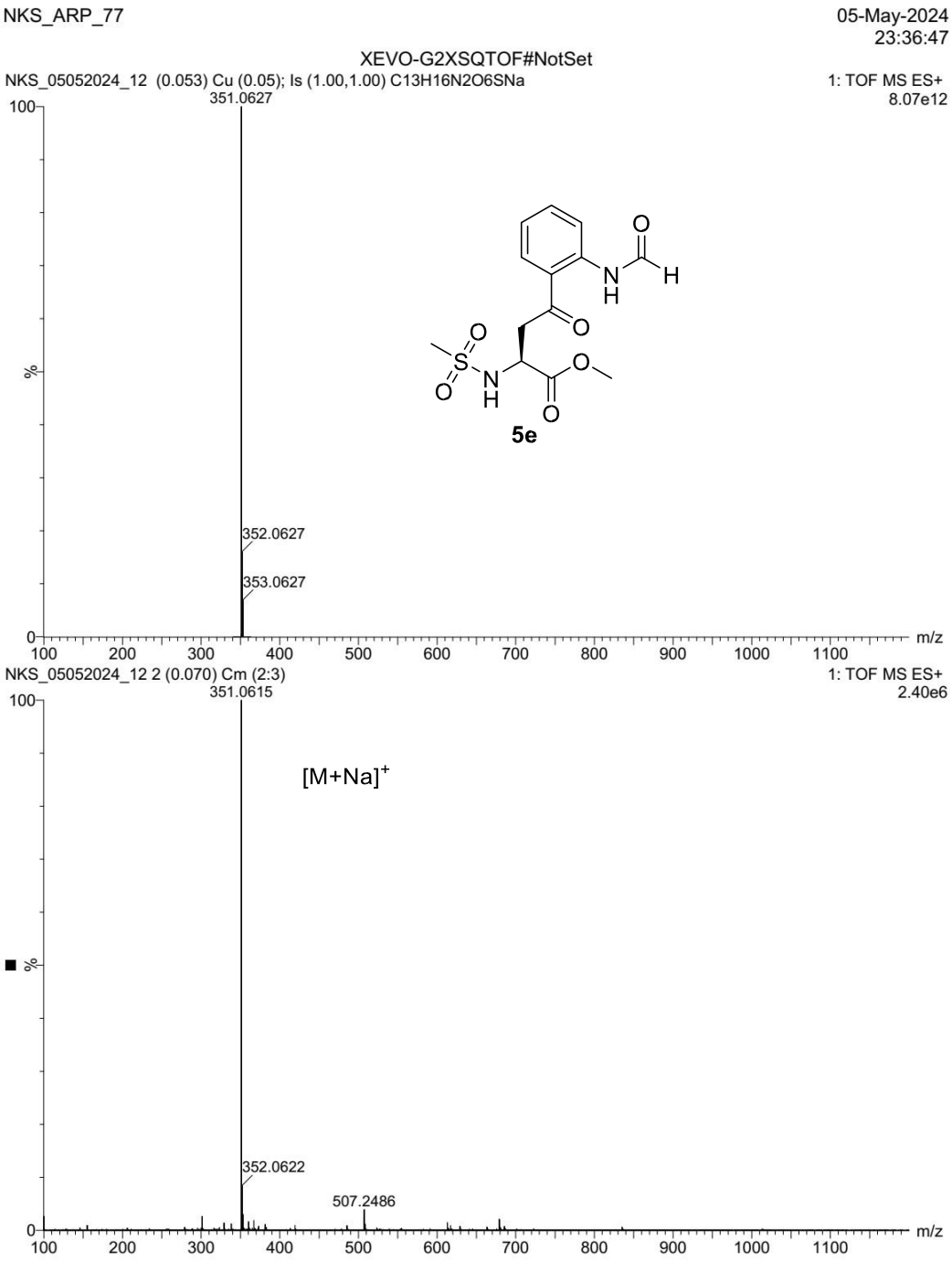

Fig S103. ESI-HRMS spectra of kynurenine derivative **5e**.

^{1}H NMR (400 MHz, $CDCl_3$)

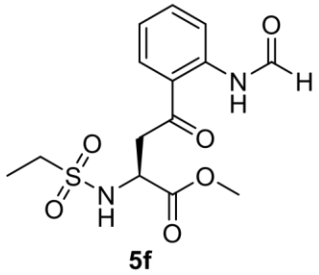

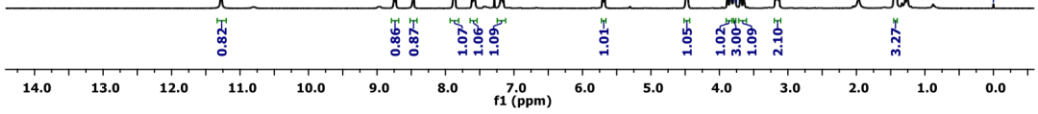

^{13}C{^{1}H} NMR (101 MHz, $CDCl_3$)

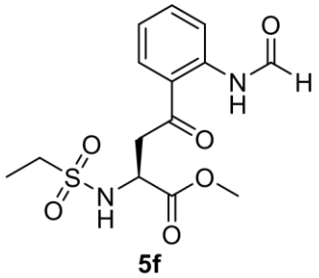

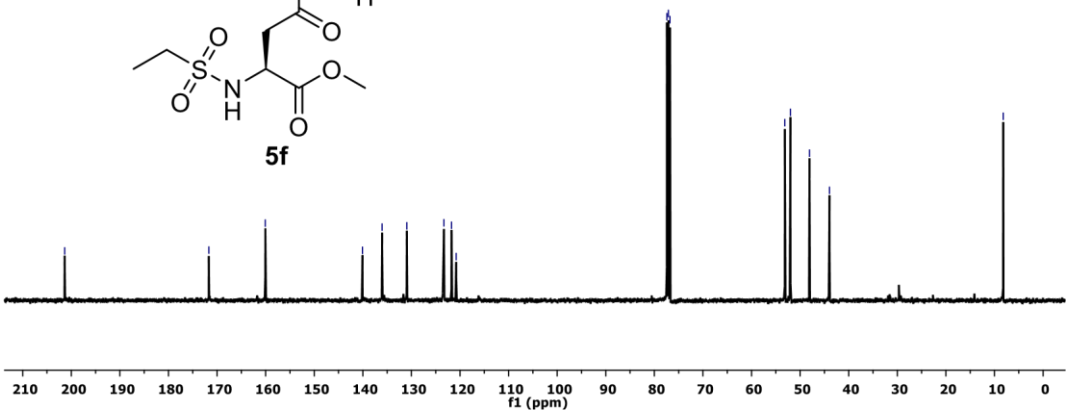

Fig S104. ^{1}H, ^{13}C $\{^{1}H\}$ NMR spectra of kynurenine derivative **5f**.

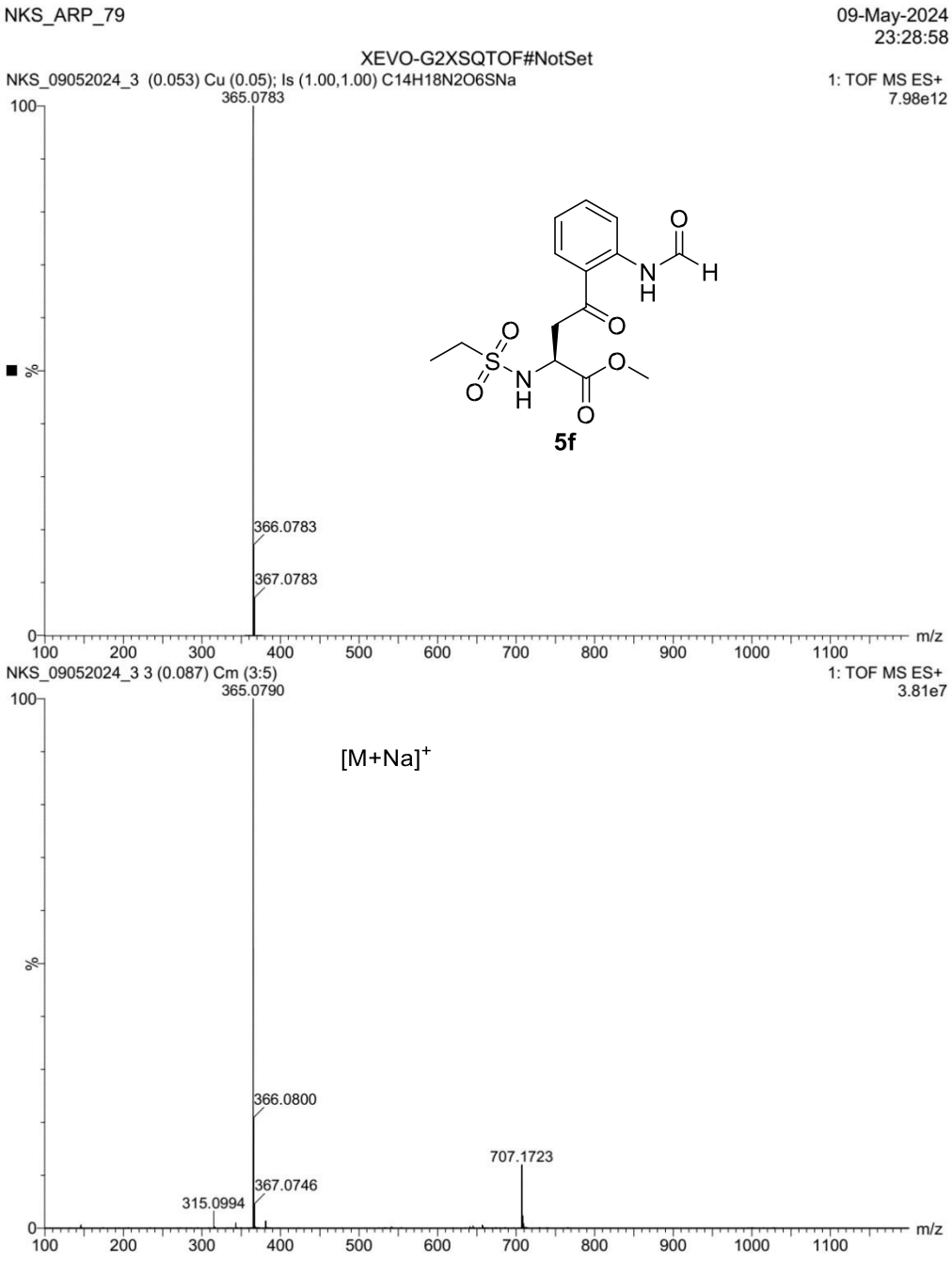

Fig S105. ESI-HRMS spectra of kynurenine derivative **5f**.

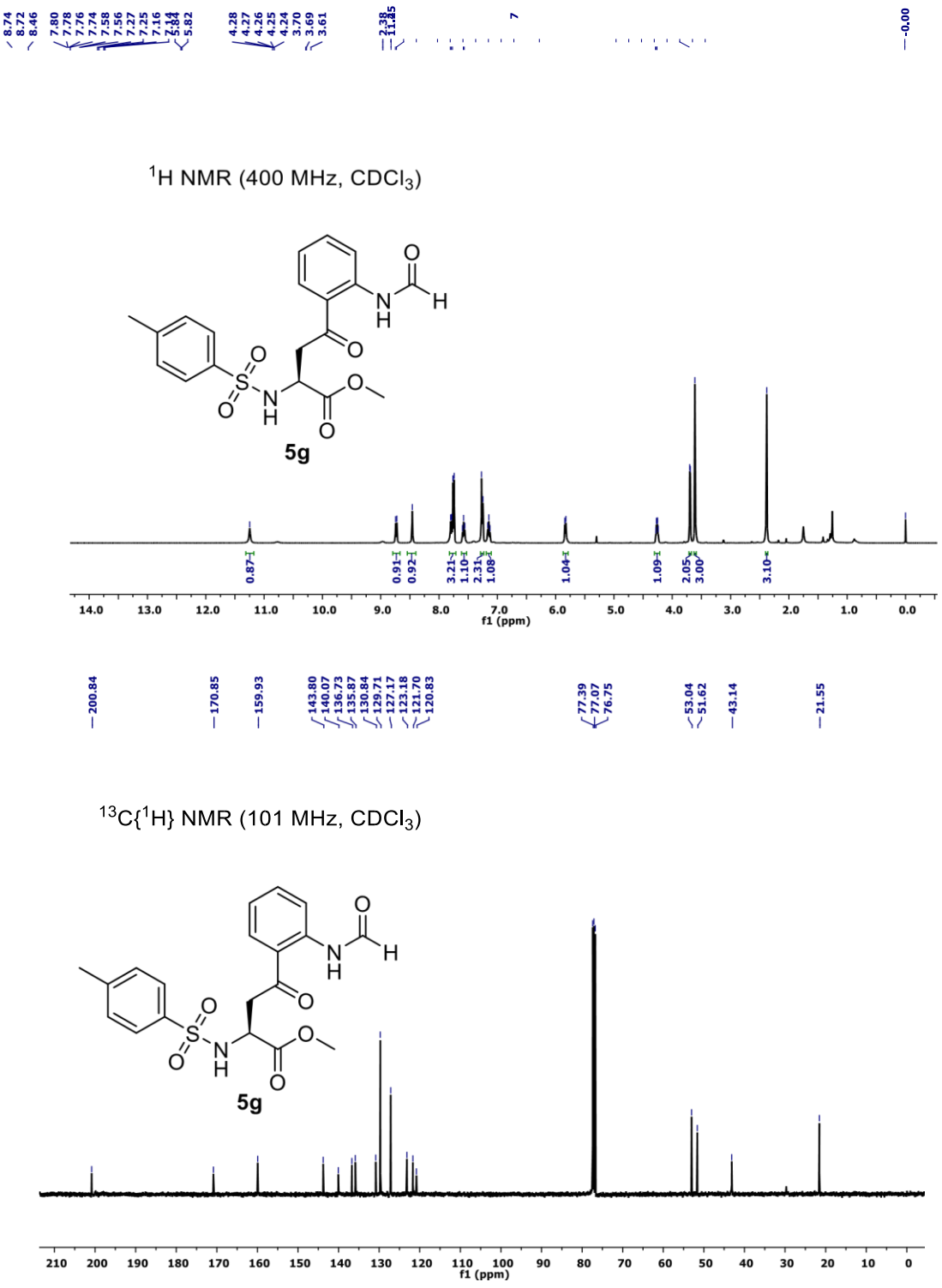

Fig S106. ^{1}H, ^{13}C $\{^{1}H\}$ NMR spectra of kynurenine derivative **5g**.

Fig ^{1}H, ^{13}C $\{^{1}H\}$ NMR spectra of

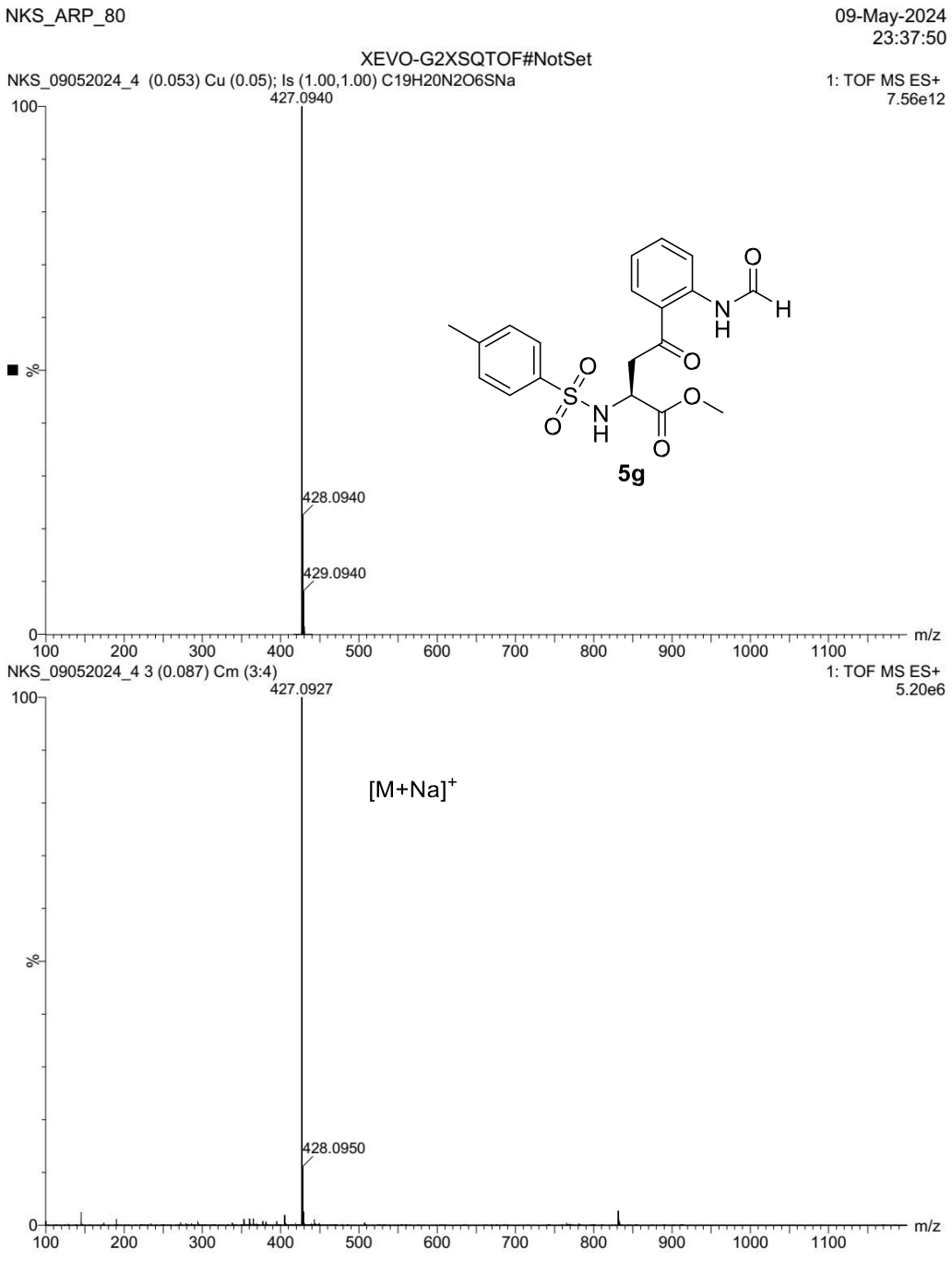

Fig S107. ESI-HRMS spectra of kynurenine derivative **5g**.

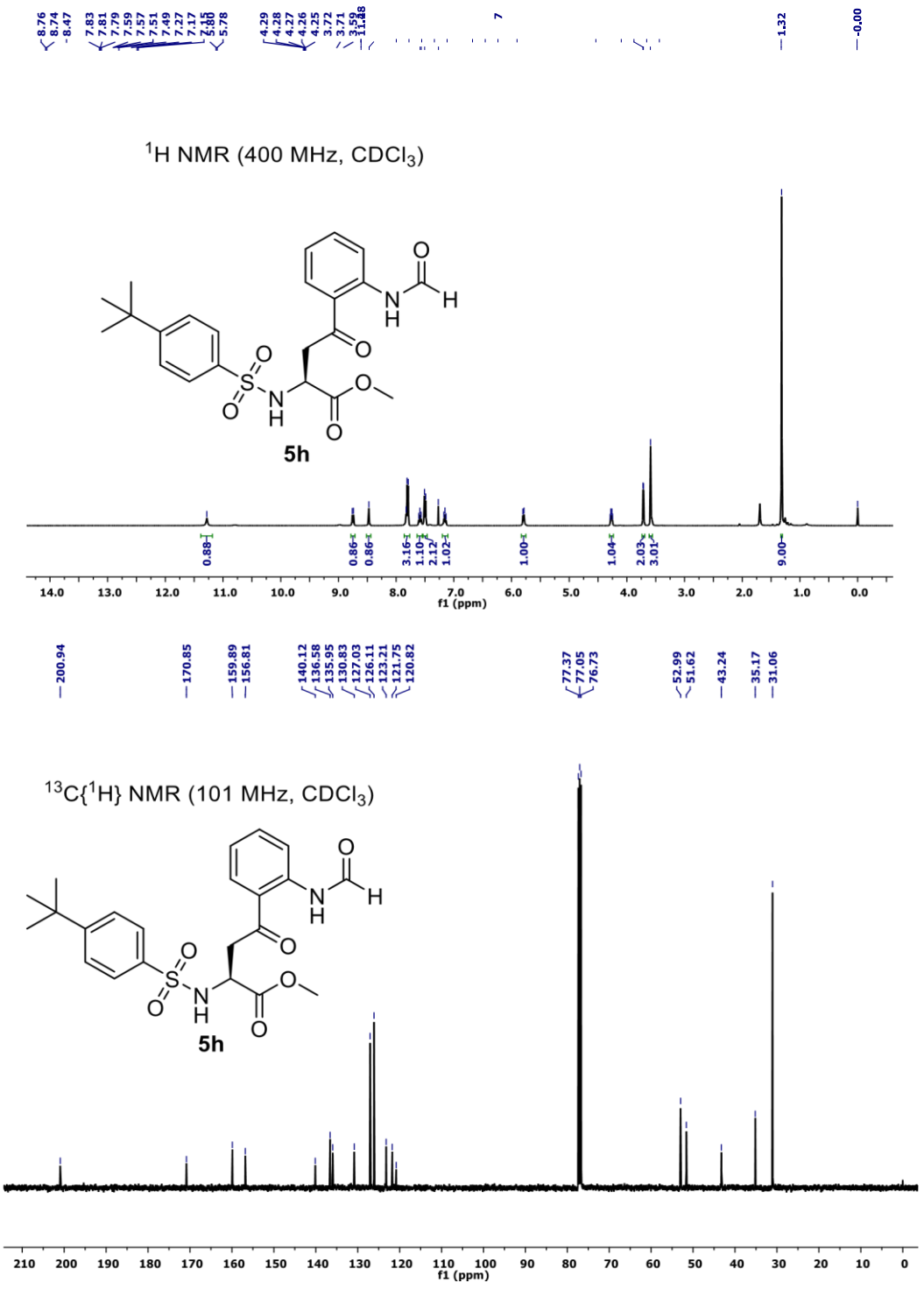

Fig ^{1}H, ^{13}C $\{^{1}H\}$ NMR spectra of

S108. kynurenine derivative **5h**.

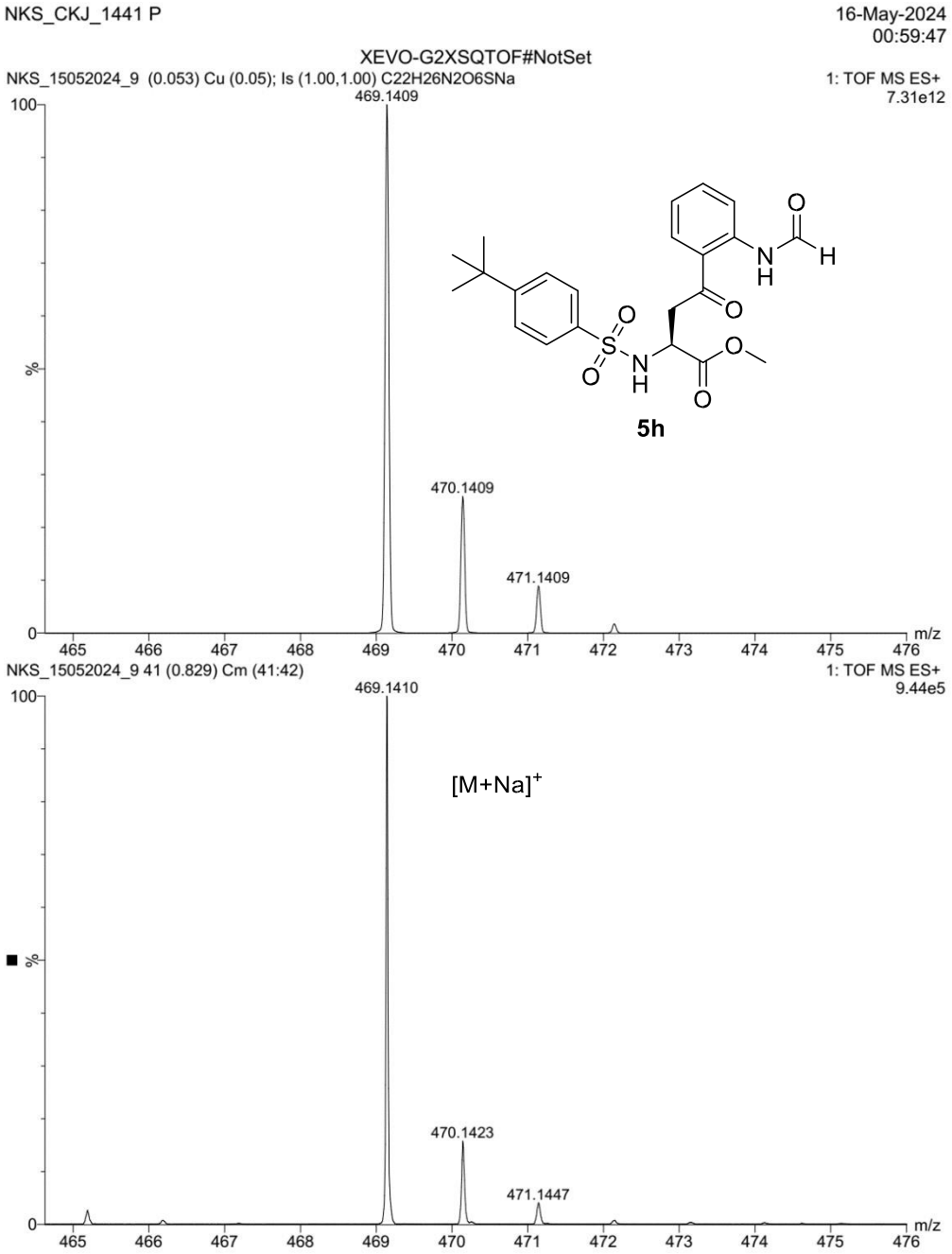

Fig S109. ESI-HRMS spectra of kynurenine derivative **5h**.

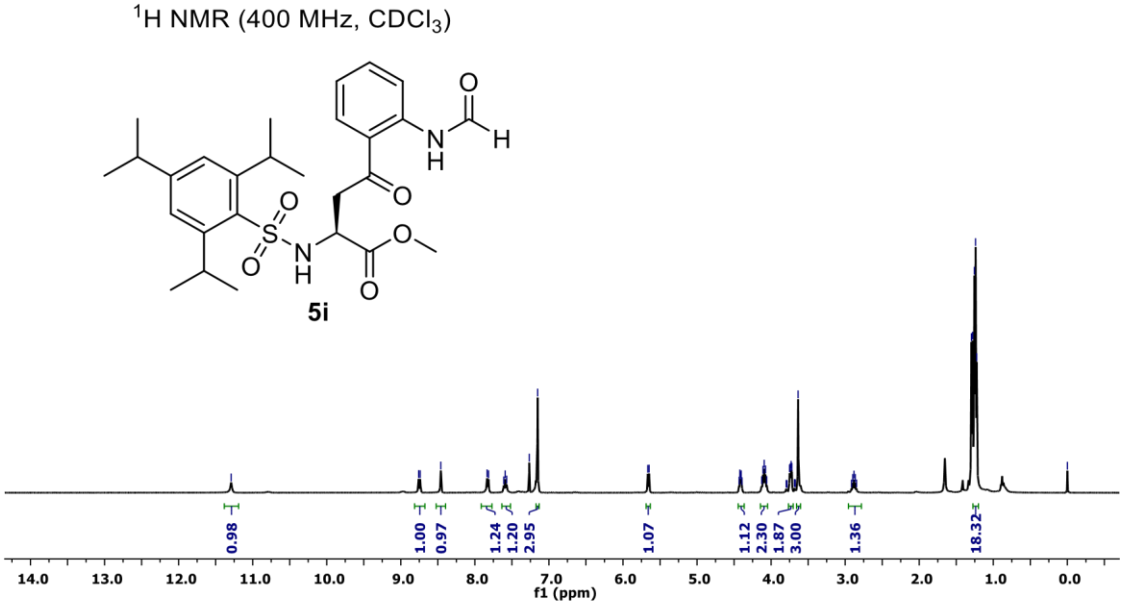

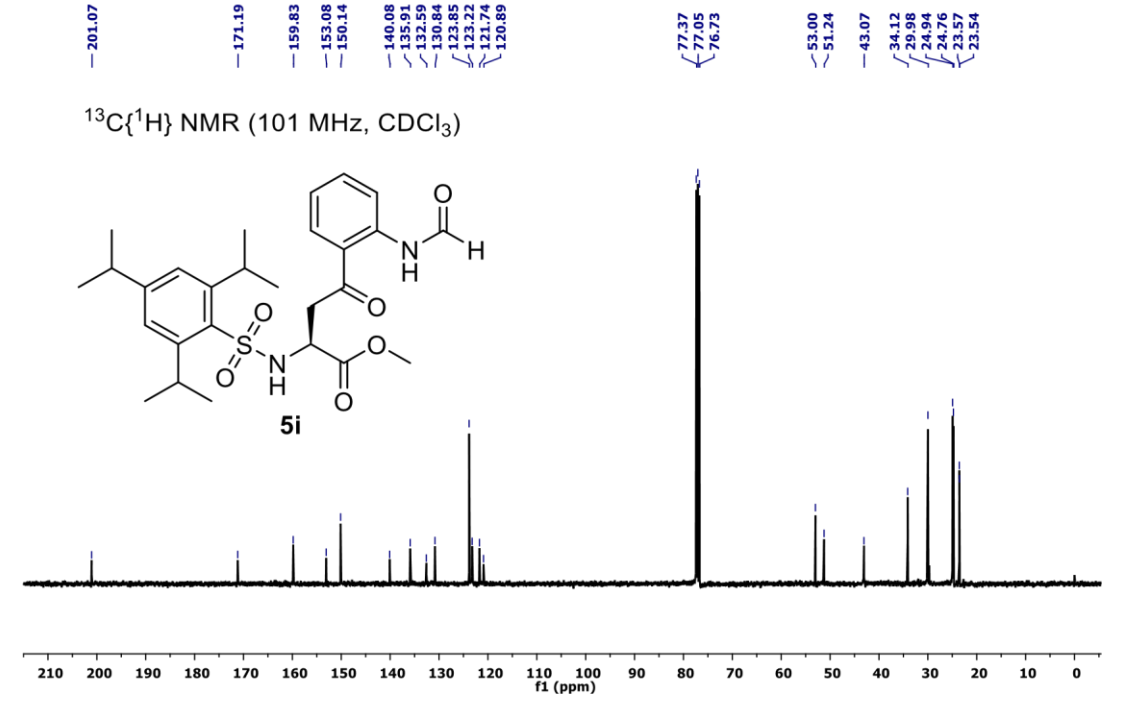

Fig ^{1}H, ^{13}C $\{^{1}H\}$ NMR spectra of

S110. kynurenine derivative **5i**.

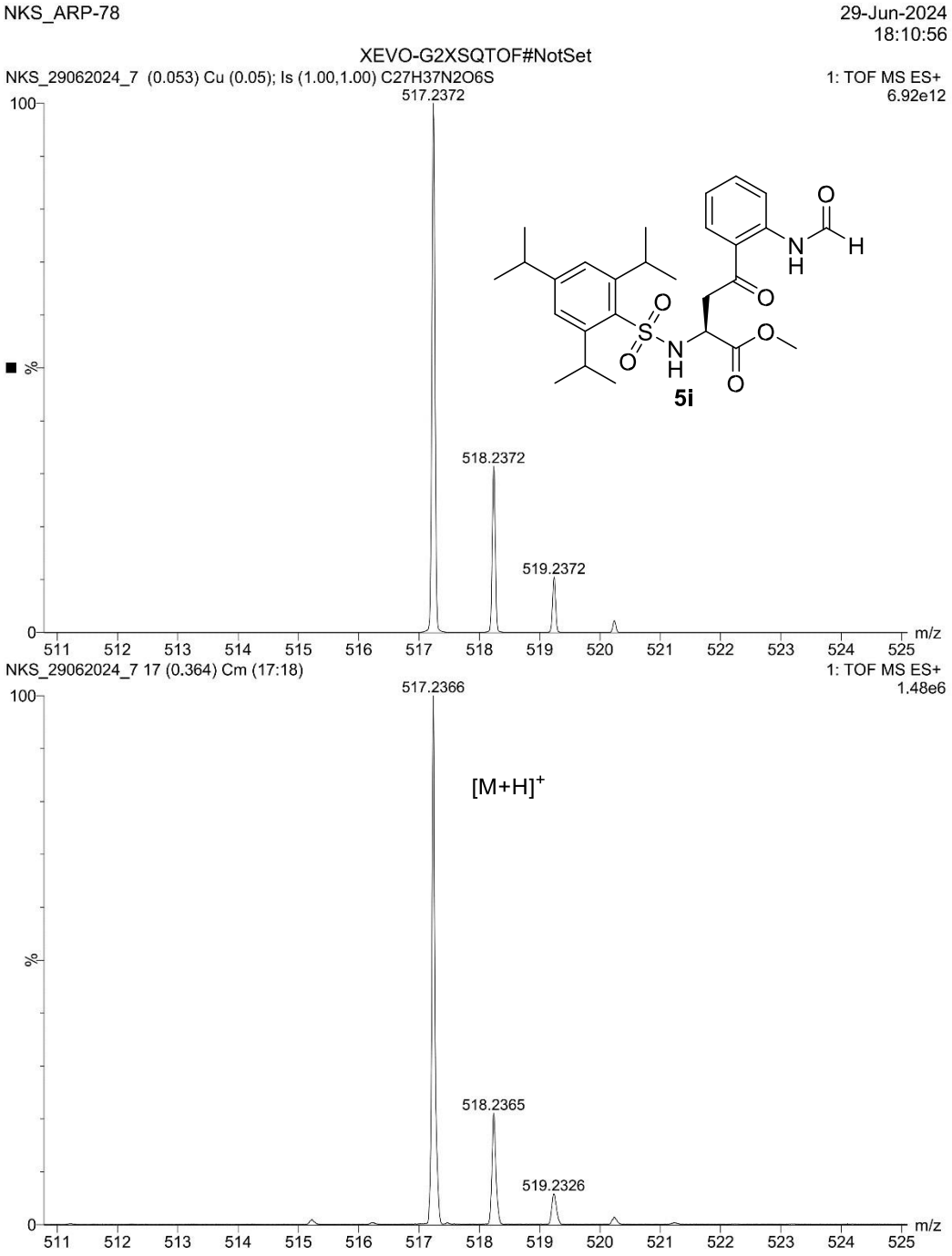

Fig S111. ESI-HRMS spectra of kynurenine derivative **5i**.

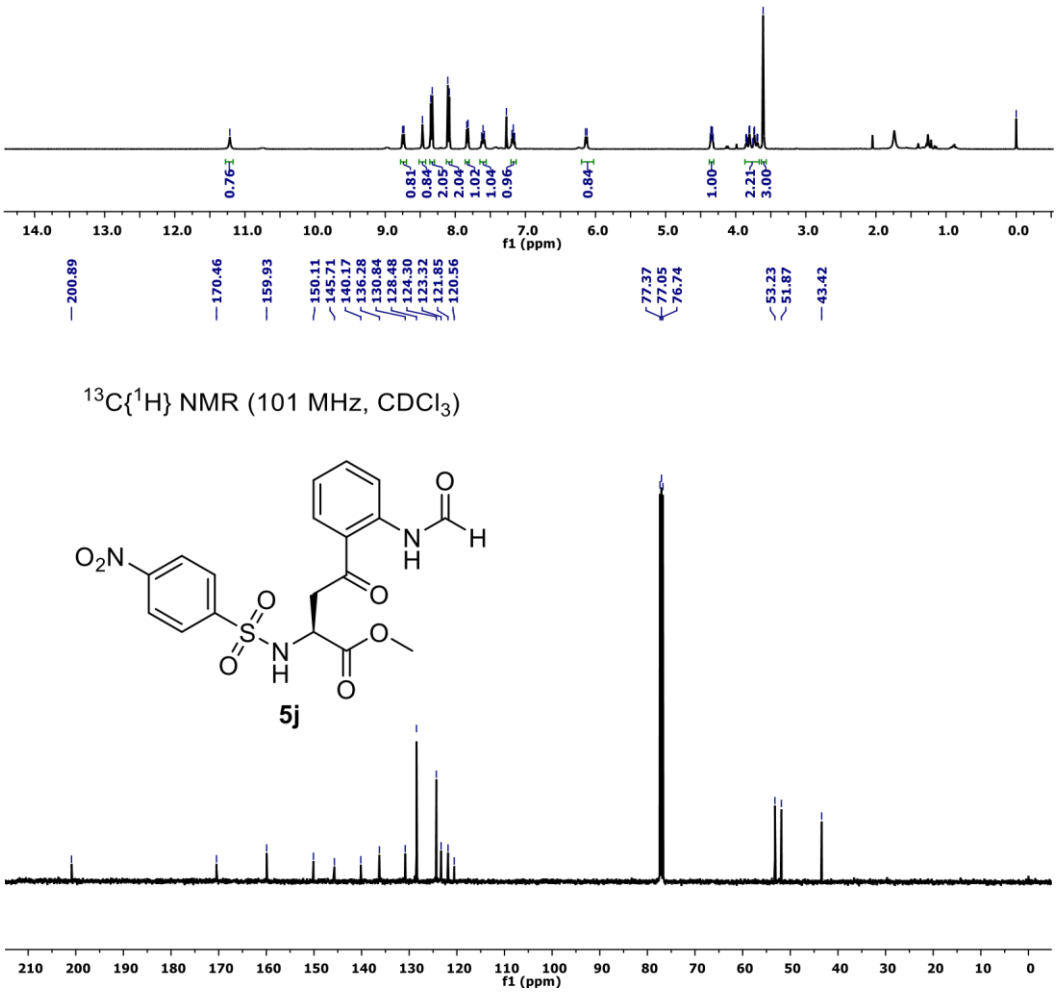

Fig ^{1}H, ^{13}C $\{^{1}H\}$ NMR spectra of

S112. kynurenine derivative **5j**.

^{1}H NMR (400 MHz, $CDCl_3$)

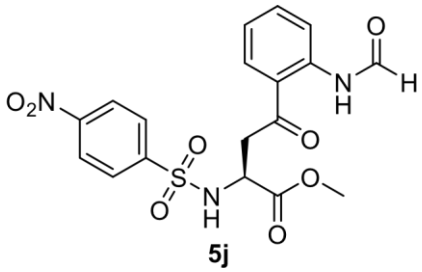

5j

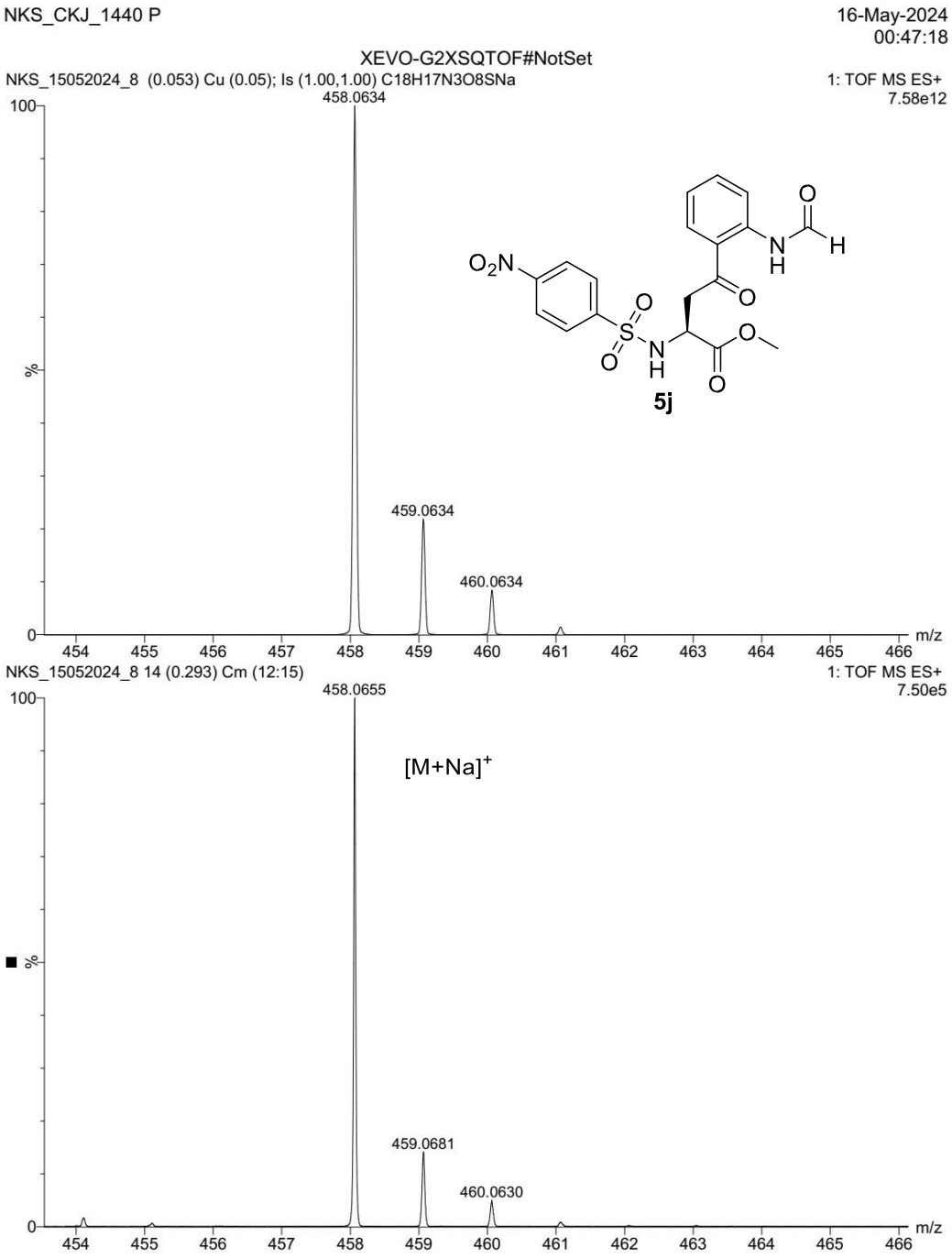

Fig ^{1}H, ^{13}C $\{^{1}H\}$ NMR spectra of

Fig S113. ESI-HRMS spectra of kynurenine derivative **5j**.

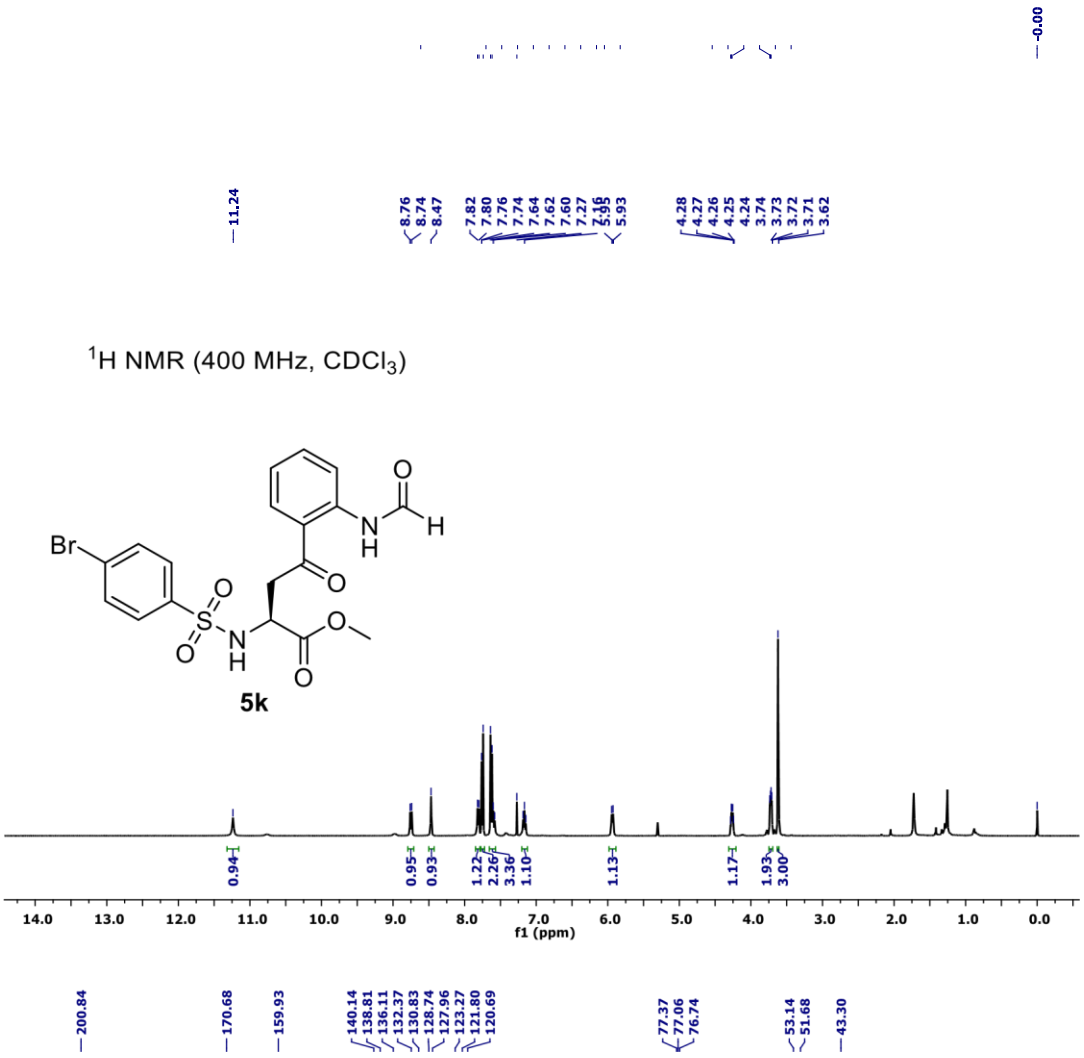

Fig ^{1}H, ^{13}C {^{1}H} NMR spectra of

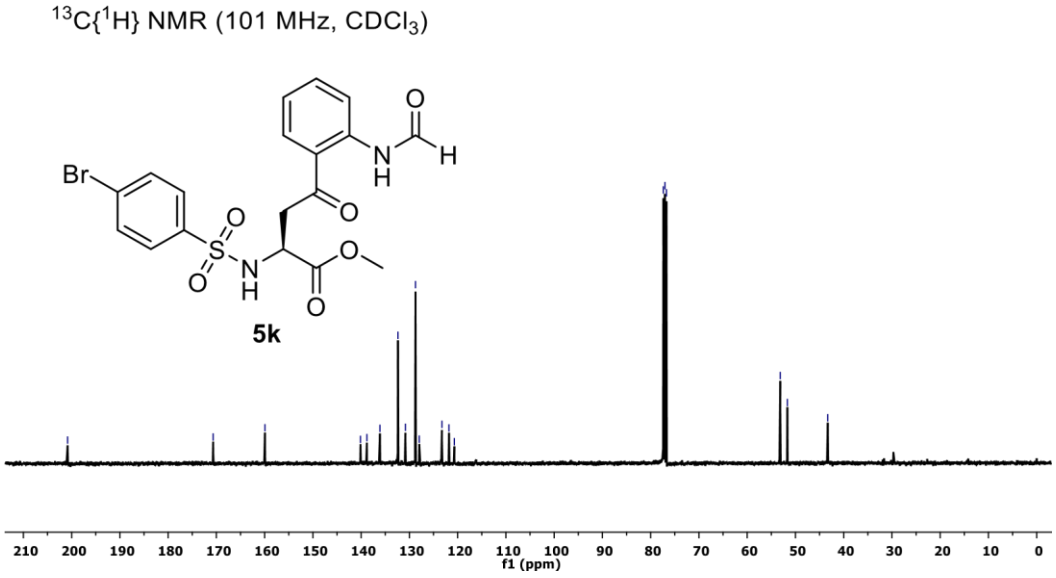

S114. kynurenine derivative **5k**.

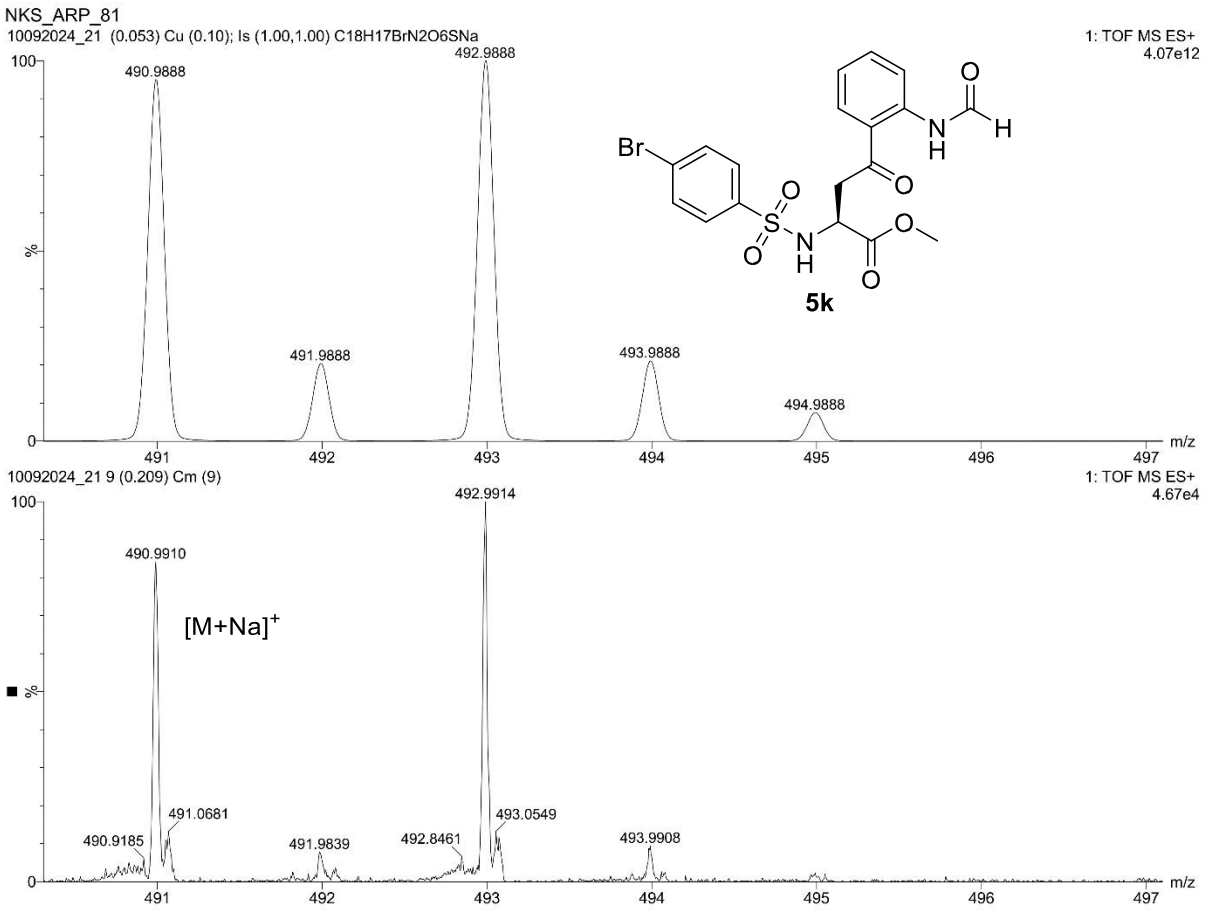

Fig S115. ESI-HRMS spectra of kynurenine derivative **5k**.

Fig ^{1}H, ^{13}C $\{^{1}H\}$ NMR spectra of

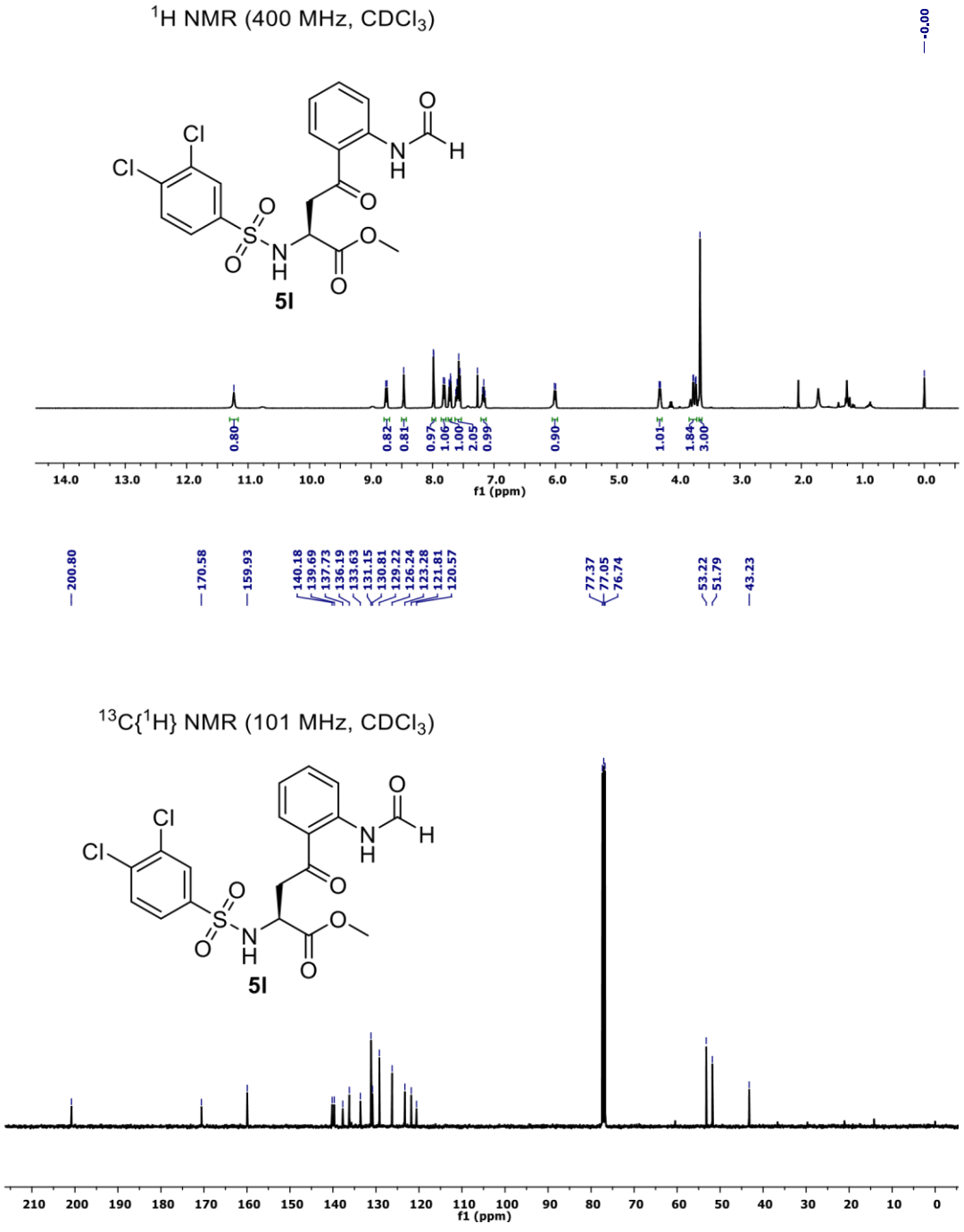

S116. kynurenine derivative **5l**.

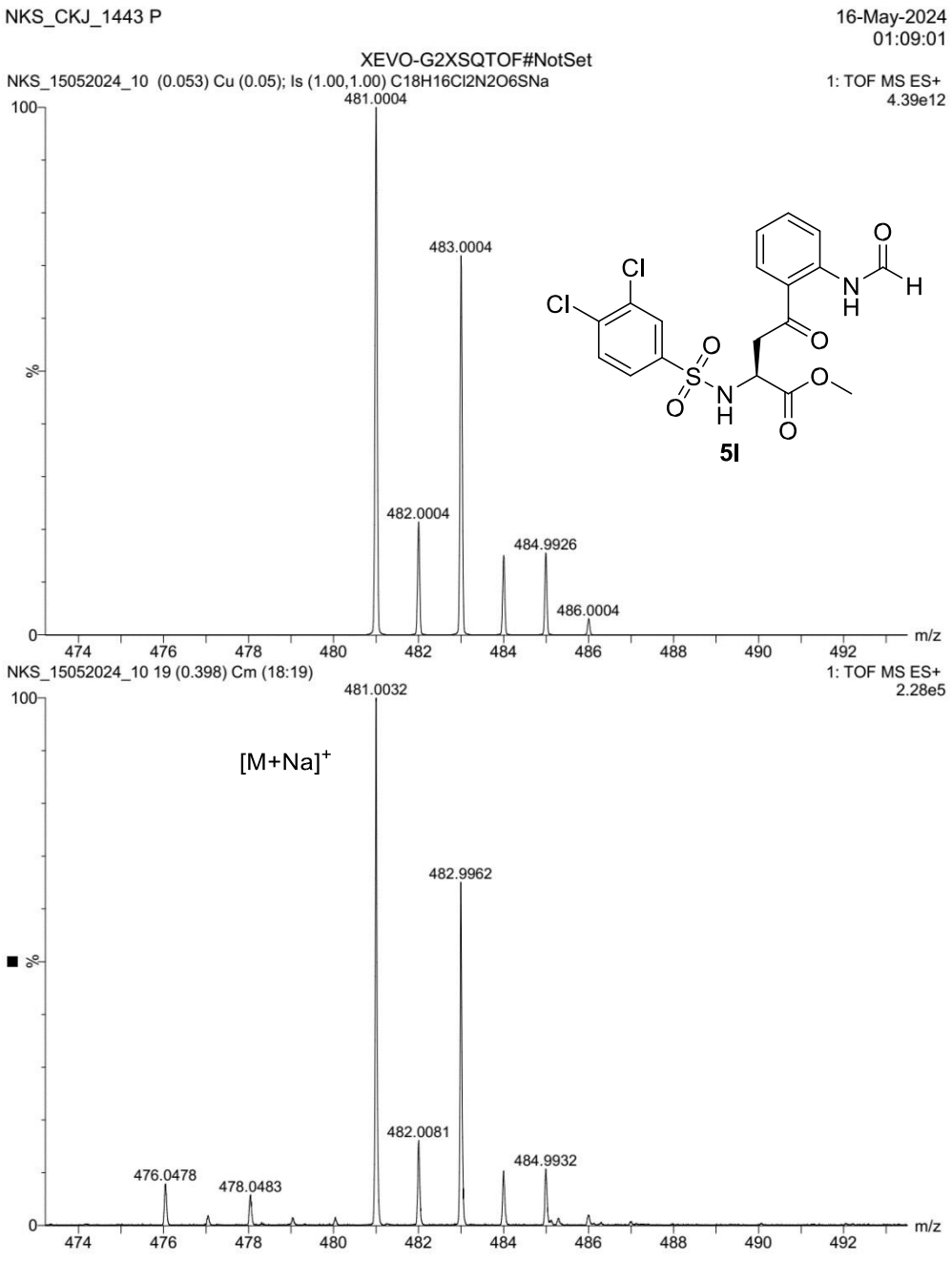

Fig ^{1}H, ^{13}C $\{^{1}H\}$ NMR spectra of

Fig S117. ESI-HRMS spectra of kynurenine derivative **5l**.

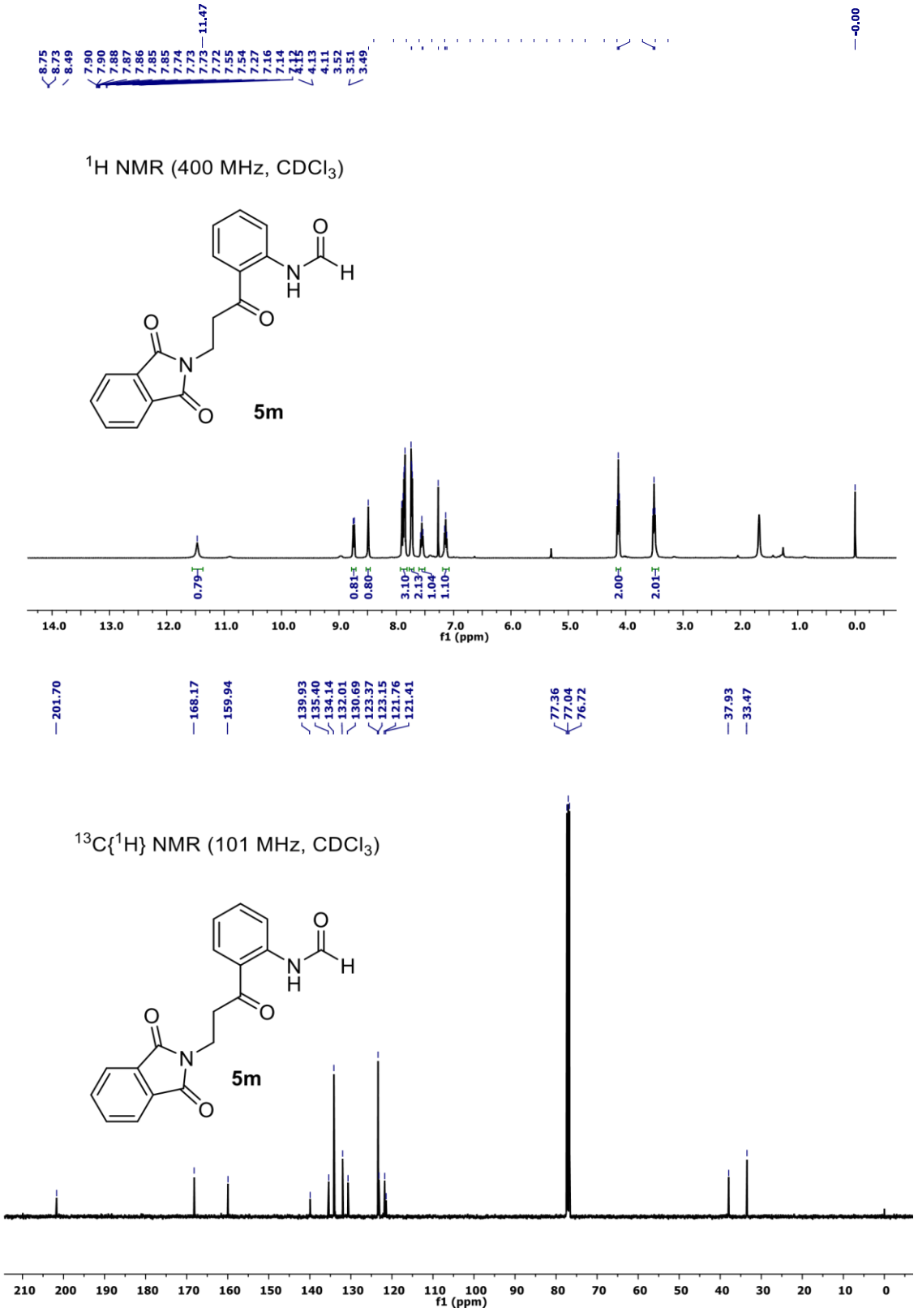

Fig S118. ^{1}H, ^{13}C {^{1}H} NMR spectra of kynurenine derivative **5m**.

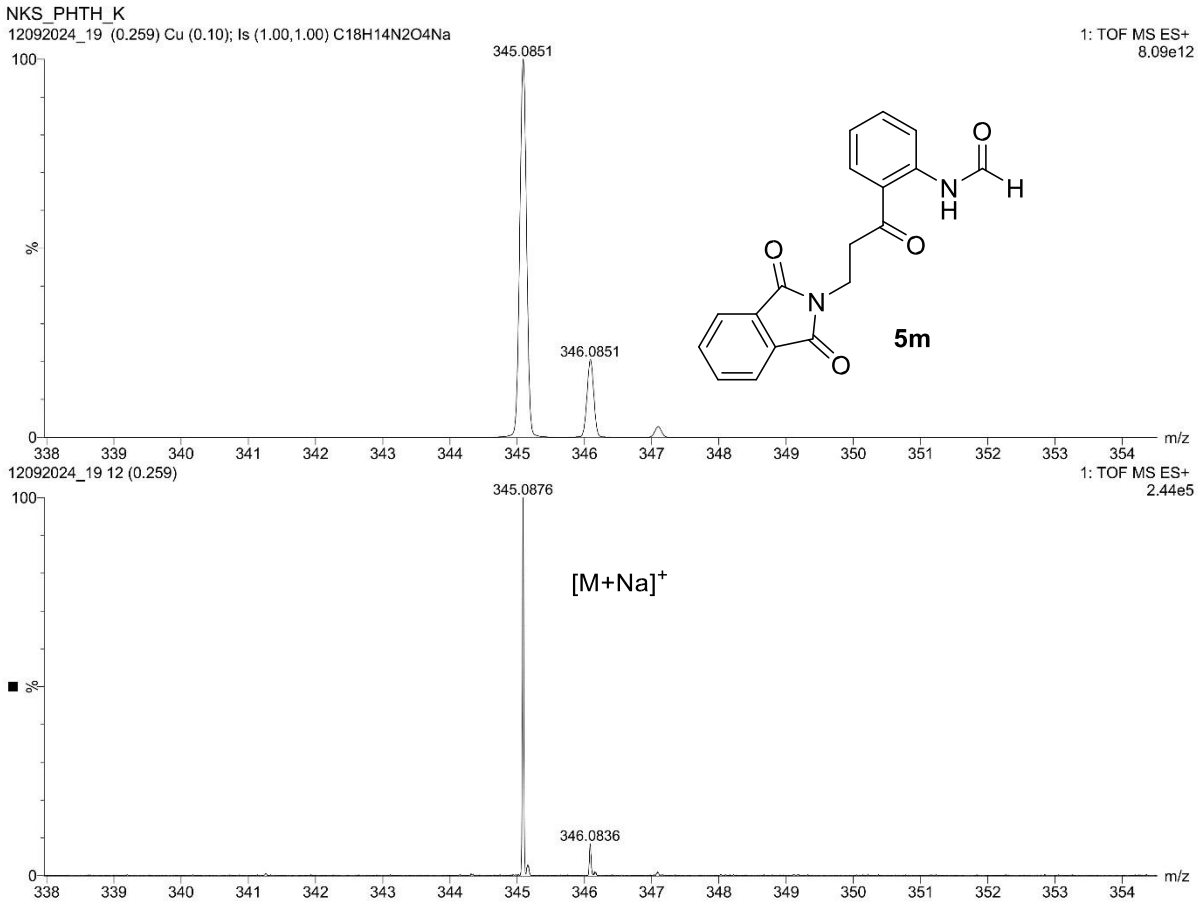

Fig S119. ESI-HRMS spectra of kynurenine derivative **5m**.

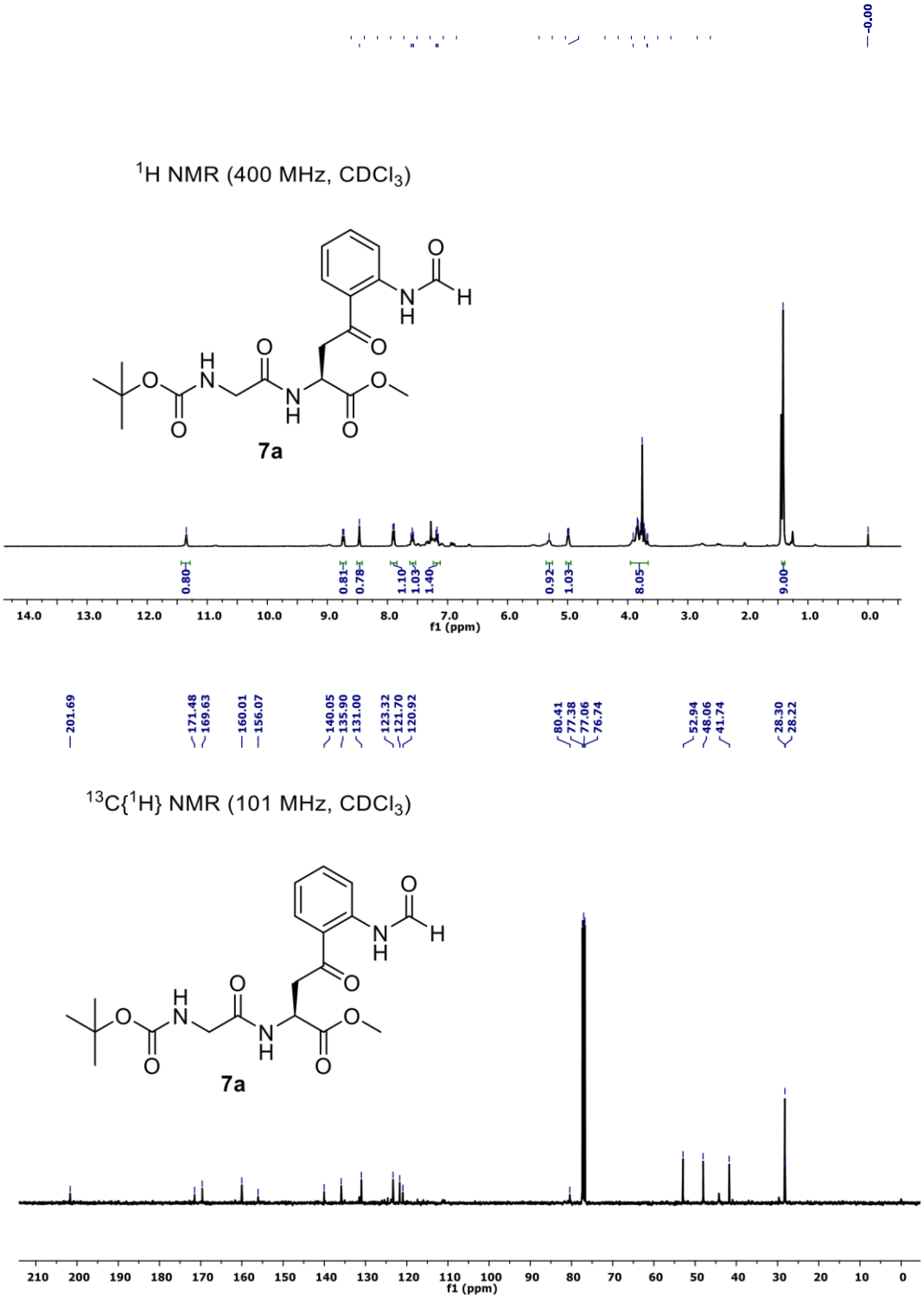

Fig S120. ^{1}H, ^{13}C {^{1}H} NMR spectra of kynurenine-containing dipeptide **7a**.

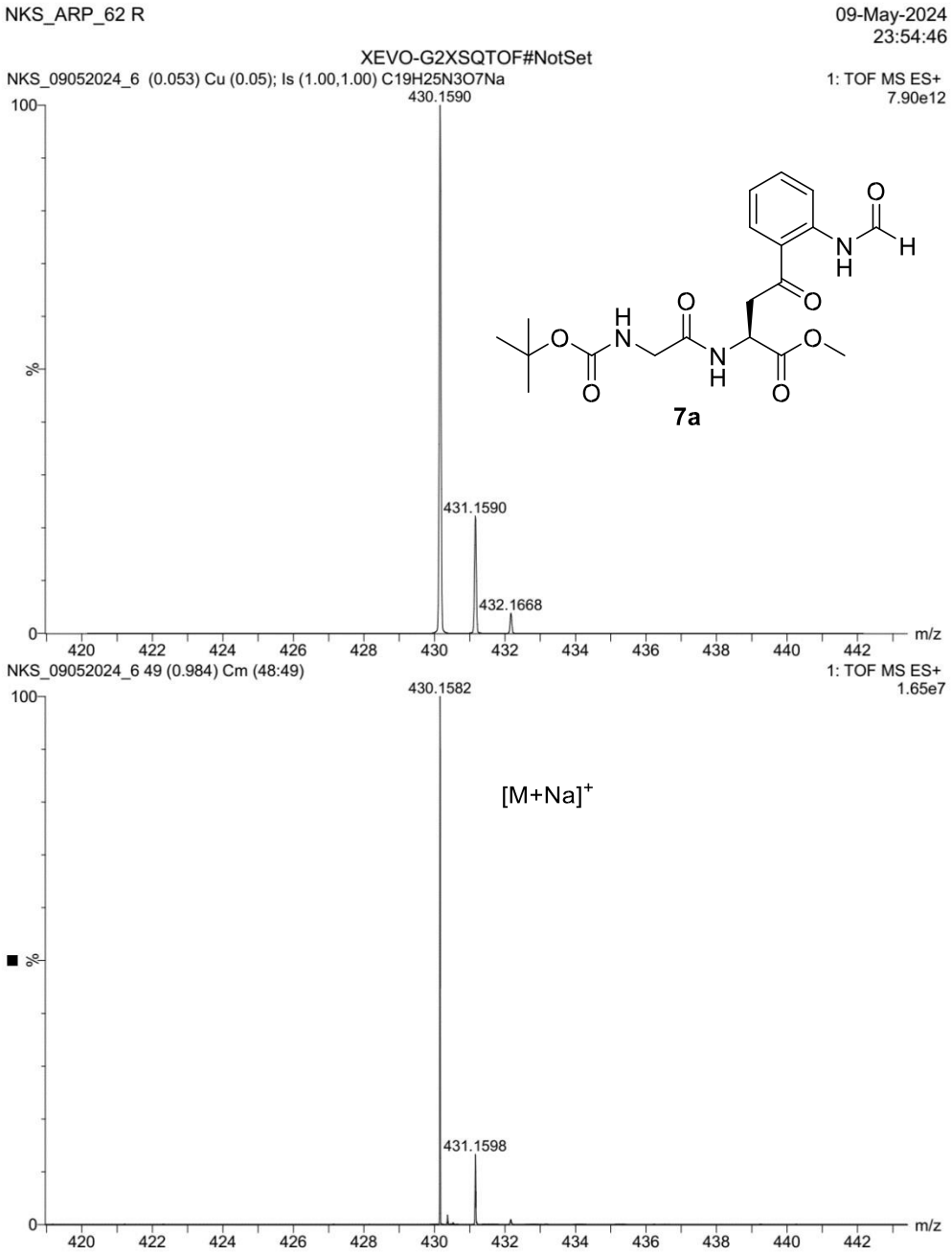

Fig S121. ESI-HRMS spectra of kynurenine-containing dipeptide **7a**.

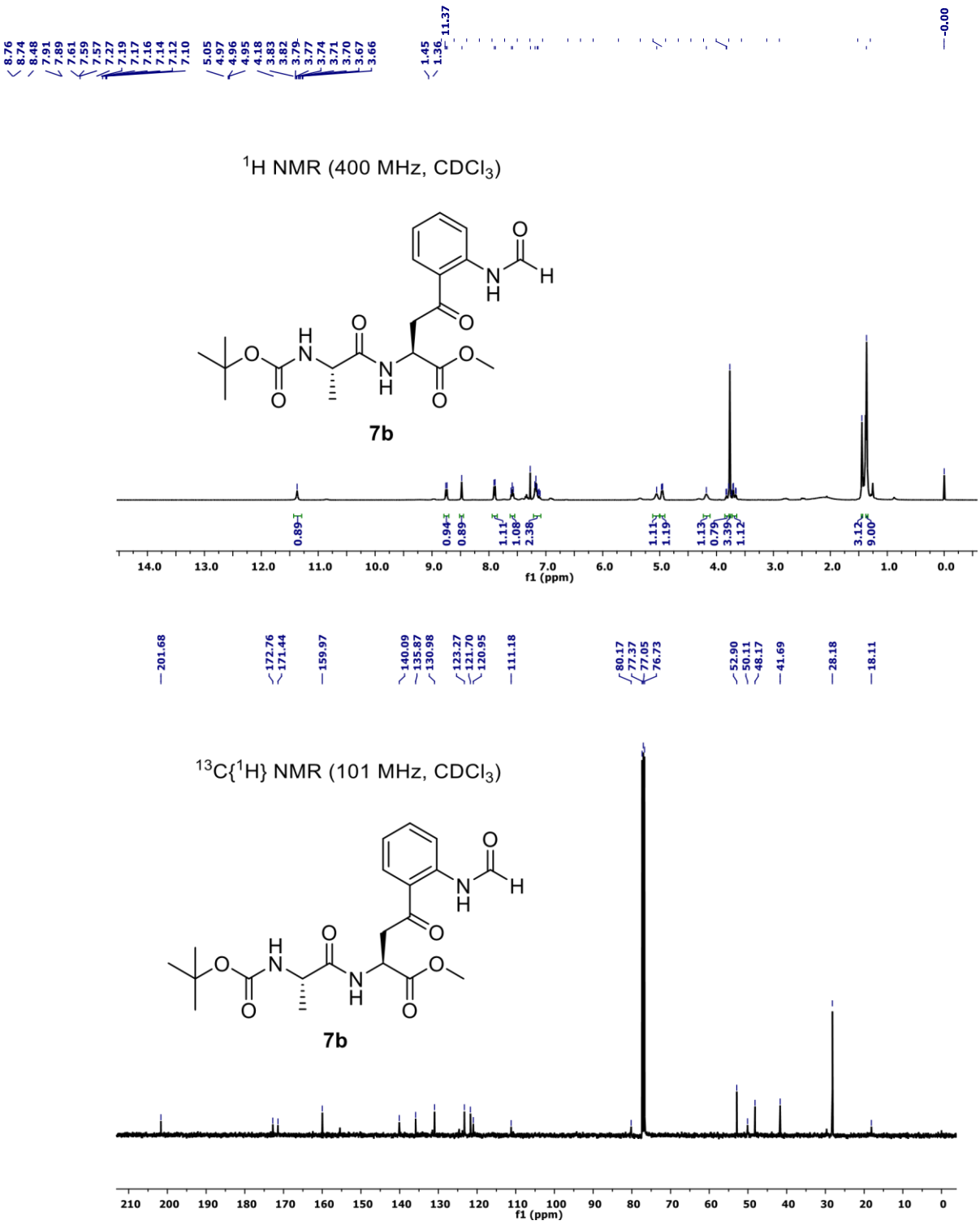

Fig S122. ^{1}H, ^{13}C {^{1}H} NMR spectra of kynurenine-containing dipeptide **7b**.

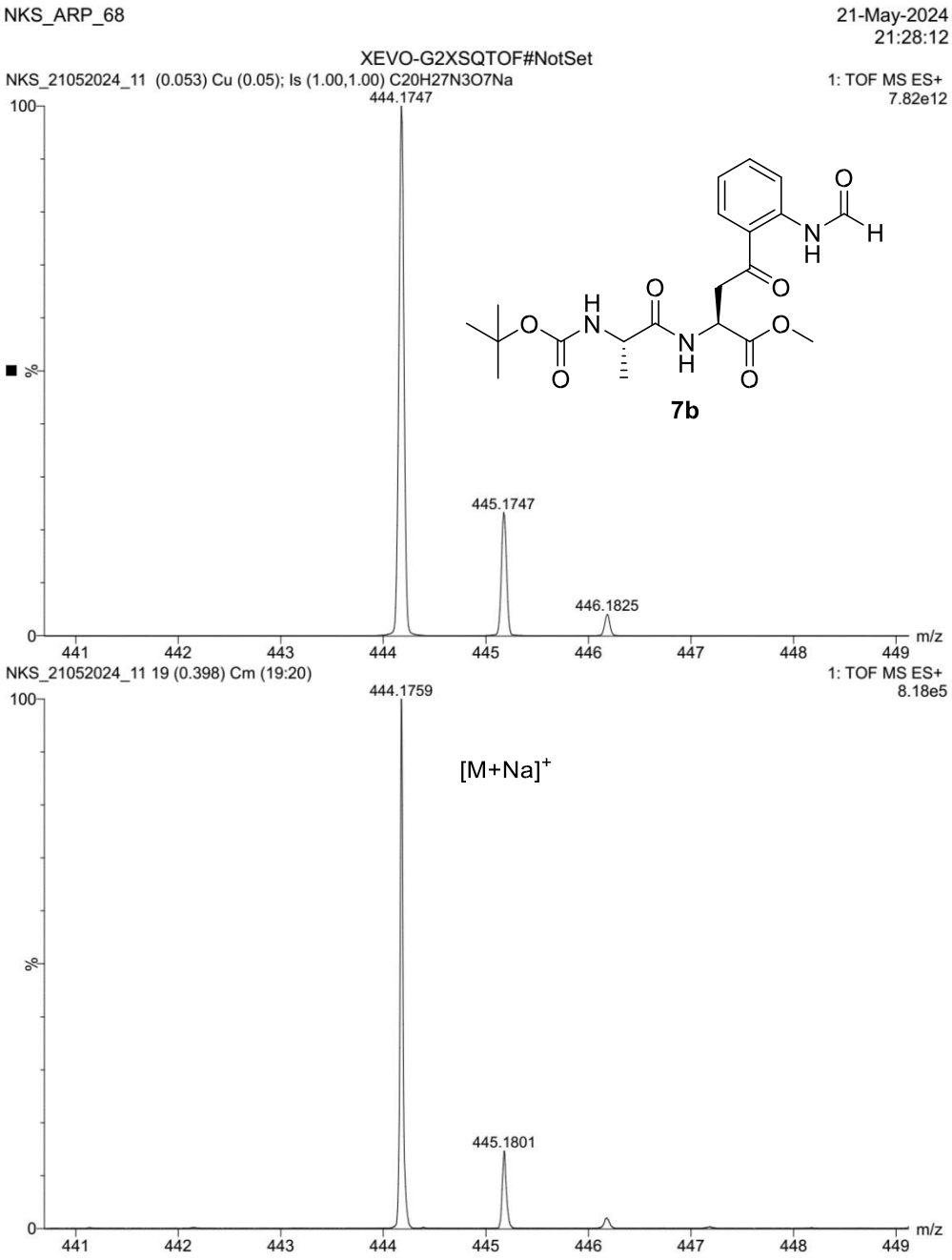

Fig S123. ESI-HRMS spectra of kynurenine-containing dipeptide **7b**.

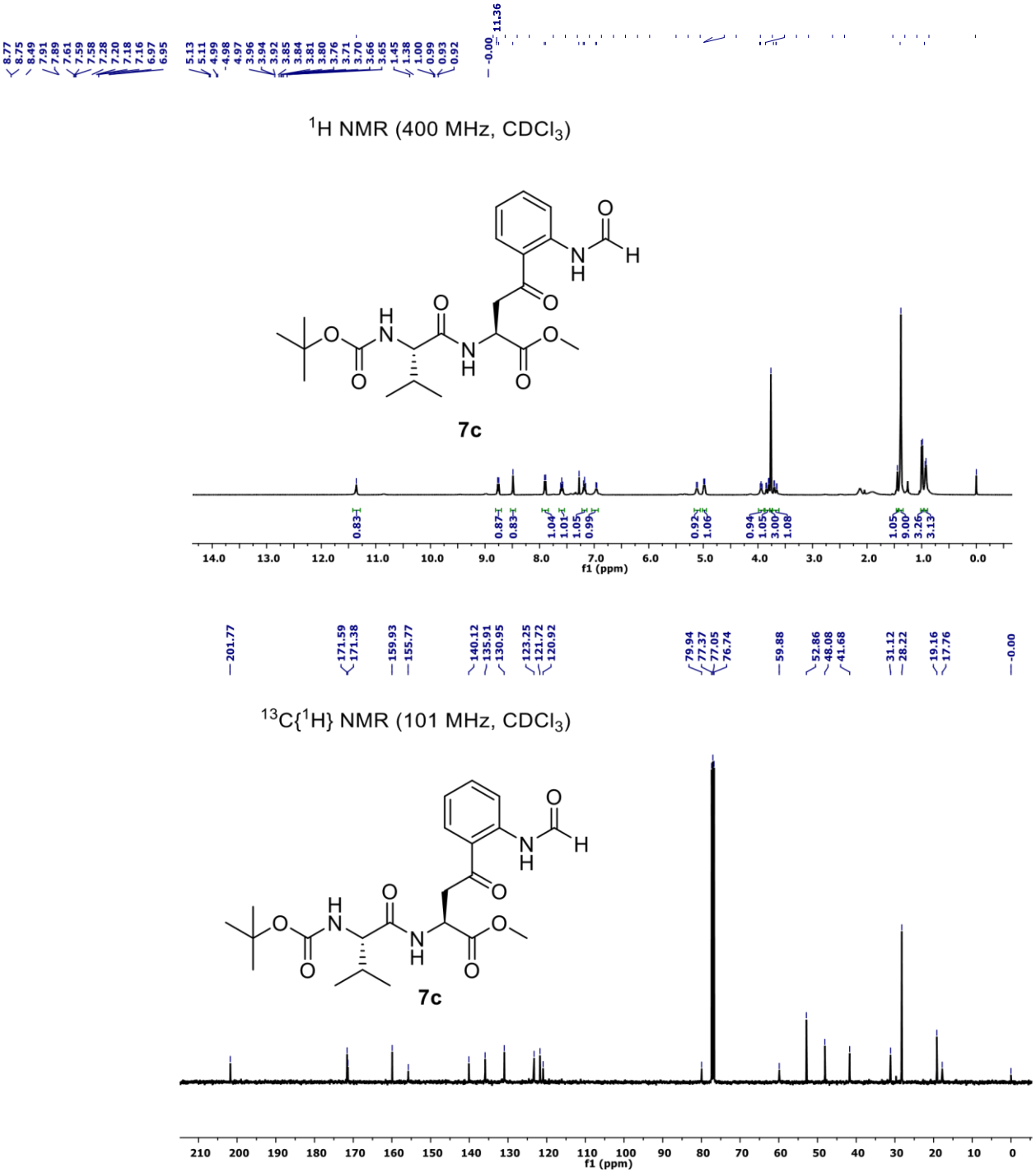

Fig S124. ^{1}H, ^{13}C $\{^{1}H\}$ NMR spectra of kynurenine-containing dipeptide **7c**.

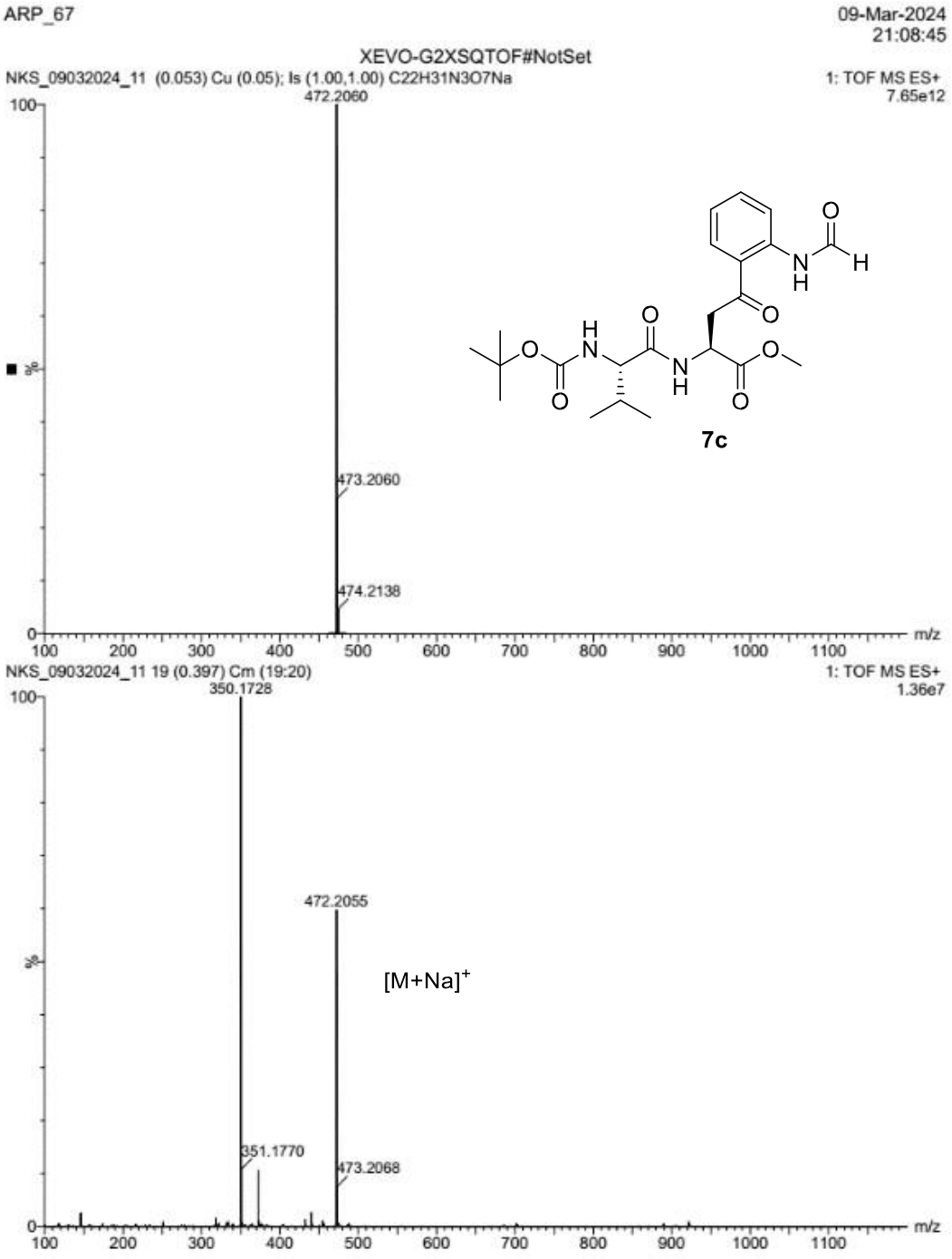

Fig S125. ESI-HRMS spectra of kynurenine-containing dipeptide **7c**.

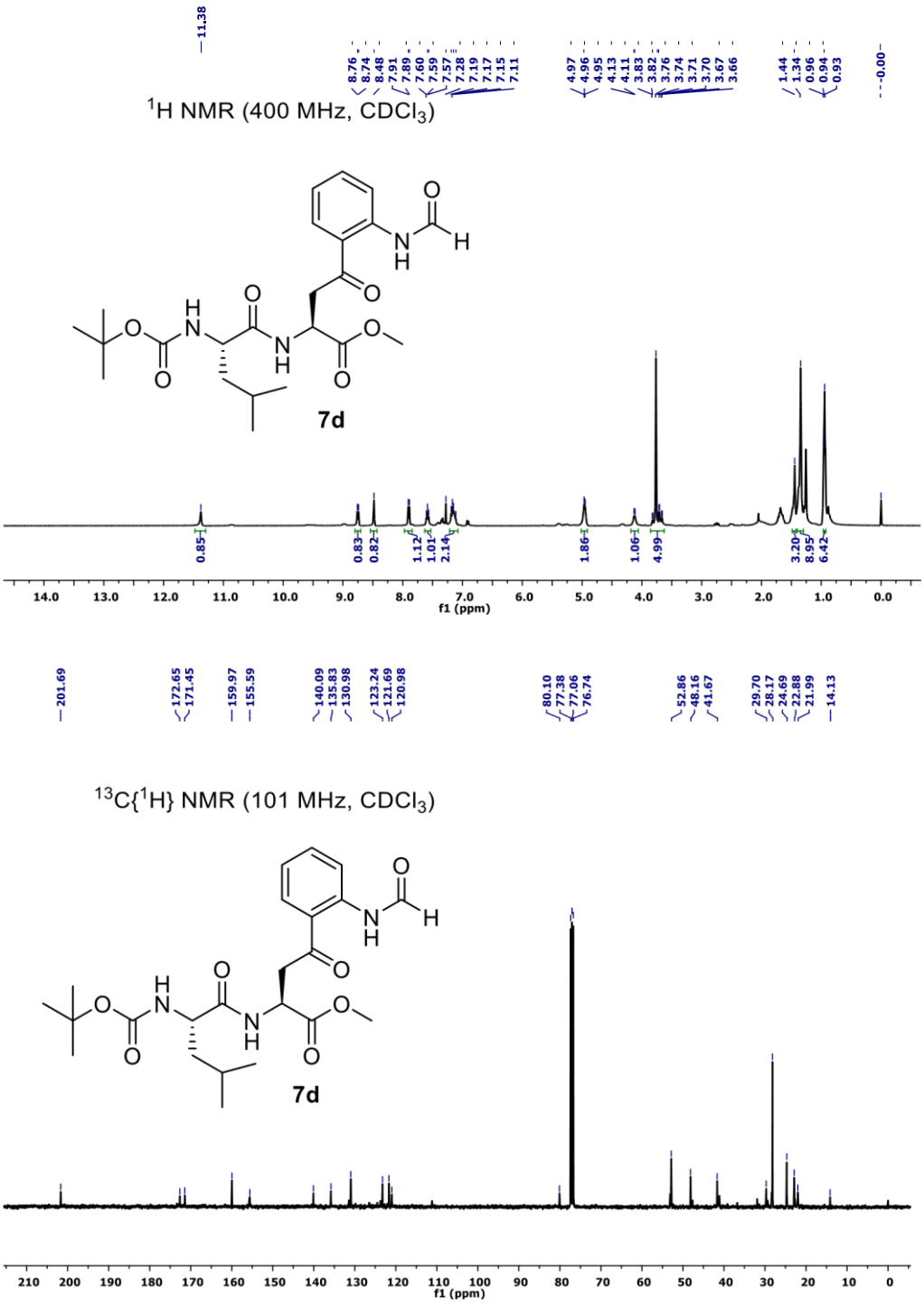

Fig S126. ^{1}H, ^{13}C $\{^{1}H\}$ NMR spectra of kynurenine-containing dipeptide **7d**.

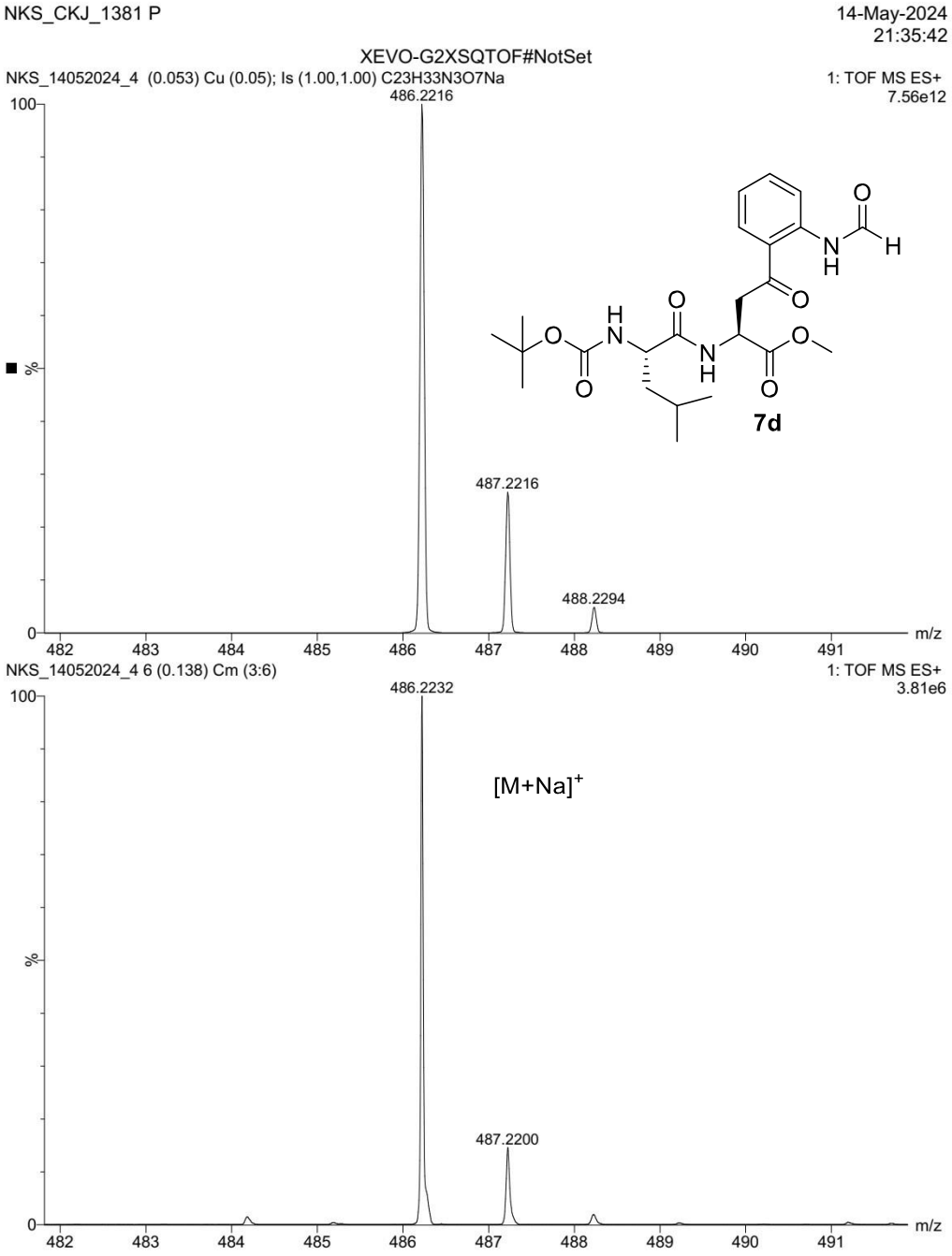

Fig S127. ESI-HRMS spectra of kynurenine-containing dipeptide **7d**.

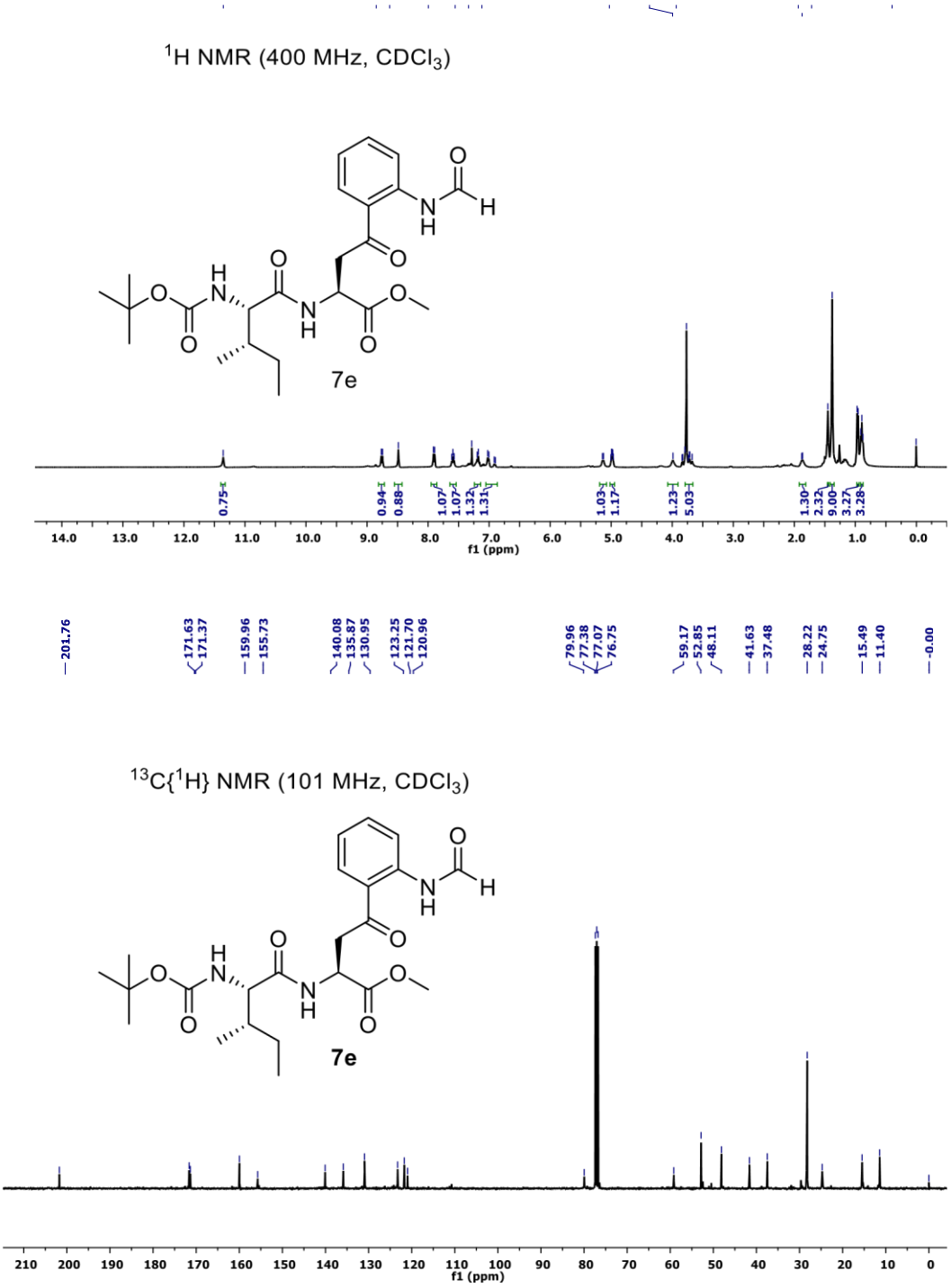

Fig S128. ^{1}H, ^{13}C {^{1}H} NMR spectra of kynurenine-containing dipeptide **7e**.

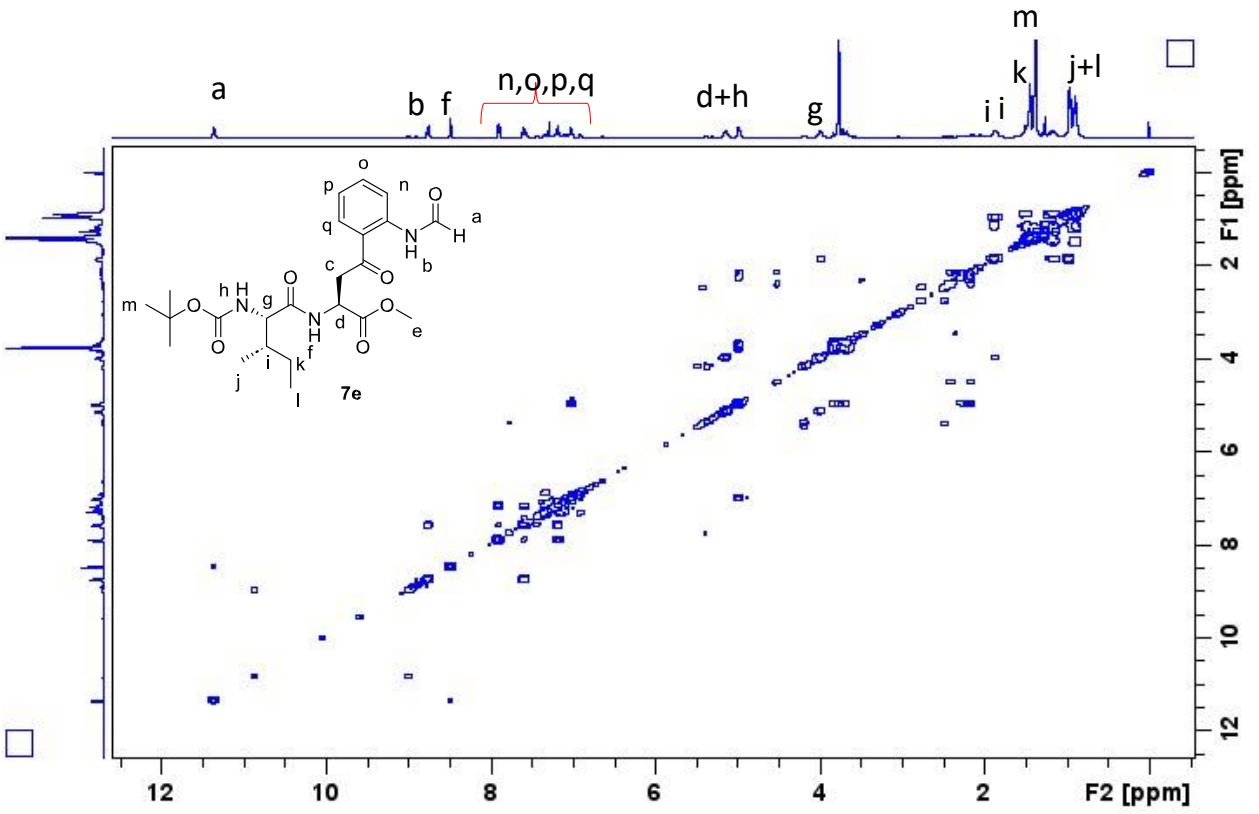

^{1}H-^{1}H COSY 2D NMR Spectra of Compound **7e** e+c

Fig S129. ^{1}H-^{1}H COSY 2D NMR Spectra of Compound **7e.**

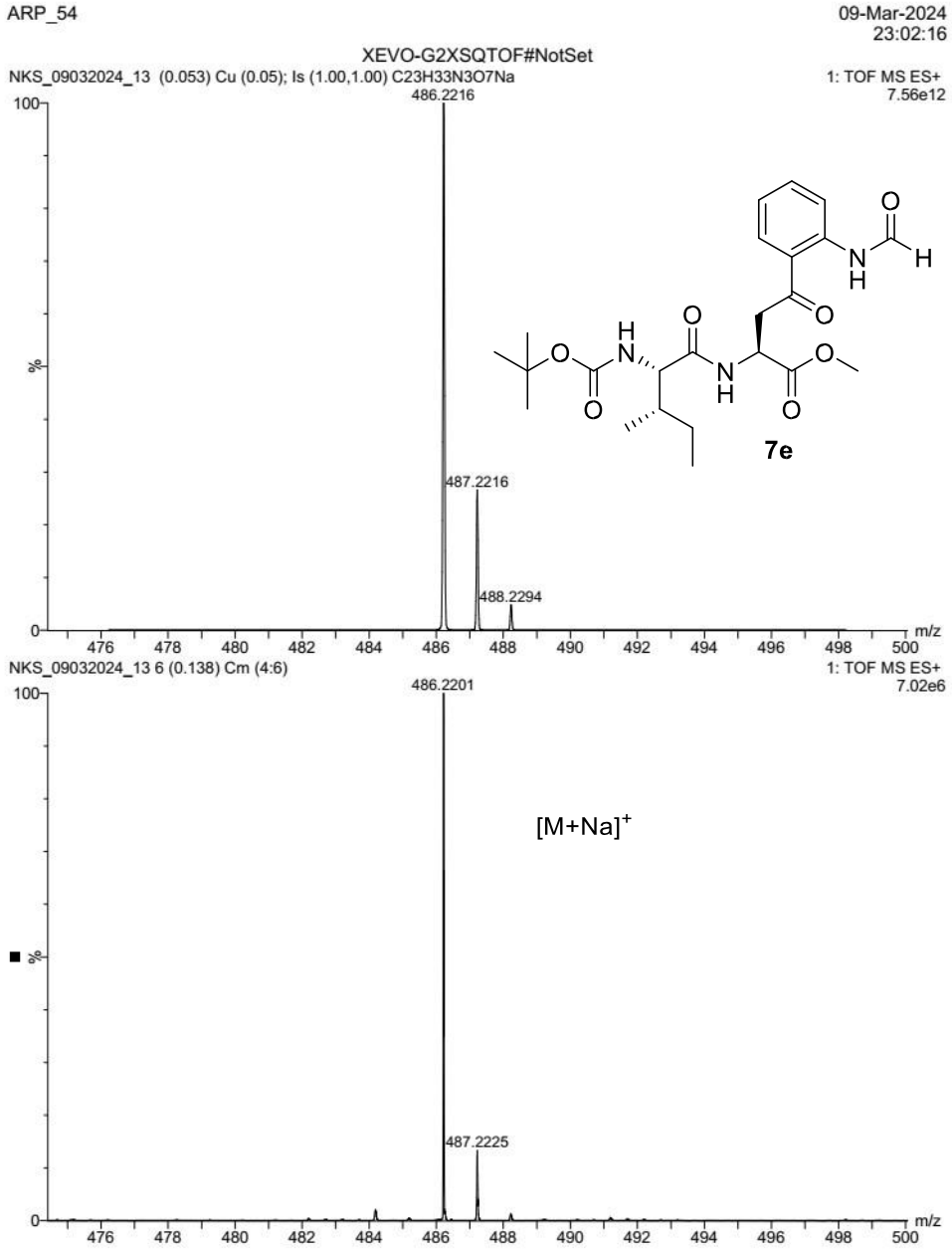

Fig S130. ESI-HRMS spectra of kynurenine-containing dipeptide **7e**.

.

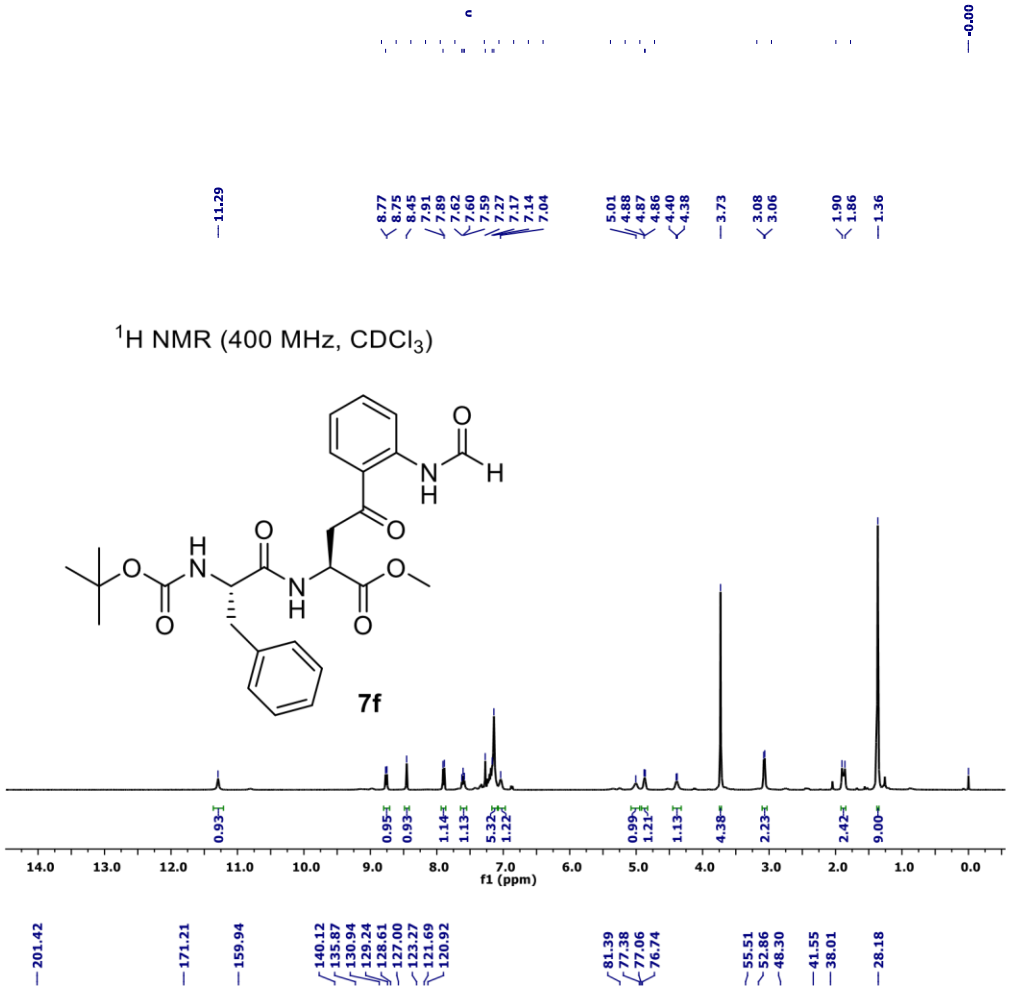
11.29
8.77
8.75
8.45
7.91
7.89
7.62
7.60
7.59
7.27
7.17
7.14
7.04
5.01
4.88
4.87
4.86
4.40
4.38
3.73
3.08
3.06
1.90
1.86
1.36
0.00
1H NMR (400 MHz, CDCl3)
7f
0.93
0.95
0.93
1.14
1.13
5.32
1.22
0.99
1.21
1.13
4.38
2.23
2.42
9.00
14.0
13.0
12.0
11.0
10.0
9.0
8.0
7.0
6.0
5.0
4.0
3.0
2.0
1.0
0.0
f1 (ppm)
201.42
171.21
159.94
140.12
135.87
130.94
129.24
128.61
127.00
123.27
121.69
120.92
81.39
77.38
77.06
76.74
55.51
52.86
48.30
41.55
38.01
28.18

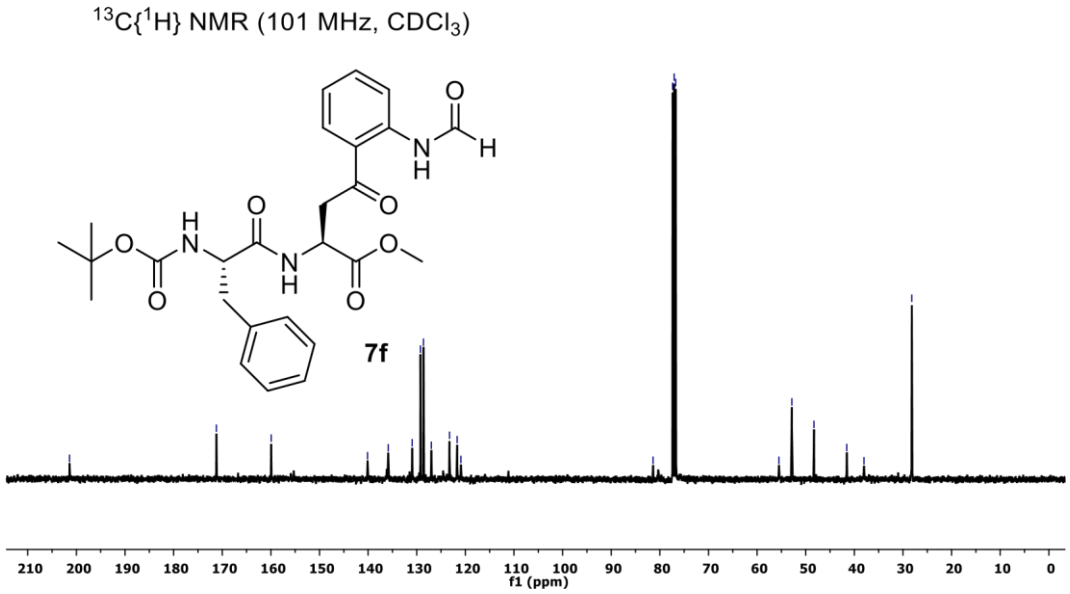

Fig S131. ^{1}H, ^{13}C $\{^{1}H\}$ NMR spectra of kynurenine-containing dipeptide **7f**.

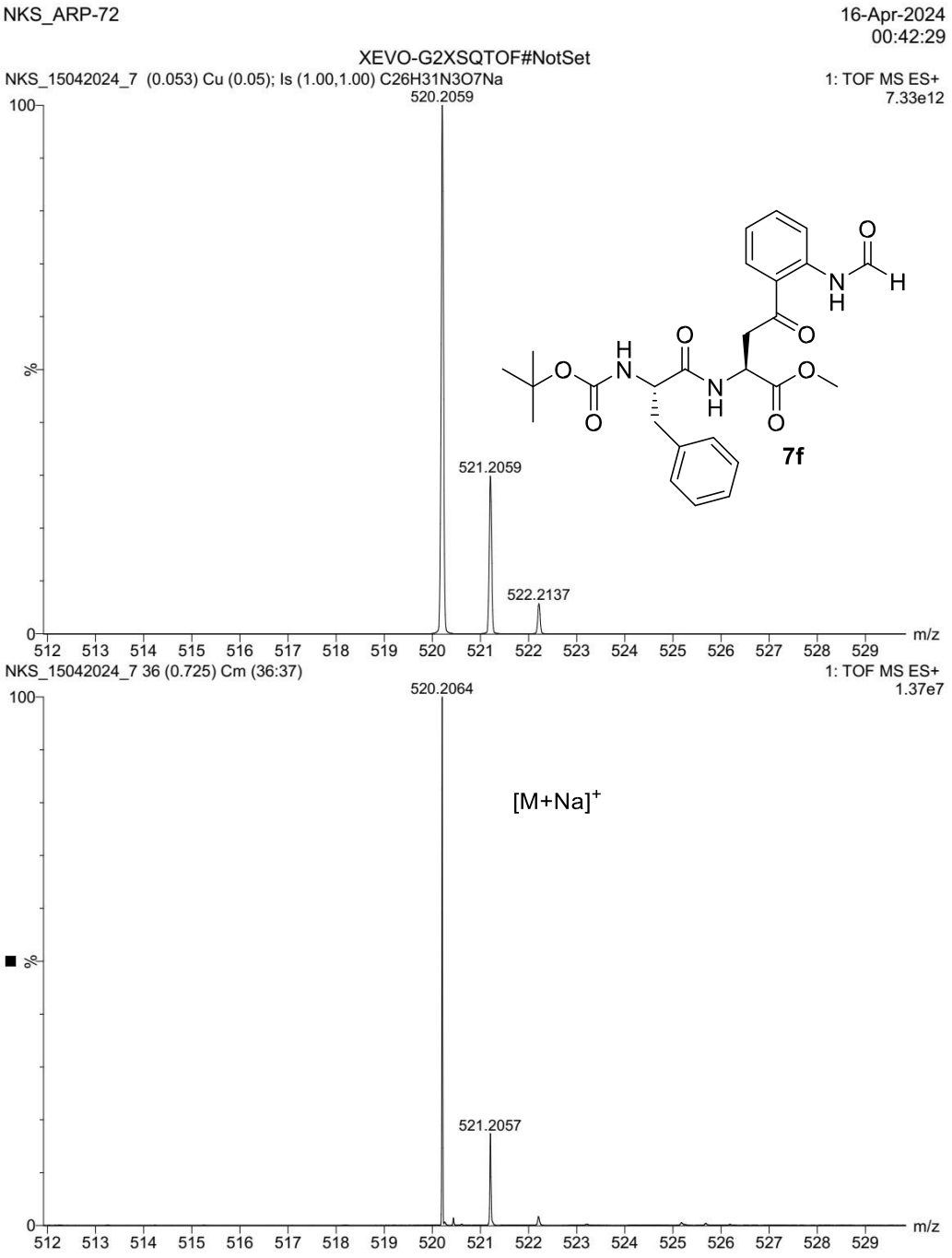
NKS_ARP-72
16-Apr-2024
00:42:29
XEVO-G2XSQTOF#NotSet
NKS_15042024_7 (0.053) Cu (0.05); Is (1.00,1.00) C26H31N3O7Na
1: TOF MS ES+
7.33e12
520.2059
521.2059
522.2137
7f
NKS_15042024_7 36 (0.725) Cm (36:37)
1: TOF MS ES+
1.37e7
520.2064
[M+Na]+
521.2057
%
m/z
100
0
512 513 514 515 516 517 518 519 520 521 522 523 524 525 526 527 528 529

Fig S132. ESI-HRMS spectra of kynurenine-containing dipeptide **7f**.

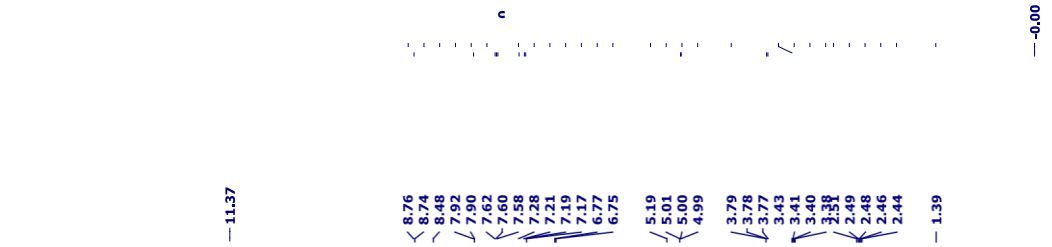

^{1}H NMR (400 MHz, $CDCl_3$)

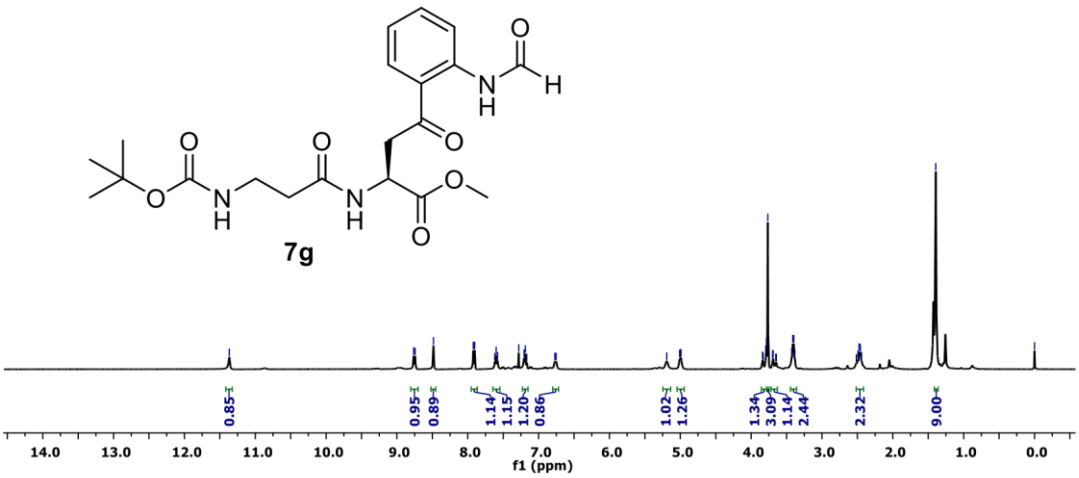

^{13}C{^{1}H} NMR (101 MHz, $CDCl_3$)

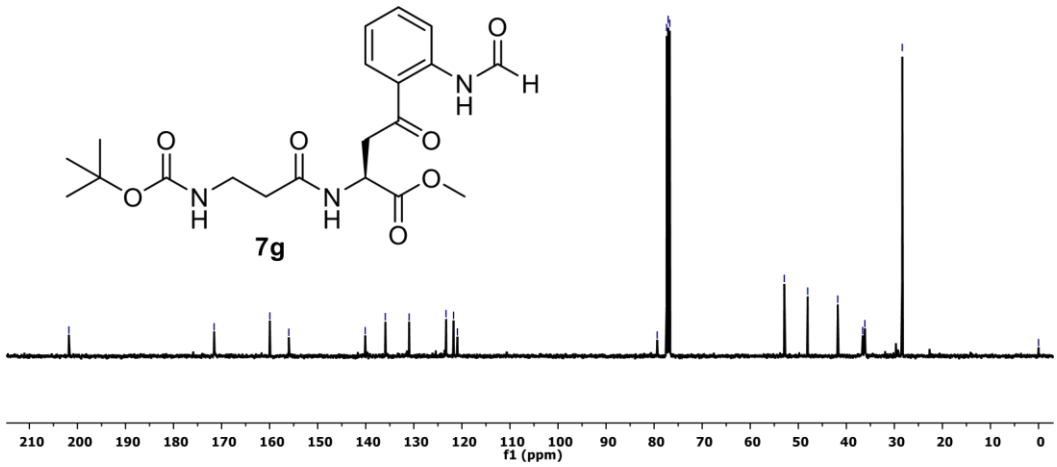

Fig S133. ^{1}H, ^{13}C $\{^{1}H\}$ NMR spectra of kynurenine-containing dipeptide **7g**.

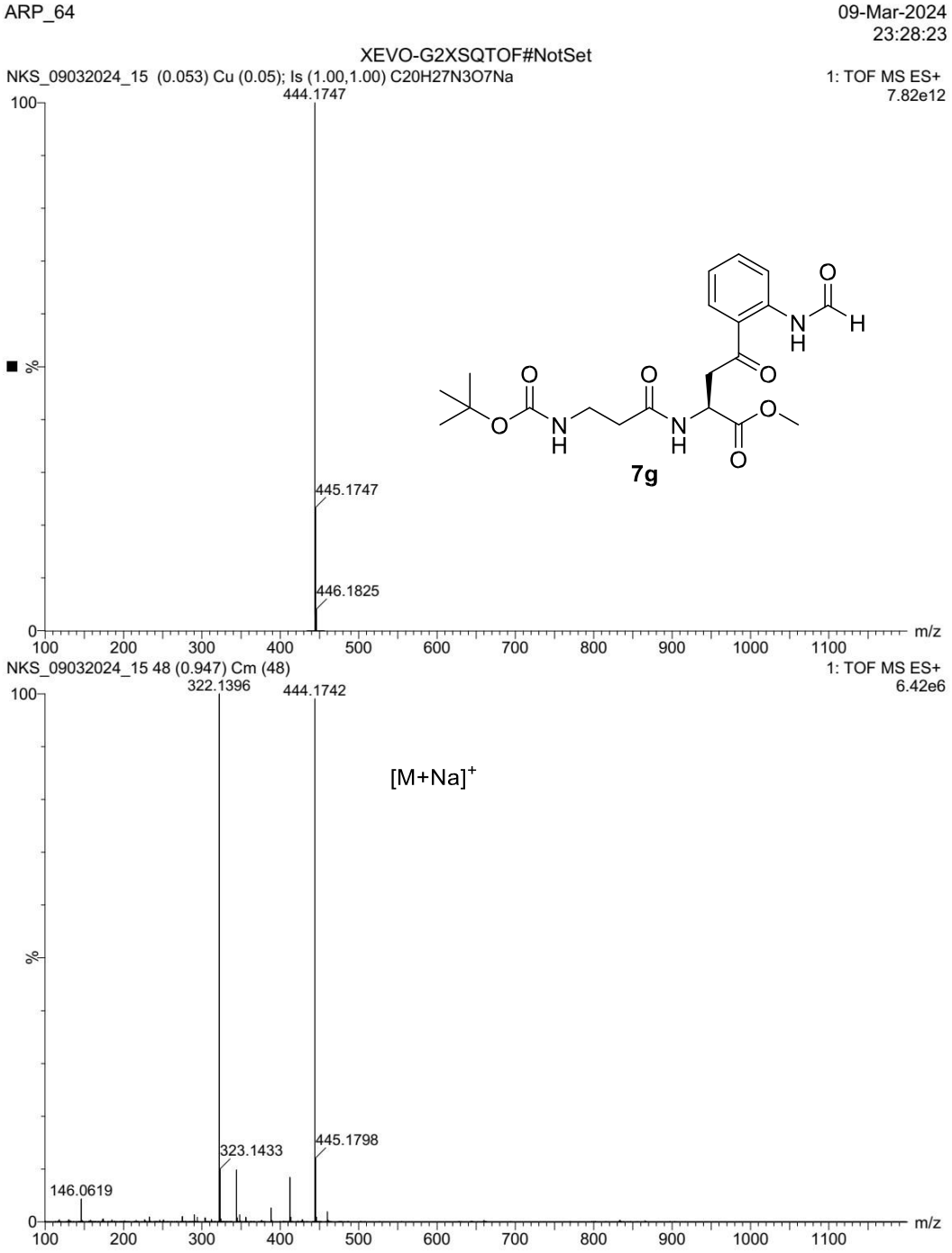

Fig S134. ESI-HRMS spectra of kynurenine-containing dipeptide **7g**.

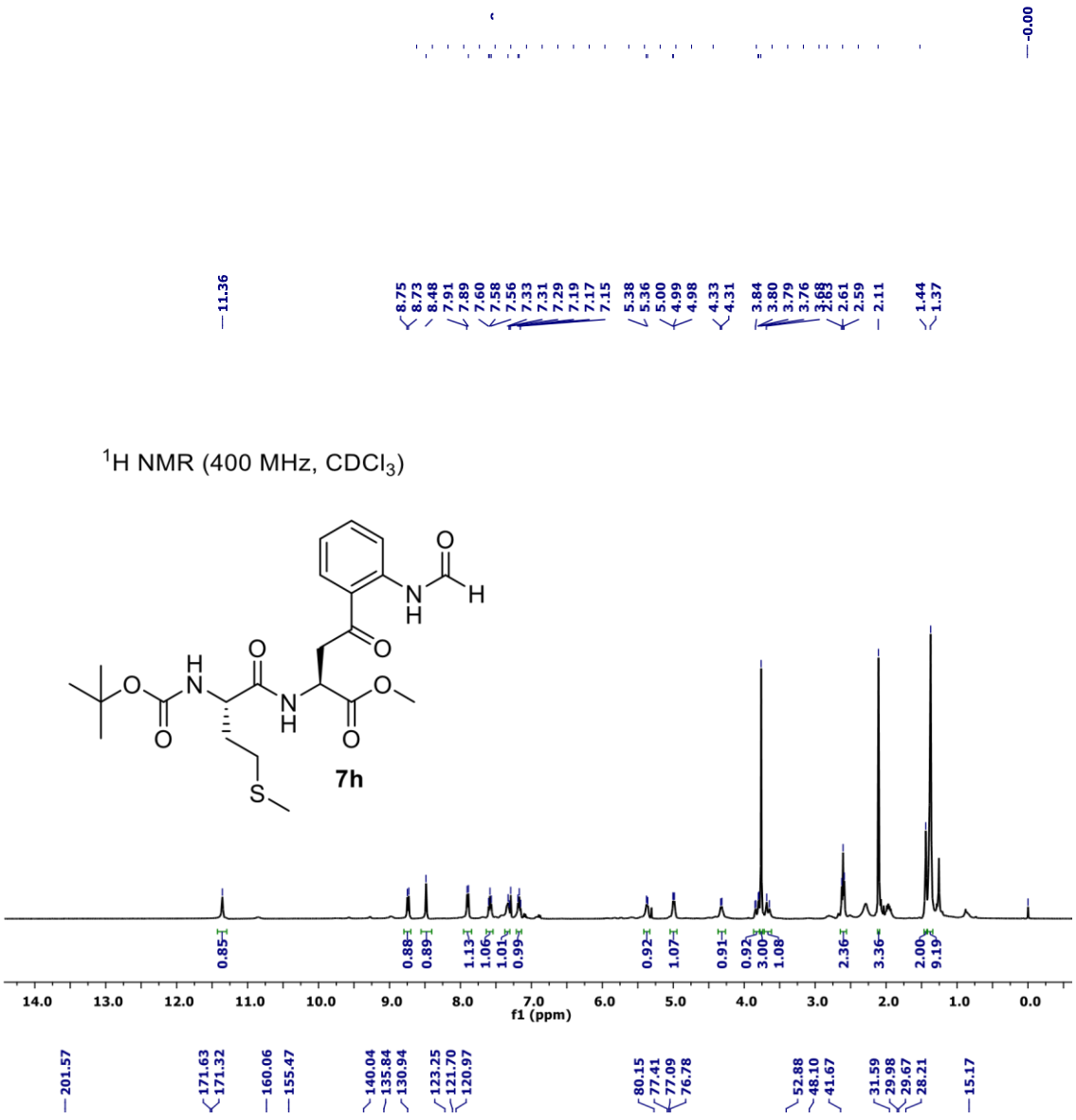
11.36
8.75
8.73
8.48
7.91
7.89
7.60
7.58
7.56
7.33
7.31
7.29
7.19
7.17
7.15
5.38
5.36
5.00
4.99
4.98
4.33
4.31
3.84
3.80
3.79
3.76
2.61
2.59
2.11
1.44
1.37
0.00
1H NMR (400 MHz, CDCl3)
7h
0.85
0.88
0.89
1.13
1.06
1.01
0.99
0.92
1.07
0.91
0.92
3.00
1.08
2.36
3.36
2.00
9.19
14.0
13.0
12.0
11.0
10.0
9.0
8.0
7.0
6.0
5.0
4.0
3.0
2.0
1.0
0.0
f1 (ppm)
201.57
171.63
171.32
160.06
155.47
140.04
135.84
130.94
123.25
121.70
120.97
80.15
77.41
77.09
76.78
52.88
48.10
41.67
31.59
29.98
29.67
28.21
15.17

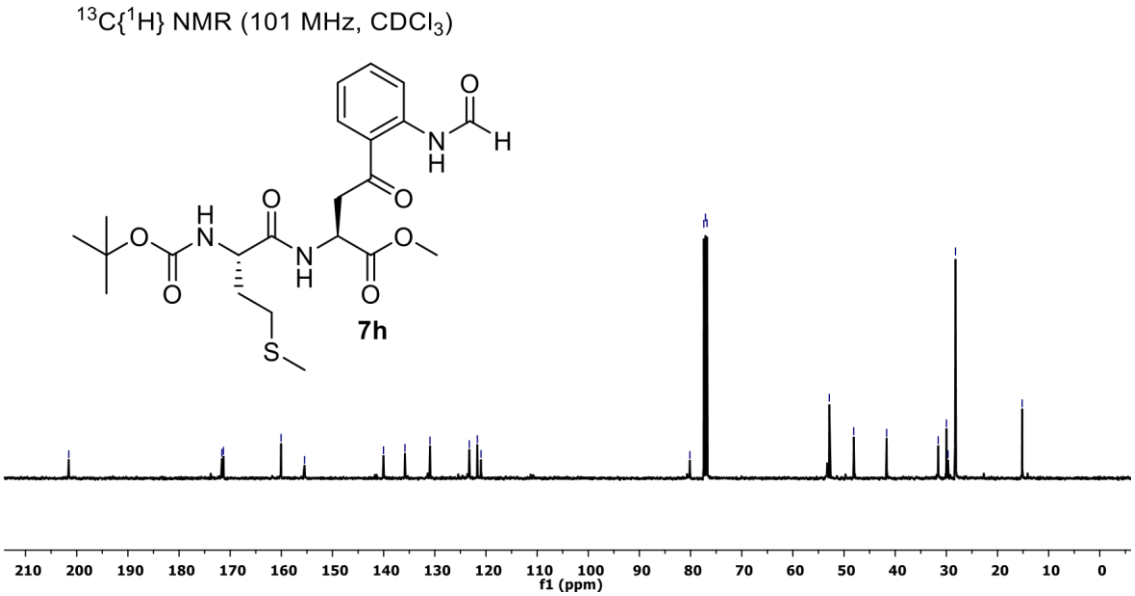

Fig S135. ^{1}H, ^{13}C $\{^{1}H\}$ NMR spectra of kynurenine-containing dipeptide **7h**.

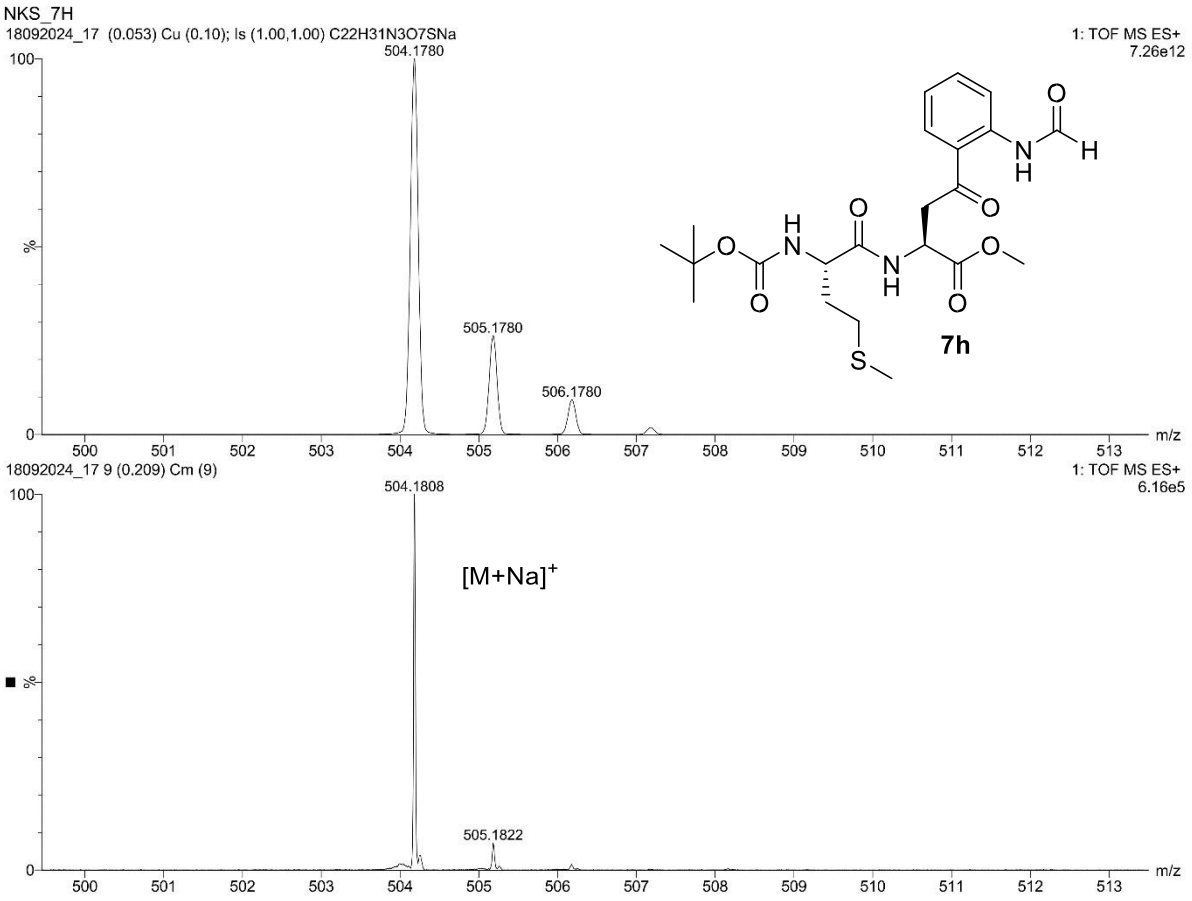

Fig S136. ESI-HRMS spectra of kynurenine-containing dipeptide **7h**.

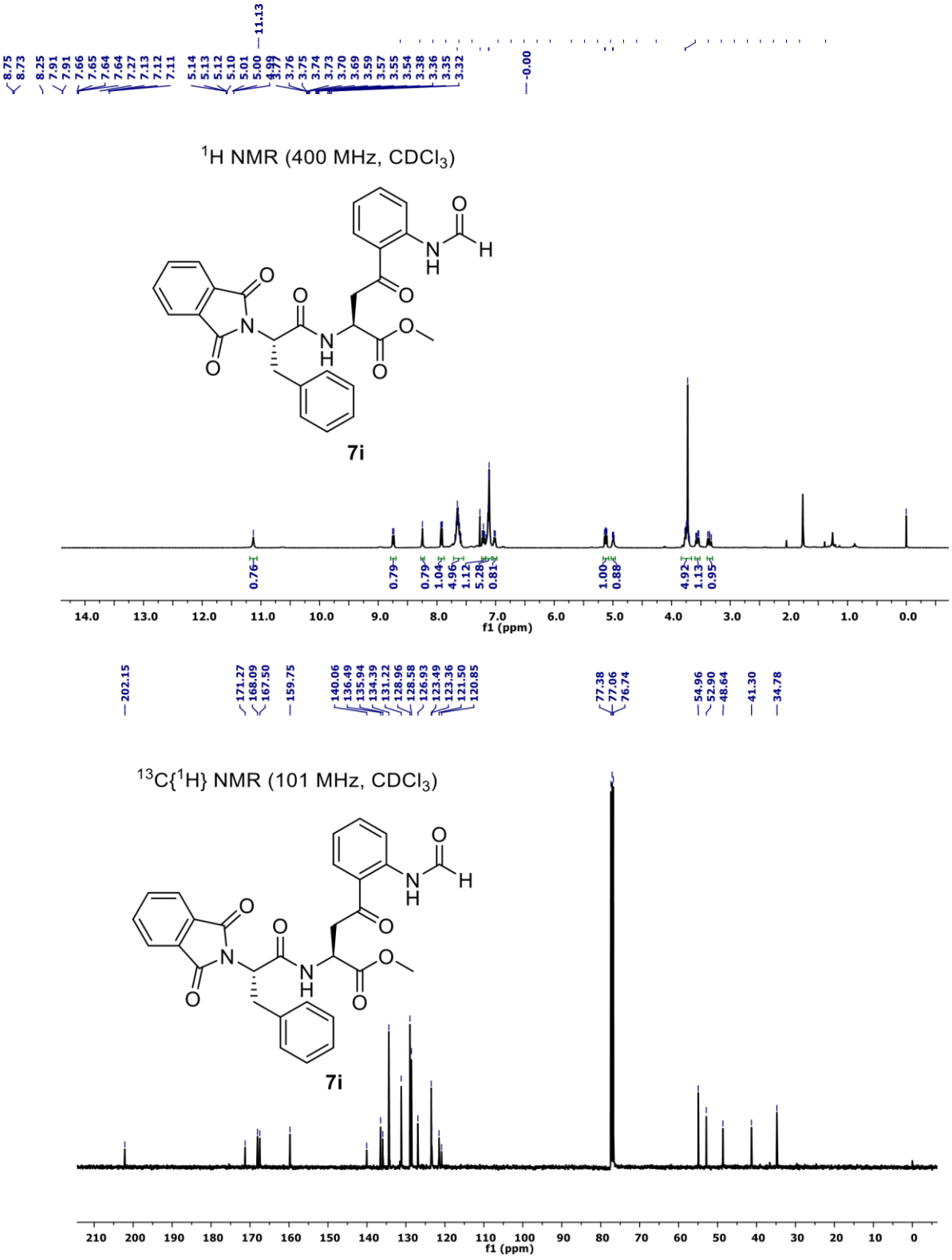

Fig S137. ^{1}H, ^{13}C {^{1}H} NMR spectra of kynurenine-containing dipeptide **7i**.

3. NMR and Mass Spectra of *N*-phenyl tryptophan (**9**) and *N*-troponyl tryptophan (**12**)

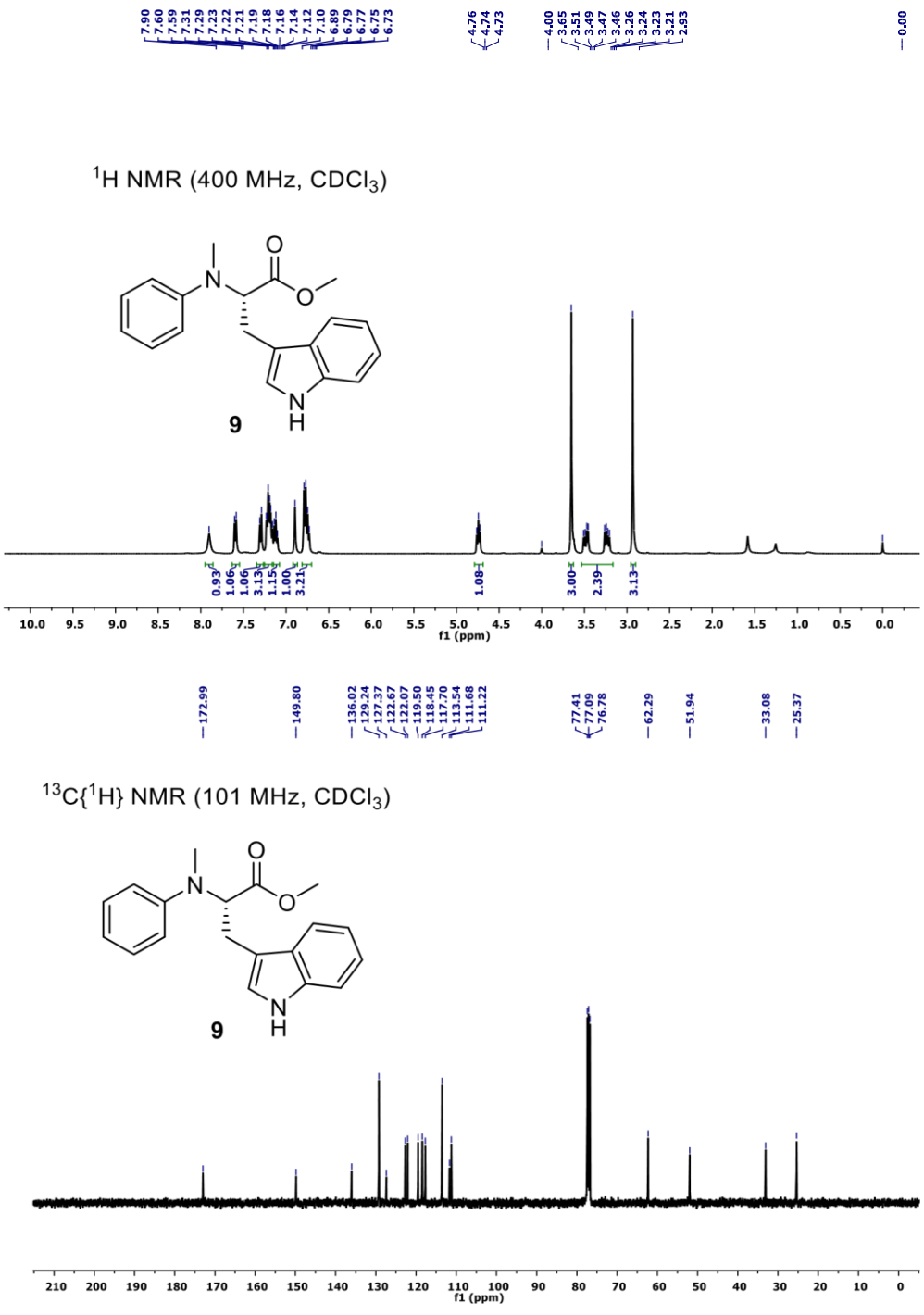

Fig S138. ^{1}H, ^{13}C $\{^1$H$\}$ NMR spectra of *N*-phenyl tryptophan **9**.

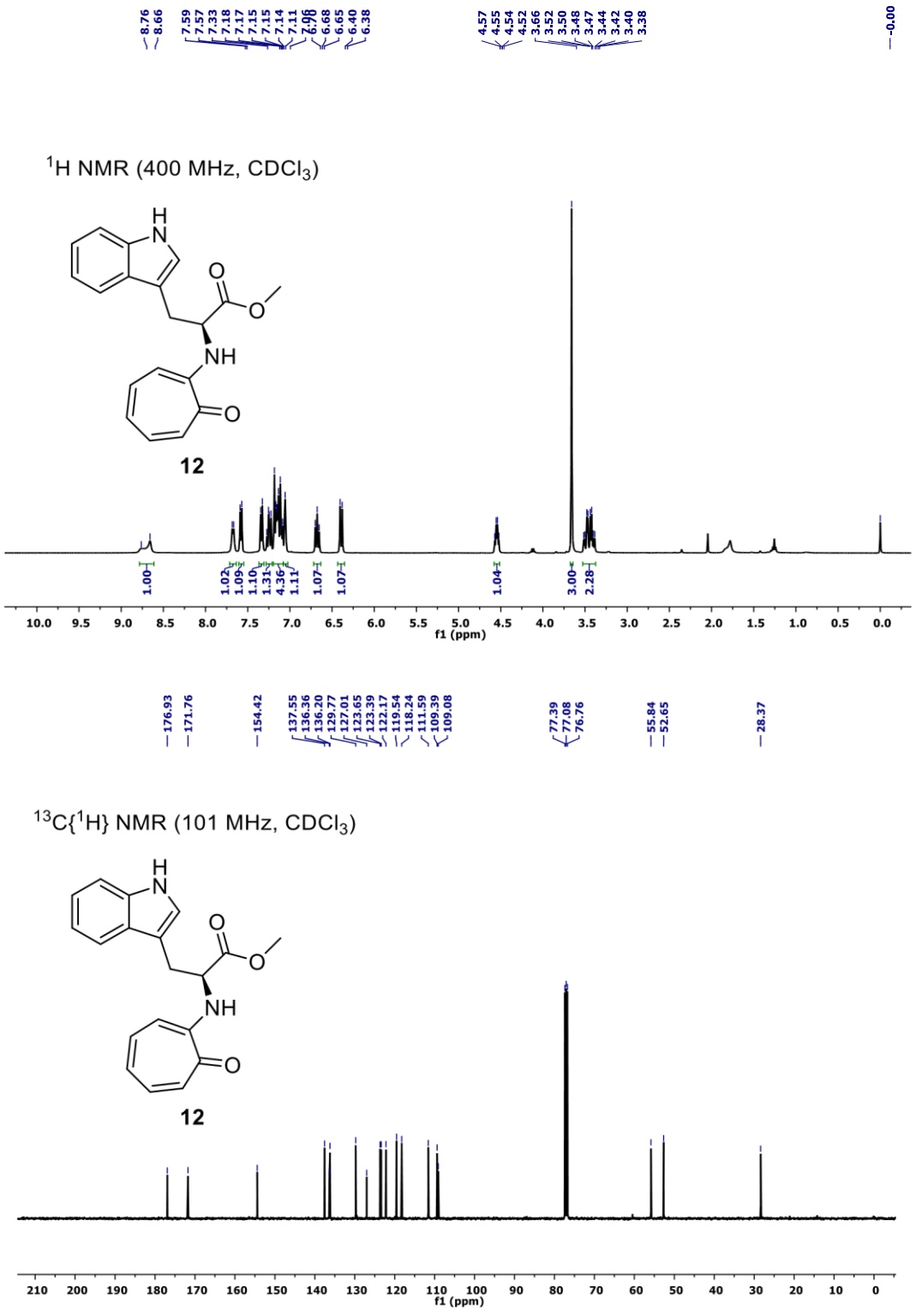

Fig S139. ^{1}H, ^{13}C $\{^{1}H\}$ NMR spectra of *N*-troponyl tryptophan **12**.

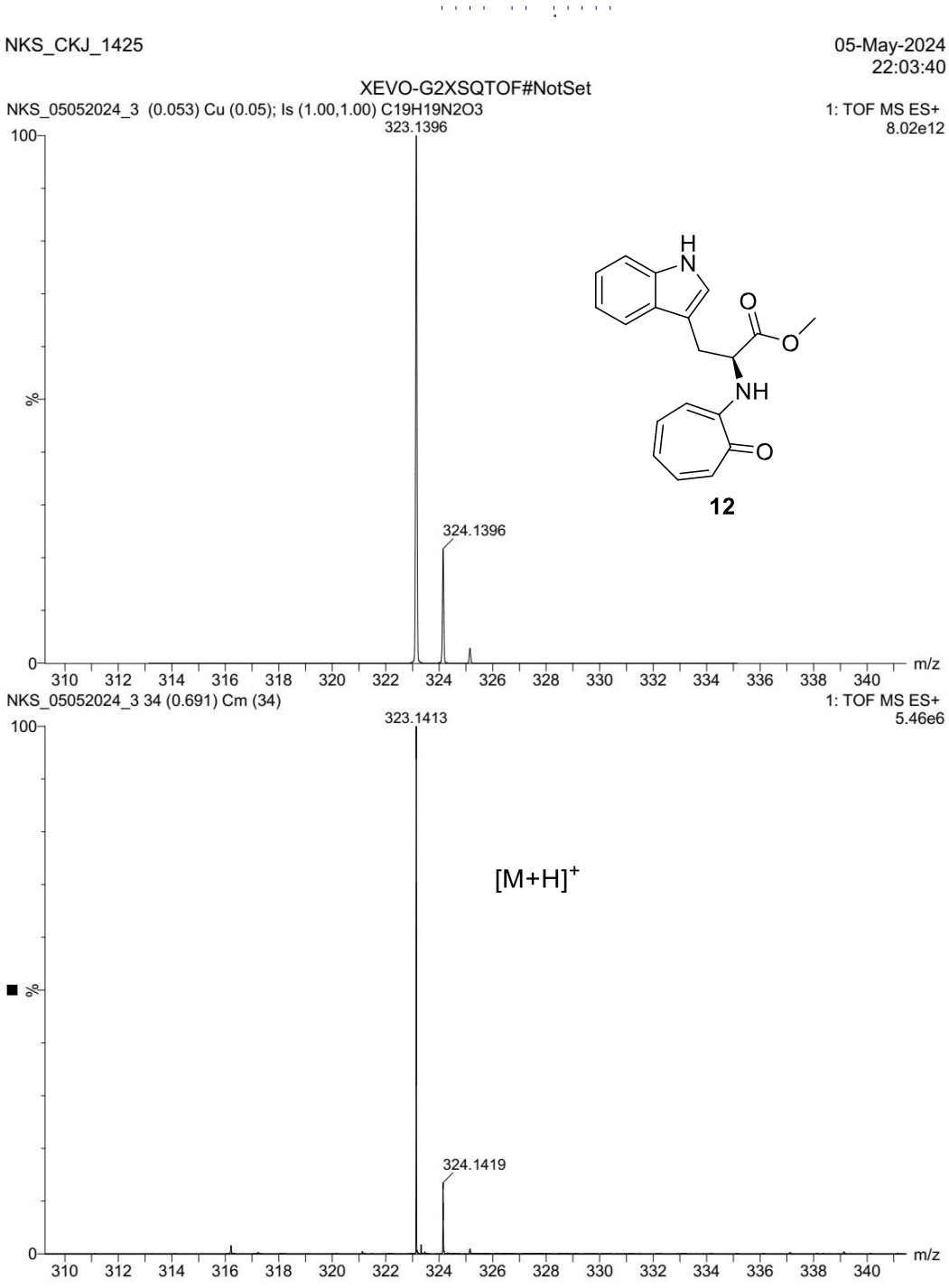

Fig S140. ESI-HRMS spectra of *N*-troponyl tryptophan **12**.

4. NMR and Mass Spectra of Spirocyclic Motifs (**8**/**10**/**13**)

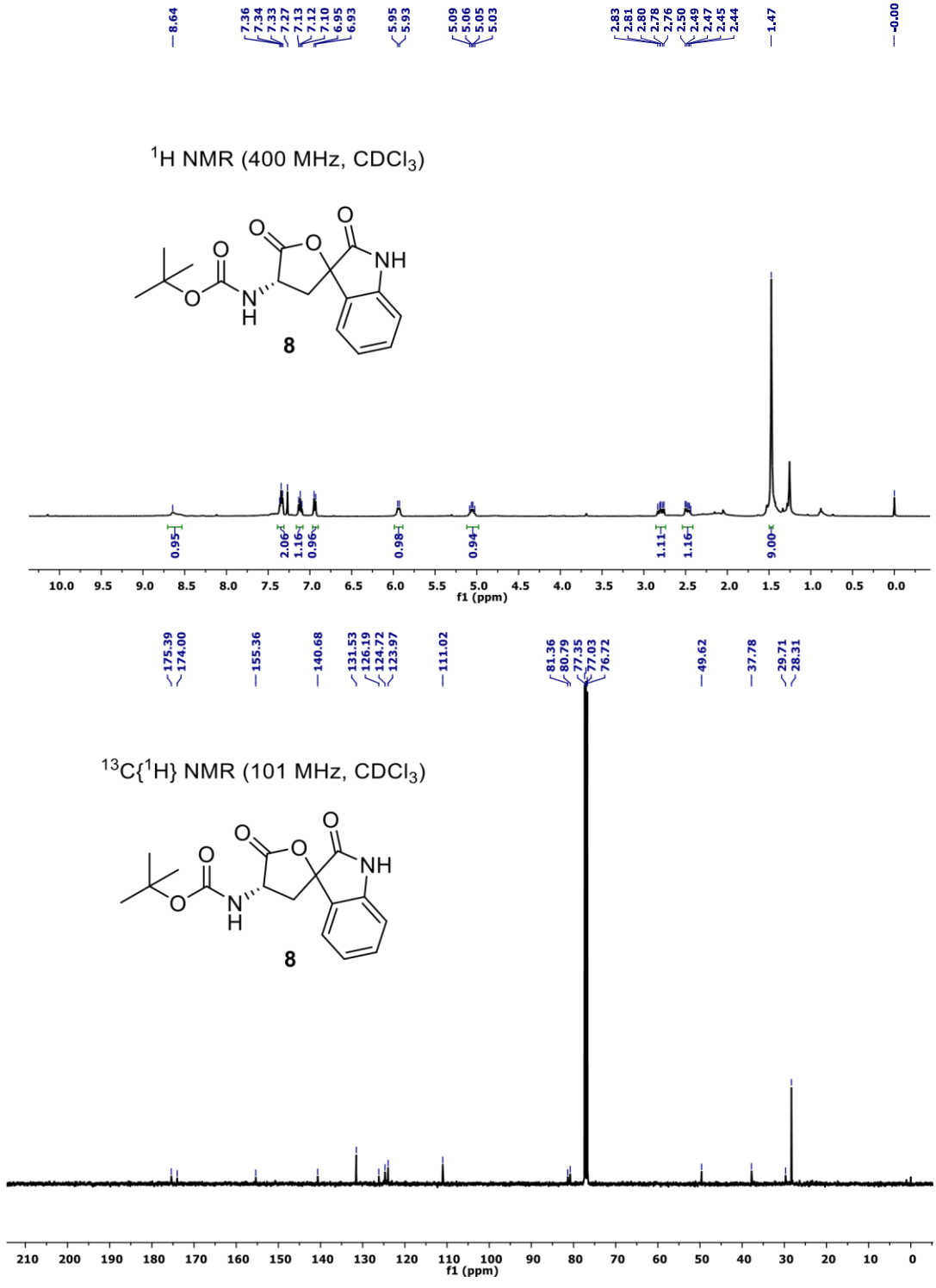

Fig S141. ^{1}H, ^{13}C {^{1}H} NMR spectra of oxaspirooxindole **8**.

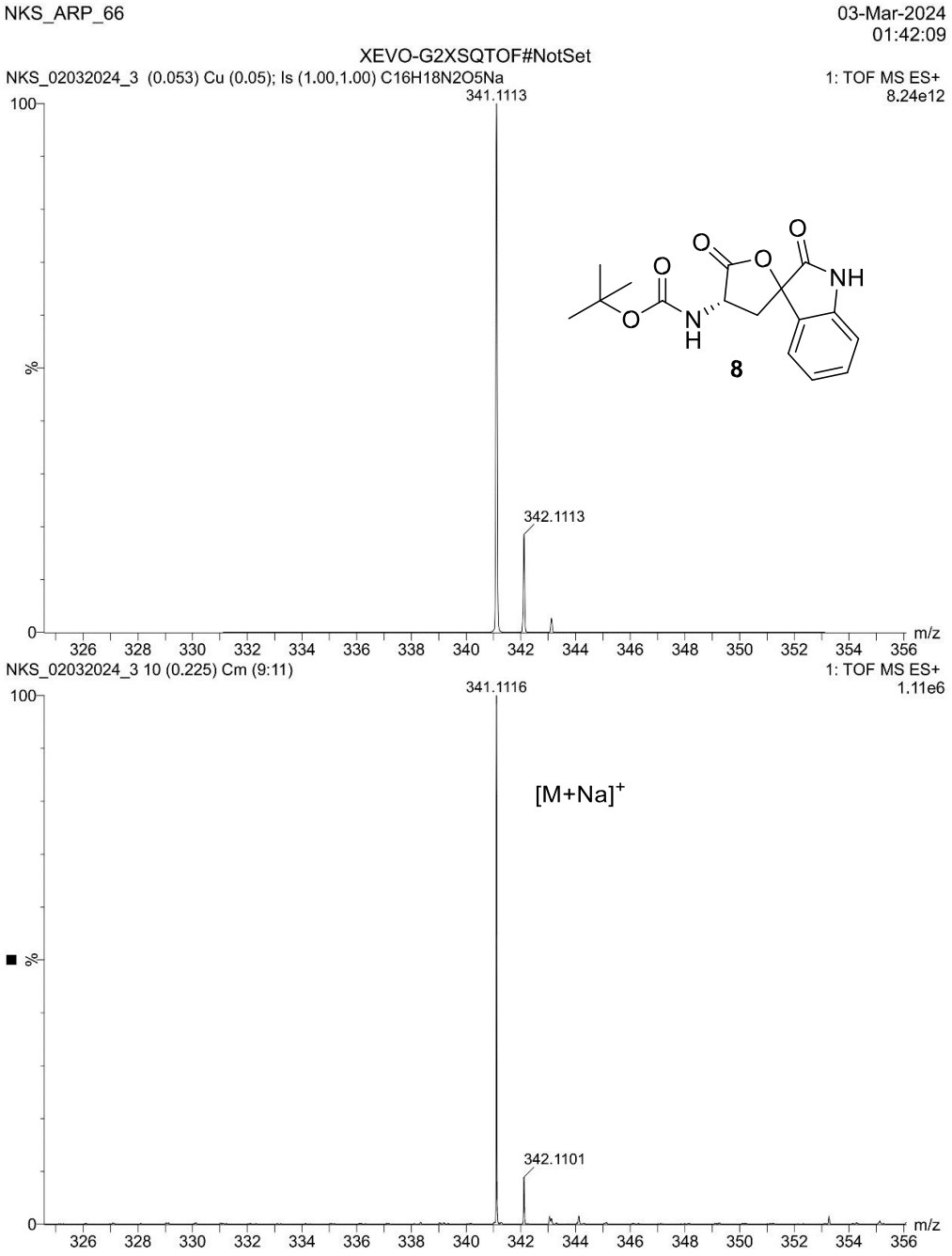

Fig S142. ESI-HRMS spectra of oxaspirooxindole **8**.

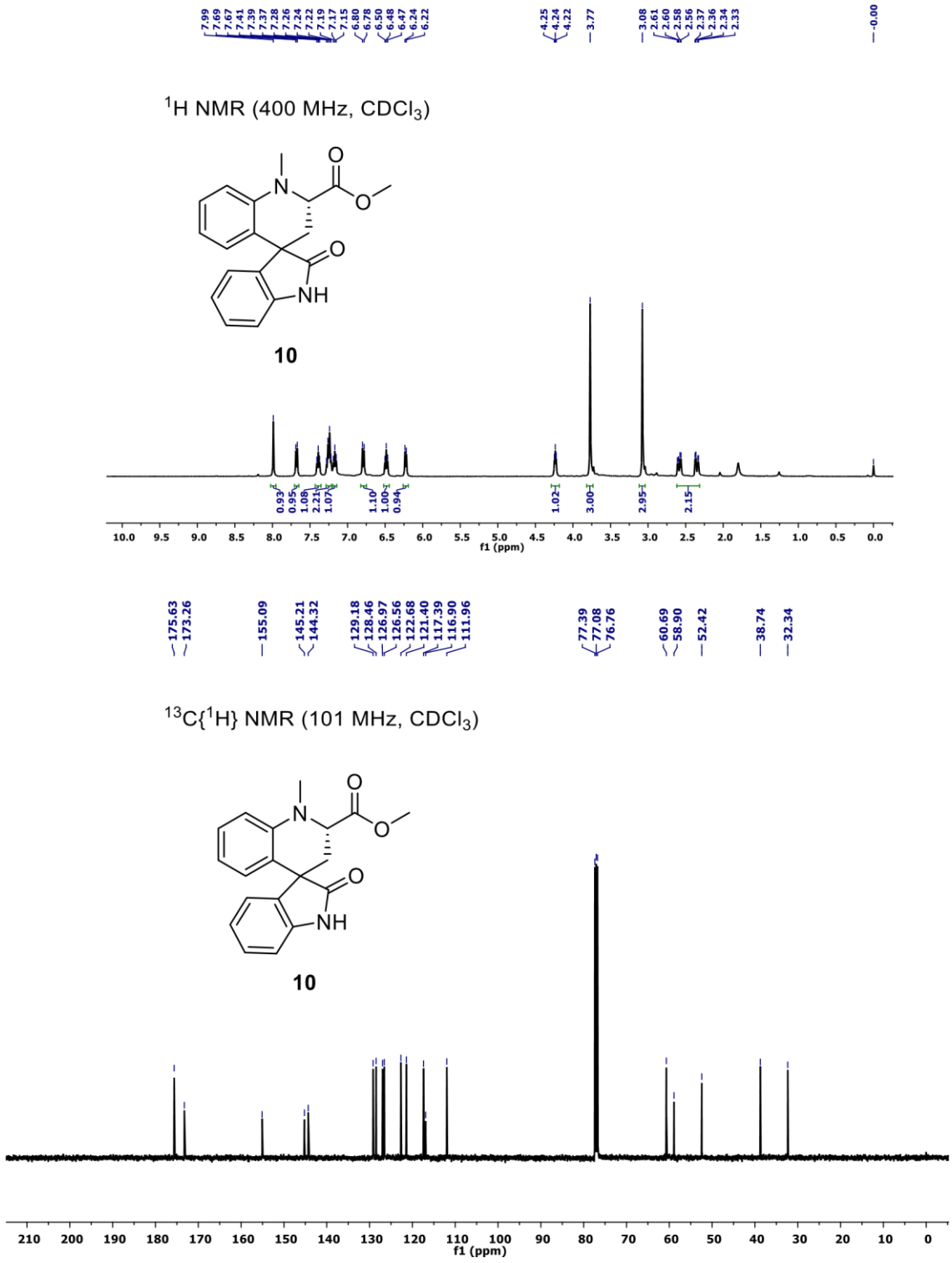

Fig S143. ^{1}H, ^{13}C $\{^{1}H\}$ NMR spectra of spirofused tetrahydroquinoline-oxindole **10**.

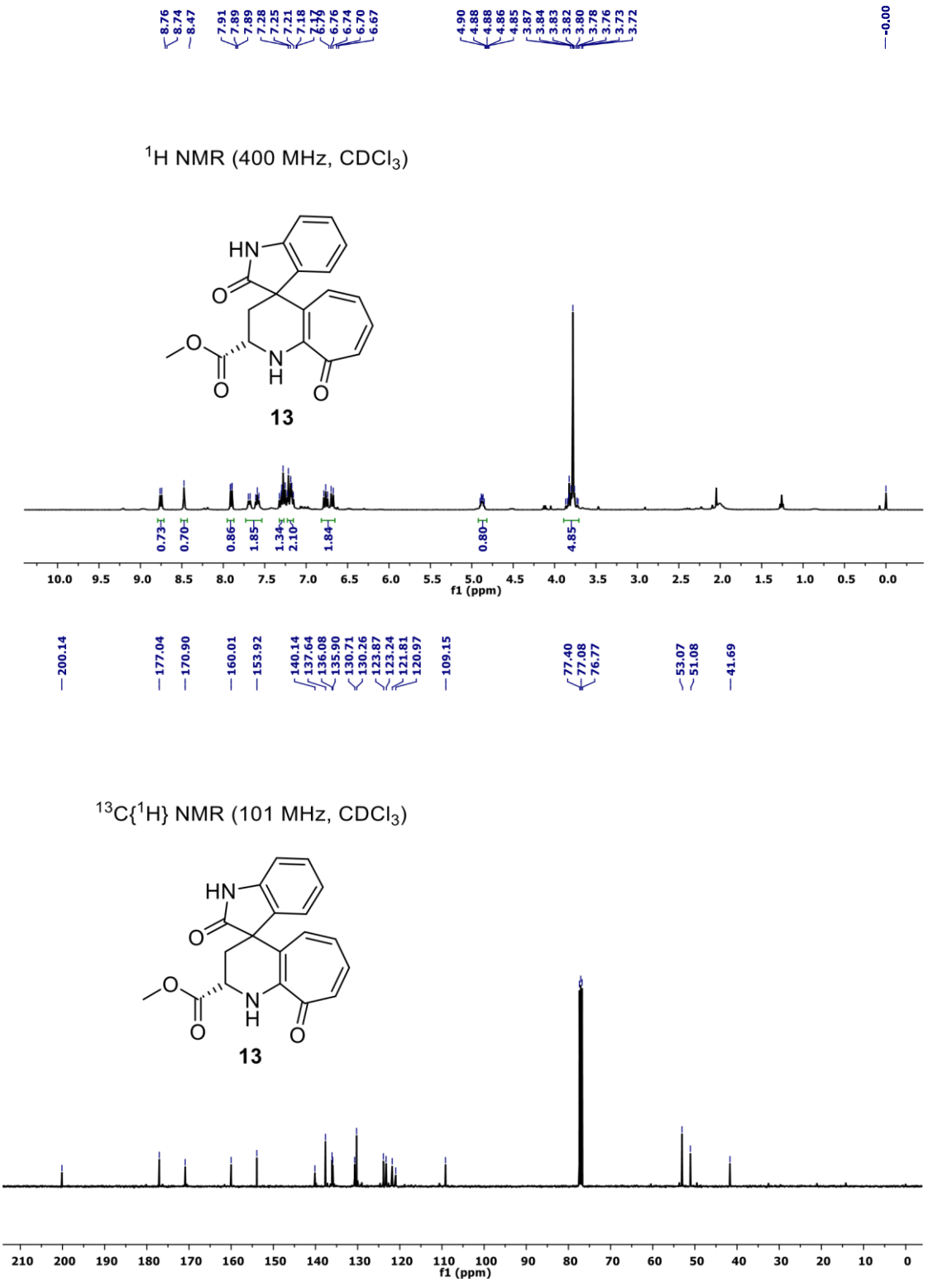

Fig S144. ^{1}H, ^{13}C $\{^{1}H\}$ NMR spectra of tropone-pipecolate fused spiro-oxindole **13**.

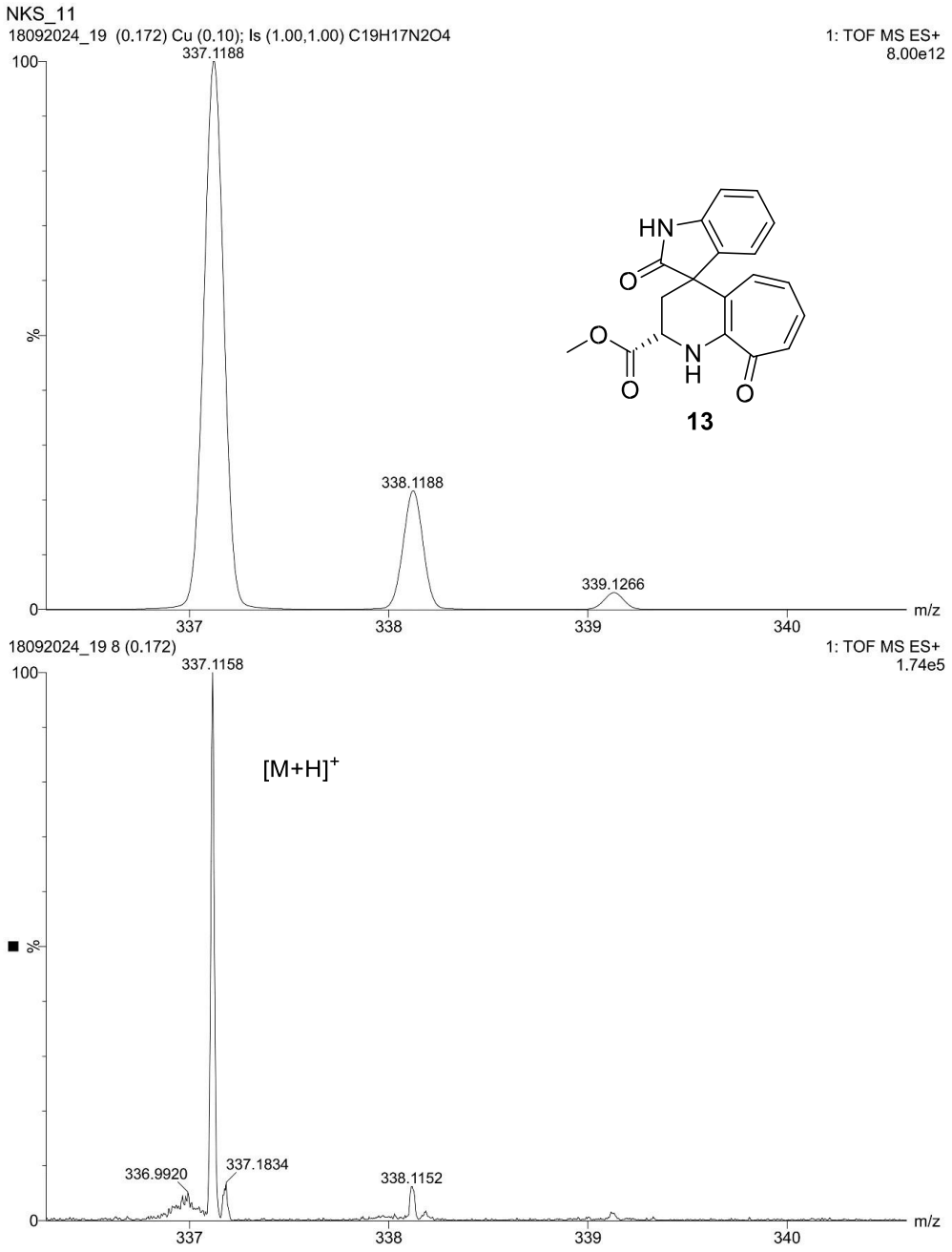

Fig S145. ESI-HRMS spectra of tropone-pipecolate fused spiro-oxindole **13**.

5. X-Ray Studies of Single Crystals

Single crystal of kynurenine derivative **(5g)** was obtained in solvent mixture ethylacetate and hexane by slow evaporation method. The crystal data of **5g** was collected on a Rigaku Oxford diffractometer at 100 K. Selected collection parameters and other crystallographic results are summarized below. The program package SHELXTL1 and Olex2 was used for structure solution and ORTEP diagram carried out by DIAMOND 3.2.

Table S1. Crystal data and structure refinement for compound **5g.**

Identification code	**5g**
Empirical formula	$C_{38}H_{40}N_4O_{12}S_2$
Formula weight	808.86
Temperature/K	100.00(10)
Crystal system	monoclinic
Space group	$P2_1$
a/Å	11.0125(2)
b/Å	8.54110(10)
c/Å	21.0020(3)
α/°	90
β/°	104.994(2)
γ/°	90
Volume/Å^3	1908.17(5)
Z	2
ρ_{calc} g/cm^3	1.408
μ/mm^{-1}	1.858
F (000)	848.0
Crystal size/mm^3	0.02 × 0.02 × 0.002
Radiation	Cu Kα (λ = 1.54184)
2Θ range for data collection/°	8.312 to 150.842
Index ranges	-13 ≤ h ≤ 13, -10 ≤ k ≤ 10, -26 ≤ l ≤ 14
Reflections collected	16144
Independent reflections	6776 [R_{int} = 0.0544, R_{sigma} = 0.0591]
Data/restraints/parameters	6776/1/517
Goodness-of-fit on F^2	1.068
Final R indexes [I>=2σ (I)]	R_1 = 0.0331, wR_2 = 0.0905
Final R indexes [all data]	R_1 = 0.0369, wR_2 = 0.0913
Largest diff. peak/hole / e Å^{-3}	0.28/-0.31
Flack parameter	0.052(8)

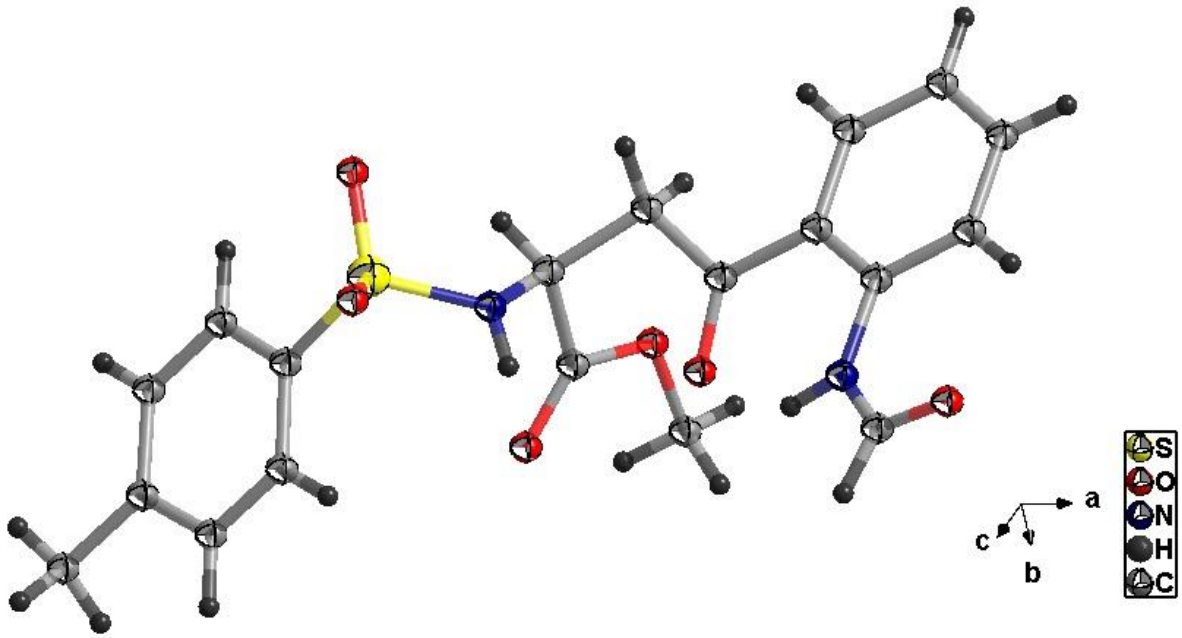

Fig S146. ORTEP diagram of kynurenine derivative **(5g)** [ellipsoid contour probability: 50%].

kynurenine derivative **(7b)** was obtained in solvent mixture ethylacetate and hexane by slow evaporation method. The crystal data of **7b** was collected on a Rigaku Oxford diffractometer at 100 K. Selected collection parameters and other crystallographic results are summarized below. The program package SHELXTL1 and Olex2 was used for structure solution and ORTEP diagram carried out by DIAMOND 3.2.

Table S2. Crystal data and structure refinement for compound **7b.**

Identification code	**7b**
Empirical formula	$C_{40}H_{54}N_6O_{14}$
Formula weight	842.89
Temperature/K	100.01(11)
Crystal system	triclinic
Space group	P1
a/Å	9.6582(4)
b/Å	10.8402(3)
c/Å	12.8768(3)
α/°	65.827(2)
β/°	69.312(3)
γ/°	63.964(3)
Volume/Å^3	1080.08(7)
Z	1
ρ_{calc} g/cm^3	1.296
μ/mm^{-1}	0.826
F (000)	448.0
Crystal size/mm^3	0.01 × 0.01 × 0.001
Radiation	Cu Kα (λ = 1.54184)
2Θ range for data collection/°	7.7 to 155.582
Index ranges	-12 ≤ h ≤ 12, -13 ≤ k ≤ 10, -16 ≤ l ≤ 15
Reflections collected	16820
Independent reflections	6208 [R_{int} = 0.0562, R_{sigma} = 0.0592]
Data/restraints/parameters	6208/3/551
Goodness-of-fit on F^2	0.979
Final R indexes [I>=2σ (I)]	R_1 = 0.0675, wR_2 = 0.1806
Final R indexes [all data]	R_1 = 0.0696, wR_2 = 0.1848
Largest diff. peak/hole / e Å^{-3}	0.63/-0.29
Flack parameter	0.06(15)

Single crystal of

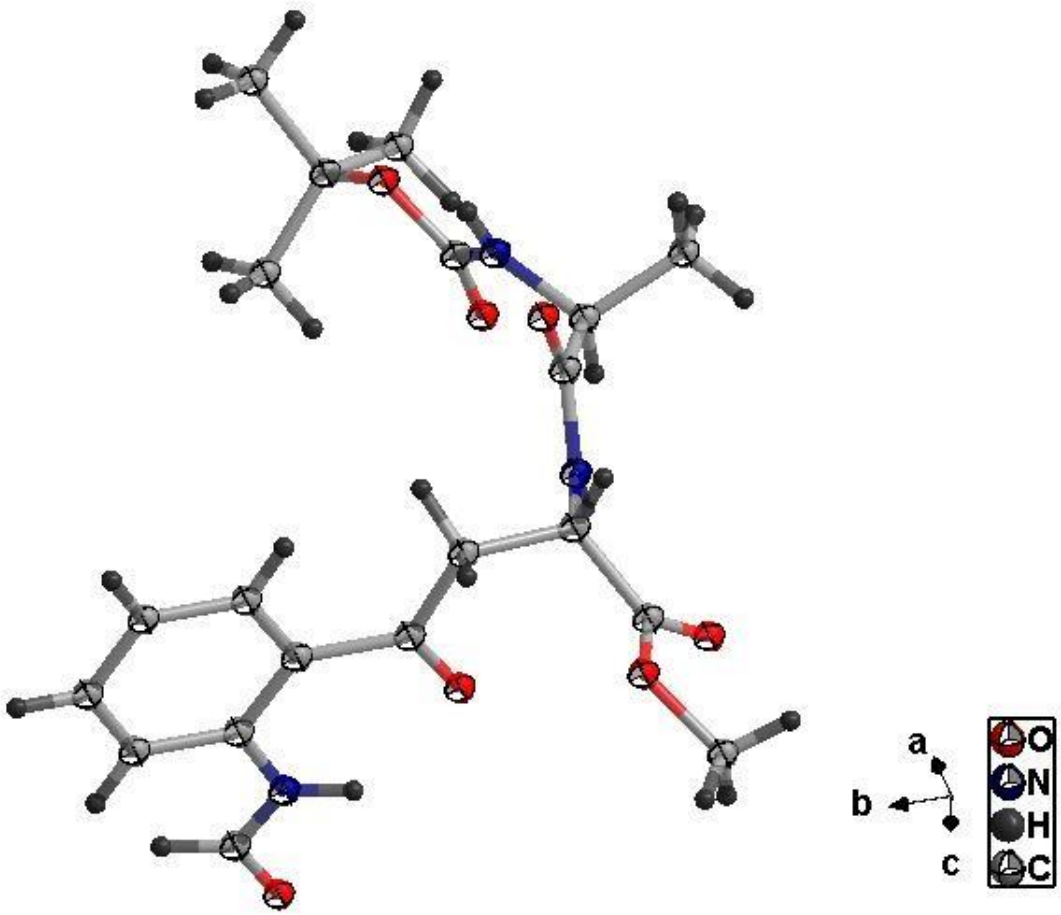

Fig S147. ORTEP diagram of kynurenine derivative **(7b)** [ellipsoid contour probability: 50%]. kynurenine derivative **(7g)** was obtained in solvent mixture ethylacetate and hexane by slow evaporation method. The crystal data of **7g** was collected on a Rigaku Oxford diffractometer at 100 K. Selected collection parameters and other crystallographic results are summarized below. The program package SHELXTL1 and Olex2 was used for structure solution and ORTEP diagram carried out by DIAMOND 3.2.

Table S3. Crystal data and structure refinement for compound **7g.**

Identification code	**7g**
Empirical formula	$C_{20}H_{27}N_3O_7$
Formula weight	421.44
Temperature/K	100.15
Crystal system	triclinic
Space group	P1 calc
a/Å	5.03333(16)
b/Å	8.5410(3)
c/Å	13.3951(4)
α/°	82.934(3)
β/°	85.650(3)
γ/°	73.874(3)
Volume/Å^3	548.46(3)
Z	1
ρ g/cm^3	1.276
μ/mm^{-1} 0.814 F (000)	224.0
Crystal size/mm^3	0.01 × 0.01 × 0.001
Radiation	CuKα (λ = 1.54184)
2Θ range for data collection/°	6.656 to 155.548
Index ranges	$-6 \le h \le 6$, $-10 \le k \le 10$, $-16 \le l \le 15$
Reflections collected	8615
Independent reflections	3497 [R_{int} = 0.0537, R_{sigma} = 0.0617]
Data/restraints/parameters	3497/3/287
Goodness-of-fit on F^2	1.060
Final R indexes [I>=2σ (I)]	R_1 = 0.0427, wR_2 = 0.1122
Final R indexes [all data]	R_1 = 0.0459, wR_2 = 0.1162
Largest diff. peak/hole / e Å^{-3}	0.20/-0.20
Flack parameter	0.2(3)

Single crystal of

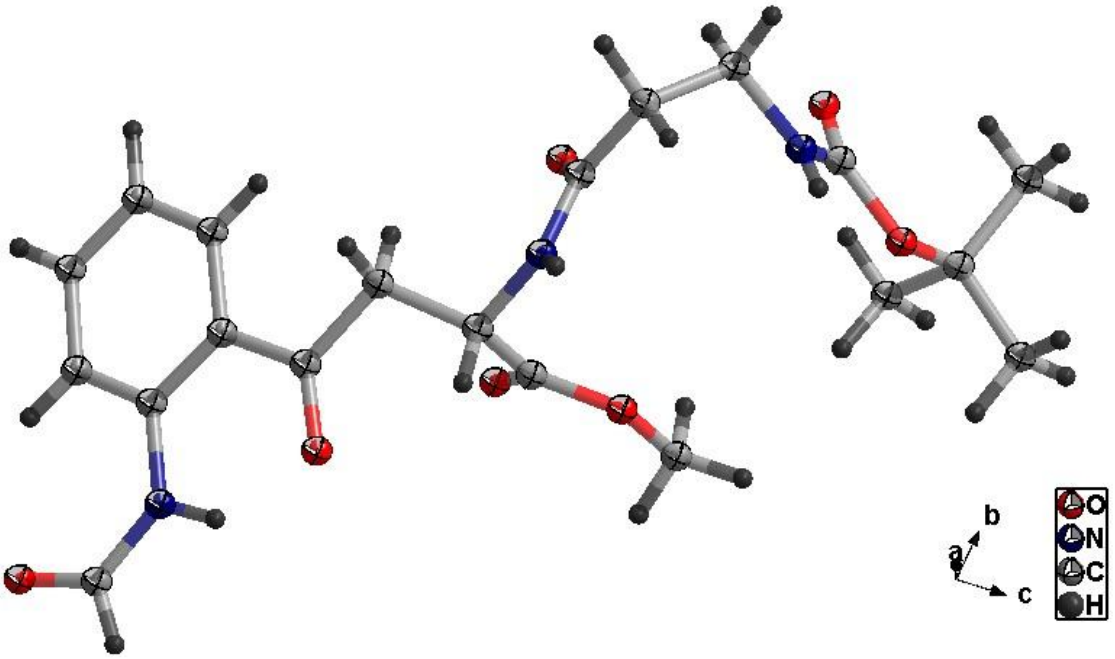

Fig S148. ORTEP diagram of kynurenine derivative **(7g)** [ellipsoid contour probability: 50%]. oxaspiro-oxindole **(8)** was obtained in solvent mixture ethylacetate and hexane by slow evaporation method. The crystal data of **8** was collected on a Rigaku Oxford diffractometer at 100 K. Selected collection parameters and other crystallographic results are summarized below. The program package SHELXTL1 and Olex2 was used for structure solution and ORTEP diagram carried out by DIAMOND 3.2.

Table S4. Crystal data and structure refinement for compound **8.**

Identification code	**8**
Empirical formula	$C_{16}H_{18}N_2O_5$
Formula weight	318.32
Temperature/K	100.15
Crystal system	orthorhombic
Space group	$P2_12_12_1$ calc
a/Å	5.6238(3)
b/Å	14.8768(8)
c/Å	19.4102(10)
α/°	90
β/°	90
γ/°	90
Volume/Å^3	1623.94(15)
Z	4
ρ g/cm^3	1.302
μ/mm^{-1} 0.817 F (000)	672.0
Crystal size/mm^3	0.02 × 0.02 × 0.002
Radiation	CuKα (λ = 1.54184)
2Θ range for data collection/°	7.488 to 155.81
Index ranges	$-6 \le h \le 6$, $-18 \le k \le 18$, $-14 \le l \le 24$
Reflections collected	7534
Independent reflections	3118 [R_{int} = 0.0436, R_{sigma} = 0.0390]
Data/restraints/parameters	3118/0/215
Goodness-of-fit on F^2	1.053
Final R indexes [I>=2σ (I)]	R_1 = 0.0410, wR_2 = 0.1118
Final R indexes [all data]	R_1 = 0.0424, wR_2 = 0.1133
Largest diff. peak/hole / e Å^{-3}	0.18/-0.33
Flack parameter	0.03(14)

Single crystal of

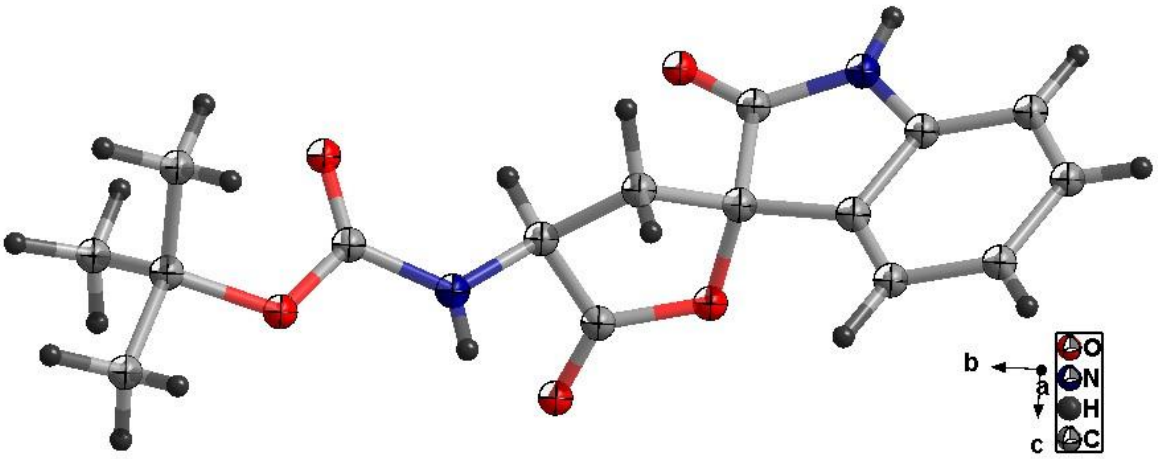

Fig S149. ORTEP diagram of oxaspirooxindole **(8)** [ellipsoid contour probability: 50%]. spiro-oxindole **(13)** was obtained in solvent mixture ethylacetate and hexane by slow evaporation method. The crystal data of **13** was collected on a Rigaku Oxford diffractometer at 243 K. Selected collection parameters and other crystallographic results are summarized below. The program package SHELXTL1 and Olex2 was used for structure solution and ORTEP diagram carried out by DIAMOND 3.2.

Table S5. Crystal data and structure refinement for compound **13.**

Identification code	**13**		
Empirical formula	$C_{19}H_{14}N_2O_4$		
Formula weight	334.32		
Temperature/K	243(60)		
Crystal system	monoclinic		
Space group	C2/c	ρ_{calc}	
a/Å	15.6051(10)	μ/mm^{-1}	0.099
b/Å	9.8026(6)	F (000)	1392.0
c/Å	21.1562(13)	Crystal size/mm^3	0.01 × 0.01 × 0.001
α/°	90	Radiation	MoKα (λ = 0.71073)
β/°	98.295(6)	2Θ range for data collection/°	6.996 to 60.464
γ/°	90	Index ranges	-21 ≤ h ≤ 21, -13 ≤ k ≤ 12, -28 ≤ l ≤ 27
Volume/$Å^3$	3202.4(3)	Reflections collected	15065
Z	8	Independent reflections	3943 [R_{int} = 0.0427, R_{sigma} = 0.0358]
ρ g/cm^3	1.387		
Data/restraints/parameters	3943/0/227		
Goodness-of-fit on F^2	1.058		
Final R indexes [I>=2σ (I)]	R_1 = 0.0647, wR_2 = 0.1742		
Final R indexes [all data]	R_1 = 0.0822, wR_2 = 0.1841	Largest diff. peak/hole / e $Å^{-3}$	0.34/-0.28

Single crystal of

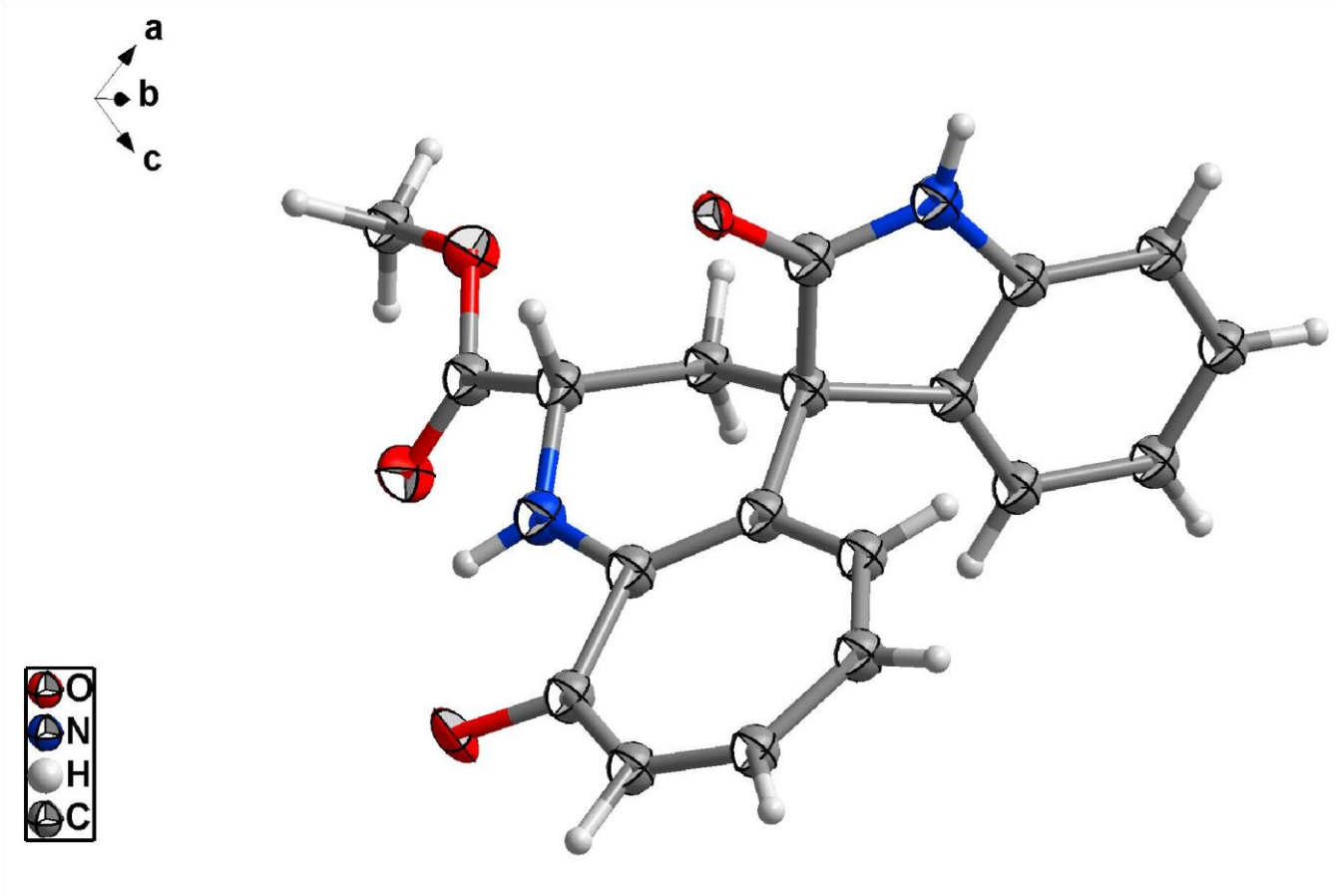

Fig S150. ORTEP diagram of spiro-oxindole **(13)** [ellipsoid contour probability: 50%].

6. Biofilm Assay

Biofilm formation ability in presence of various synthesized kynurenine derivatives was studied qualitatively and quantitatively by falcon tube and microtitre plate assay. For qualitative analysis, 20 µL of overnight grown culture (OD595 adjusted to 0.5) of *Pseudomonas aeruginosa* (PA14) was inoculated into 2 ml LB broth supplemented with 100 µM of the kynurenine moieties and incubated at 37°C for 48 h. After incubation the culture was carefully decanted and the tube was rinsed twice by milli-Q water followed by staining with 0.1% aqueous solution of crystal violet for 30 min at room temperature. The crystal violet stain was carefully decanted and the tubes were washed with milli-Q water thrice followed by air drying and crystal violet ring observation.

For quantitative analysis, 10 µL of overnight grown culture (OD595 adjusted to 0.5) of PA14 was inoculated into 100 µL LB broth supplemented with 100 µg/ ml of the synthesized compounds taken in a micro-titre plate and incubated at 37°C for 48 h under moist condition. After incubation the supernatant were carefully taken off and unattached cells in the supernatant were carefully removed followed by washing with milliQ water twice. 125 µL of 0.1% crystal violet solution was added and micro-titre plate was incubated for 30 min followed by washing with milli-Q water thrice. The plates were air-dried and de-stained with 200 µL of 30% acetic acid and biofilm formation was indirectly quantified in terms of optical density of dissolved crystal violet at 595nm. Compounds showing significant biofilm reduction were further tested for their anti-biofilm activity in dose dependent manner taking concentration range from 20 µM to 100 µM and their IC50 values for biofilm formation were obtained.

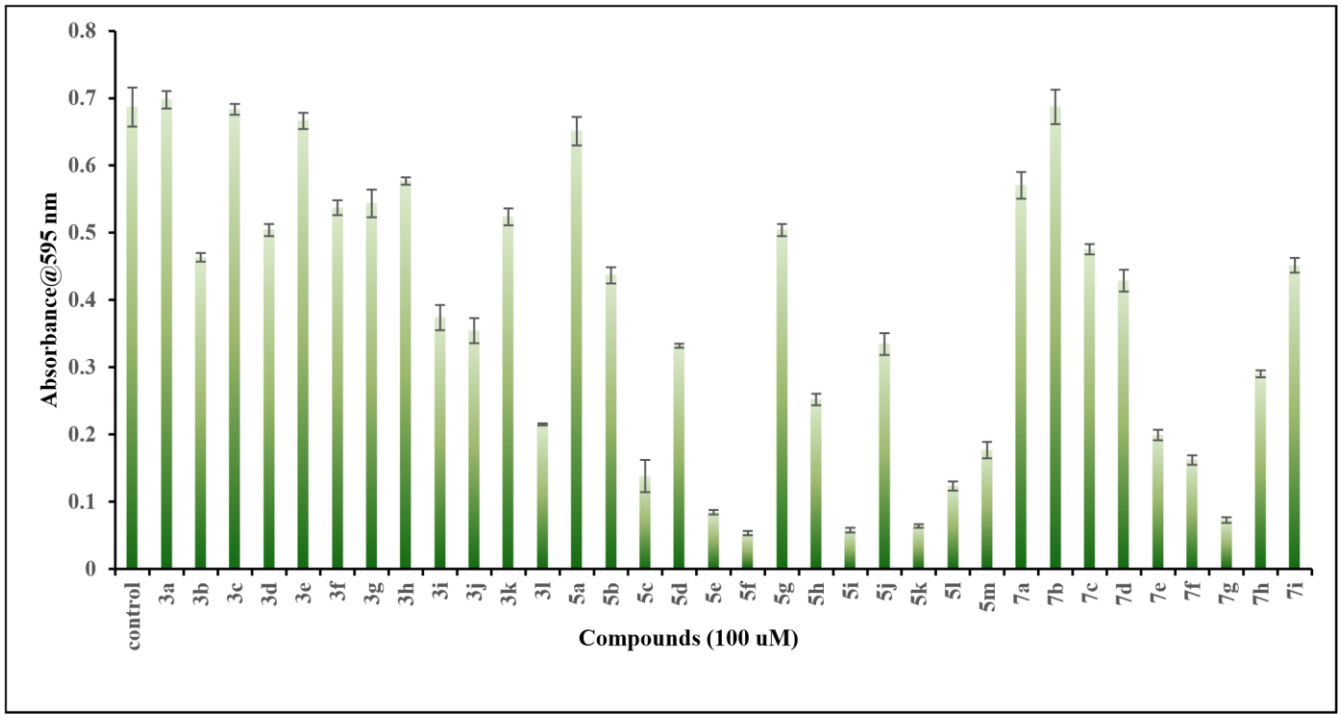

Fig S151. Quantitative analysis of *P. aeruginosa* biofilm formation in absence (control) or presence of kynurenine derivatives (**3a-3l**/**5a-5m**/**7a-7i**) at 100 µM concentration. Error bars are mean ± standard deviation (SDs).

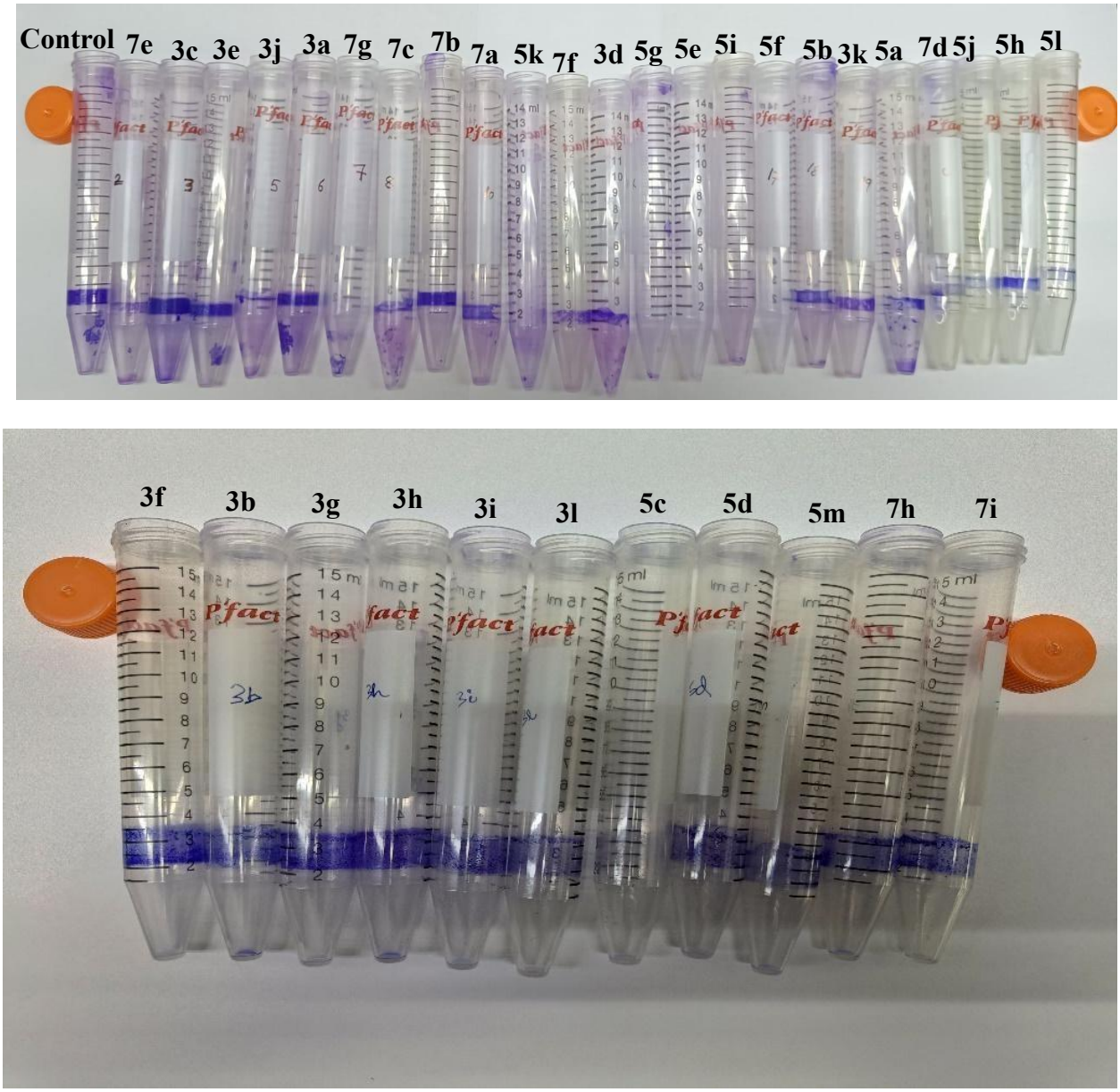

Fig S152. Images of biofilm formation for control and all the kynurenine derivatives (**3a-3l/5a5m/7a-7i**) tested for 100 μM concentration.

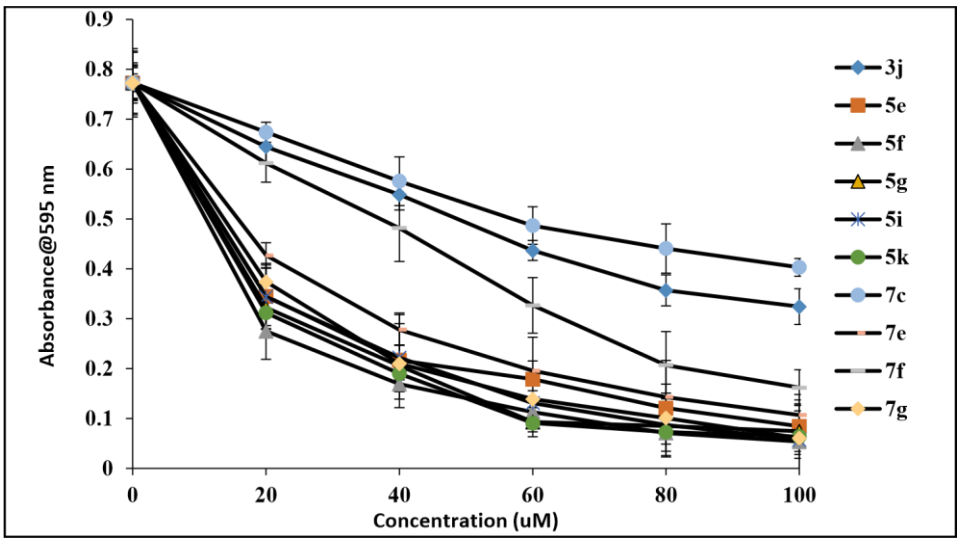

Fig S153. Concentration dependent quantitative biofilm assay. Error bars are mean ± standard deviation (SDs).

Table S6. IC-50 values analysed from biofilm assay.

Compound	IC-50 (concentration in µM)
3j	64.06
5e	32.46
5g	17.81
5i	28.85
5f	15.52
5k	15.68
7c	53.35
7e	30.25
7f	76.14
7g	20.65

7. Pyocyanin Assay

In order to assess the effect of synthesized kynurenine derivatives on pyocyanin production, *PA 14* were grown overnight in 5 mL minimal media (Himedia) in presence of 100 µM of the synthesized compounds (only the substrates showing significant result in biofilm assay) under shaking condition. After incubation, supernatant was collected from the 5 mL culture by centrifugation of the entire culture at 5000 rpm for 15 min at room temperature. The pyocyanin fraction was further extracted by adding 3 mL chloroform in the supernatant. Pyocyanin was then re-extracted into 1 mL of acidified water (0.2 mol/L HCl) which gave a pink–red solution. For the quantitation of the pyocyanin within the solution, the absorbance was measured at 520 nm. Pyocyanin inhibition was also performed at variable concentration to analyze their IC_{50} values for pyocyanin production.

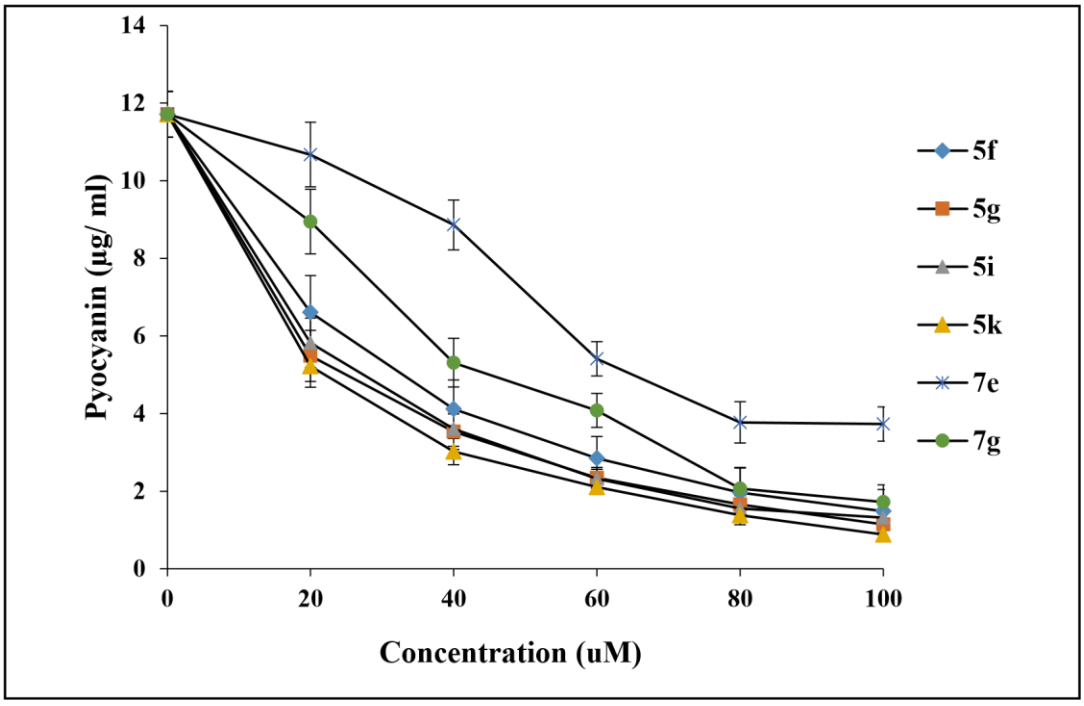

Fig S154. Concentration dependent quantitative pyocyanin assay. Error bars are mean ± standard deviation (SDs).

Table S7. IC-50 values analysed from pyocyanin assay.

Compound	IC-50 (concentration in µM)
5f	28.07
5g	27.73
5i	22.26
5k	20.56
7e	51.45
7g	39.74

8. Swarming Motility Assay

Swarming motility assays were performed in M9 medium (Himedia) amended with 0.5% Bacto™casamino acids (BD) and solidified with 0.6% Bacto™ agar (BD). 10 ml of swarm media supplemented with 100 µM of different kynurenine derivatives were poured on petridishes (60 mm diameter) and were allowed to dry for 30 min. The plates were spot inoculated at the centre with one isolated colony grown on LB with the help of a straight wire loop. The plates were incubated in upright position at 37 °C for 24 hours. The plates were carefully taken out and observed for tendril formation. Images were taken in Gel Doc™ XR+ and processed by using Image lab™ software.

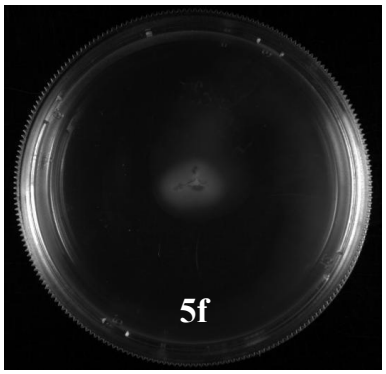

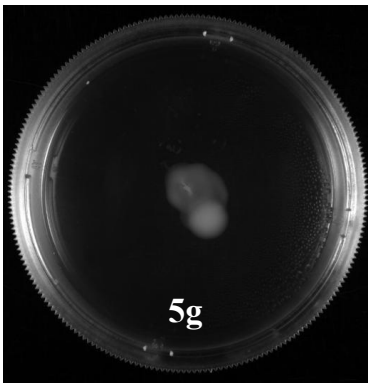

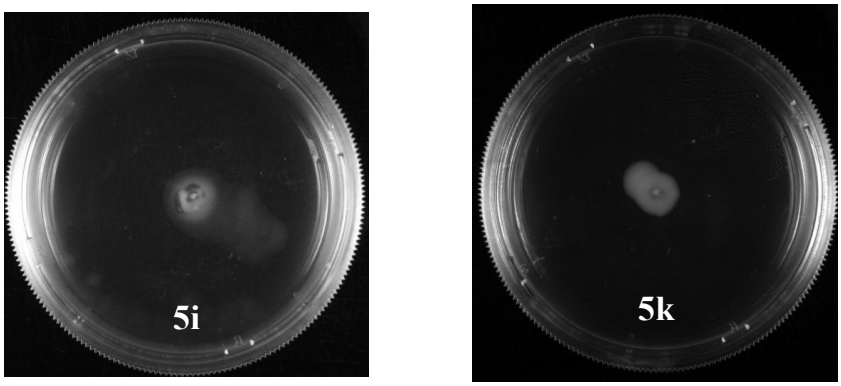

Fig S155. Swarming images of *P. aeruginosa (*PA14) in the absence (DMSO control) or presence of compounds (**5f, 5g, 5i** and **5k**; 100 µM concentration)

9. Scanning Electron Microscopy (SEM) Analysis

Bacterial biofilm was grown on silicon wafer substrate by inoculating 10 µL of overnight grown culture of *PA14 into 1mL LB broth supplemented with* 100 µM of the kynurenine derivatives and incubated at 37°C for 48 h. The biofilm substrate was then removed from the growth medium and rinsed with phosphate-buffered saline (PBS) to remove any non-adherent bacteria. The biofilm was then fixed with 2.5% glutaraldehyde in PBS for 12 h at 4 °C. It was then subjected to a graded ethanol series for dehydration and then allowed to air dry. The substrates were then sputter-coated with platinum to increase their conductivity and SEM images were recorded.

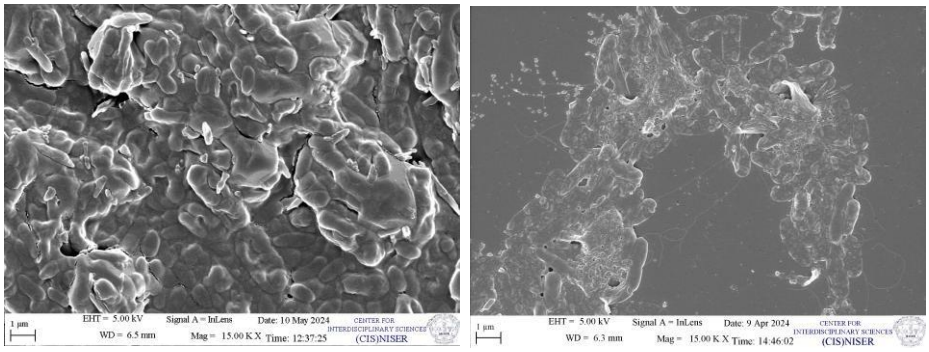

Control **5f**

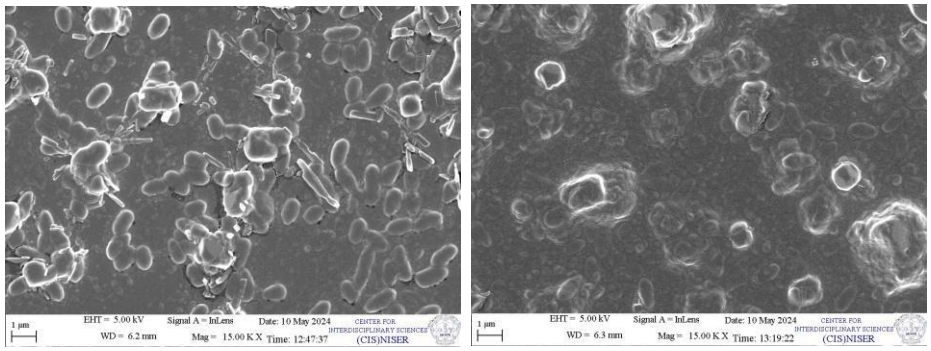

5g **5i**

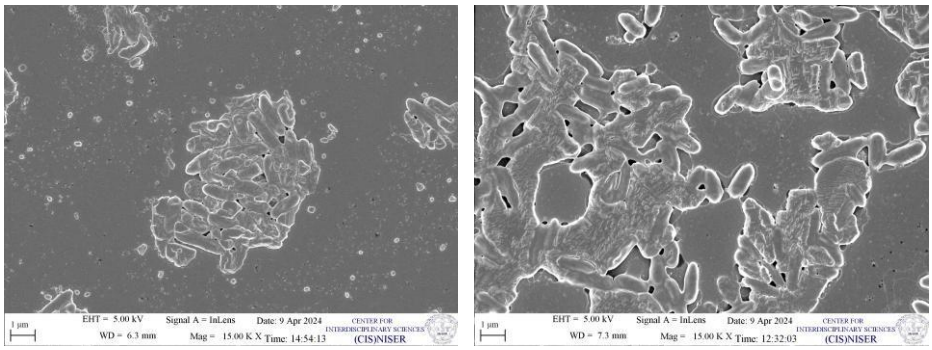

5k **7e**

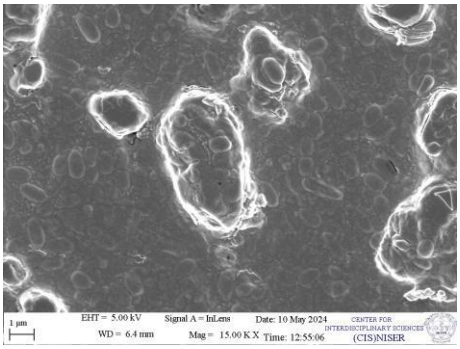

7g

Fig S156. SEM images of biofilms developed by *P. aeruginosa* illustrating the effect of kynurenine derivatives (**5f/5g/5i/5k/7e/7g**) at 100 µM concentration on biofilm formation.

10. Bacterial Growth Curve Measurement

A single colony of the bacterial strain was inoculated into small volume of LB media. The overnight culture was diluted to OD600 of approximately 0.1 in fresh growth medium. 200 µL of the diluted bacterial culture along with 100 µM of the kynurenine derivatives were added into each well of the 96-well microtitre plate. OD was recorded at 600 nm in every 15min interval for an overall period of 24 h using a plate reader.

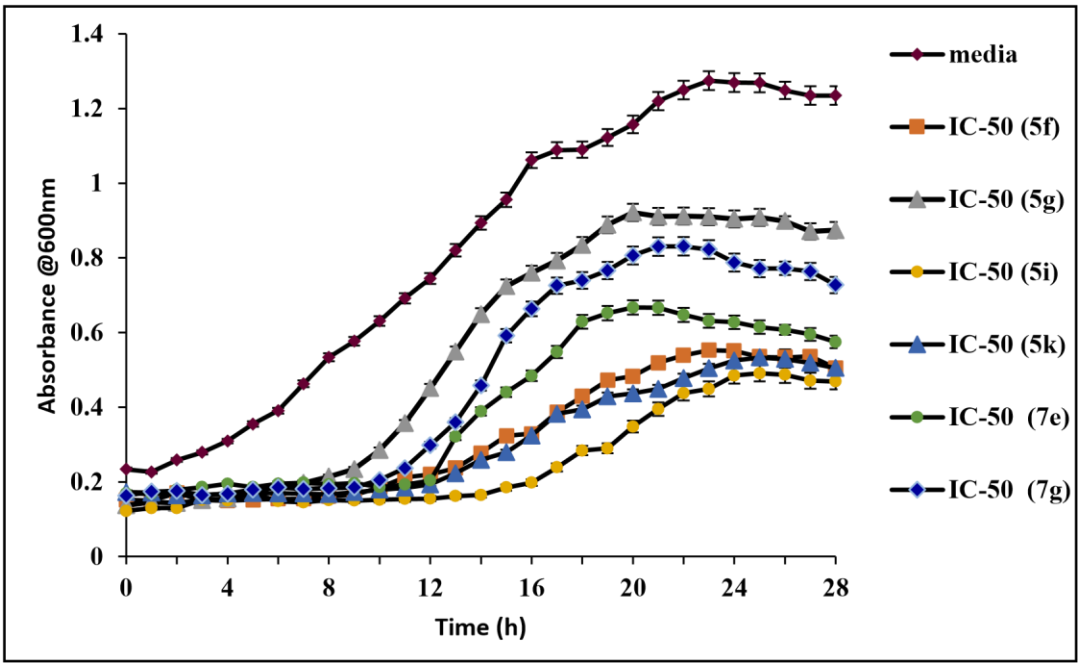

Fig S157. Growth curve of *P. aeruginosa* grown at 37 ºC for 24 h treated with different kynurenine derivatives at their respective IC-50 concentration. Error bars are mean ± standard deviations (SDs).

11. QRT-PCR (Quantitative Real-Time Polymerase Chain Reaction) Analysis

RNA was extracted from overnight grown 2 mL culture of PA14 treated with kynurenine derivatives using the RiboPur™ kit (Ambion) according to the manufacturer's instruction. RNA purity was assessed by spectrophotometer (NanoDrop ND-1000). Samples showing ratios of A_{260}/A_{280} close to 2.0 were selected. First strand cDNA was synthesized from 1 µg of treated RNAusing the Verso cDNA synthesis kit (Thermo Scientific) as per manufacture's guidelines. Primers were designed for *lasI*, *lasB*, *lasR* genes using the sequences obtained from pseudomonas database (https://www.pseudomonas.com/) (Table S8). cDNA was diluted 10-fold and combined with primer pairs and PowerU™ SYBR® Green Master Mix (Thermo Scientific) on an Applied Biosystems real-time PCR system (QuantStudio 6 and 7 Flex Real Time PCR System) according to the following protocol: 95°C for 2 min; 40 cycles of 95°C for 3 sec, 60°C for 30 sec; followed by a melt curve cycle. The housekeeping gene 16S ribosomal RNA (rRNA) was used as an internal standard for quantification of the total RNA. For each gene, a common threshold setting applied to each of the three biological replicates determined the threshold cycle (C_T). Relative abundance of each gene was determined by the $2^{-\Delta\Delta Ct}$ method.

TABLE S8. Primers used for quantitative RT-PCR.

Gene	PCR primer sequence (5' – 3')
lasI	Fw: GGTTATGACGCACTCAGTCC
	Rv: TTCAGCATGTAGGGGCCAGT
lasR	Fw: GTGGAAAATTGGAGTGGAGC
	Rv: ACGATGAAGGCGTTCTCGTA
lasB	Fw: GACCTGATCGACGTGTCCAA
	Rv: ATCGCTTTCAGTTCGTCGGC
16s	Fw: TAAGCACCGGCTAACTTCGT
	Rv: AACCACCTACGCGCGCTTTA

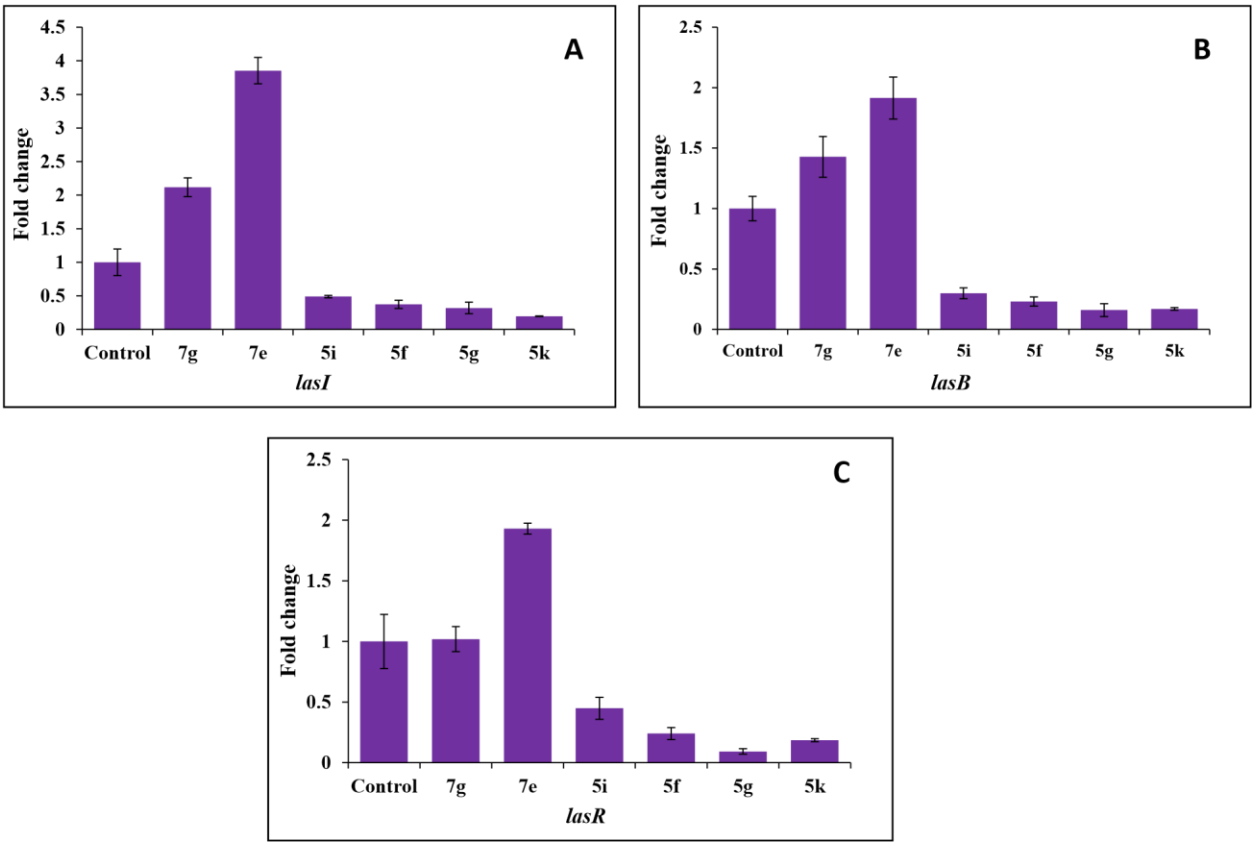

Fig S158. Effect of kynurenine treatment on expression of QS-related genes, Quantitative realtime PCR analysis showing the transcript levels of (A) *lasI* genes and (B) *lasB* genes and (C) *lasR* genes in the presence of kynurenine derivatives (**5f**, **5g**, **5i**, **5k**, **7e**, **7g**) at their IC-50 concentration. Error bars are mean ± standard deviations (SDs).

12. Plausible Mechanisms for the Synthesis of Spirocyclic Motifs

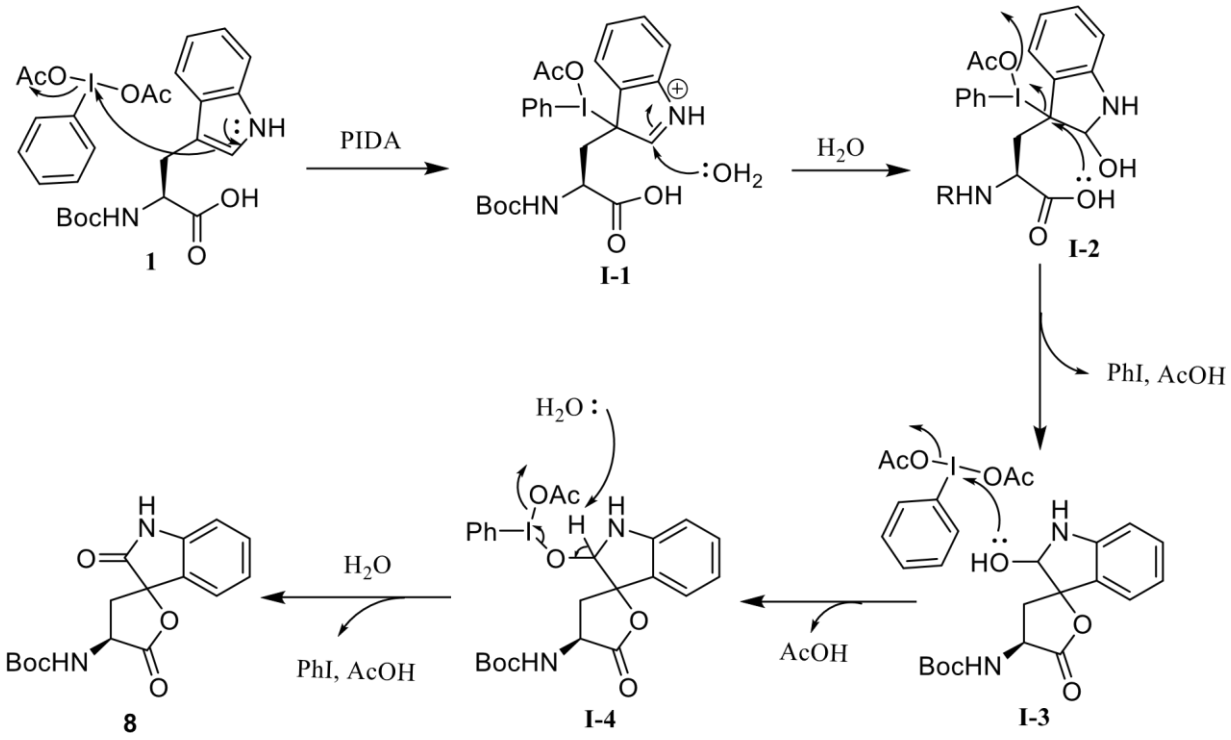

Fig S159. Plausible mechanism for the synthesis of oxaspiro-oxindole **8**.

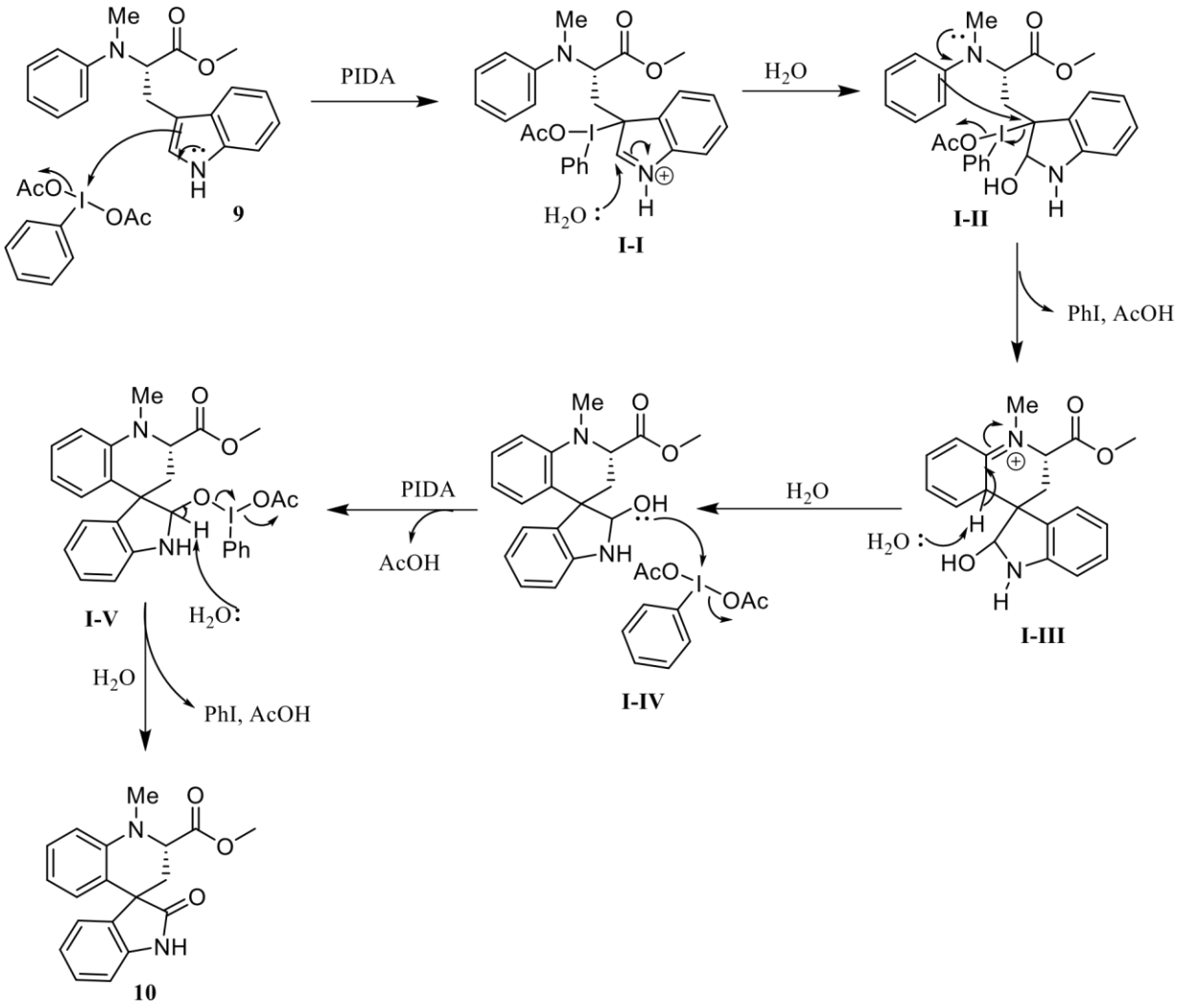

Fig S160. Plausible mechanism for the synthesis of spiro-oxindole **10**.

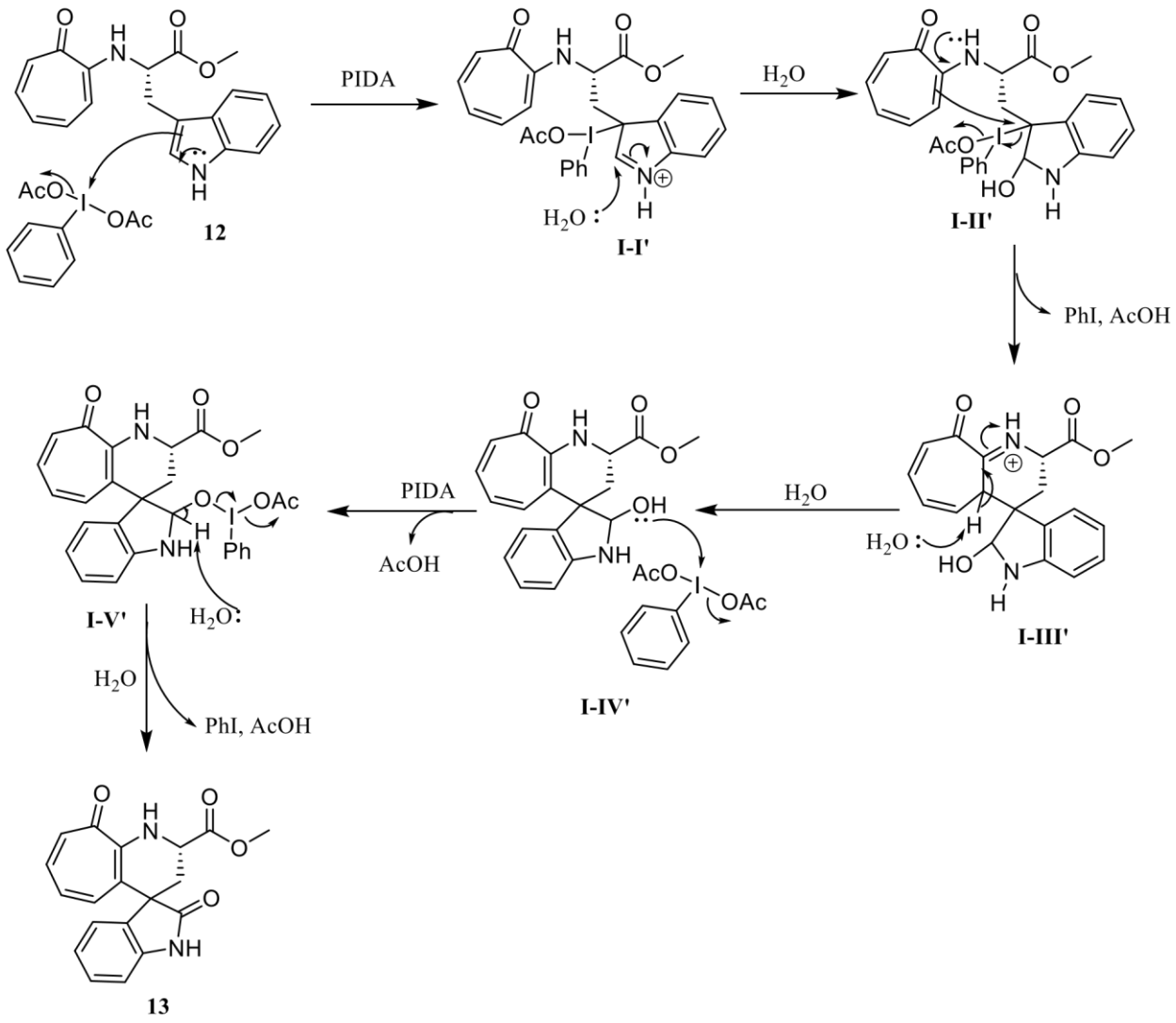

Fig S161. Plausible mechanism for the synthesis of spiro-oxindole **13**.